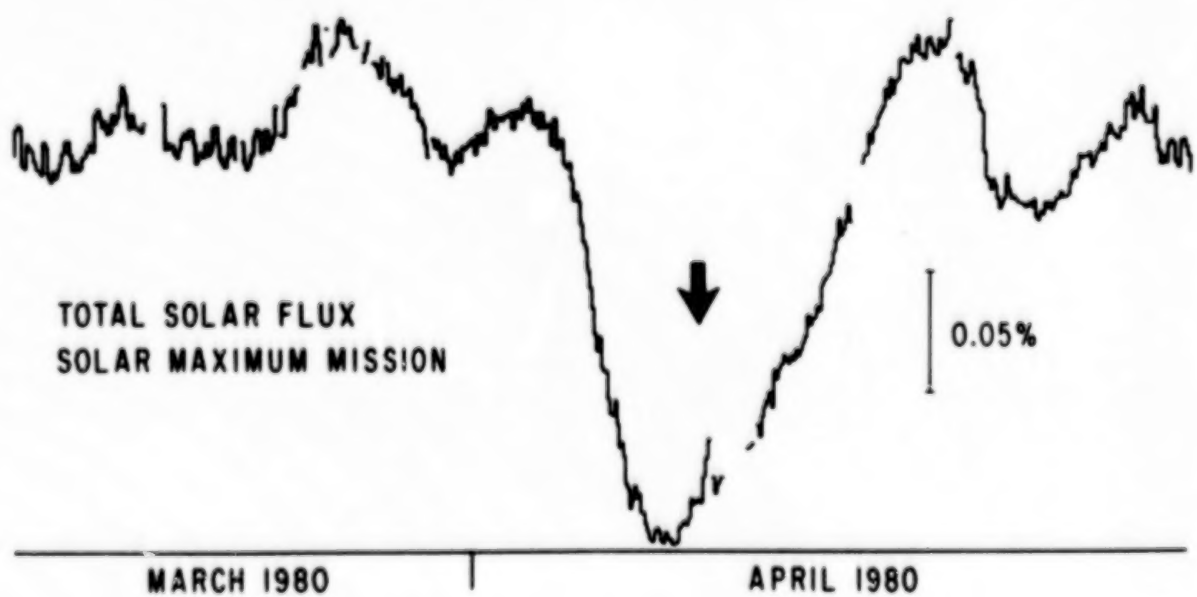
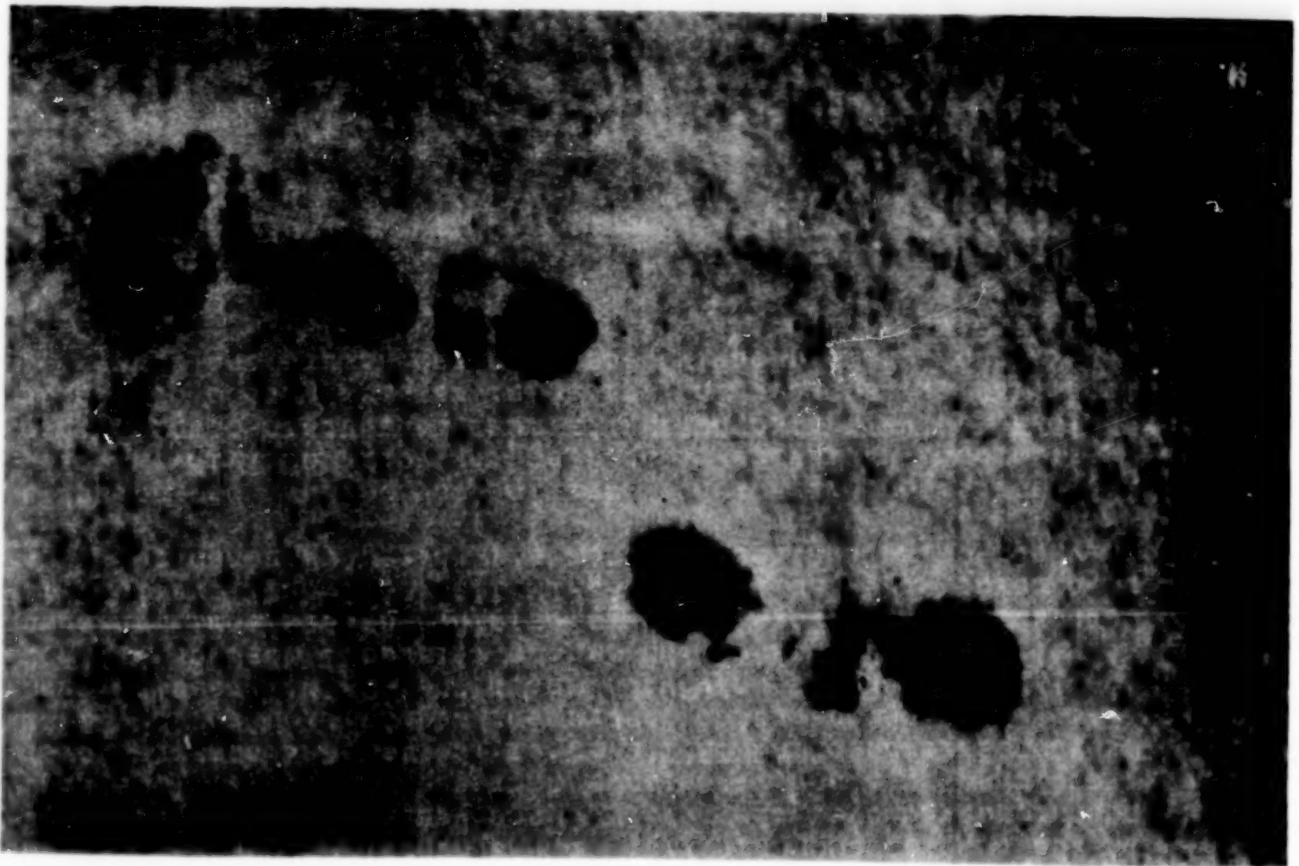


8 APRIL 1980



BEST COPY AVAILABLE

NASA Conference Publication 2310

Solar Irradiance Variations on Active Region Time Scales

Edited by
B. J. LaBonte
University of Hawaii at Manoa
Honolulu, Hawaii

G. A. Chapman
California State University at Northridge
Northridge, California

H. S. Hudson
University of California at San Diego
La Jolla, California

R. C. Willson
Jet Propulsion Laboratory
California Institute of Technology
Pasadena, California

Proceedings of a workshop held at
The California Institute of Technology
Pasadena, California
June 20-21, 1983

NASA

National Aeronautics
and Space Administration

Scientific and Technical
Information Branch

1984

BEST COPY AVAILABLE

BLANK PAGE

PREFACE

The variations of the total solar irradiance have become in the past few years an important new tool for studying the sun, thanks to the development of very precise sensors such as the ACRIM instrument on board the Solar Maximum Mission. The study of variations of the spectral irradiance observed in the EUV has also developed rapidly. The largest variations of the total irradiance occur on time scales of a few days and are caused by solar active regions, and especially sunspots. Several independent efforts have been underway to describe the active-region effects on total and spectral irradiance, and a first round of results from these efforts has appeared in the literature. Needless to say, disagreements on interpretation have quickly surfaced in this new field, and it therefore seemed very appropriate to have a topical workshop in which informal discussions could take place on this subject. Accordingly, the workshop took place June 20-21 in Pasadena, California, and was attended by most of the active workers in this field. The papers resulting from this workshop are collected here, along with much of the discussion. Gordon Newkirk provided a very nice introduction to the general discussion, which is printed here (p. 131) and provides a good summary of the entire two days of the workshop.

Most of the participants regarded this workshop as an extension of earlier workshops on the solar constant held in 1975 at Big Bear Solar Observatory (Zirin and Walter, BBSO 0149) and in 1980 at NASA Goddard Space Flight Center (Sofia, NASA-CP-2191). The organizers, however, had an ulterior motive in focusing the workshop on one particular component of the solar-constant variability. Much of the interpretation of the observed variations depends on the quality of supporting ground-based observations. Great improvements in these data can and should be made, especially to accompany future precise solar-constant measurements from a repaired Solar Maximum Mission. We attempted therefore to stimulate discussions of the types and quality of data best suited for these comparisons. Several persons provided short discussions of these needs, which are printed here, and we have also written our own summary of what we felt to be desirable ("A Global Irradiance Program," p. 311). We expect that the actual improvements in supporting data that do occur will differ somewhat from our desires, but we hope that this will happen because the community has been stimulated to have better ideas!

Finally, the meeting took place under excellent conditions at Caltech, and we would like to thank Hal Zirin and the Caltech solar astronomy group for helping us with local arrangements.

B. J. LaBonte
G. A. Chapman
H. S. Hudson
R. C. Willson

NOTE ON THE TRANSCRIPTION OF DISCUSSIONS

The idea of transcribing the discussions occurred to us at the last minute, and the equipment used (pencil and paper for the morning of the first day, tape recorders later on) was ad hoc and noisy. Nevertheless we enjoyed the discussions so much that we thought others might appreciate the flavor of the remarks. As we did the transcription we were very impressed at the remarkable difference in form and content between what scientists say and what they write. Since we wished to publish these proceedings promptly, we decided not to send the discussion around for comments by the participants. We have all worked on the transcripts and sincerely hope that they are accurate enough in spite of the noise. We do apologize in advance for any mis-identified speakers or mis-quoted remarks. We also apologize for omissions which may have occurred.

B. J. LaBonte
G. A. Chapman
H. S. Hudson
R. C. Willson

Table of Contents

Preface	iii
Note on Transcriptions of Discussions	iv
Table of Contents	v
Solar Total Irradiance Variability Measurements by the SMM/ACRIM I Experiment, R. C. Willson	1
Status of Solar Measurements and Data Reduction for ERB-Nimbus 7, J. R. Hickey and B. M. Alton	43
Facular Limb-Darkening Functions for Irradiance Modeling, T. Hirayama, T. Okamoto, and H. S. Hudson	59
Ground-Based Measurements of Solar Irradiance Variations, G. A. Chapman	73
Two-Dimensional Photometry of Active Regions, J. K. Lawrence, G.A. Chapman, A. D. Herzog, and J. C. Shelton	91
Photometric Studies of Heat Flow at the Photosphere, P. Foukal	97
Interaction of Convection and Small-Scale Magnetic Fields: Influ- ence on the Solar Luminosity, Åke Nordlund	121
Energy Flow Continuity in Solar Active Regions, K. H. Schatten	125
Active Region Contributions to Solar Irradiance Variation, Discus- sion, Afternoon 20 June 1983: Introductory Remarks, G. Newkirk	133
The Goddard Model of ACRIM Data, Sabatino Sofia	137
The Quality of Existing Spot and Facular Data, Jack Eddy	141
A Model for Balancing Spot and Facular Emission, Ken Schatten	145
What are Faculae? Gary Chapman	149
Recent Ground-based Observations of the Global Properties of the Sun, B. J. LaBonte	151
Limb-Darkening Variations, D. H. Bruning	165
Photometric Variations of Solar-Type Stars: Results of the Cloud- croft Survey, M. S. Giampapa	173
A Stellar Analogue of Solar Variability: The K-Dwarf V 471 Tau, A. Skumanich and A. Young	185
Helium 10830Å Irradiance: 1975-1983, J. W. Harvey	197
The Solar Constant, Climate, and some Tests of the Storage Hypo- thesis, J. A. Eddy	213
Temporal Variations of Solar UV Spectral Irradiance Caused by Rotation and Active Region Evolution, R. F. Donnelly, D. F. Heath, J. L. Lean, and G. J. Rottman	233
Modelling Solar Spectral Irradiance Variations at UV Wavelengths, J. L. Lean, W. C. Livingston, O. R. White, and A. Skumanich	253
Partial Summary of Heath's Presentation	291
Discussion of ACRIM "Spin-mode" Data	293

Final Discussion of Ground-based Observing Programs	295
Drift Scan Photometry and Astrometry, H. S. Hudson	297
Facular Data Base for SMM-ACRIM Comparisons, D. L. Glackin and R. C. Willson	299
New Techniques for Global Activity Monitoring, H. Zirin	301
Solar and Terrestrial Atmospheric Spectrometer - STAS, P. L. Smith, W. H. Parkinson, and W. K. Fowler	303
Status Report - Arizona Solar Variability Monitoring Program, J. M. Palmer	307
Comments on Ground-based Observations for Research on Solar Variability on Active-Region Time Scales, R. F. Donnelly	309
Comments, D. H. Bruning	311
A Global Irradiance Program, H. S. Hudson, G. A. Chapman, B. J. LaBonte	313
List of Participants	317

SOLAR TOTAL IRRADIANCE VARIABILITY MEASUREMENTS

BY THE SMM/ACRIM I EXPERIMENT

Richard C. Willson

Jet Propulsion Laboratory
Calif. Inst. of Technology
Pasadena, CA 91109

8/22/83

ABSTRACT

Convincing evidence of solar total irradiance variability and its relationships with solar activity has been provided by the Active Cavity Radiometer Irradiance Monitor I (ACRIM I) experiment on the NASA Solar Maximum Mission (SMM). SMM/ACRIM I, the first flight experiment dedicated to the task of solar irradiance monitoring, has produced a multi-year solar total irradiance data base with $\pm 0.02\%$ or better long term precision since its launch in February, 1980. While the climatological significance of the results will not be apparent until many more years of continuous data are acquired, the discovery of variability on solar active region time scales has provided new insight into the physics of solar activity in the early years of the mission.

INTRODUCTION

The first Active Cavity Radiometer Irradiance Monitor (ACRIM I) experiment was launched in Feb., 1980 on NASA's Solar Maximum Mission and has monitored solar total irradiance on a nearly continuous basis since. Its objectives were to begin a program of long term solar monitoring with the maximum precision and accuracy presently achievable to detect both long and short term solar variations of significance to climate and solar physics.

The ACRIM experiment operates in the electrically self calibrated mode at all times to realize maximum accuracy and precision. During normal SMM operations its shutters on active sensors open or close every 64 seconds, providing solar and internal reference data (respectively) 50 % of the time. In this mode more than 800 independent samples of total solar irradiance are acquired during the 55 sunlit minutes of each 96 minute SMM orbit.

The ACRIM I experiment and its early results have been described elsewhere (refs. 1-10). The uncertainty of the observations relative to the International System of units (SI) is less than $\pm 0.2\%$. In flight the three ACRIM I sensors agree within $\pm 0.04\%$ of their average result. A sounding rocket solar

irradiance experiment in May, 1980 compared two ACRIM's on the rocket with ACRIM I, finding agreement between all five ACR type IV sensors to within $\pm 0.05\%$ of their combined average result.

Two of ACRIM I's three active cavity radiometer type IV sensors, kept shuttered most of the time, are used sparingly to calibrate degradation of the continuously monitoring sensor. A measurement precision smaller than $\pm 0.002\%$ was sustained using this technique during the first 300 days of (normal) SMM operation. The standard error of single orbit averages of solar flux during this period were frequently as small as $\pm 0.001\%$ (ref. 10).

The solar pointing system of the SMM failed in Dec., 1980 and the satellite was placed into a spin stabilized mode with its spin axis nominally directed at the sun. Since SMM was not designed for spin stabilization this axis wobbles slowly about the solar direction with a maximum pointing error of about 10 degrees.

The ACRIM I experiment was placed into a new operating mode to take maximum advantage of the limited solar pointing provided by the spin stabilized spacecraft. In place of the normal procedure of opening or closing ACRIM I's shutters every 64 seconds, they are opened at orbit sunrise and closed at sunset. This procedure, with ACRIM I's tolerance for off-sun pointing of ± 0.75 degrees, has produced an average of 100 solar observations per day during the spin stabilized operation of the SMM. After correcting for small systematic differences between ACRIM I's response to solar irradiance in the normal and spin modes of solar pointing, (the largest of which was -0.12%) the relativity of the observations in the two phases of SMM operation are known with no more than $\pm 0.02\%$ uncertainty (ref. 11).

ACRIM I observations from launch through the middle of 1982 are shown in figure 1 as the percentage variation about the mean 1 A.U. solar total irradiance. The general character of the record is that of continuous variability whose major features are irradiance decreases lasting from a few days to a few weeks with a maximum amplitude of about -0.25% . The timescale of variability ranges from seconds to the duration of the record (refs. 3-8,10).

The effects of the decreased quantity and quality of ACRIM I data in the spin mode can be seen in fig. 1 as visible measurement noise in the results following 1980 day 350. The average standard error of daily mean results increased by a factor of about 5, from 0.002% during the normal operation of SMM to 0.01% in the spin mode. Some of the information available from the normal 300 mission days in 1980, particularly that used to detect the signature of the 5 minute solar global oscillation in the total irradiance, appears to be unavailable in data of the spin mode. All the major irradiance events on timescales of days and longer, particularly those related with solar activity, continue to be clearly resolved. A tabulation of the

daily mean 1 A.U. solar total irradiance results from ACRIM I is included as Appendix C.

SOLAR VARIABILITY ON TIMESCALES OF ACTIVE REGION LIFETIMES

The most significant result of the ACRIM I experiment thus far has been the first clear detection of solar total irradiance variability. The variations on time scales of days to weeks have been found to result from the modulation of the average solar irradiance by sunspots and faculae in active regions (see Fig. 2) (refs. 2-4,6-10,12-14).

Temporary decreases in solar total irradiance caused by the transit of magnetically active regions containing sunspot area across the earth's side of the sun are the dominant variation. These radiative deficits, lasting from days to weeks, have amplitudes as large as -0.25% of the average total irradiance. The detailed correspondence of the sunspot area projected in the earth's direction with most of the irradiance decreases can be seen in Fig. 2 (bottom panel).

Sunspots have long been assumed to be a potential cause of variations in the solar radiative output. Measurement of their effects on total irradiance by ACRIM I has verified this assumption and provided quantitative evidence that can lead to an improved understanding of the energetics of active region evolution (refs. 10,13,15).

The large faculae frequently present in the same active regions as sunspots appear to be responsible for solar radiative excesses, smaller in magnitude than sunspot deficits, but detectable in the ACRIM I results. Faculae in active regions usually develop to their maximum size after the associated sunspots, average five times the spot area, persist about twice as long and radiate about 3% more flux than the undisturbed photosphere. Preliminary analyses, based on their temporal and areal distribution during the period of ACRIM I observations, indicates that they are responsible for irradiance peaks before and after many deficits, and can at least partially offset sunspot radiative deficit (ref. 10).

Examples of irradiance peaking due to large faculae (whose presence and areas are inferred from NOAA Geophysical Quantities Ca plage data) can be seen in Fig. 2 as the maxima just following the first major decrease near 1980 day 100 and that following a decrease near day 200. Examples of facular excess flux offsetting the deficit of sunspots are found near 1980 day 210 and 1981 day 315. The amplitudes of the irradiance decreases in these cases were smaller in proportion to the projected sunspot areas than in cases when little facular area was present (eg. 1980 day 250, 1981 day 210.)

The most obvious effects on irradiance of sunspot and facular area occur at different times during the rotation of the active regions containing them across the solar disk. This is

caused by the different distribution of the radiative phenomena associated with sunspots and faculae in the horizontal and vertical extent of the photosphere and chromosphere.

Sunspots, located in the photosphere, appear to obey a limb darkening law that is little different from that of the undisturbed photosphere. Their maximum radiative effect occurs when they are on the longitude of the center of the solar disk (as seen from the earth.)

Faculae are more apparent near the solar limb than sunspots at the same solar longitude because of their flatter limb-darkening function. Additionally, they usually have a larger total area and horizontal extent than the sunspots in an active region, making them the first and last component of a radiatively active region to be seen from the earth during its transit across our field of view.

The enhanced visibility of facular radiative effects near the solar limb and their poor contrast near disk center have led some researchers to ascribe a highly non-isotropic character to their emittance, concluding that their affects on the total irradiance are inconsequential except at the limb (ref. 13). This is not supported by the ACRIM I observations in which the radiative excess of large facular area have been observed to offset sunspot deficit throughout the transit of radiatively active regions across the visible solar disk (ref. 10).

Investigation of a fairly regular recurrence of sunspot induced irradiance dips in the ACRIM I results led to the discovery of a related and even more regular recurrence of solar active regions over a six month period early in the SMM. The irradiance decreases demonstrated an average period of 24 days from April to October, 1980, with a maximum deviation of 5 days. The principal solar active regions containing the sunspots responsible for the irradiance dips were also found to recur with an average period of 24 days but with a deviation of less than three days when the combined spot and plage areas were used to define the extent of the active regions. During this six month interval the majority of the active regions were confined to one solar hemisphere. Time series analyses revealed prominent periods for both the ACRIM I irradiance and the total sunspot area near the 1st, 2nd and 3rd harmonics of the 24 day periodicity, providing an analytical link between the two (ref. 10).

DETECTION OF "5 MINUTE" SOLAR GLOBAL OSCILLATION

The precision of the ACRIM I results led Hudson (ref. 16) and Frohlich (ref. 17) to search for the effects of solar global oscillation phenomena in the total irradiance. They separately detected the low degree p-modes ($l = 0, 1, 2$) of a 5 minute oscillation in the ACRIM I results with amplitudes of a few parts per million (ppm) and coherence lifetimes of at least one week, in agreement with the predictions of Gough (ref. 18). The analysis of Woodard and Hudson confirmed the frequencies derived

from ground based data. Evidence of the 160 minute oscillation reported by Severny (ref. 19) was not found in the ACRIM I results. A detection limit of 5 ppm of the total irradiance signal was derived by Woodard and Hudson (ref. 16) as the sensitivity threshold of the ACRIM I data for detection of this oscillatory phenomenon.

REFERENCES

1. Willson, R. C.: Active cavity radiometer type IV. J. Applied Optics, 1979, vol. 18, p. 179.
2. Willson, R. C.: Solar irradiance observations from the SMM/ACRIM experiment. American Geophysical Union, Toronto, Canada, May, 1980.
3. Willson, R. C.: Solar Irradiance Variations, XIV ESLAB Symposium on physics of solar variations, Scheveningen, The Netherlands, Sept., 1980.
4. Willson, R. C.: Solar total irradiance observations by active cavity radiometers. Solar Physics, 1981, vol. 74, p. 218.
5. Willson, R. C., Hudson, H. S.: Astroph. J. Lett., 1981, vol. 24, p. 185.
6. Willson, R. C., Gulkis, S., Janssen, M., Hudson, H. S., Chapman, G. A.: Observations of solar irradiance variability. Science, 1981, vol. 211, p. 700.
7. Willson, R. C.: Observation of solar irradiance variations in balloon, rocket and satellite experiments. Proc. of IAMAP 3rd Scientific Assembly, Hamburg, FRG, August, 1981.
8. Hudson, H. S., Willson, R. C.: Sunspots and solar variability. Proc. Conference on Sunspots, 1981, Sunspot, AZ.
9. Hudson, H. S., Silva, S., Woodard, M., Willson, R. C.: Effects of Sunspots on Solar Irradiance. Solar Physics, 1981, in press.
10. Willson, R. C.: Solar irradiance variations and solar activity, J. Geoph. Res., 1982, vol. 86, p. 4319.
11. Willson, R. C.: Solar irradiance variability from 1980-83. In press, 1983.
12. Eddy, J. A., Hoyt, D.V., White, O. R.: Reconstructed values of the solar constant from 1874 to the present. Collection of extended abstracts presented at The Symposium on the Solar Constant and the Spectral Distribution of Solar Irradiance, IAMAP 3rd Scientific Assembly, 17-28 Aug., 1981, Hamburg, FRG, 1982.
13. Oster, L. F., Schatten, K. H., Sofia, S.: Solar irradiance variations due to active regions. Astrophys. J., 1982, vol. 256, p. 768.

14. Newkirk, G. N. Jr.: Variations in solar luminosity. Annual Reviews of Astronomy and Astrophysics, 1983, vol. 21, p. 382.
15. Eddy, J. A., Gilliland, R. L., Hoyt, D. V.: Changes in the solar constant and climatic effects. Nature, Dec. 1982, vol. 300, p. 689.
16. Woodard, M., Hudson, H.: Solar oscillations observed in the total irradiance. Solar Physics, 1983, in press.
17. Frohlich, C.: Radiometry of solar irradiance variations over long time scales. 18th General Assembly of the International Astronomical Union, Patras, Greece, August, 1982.
18. Gough, D. O.: Internal rotation and gravitational quadrupole moment of the sun. Nature, 1982, vol. 298, p. 334.
19. Severny, A. B., Kotov, V. A., Tsap, T. T.: Nature, 1976, v. 259, p. 87.
20. Hickey, J.R., Griffin, F.J., Solar Radiation Measurements from NIMBUS 6, Third AMS Conference on Radiation, Fort Collins, CO, 1979
21. Hickey, J.R., Stowe, L.L., Jacobowitz, H., Pellegrino, P., Maschoff, R.H., House, F., Vonder Haar, T.H., Initial Solar Irradiance Determinations from Nimbus 7 Cavity Radiometer Measurements, Science, v. 208, p. 281, 1980
22. Vonder Haar, T.H., Campbell, G.G., Smith, E.A., Arking, A., Coulson, K., Hickey, J., House, F., Ingersoll, A., Jacobowitz, H., Smith, L., Stowe, L., Measurements of the earth radiation budget during the first GARP experiment, Adv. Space Res. (COSPAR), v. 1, p. 285, 1981
23. Hickey, J. R., Alton, B. M., Griffin, F. J., Jacobowitz, H., Pellegrino, P., Smith, E. A., Vonder Haar, T. H., Maschoff, R. H.: Extraterrestrial solar irradiance variability: two and one-half years of measurements from Nimbus 7. J. Solar Energy, vol. 29, p. 125, 1982
24. Hickey, J. R.: Private communication, Sept., 8, 1981.
25. Hickey, J. R.: Results from Nimbus 7 ERB solar observations, Workshop on Solar Variability on Active Region Timescales. Calif. Inst. of Technology, June 20-21, 1983.

APPENDIX A

SOLAR IRRADIANCE VARIABILITY ON TIMESCALES OF YEARS

The SMM/ACRIM I results have provided a record of solar variability over a multi-year period with adequate precision to unambiguously detect subtle long term trends in irradiance. Although increases and decreases lasting up to six months can be seen in the results shown in Fig. 1, a sustained downward trend has been resolved over the nearly three years data analyzed thus far, resulting in a net irradiance decrease of 0.08 %. (See Fig. 3) Intercomparisons of ACRIM I's three independent sensors over this time have demonstrated instrument degradation to be less than the ± 0.02 % uncertainty with which the ACRIM I results from the normal and spin mode of SMM can be related. Most or all of the decrease is therefore solar in origin, unless some unknown factor outside the ability of ACRIM I's self calibration is uniformly affecting the results from all three ACR sensors.

The sustained irradiance decline may be the beginning a solar irradiance variation related to the solar activity cycle. Observations equivalent to ACRIM I's must be sustained well into the late 1980's, approaching the solar maximum period of solar cycle #22, to unambiguously determine the nature and cause of this long term variation.

APPENDIX B

COMPARISON OF SMM/ACRIM I AND NIMBUS 7/ERB RESULTS

The Nimbus 7 Earth Radiation Budget (ERB) experiment includes an electrically self-calibrating cavity solar total irradiance sensor of the type referred to as the Hickey-Freidan (HF) by its developers (ref. 20). The HF has been acquiring data since the launch of Nimbus 7 in late 1978, a significant fraction of one solar cycle.

The complete set of HF results has been published by Hickey et.al. (ref.s 20-25). Here the results for a 1050 day period following the start of the SMM/ACRIM I experiment in early 1980 are shown for comparison purposes. (Fig. 3) A least mean squares linear fit to the Nimbus 7/ERB results has a small negative slope with -0.03 % net change over the period, much less than the -0.08 % net change of the ACRIM I results for the same period.

The net change in the linear fit to the ACRIM I results is believed to be uncertain by no more ± 0.02 % over the 1050 days shown in fig. 3. The significance of the trend is that it may be the subtle total irradiance signature of the solar activity cycle, a potentially important result. It is therefore worthwhile to attempt to identify the cause of disagreement between ERB and ACRIM I as a means of adding confidence to the ACRIM I result.

There are several possible reasons why the ERB results might not agree with the ACRIM I trend and they fall into two general categories: First, the ERB experiment may lack the long term precision to resolve the trend, in which case, no further analysis is required. The second category assumes the -0.03 % slope of the ERB results is significant relative to the long term precision and includes two possibilities: 1) the large number of missing days of ERB data in 1981-82 may have biased the slope of its linear fit to a smaller value, and/or 2) there may have been an intentional detrending of ERB data.

The issue of ERB long term precision is difficult to resolve since it has never been succinctly discussed in the literature by the experimenters. The picture of long term precision must be pieced together from various published descriptions of ERB data processing and analysis. The data has been re-evaluated at least twice during the six years of the Nimbus 7 Mission and the value of the average 1 A.U. irradiance has been successively revised downward by nearly 0.04 %. The initially reported value of 1376 W/m² (ref.s 20-22) was decreased by 0.2 % in 1982 to 1373 W/m² (ref. 23) and further decreased to 1371 W/m² in 1983 [Hickey (1983)]. Downward re-evaluations of the SI value of the results would not necessarily change their slope, but such successive manipulations would have the potential of decreasing the experiment's long term precision.

The stability of ERB's sensitivity during the first two years of operation was quoted as $\pm 0.16\%$ by Hickey in 1980 (ref. 21). If this accurately represents the experiment's ability to relate measurements over the 1050 days of data analyzed here, it may represent the lower limit for detection of trends in the ERB results. This would obviate further searching for the reason for ERB/ACRIM I disagreement since the ACRIM I trend would be undetectable by ERB.

The basic assumption of the second category of reasons for disagreement is that the -0.03% ERB trend is significant relative to ERB's long term precision. The first candidate cause in this category is that during 1981-82 ERB did not acquire solar data much of the time when large irradiance decreases were observed by ACRIM I (see Fig. 3). The absence of these data from ERB's database may have biased the slope of a linear fit to a smaller negative value. To test for this possibility, gaps in the ERB record were filled using daily mean values proportional to the percentage variability detected by the ACRIM I experiment (wherever it had data and ERB did not.) Care was taken to scale the added data to the average value of the ERB irradiance as published by Hickey, et.al. in 1982 (ref. 23).

The results of this test are plotted in Fig. 3, panel C. The period of time shown covers the 1050 days for which ERB results are presently available following the SMM/ACRIM I launch. The least mean square linear fits made to each of the ACRIM I, ERB and augmented ERB (ERBMOD) results are shown superimposed on the data sets. The restoration of missing data to the ERB record produces a net irradiance change of -0.06% over the 1050 day period, which agrees with the ACRIM I slope to just within the uncertainty of the long term precision of both experiments.

The second possible cause of disagreement in this category is that the 1982 re-evaluation of NIMBUS 7/ERB data appears to have not only decreased the average value of the results, but also decreased the slope of their trend over at least part of the 1050 days. Early in 1981 the data from the ACRIM I experiment during the 300 days of "normal" SMM spacecraft operation (1980 days 47-347) were compared with the corresponding 300 days results from the Nimbus 7/ERB. At that time Hickey's analysis showed a -0.049% net change for the linear fit to the ERB results over this period (ref. 24) and Willson found a -0.04% slope for the ACRIM I results (ref. 10).

The comparative 1980 results for ACRIM I, ERB (the 1982 re-evaluation) and ERBMOD are plotted for 1980 days 50 to 347 in Fig. 4. During this period the long term precision of the ACRIM I results was smaller than $\pm 0.002\%$, making its -0.04% net change significant with less than $\pm 5\%$ uncertainty (ref. 10). The -0.02% net change of the linear fit to the revised ERB results is less than half that found by Hickey using their original version values.

It is clear that slope was removed as part of the re-evaluation of the Nimbus 7/ERB data and there has been no published statement to that effect or a rationale for it. Hickey regularly removed long term slope from the results of the NIMBUS 6/ERB on the assumption that the systematic decreases in its results were due to sensor degradation (ref. 20). There was justification for doing so, since the instrument had a flat plate detector that could not attenuate degradation of its solar absorbing surface. Since there was no capability within the experiment to separate solar trends from degradation, the detrending removed all long term slope from the data, producing constant results to within the precision limit of the approach.

The same detrending is probably not justified for the Nimbus 7/ERB. Its cavity detector has similar properties to the ACR detectors in the ACRIM I experiment and might reasonably be expected to have a similarly small sensitivity to degradation of its surface coating. Internal self calibration by the three ACRIM I ACR's placed an upper limit of 0.02 percent on their degradation during the 1050 days shown in Fig. 3. The upper limits on ERB degradation should not be very different.

In summary, the ERB data lack the long term precision to confirm or contradict the solar trend in the ACRIM I results. The published ERB stability limit of $\pm 0.16\%$ is consistent with apparent noise in the database (see panels b in Fig.'s 3 and 4) and probably represents an upper limit to the experiment's precision. Trends in the ERB database much smaller than 0.16% lack significance and are artifacts of specific re-scaling and detrending algorithms used in the various re-evaluations. The agreement between the ERBMOD and ACRIM I trends within 0.02% is therefore fortuitous and only serves to indicate that the missing ERB data does bias the slope of their results to smaller negative values.

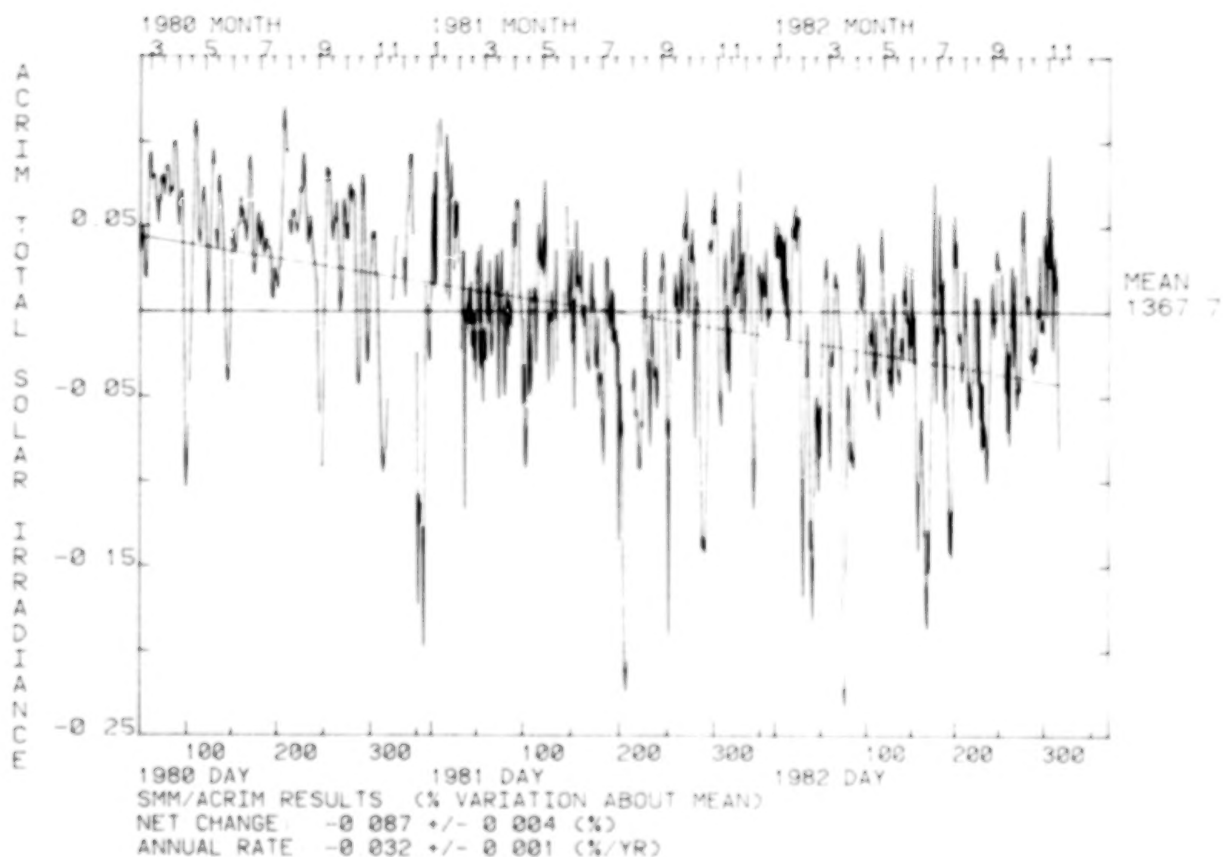


Figure 1 - Percentage variation of the 1 A.U. daily mean solar total irradiances derived from observations by the SMM/ACRIM I experiment. Results for adjacent days have been connected by lines to more clearly delineate major variabilities. The decreased quality of the results from the experiment beginning on 1980 day 350 marks the loss of precision solar pointing capability by the SMM spacecraft and the start of spin stabilized operation. The mean value of the total irradiance at 1 A.U. over the period is 1367.7 W/m². During the 300 days of normal SMM operation in 1980 all variations visible on this scale are believed to be solar in origin. In the SMM spin mode variability exceeding $\pm 0.01\%$ is solar in origin. The linear least mean square fit to the results exhibited a net decrease of about 0.09% over the 1010 days of the mission shown here. Repair of the SMM solar pointing capability by the shuttle in 1984 should restore the high quality results available during normal operation in 1980.

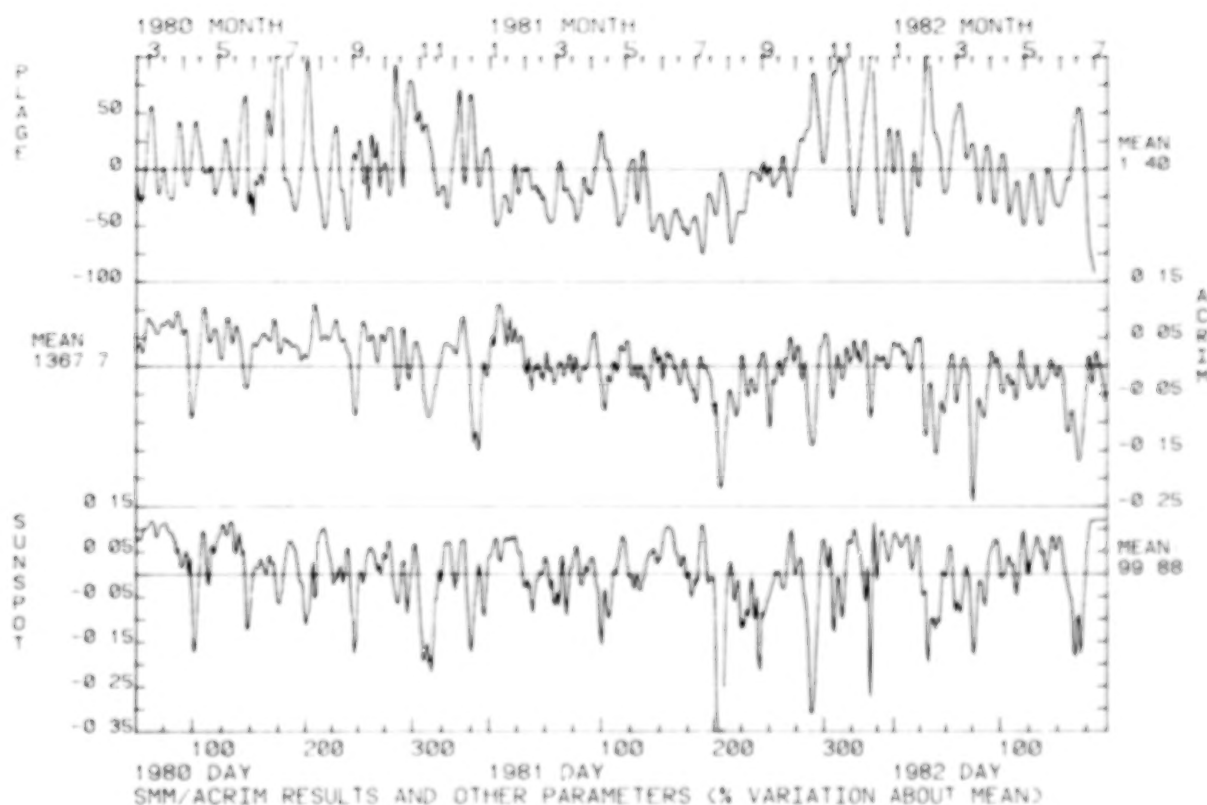


Figure 2 - Percentage variation of the total solar irradiance derived from the SMM/ACRIM 1 experiment (middle panel) plotted with the total plage (top panel) and sunspot areas (bottom panel) projected in the earth's line of sight. Gaps in the data sets have been filled by linear interpolation and three day running means of the three solar parameters shown have been used as a low pass filters to emphasize their variability on longer timescales. The fraction of the visible solar disk not covered by sunspots is plotted to produce variation in the same direction as the irradiance deficits. Means for plage and sunspot are in percentage units, that for ACRIM 1 is total irradiance at 1 A.U. in W/m². The close correlation between most irradiance dips and projected sunspot area, the so-called sunspot deficit effect, is readily apparent. The plage radiative excess effect is more subtle, causing some irradiance peaks and offsetting the sunspot deficit in some cases, decreasing the amplitude of some sunspot induced dips. Sunspot and plage areas were derived from NOAA Geophysical Parameters.

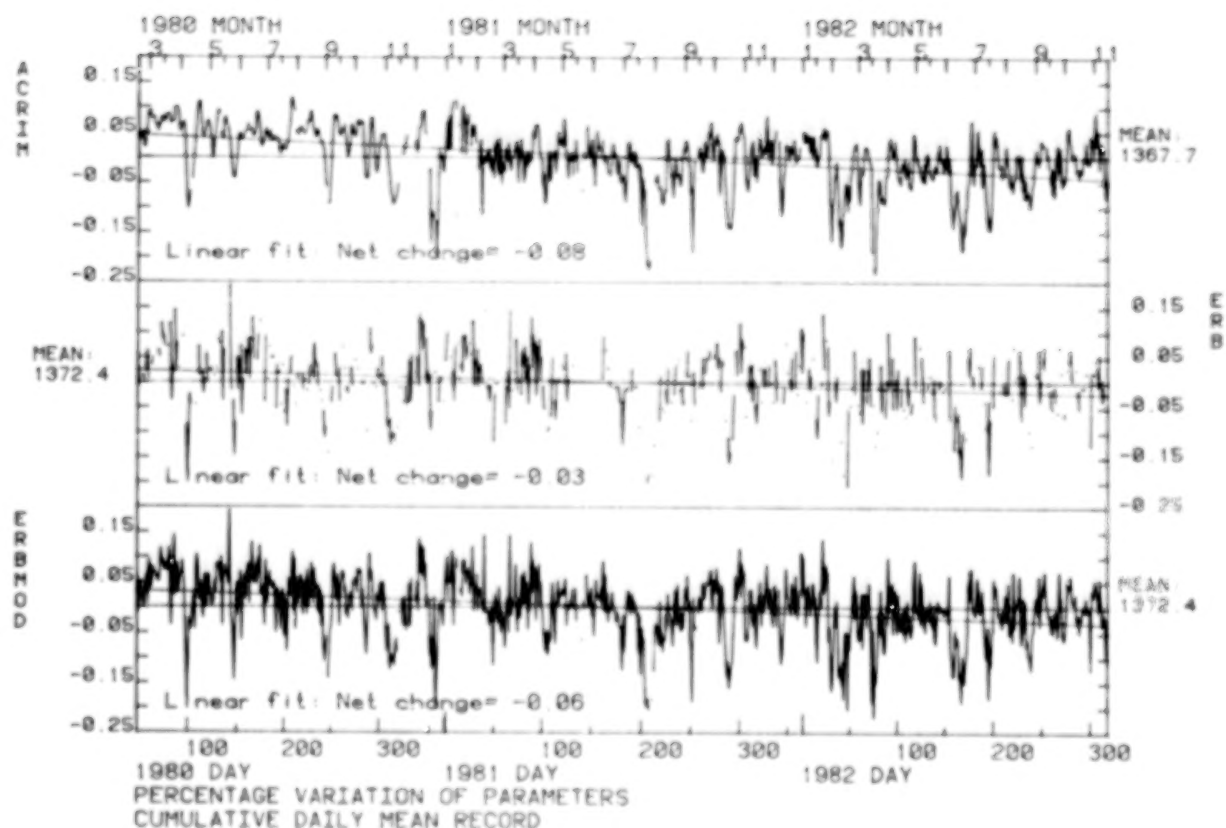


Figure 3 - Comparison plots of the percentage variation of the daily mean solar total irradiance observations made by the SMM/ACRIM I (top panel) and NIMBUS 7/ERB (middle panel) experiments from the start of the SMM through the end of 1982. The results from both are plotted with lines connecting observations made on adjoining days to emphasize the features of solar variability and the amount of missing data in both records. The bottom panel (ERBMOD) was compiled by adding data to the ERB record from the SMM/ACRIM I results for days when ACRIM I had results and ERB did not. The average results (in W/m^2 at 1 A.U.) and the net change in irradiance (in percentage units) resulting from the linear least mean square fits to the three records are shown. The remaining difference between ACRIM I and ERBMOD slopes is not significant with respect to the uncertainties in the long term precision of the irradiance records.

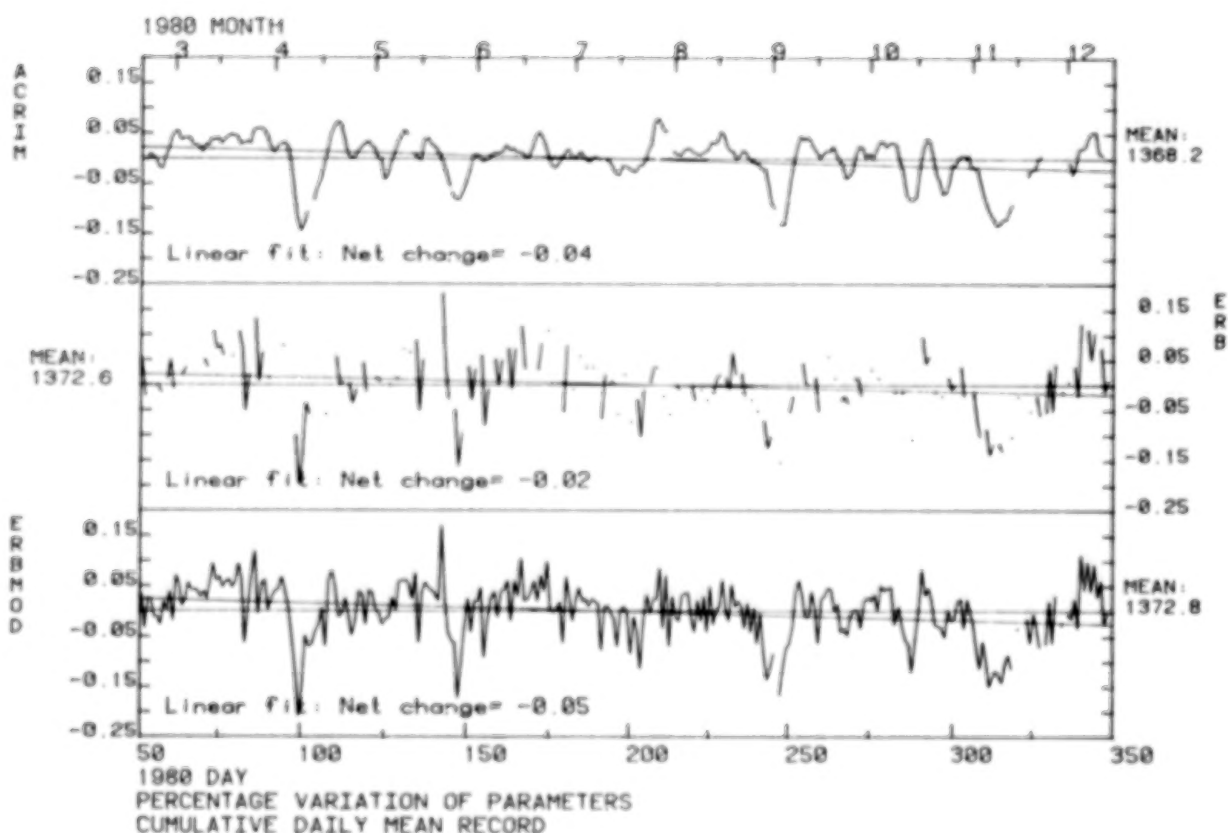


Figure 4 - Comparison plots of the percentage variation of the daily mean solar total irradiance observations made by the SMM/ACRIM I (top panel) and NIMBUS 7/ERB (middle panel) experiments during the 300 days of normal operation of the SMM in 1980. The results from both are plotted with lines connecting observations made on adjoining days to emphasize the features of solar variability and amount of missing data in both records. The bottom panel (ERBMOD) was compiled by adding data to the ERB record from the SMM/ACRIM I results for days when ACRIM I had results and ERB did not. The mean results (in W/m^2 at 1 A.U.) and the net change in irradiance over the 300 days (in percentage units) resulting from the linear least mean square fits to the three records are shown. ACRIM I precision over this period was better than $\pm 0.002\%$. Agreement between the ACRIM I and ERBMOD slopes to within 0.01% is within the uncertainty of constructing ERBMOD.

APPENDIX - C

TABULATION OF RESULTS

ACTIVE CAVITY RADIOMETER IRRADIANCE MONITOR EXPERIMENT

THE SOLAR MAXIMUM MISSION

Table 1. Daily mean results for the 1 A.U. solar total irradiance and their standard errors. The individual solar irradiance observations made by ACRIM I (410000 daily on average) are corrected for the satellite - sun distance and for the relativistic effect of the satellite - sun relative velocity. Irradiance units are W/m². Statistical uncertainty is the standard error of the daily mean in percentage units based on all the individual samples taken each day.

TABLE 1

SMM ACRIM SUMMARY FOR CHANNEL A SENSOR *** MEAN VALUES FOR DAYS

1980 DAY	1AU SOLAR IRRADIANCE (W/M2)	STATISTICAL UNCERTAINTY (PERCENT)	1980 DAY	1AU SOLAR IRRADIANCE (W/M2)	STATISTICAL UNCERTAINTY (PERCENT)
1	NO DATA	*****	26	NO DATA	*****
2	NO DATA	*****	27	NO DATA	*****
3	NO DATA	*****	28	NO DATA	*****
4	NO DATA	*****	29	NO DATA	*****
5	NO DATA	*****	30	NO DATA	*****
6	NO DATA	*****	31	NO DATA	*****
7	NO DATA	*****	32	NO DATA	*****
8	NO DATA	*****	33	NO DATA	*****
9	NO DATA	*****	34	NO DATA	*****
10	NO DATA	*****	35	NO DATA	*****
11	NO DATA	*****	36	NO DATA	*****
12	NO DATA	*****	37	NO DATA	*****
13	NO DATA	*****	38	NO DATA	*****
14	NO DATA	*****	39	NO DATA	*****
15	NO DATA	*****	40	NO DATA	*****
16	NO DATA	*****	41	NO DATA	*****
17	NO DATA	*****	42	NO DATA	*****
18	NO DATA	*****	43	NO DATA	*****
19	NO DATA	*****	44	NO DATA	*****
20	NO DATA	*****	45	NO DATA	*****
21	NO DATA	*****	46	NO DATA	*****
22	NO DATA	*****	47	1367.78	0.007139
23	NO DATA	*****	48	1367.90	0.003984
24	NO DATA	*****	49	1368.06	0.001865
25	NO DATA	*****	50	NO DATA	*****

SMN ACRIM SUMMARY FOR CHANNEL A SENSOR *** MEAN VALUES FOR DAYS

1980 DAY	1AU SOLAR IRRADIANCE (W/M2)	STATISTICAL UNCERTAINTY (PERCENT)	1980 DAY	1AU SOLAR IRRADIANCE (W/M2)	STATISTICAL UNCERTAINTY (PERCENT)
51	1368.20	0.001007	76	1368.76	0.001815
52	1368.38	0.002038	77	1368.82	0.001654
53	1368.30	0.001757	78	1368.88	0.001204
54	1368.22	0.002154	79	1368.87	0.001235
55	1367.99	0.002253	80	1368.82	0.001032
56	1367.96	0.002126	81	1368.61	0.001857
57	1368.28	0.001761	82	1368.68	0.001581
58	1368.49	0.002058	83	1368.70	0.000955
59	1368.79	0.001271	84	1368.66	0.001312
60	1368.97	0.006580	85	1369.01	0.000857
61	1368.98	0.008617	86	1369.06	0.001425
62	1368.75	0.001517	87	1369.08	0.000951
63	1368.79	0.002222	88	1369.01	0.001413
64	1368.80	0.001665	89	1368.87	0.001218
65	1368.79	0.001410	90	1368.56	0.001672
66	1368.60	0.001079	91	1368.39	0.000999
67	1368.60	0.002027	92	1368.57	0.001524
68	1368.58	0.001045	93	1368.63	0.001425
69	1368.41	0.000961	94	1368.68	0.001782
70	1368.63	0.001476	95	1368.57	0.001690
71	1368.59	0.001670	96	1368.13	0.001416
72	1368.79	0.001778	97	1367.35	0.001211
73	1368.73	0.001078	98	1366.62	0.001857
74	1368.81	0.001143	99	1366.28	0.001258
75	1368.64	0.001050	100	1366.48	0.001517

SNM ACRIM SUMMARY FOR CHANNEL A SENSOR *** MEAN VALUES FOR DAYS

1980 DAY	1AU SOLAR IRRADIANCE (W/M2)	STATISTICAL UNCERTAINTY (PERCENT)	1980 DAY	1AU SOLAR IRRADIANCE (W/M2)	STATISTICAL UNCERTAINTY (PERCENT)
101	1366.79	0.001780	126	1368.16	0.001742
102	NO DATA	*****	127	1368.40	0.002327
103	1367.13	0.001387	128	1368.66	0.003113
104	1367.47	0.001463	129	1368.85	0.003111
105	1367.68	0.001735	130	1369.01	0.002538
106	1368.10	0.002106	131	1368.88	0.001895
107	1368.47	0.002770	132	NO DATA	*****
108	1368.91	0.001985	133	1368.35	0.002099
109	1369.11	0.001732	134	1368.28	0.002775
110	1369.24	0.002187	135	1368.19	0.001802
111	1369.16	0.002376	136	1368.72	0.001575
112	1368.77	0.001839	137	1368.81	0.002262
113	1368.37	0.002414	138	1368.64	0.001920
114	1368.27	0.002296	139	1368.59	0.001935
115	1368.25	0.002988	140	1368.48	0.002209
116	1368.43	0.001595	141	1368.30	0.002777
117	1368.57	0.002524	142	1368.11	0.001521
118	1368.64	0.001085	143	1367.82	0.003121
119	1368.71	0.002531	144	1367.50	0.001965
120	1368.59	0.001874	145	1367.23	0.003036
121	1368.51	0.004391	146	1367.13	0.002010
122	1368.24	0.001590	147	1367.15	0.002100
123	1368.23	0.037975	148	1367.36	0.002097
124	1367.67	0.001409	149	1367.58	0.001239
125	1367.82	0.002267	150	1367.88	0.002285

SMM ACRIM SUMMARY FOR CHANNEL A SENSOR *** MEAN VALUES FOR DAYS

1980 DAY	1AU SOLAR IRRADIANCE (W/M2)	STATISTICAL UNCERTAINTY (PERCENT)	1980 DAY	1AU SOLAR IRRADIANCE (W/M2)	STATISTICAL UNCERTAINTY (PERCENT)
151	1368.25	0.002372	176	1367.99	0.001474
152	1368.37	0.002631	177	1368.11	0.002583
153	1368.29	0.001435	178	1368.26	0.004340
154	1368.17	0.002545	179	1368.40	0.001244
155	1368.20	0.001721	180	1368.50	0.001362
156	1368.26	0.002520	181	1368.36	0.001863
157	1368.37	0.001537	182	1368.23	0.001515
158	1368.40	0.003600	183	1368.34	0.002016
159	1368.40	0.002204	184	1368.43	0.001666
160	1368.45	0.001956	185	1368.29	0.001483
161	1368.62	0.011571	186	1368.18	0.001848
162	1368.47	0.001419	187	1368.16	0.001607
163	1368.53	0.001536	188	1368.28	0.001731
164	1368.41	0.003145	189	1368.28	0.001300
165	1368.43	0.001253	190	1368.21	0.002903
166	1368.38	0.001790	191	NO DATA	*****
167	1368.26	0.001535	192	1368.21	0.001947
168	1368.36	0.001799	193	1368.17	0.001447
169	1368.56	0.001924	194	1368.02	0.002004
170	1368.85	0.001355	195	1367.82	0.001265
171	1368.96	0.001619	196	1367.80	0.001615
172	1368.81	0.001185	197	1368.05	0.001524
173	1368.57	0.001171	198	1368.03	0.001399
174	1368.27	0.001214	199	1367.99	0.002271
175	1368.03	0.001338	200	1367.91	0.003316

SMM ACRIM SUMMARY FOR CHANNEL A SENSOR *** MEAN VALUES FOR DAYS

1980 DAY	1AU SOLAR IRRADIANCE (W/M2)	STATISTICAL UNCERTAINTY (PERCENT)	1980 DAY	1AU SOLAR IRRADIANCE (W/M2)	STATISTICAL UNCERTAINTY (PERCENT)
201	1367.88	0.001224	226	1368.66	0.001144
202	1368.06	0.001006	227	1368.71	0.007314
203	1368.06	0.001059	228	1368.98	0.001077
204	1368.19	0.001374	229	1368.89	0.001349
205	1368.48	0.001895	230	1368.60	0.001395
206	1368.64	0.001117	231	1368.46	0.001151
207	1369.23	0.019230	232	1368.43	0.000981
208	1369.34	0.009914	233	1368.24	0.000484
209	1369.18	0.001348	234	1368.31	0.001308
210	1368.97	0.001403	235	1368.48	0.001156
211	1369.00	0.004701	236	1368.41	0.000963
212	NO DATA	*****	237	1368.25	0.000951
213	1368.43	0.000111	238	1368.19	0.001590
214	1368.35	0.001252	239	1368.11	0.001505
215	1368.31	0.001267	240	1368.10	0.000879
216	1368.46	0.000941	241	1367.97	0.001738
217	1368.52	0.001321	242	1367.95	0.001060
218	1368.51	0.004832	243	1367.54	0.001187
219	1368.43	0.001290	244	1367.03	0.000885
220	1368.39	0.001174	245	1366.88	0.001118
221	1368.33	0.000748	246	NO DATA	*****
222	1368.39	0.001652	247	1366.45	0.002350
223	1368.45	0.000846	248	1366.46	0.001227
224	1368.50	0.001159	249	1367.01	0.001198
225	1368.70	0.001594	250	1367.64	0.001124

SNM ACRIM SUMMARY FOR CHANNEL A SENSOR *** MEAN VALUES FOR DAYS

1980 DAY	1AU SOLAR IRRADIANCE (W/M2)	STATISTICAL UNCERTAINTY (PERCENT)	1980 DAY	1AU SOLAR IRRADIANCE (W/M2)	STATISTICAL UNCERTAINTY (PERCENT)
251	1368.15	0.001520	276	1368.48	0.001360
252	1368.56	0.002624	277	1368.70	0.001319
253	1368.87	0.001675	278	1368.73	0.001054
254	1368.75	0.001070	279	1368.57	0.020195
255	1368.84	0.000984	280	1368.68	0.002218
256	1368.73	0.000958	281	1368.67	0.001088
257	1368.56	0.001247	282	1368.62	0.000954
258	1368.43	0.001114	283	1368.16	0.001471
259	1368.27	0.001336	284	1367.86	0.001842
260	1368.36	0.001250	285	1367.27	0.000917
261	1368.45	0.003267	286	1367.12	0.001785
262	1368.43	0.005205	287	1367.11	0.001555
263	1368.59	0.000986	288	1367.22	0.001712
264	1368.38	0.001468	289	1367.99	0.001643
265	1368.22	0.001856	290	1368.51	0.000972
266	1368.08	0.000972	291	1368.81	0.001097
267	1367.70	0.001038	292	1368.71	0.001065
268	1367.79	0.001212	293	1368.29	0.002058
269	1367.92	0.001085	294	1367.84	0.001594
270	1368.36	0.001379	295	1367.62	0.001330
271	1368.61	0.001307	296	1367.28	0.001005
272	1368.53	0.001381	297	1367.32	0.001130
273	1368.29	0.004288	298	1367.59	0.000663
274	1368.40	0.001274	299	1368.08	0.000969
275	1368.27	0.005130	300	1368.09	0.001370

SNM ACRIM SUMMARY FOR CHANNEL A SENSOR *** MEAN VALUES FOR DAYS

1980 DAY	1AU SOLAR IRRADIANCE (W/M2)	STATISTICAL UNCERTAINTY (PERCENT)	1980 DAY	1AU SOLAR IRRADIANCE (W/M2)	STATISTICAL UNCERTAINTY (PERCENT)
301	1368.29	0.001063	326	1368.19	0.000880
302	1368.34	0.001336	327	1368.32	0.000743
303	1368.28	0.001104	328	NO DATA	*****
304	1368.34	0.000940	329	NO DATA	*****
305	1367.99	0.000761	330	NO DATA	*****
306	1368.01	0.001460	331	NO DATA	*****
307	1367.90	0.001415	332	NO DATA	*****
308	1367.55	0.001984	333	NO DATA	*****
309	1367.21	0.000838	334	NO DATA	*****
310	1366.95	0.000849	335	NO DATA	*****
311	1366.72	0.001484	336	1368.13	0.013940
312	1366.60	0.001281	337	1367.82	0.001676
313	1366.40	0.001098	338	1368.09	0.003181
314	1366.48	0.001013	339	1368.51	0.008483
315	1366.59	0.001360	340	1368.53	0.006979
316	1366.61	0.001208	341	1368.60	0.010853
317	1366.83	0.001156	342	1368.87	0.004912
318	1367.00	0.001072	343	1368.96	0.005004
319	NO DATA	*****	344	1368.97	0.006984
320	NO DATA	*****	345	1368.40	0.018978
321	NO DATA	*****	346	1368.33	0.002297
322	NO DATA	*****	347	NO DATA	*****
323	1367.80	0.001432	348	NO DATA	*****
324	1367.95	0.001439	349	NO DATA	*****
325	1367.96	0.002551	350	1367.37	0.011848

SMM ACRIM SUMMARY FOR CHANNEL A SENSOR *** MEAN VALUES FOR DAYS

1980 DAY	1AU SOLAR IRRADIANCE (W/M2)	STATISTICAL UNCERTAINTY (PERCENT)	1980 DAY	1AU SOLAR IRRADIANCE (W/M2)	STATISTICAL UNCERTAINTY (PERCENT)
351	1365.34	0.006215	***	* 1981	*****
352	1366.23	0.012360	***	* 1981	*****
353	1365.99	0.003989	***	* 1981	*****
354	1366.15	0.007300	***	* 1981	*****
355	NO DATA	*****	***	* 1981	*****
356	1365.95	0.024423	***	* 1981	*****
357	1365.00	0.006184	***	* 1981	*****
358	1366.30	0.009783	***	* 1981	*****
359	1367.29	0.011374	***	* 1981	*****
360	1367.92	0.013235	***	* 1981	*****
361	NO DATA	*****	***	* 1981	*****
362	1367.75	0.002648	***	* 1981	*****
363	1367.39	0.005982	***	* 1981	*****
364	1367.30	0.005442	***	* 1981	*****
365	1367.79	0.010836	***	* 1981	*****
366	1367.92	0.004773	***	* 1981	*****
***	* 1981	*****	***	* 1981	*****

SNM ACRIM SUMMARY FOR CHANNEL A SENSOR *** MEAN VALUES FOR DAYS

1981 DAY	1AU SOLAR IRRADIANCE (W/M2)	STATISTICAL UNCERTAINTY (PERCENT)	1981 DAY	1AU SOLAR IRRADIANCE (W/M2)	STATISTICAL UNCERTAINTY (PERCENT)
1	1368.22	0.007851	26	1368.60	0.005893
2	1368.65	0.005785	27	1368.29	0.007790
3	1367.89	0.022930	28	1368.54	0.003869
4	1368.83	0.004528	29	1368.59	0.006621
5	1367.93	0.026722	30	1368.09	0.002683
6	1368.91	0.004255	31	NO DATA	*****
7	1369.22	0.013995	32	NO DATA	*****
8	NO DATA	*****	33	1367.39	0.009976
9	NO DATA	*****	34	1367.55	0.005838
10	1369.25	0.005862	35	1368.19	0.006384
11	1369.03	0.004966	36	1368.17	0.014629
12	NO DATA	*****	37	1366.11	0.006761
13	NO DATA	*****	38	1367.71	0.004675
14	1368.59	0.010249	39	1367.56	0.007014
15	NO DATA	*****	40	1367.77	0.002824
16	1367.85	0.009420	41	1367.52	0.010064
17	1369.13	0.004477	42	1367.89	0.003111
18	1368.98	0.008732	43	1367.61	0.006453
19	1368.63	0.003346	44	1367.94	0.006228
20	1367.78	0.011320	45	1367.43	0.019985
21	1368.49	0.010653	46	1367.68	0.010689
22	1368.90	0.006576	47	1367.31	0.003813
23	1368.62	0.004334	48	1367.68	0.023876
24	NO DATA	*****	49	1367.13	0.009306
25	1368.04	0.006943	50	1368.06	0.006836

SMM ACRIM SUMMARY FOR CHANNEL A SENSOR *** MEAN VALUES FOR DAYS

1981 DAY	1AU SOLAR IRRADIANCE (W/M2)	STATISTICAL UNCERTAINTY (PERCENT)	1981 DAY	1AU SOLAR IRRADIANCE (W/M2)	STATISTICAL UNCERTAINTY (PERCENT)
51	1368.04	0.013677	76	1367.96	0.005875
52	1368.19	0.005227	77	1368.21	0.006685
53	1367.38	0.009319	78	1367.60	0.006829
54	1367.24	0.003362	79	1367.74	0.008108
55	1368.24	0.005189	80	1367.02	0.013502
56	1367.57	0.009681	81	1367.26	0.007907
57	1366.97	0.021467	82	1367.76	0.005895
58	1367.58	0.008808	83	1367.88	0.007720
59	1367.33	0.018376	84	1367.42	0.008664
60	1367.30	0.014692	85	1367.79	0.007879
61	1367.93	0.006592	86	1367.66	0.004228
62	1367.83	0.008795	87	1367.57	0.009178
63	1367.60	0.003943	88	1367.88	0.005846
64	1368.12	0.010232	89	1367.98	0.006602
65	1367.68	0.007314	90	1368.42	0.006838
66	1367.34	0.009284	91	1368.22	0.006449
67	1367.43	0.002518	92	1368.54	0.003498
68	1367.75	0.004110	93	1368.60	0.005550
69	1367.75	0.004108	94	1368.58	0.010285
70	1367.82	0.003536	95	1368.47	0.011472
71	1367.98	0.003241	96	1367.85	0.004180
72	1368.17	0.004553	97	1367.79	0.006612
73	1367.95	0.003916	98	1367.64	0.012856
74	1366.99	0.020793	99	1367.63	0.005671
75	1367.74	0.003401	100	1366.95	0.015519

SAN ACRIM SUMMARY FOR CHANNEL A SENSOR *** MEAN VALUES FOR DAYS

1981 DAY	1AU SOLAR IRRADIANCE (W/M2)	STATISTICAL UNCERTAINTY (PERCENT)	1981 DAY	1AU SOLAR IRRADIANCE (W/M2)	STATISTICAL UNCERTAINTY (PERCENT)
101	1367.27	0.014759	126	1367.13	0.005279
102	1366.44	0.017851	127	1367.68	0.007637
103	1366.48	0.018765	128	1367.62	0.014042
104	1367.03	0.010446	129	1367.87	0.004299
105	1367.58	0.006734	130	1367.77	0.004768
106	1367.89	0.009436	131	1367.19	0.009549
107	1367.03	0.004199	132	NO DATA	*****
108	1367.15	0.004780	133	1367.65	0.005340
109	1367.81	0.005232	134	1368.20	0.009312
110	1367.78	0.012396	135	1367.30	0.011868
111	1367.90	0.007086	136	NO DATA	*****
112	1367.86	0.012555	137	NO DATA	*****
113	1367.29	0.007649	138	1367.62	0.013241
114	1367.60	0.004457	139	NO DATA	*****
115	1368.08	0.004521	140	1366.80	0.007631
116	1368.42	0.011726	141	NO DATA	*****
117	1368.20	0.004661	142	1367.86	0.004496
118	1368.04	0.009749	143	1367.64	0.007633
119	1368.06	0.004145	144	NO DATA	*****
120	1368.29	0.010783	145	1368.55	0.005354
121	1367.98	0.009060	146	1367.98	0.005940
122	1368.77	0.005292	147	1367.69	0.006734
123	1368.32	0.004785	148	1367.73	0.013475
124	1367.74	0.004057	149	1368.10	0.006368
125	1367.67	0.009633	150	1368.21	0.007657

SNM ACRIM SUMMARY FOR CHANNEL A SENSOR *** MEAN VALUES FOR DAYS

1981 DAY	1AU SOLAR IRRADIANCE (W/M2)	STATISTICAL UNCERTAINTY (PERCENT)	1981 DAY	1AU SOLAR IRRADIANCE (W/M2)	STATISTICAL UNCERTAINTY (PERCENT)
151	1367.44	0.022891	176	1367.25	0.006560
152	1367.80	0.015871	177	1367.66	0.003386
153	1366.90	0.028597	178	1366.99	0.012744
154	1367.77	0.010406	179	1367.12	0.005313
155	1368.44	0.007289	180	1367.21	0.009766
156	1367.90	0.005883	181	1367.20	0.007390
157	NO DATA	*****	182	1366.81	0.003417
158	1367.98	0.005373	183	1366.47	0.010925
159	1367.85	0.005599	184	1367.37	0.005367
160	1368.19	0.006493	185	1367.59	0.005608
161	1367.66	0.005611	186	1368.14	0.007689
162	1367.73	0.011938	187	1368.08	0.007399
163	1367.58	0.008681	188	1367.67	0.016093
164	1367.76	0.005936	189	1367.56	0.003313
165	1367.55	0.004526	190	1367.77	0.004798
166	1367.31	0.003836	191	1367.89	0.005310
167	1367.29	0.003624	192	1367.46	0.007481
168	1367.21	0.003140	193	1367.84	0.007231
169	1367.56	0.008878	194	1367.43	0.005446
170	1367.90	0.005483	195	1367.45	0.008929
171	1368.10	0.004982	196	1367.56	0.008905
172	1367.72	0.003411	197	1367.10	0.009604
173	1367.81	0.007918	198	1367.45	0.008955
174	1367.61	0.004905	199	1365.85	0.013955
175	1367.28	0.008039	200	1367.12	0.032133

SMM ACRIM SUMMARY FOR CHANNEL A SENSOR *** MEAN VALUES FOR DAYS

1981 DAY	IAU SOLAR IRRADIANCE (W/M2)	STATISTICAL UNCERTAINTY (PERCENT)	1981 DAY	IAU SOLAR IRRADIANCE (W/M2)	STATISTICAL UNCERTAINTY (PERCENT)
201	1366.70	0.015250	226	1368.22	0.005999
202	1366.81	0.009630	227	1367.60	0.009543
203	1365.74	0.006902	228	1367.44	0.003298
204	1365.04	0.003941	229	1367.17	0.006335
205	1364.82	0.009914	230	1367.31	0.004523
206	1364.64	0.007850	231	1366.61	0.005663
207	1364.88	0.006325	232	1367.03	0.003802
208	NO DATA	*****	233	1367.69	0.012186
209	NO DATA	*****	234	1367.49	0.008079
210	NO DATA	*****	235	1367.17	0.018944
211	NO DATA	*****	236	1367.18	0.014230
212	NO DATA	*****	237	1367.26	0.011717
213	1367.05	0.004859	238	1366.91	0.006369
214	1367.25	0.006477	239	1367.03	0.003017
215	1367.19	0.006472	240	1367.67	0.006971
216	1366.85	0.005034	241	1367.68	0.009675
217	1366.90	0.004027	242	1367.98	0.004323
218	1366.81	0.007122	243	1367.85	0.008754
219	1366.64	0.005346	244	1368.19	0.005082
220	1366.42	0.005251	245	1368.08	0.004504
221	1366.45	0.005505	246	1367.96	0.011033
222	1366.82	0.005314	247	1367.59	0.003484
223	1366.77	0.005752	248	1367.40	0.005382
224	1367.61	0.008761	249	1366.71	0.010421
225	1368.13	0.004146	250	1366.83	0.006462

SNN ACRIN SUMMARY FOR CHANNEL A SENSOR *** MEAN VALUES FOR DAYS

1981 DAY	1AU SOLAR IRRADIANCE (W/M2)	STATISTICAL UNCERTAINTY (PERCENT)	1981 DAY	1AU SOLAR IRRADIANCE (W/M2)	STATISTICAL UNCERTAINTY (PERCENT)
251	1365.10	0.003942	276	1368.37	0.004351
252	1367.19	0.007452	277	1368.00	0.005087
253	1367.63	0.003754	278	1368.14	0.004769
254	NO DATA	*****	279	1366.68	0.021437
255	1367.13	0.004346	280	1367.56	0.009916
256	NO DATA	*****	281	1367.96	0.003614
257	1367.75	0.004747	282	1367.74	0.004042
258	1368.01	0.007137	283	1367.77	0.003744
259	1367.73	0.006081	284	1367.16	0.005432
260	1367.88	0.005233	285	1366.71	0.004044
261	1367.31	0.005505	286	1366.25	0.007205
262	1367.32	0.004664	287	1365.80	0.005541
263	1367.89	0.005469	288	1365.89	0.004837
264	1368.16	0.004246	289	1365.78	0.004208
265	1367.73	0.003492	290	1365.75	0.004118
266	1367.71	0.014820	291	1366.00	0.006055
267	1368.30	0.005995	292	1366.42	0.006082
268	1368.41	0.010024	293	1366.91	0.005113
269	1368.27	0.009973	294	1367.55	0.003571
270	1368.69	0.008468	295	1368.22	0.006062
271	1367.93	0.005710	296	1368.27	0.005266
272	1367.65	0.010166	297	1368.16	0.005746
273	1367.87	0.003686	298	1368.24	0.010422
274	1368.22	0.003947	299	1368.52	0.005570
275	1368.11	0.005333	300	1368.40	0.004873

SMN ACRIM SUMMARY FOR CHANNEL A SENSOR *** MEAN VALUES FOR DAYS

1981 DAY	1AU SOLAR IRRADIANCE (W/M2)	STATISTICAL UNCERTAINTY (PERCENT)	1981 DAY	1AU SOLAR IRRADIANCE (W/M2)	STATISTICAL UNCERTAINTY (PERCENT)
301	1368.68	0.004167	326	1367.85	0.005501
302	1368.41	0.005596	327	1368.42	0.005532
303	1368.35	0.005321	328	1368.86	0.004714
304	1368.14	0.006440	329	1367.63	0.016749
305	1367.42	0.006792	330	1367.97	0.013086
306	1367.12	0.008031	331	1368.19	0.004904
307	1366.92	0.005582	332	1368.17	0.005226
308	1366.77	0.004556	333	1367.53	0.007868
309	1367.36	0.005757	334	1367.75	0.005751
310	1367.80	0.006347	335	1368.22	0.006994
311	1367.85	0.006823	336	1368.21	0.012113
312	1368.07	0.007086	337	1368.46	0.006768
313	1368.19	0.003521	338	NO DATA	*****
314	1367.21	0.008858	339	NO DATA	*****
315	1367.75	0.004803	340	1368.16	0.007123
316	1367.44	0.007511	341	1367.08	0.004678
317	1367.04	0.011190	342	1366.85	0.003873
318	1367.73	0.004076	343	1366.11	0.003767
319	1367.99	0.003957	344	1366.46	0.003884
320	1368.23	0.007079	345	1367.17	0.004811
321	1368.39	0.006446	346	1367.45	0.004798
322	1367.73	0.003542	347	1367.85	0.006721
323	1367.74	0.004722	348	1368.09	0.008288
324	1367.92	0.003899	349	1368.00	0.006165
325	1368.03	0.004843	350	1367.97	0.004841

SMM ACRIM SUMMARY FOR CHANNEL A SENSOR *** MEAN VALUES FOR DAYS

1981 DAY	1AU SOLAR IRRADIANCE (W/M2)	STATISTICAL UNCERTAINTY (PERCENT)	1981 DAY	1AU SOLAR IRRADIANCE (W/M2)	STATISTICAL UNCERTAINTY (PERCENT)
351	1367.61	0.009716	***	* 1982	*****
352	1368.03	0.003085	***	* 1982	*****
353	1367.95	0.006755	***	* 1982	*****
354	1367.93	0.005540	***	* 1982	*****
355	1367.82	0.007153	***	* 1982	*****
356	1368.21	0.007295	***	* 1982	*****
357	1367.84	0.005102	***	* 1982	*****
358	1367.56	0.004780	***	* 1982	*****
359	1367.72	0.007835	***	* 1982	*****
360	1367.65	0.006285	***	* 1982	*****
361	1367.71	0.005244	***	* 1982	*****
362	1368.02	0.006973	***	* 1982	*****
363	NO DATA	*****	***	* 1982	*****
364	NO DATA	*****	***	* 1982	*****
365	NO DATA	*****	***	* 1982	*****
***	* 1982	*****	***	* 1982	*****

SNN ACRIM SUMMARY FOR CHANNEL A SENSOR *** MEAN VALUES FOR DAYS

1982 DAY	1AU SOLAR IRRADIANCE (W/M2)	STATISTICAL UNCERTAINTY (PERCENT)	1982 DAY	1AU SOLAR IRRADIANCE (W/M2)	STATISTICAL UNCERTAINTY (PERCENT)
1	1368.42	0.004305	26	1368.41	0.004127
2	1368.14	0.006642	27	1368.46	0.002822
3	1368.13	0.010226	28	1367.95	0.006765
4	1368.40	0.005527	29	1366.60	0.009424
5	1368.13	0.007063	30	1366.34	0.008526
6	1368.31	0.004668	31	1365.40	0.005547
7	1368.32	0.008071	32	1366.40	0.008783
8	1367.88	0.009942	33	1366.60	0.008698
9	1368.27	0.006440	34	1367.19	0.006319
10	1367.75	0.005333	35	1367.18	0.004450
11	1368.22	0.004718	36	1367.61	0.004882
12	1368.31	0.003546	37	1367.15	0.003950
13	1367.66	0.006676	38	1366.60	0.005116
14	1367.97	0.004293	39	1365.79	0.005855
15	1367.47	0.003859	40	1366.02	0.005610
16	1367.51	0.004019	41	1365.22	0.005649
17	1367.76	0.006194	42	1365.55	0.005588
18	1367.79	0.005865	43	1366.21	0.005832
19	1368.13	0.005485	44	1366.49	0.004529
20	1368.38	0.003874	45	1366.78	0.004452
21	1368.36	0.003103	46	1367.03	0.006228
22	1368.28	0.005405	47	1366.86	0.006461
23	1368.56	0.003526	48	1366.25	0.006451
24	1368.18	0.004299	49	1366.94	0.006052
25	1368.46	0.003415	50	1366.53	0.004127

SMM ACRIM SUMMARY FOR CHANNEL A SENSOR *** MEAN VALUES FOR DAYS

1982 DAY	1AU SOLAR IRRADIANCE (W/M2)	STATISTICAL UNCERTAINTY (PERCENT)	1982 DAY	1AU SOLAR IRRADIANCE (W/M2)	STATISTICAL UNCERTAINTY (PERCENT)
51	1367.17	0.007719	76	1364.66	0.005976
52	1367.34	0.011638	77	1364.52	0.006046
53	1367.56	0.004474	78	1365.61	0.009127
54	1367.89	0.002825	79	1366.38	0.005209
55	1367.95	0.008658	80	1366.78	0.006388
56	1368.02	0.004320	81	1367.13	0.007780
57	1368.14	0.002755	82	1366.98	0.004593
58	1367.84	0.004361	83	1366.49	0.004351
59	1367.31	0.005956	84	1366.65	0.005699
60	1366.76	0.006997	85	1366.54	0.007691
61	1366.42	0.008218	86	1366.47	0.005587
62	1367.35	0.005652	87	1366.43	0.006453
63	1367.38	0.006808	88	1367.09	0.007522
64	1367.25	0.005163	89	1367.25	0.006671
65	1367.76	0.003663	90	1367.23	0.007689
66	1367.90	0.005788	91	1367.97	0.003969
67	1368.02	0.006560	92	1368.05	0.004398
68	1367.90	0.005000	93	1368.26	0.003476
69	1367.92	0.004658	94	1367.94	0.003697
70	1367.71	0.005727	95	1367.73	0.005906
71	1367.61	0.006298	96	1367.71	0.004405
72	1367.56	0.003383	97	1367.92	0.003520
73	1367.38	0.004449	98	1368.18	0.003523
74	1365.89	0.013197	99	1367.71	0.008665
75	1364.15	0.008818	100	1367.51	0.004185

SMM ACRIM SUMMARY FOR CHANNEL A SENSOR *** MEAN VALUES FOR DAYS

1982 DAY	1AU SOLAR IRRADIANCE (W/M2)	STATISTICAL UNCERTAINTY (PERCENT)	1982 DAY	1AU SOLAR IRRADIANCE (W/M2)	STATISTICAL UNCERTAINTY (PERCENT)
101	1367.16	0.004514	126	1367.23	0.005853
102	1367.15	0.008013	127	1367.06	0.004855
103	1367.07	0.004303	128	1367.19	0.005776
104	1366.96	0.005209	129	1367.57	0.008946
105	1367.55	0.004051	130	1367.00	0.008398
106	1367.49	0.005978	131	1367.73	0.005876
107	1367.43	0.007110	132	1367.85	0.004416
108	1367.70	0.007855	133	1367.68	0.003246
109	1367.24	0.006600	134	1367.33	0.007267
110	1367.16	0.013241	135	1367.25	0.008999
111	1367.38	0.005528	136	1367.23	0.005566
112	1367.65	0.004612	137	1367.16	0.005449
113	1366.93	0.004654	138	1367.11	0.004163
114	1366.91	0.005355	139	1367.38	0.008883
115	1366.83	0.005622	140	1367.49	0.009200
116	1367.18	0.006781	141	1367.39	0.003615
117	1367.59	0.007262	142	1367.30	0.008361
118	1368.37	0.005345	143	1367.88	0.004520
119	1368.24	0.003245	144	1367.77	0.004119
120	1367.82	0.005754	145	1368.10	0.003890
121	1367.58	0.004182	146	1367.61	0.005628
122	1367.65	0.004099	147	1367.64	0.004496
123	1367.46	0.010018	148	1367.68	0.006495
124	1367.49	0.004551	149	1367.29	0.006648
125	1367.22	0.005663	150	1367.62	0.004413

SMN ACRIM SUMMARY FOR CHANNEL A SENSOR *** MEAN VALUES FOR DAYS

1982 DAY	1AU SOLAR IRRADIANCE (W/M2)	STATISTICAL UNCERTAINTY (PERCENT)	1982 DAY	1AU SOLAR IRRADIANCE (W/M2)	STATISTICAL UNCERTAINTY (PERCENT)
151	1367.42	0.008808	176	1367.34	0.010629
152	1368.07	0.003063	177	1367.84	0.006239
153	1367.67	0.010346	178	1368.74	0.004858
154	1367.28	0.011617	179	1367.33	0.007174
155	1367.67	0.005650	180	1366.97	0.007769
156	1367.30	0.009287	181	1367.59	0.005162
157	1366.40	0.008015	182	1367.45	0.013092
158	1366.29	0.004111	183	1367.88	0.006978
159	1365.77	0.012880	184	1368.50	0.007048
160	1366.29	0.005092	185	1367.92	0.005065
161	1366.37	0.006734	186	1367.52	0.008378
162	1366.70	0.013237	187	1367.90	0.008062
163	1366.85	0.009891	188	1367.97	0.006524
164	1366.42	0.007616	189	1366.89	0.009796
165	1366.13	0.003567	190	1367.58	0.008080
166	1365.90	0.007875	191	1367.30	0.004080
167	1365.94	0.005863	192	1366.88	0.002961
168	1365.21	0.007032	193	1366.49	0.004337
169	1365.15	0.010206	194	1366.28	0.005879
170	1365.94	0.012175	195	1365.76	0.004601
171	1365.60	0.008753	196	1366.09	0.005869
172	1366.22	0.006104	197	1365.71	0.005459
173	1366.43	0.005994	198	1366.08	0.007804
174	1366.97	0.016202	199	1366.96	0.007455
175	1367.06	0.007040	200	1368.01	0.005406

SMM ACRIM SUMMARY FOR CHANNEL A SENSOR *** MEAN VALUES FOR DAYS

1982 DAY	1AU SOLAR IRRADIANCE (W/M2)	STATISTICAL UNCERTAINTY (PERCENT)	1982 DAY	1AU SOLAR IRRADIANCE (W/M2)	STATISTICAL UNCERTAINTY (PERCENT)
201	1368.48	0.006545	226	1367.79	0.006509
202	1368.06	0.005759	227	1367.30	0.013327
203	1368.26	0.005155	228	1367.11	0.008204
204	1368.01	0.004655	229	1367.82	0.008856
205	1367.53	0.010174	230	1366.85	0.007139
206	1367.44	0.007353	231	1367.13	0.007608
207	1367.46	0.012317	232	1366.58	0.008168
208	1367.54	0.010417	233	1367.13	0.005129
209	1367.13	0.011938	234	1366.61	0.010530
210	1367.27	0.009349	235	1366.79	0.006396
211	1367.26	0.005770	236	1366.69	0.006512
212	1367.63	0.007742	237	1366.54	0.004768
213	1368.03	0.008439	238	1366.32	0.005752
214	1367.63	0.006817	239	1366.63	0.013074
215	1367.44	0.007154	240	1366.96	0.005223
216	1367.22	0.005703	241	1367.05	0.006541
217	1366.93	0.011315	242	1367.50	0.004535
218	1367.13	0.004530	243	1367.63	0.008924
219	1366.93	0.006912	244	1367.94	0.004693
220	1366.76	0.007867	245	1367.73	0.005071
221	1367.14	0.004098	246	1367.49	0.007384
222	1367.13	0.004320	247	1367.65	0.006893
223	1367.52	0.003836	248	1367.63	0.009912
224	1367.79	0.011973	249	1368.20	0.009428
225	1367.82	0.011360	250	1368.09	0.003501

SNM ACRIM SUMMARY FOR CHANNEL A SENSOR *** MEAN VALUES FOR DAYS

1982 DAY	IAU SOLAR IRRADIANCE (W/M2)	STATISTICAL UNCERTAINTY (PERCENT)	1982 DAY	IAU SOLAR IRRADIANCE (W/M2)	STATISTICAL UNCERTAINTY (PERCENT)
251	1368.03	0.011601	276	1367.93	0.005274
252	1368.06	0.005666	277	1368.45	0.005377
253	NO DATA	*****	278	1368.53	0.005266
254	1368.01	0.006613	279	1368.20	0.006132
255	1367.71	0.005755	280	1368.07	0.005629
256	1367.79	0.015458	281	1367.83	0.005047
257	1367.43	0.010106	282	1367.68	0.004928
258	NO DATA	*****	283	1367.82	0.007970
259	1367.06	0.013885	284	1367.83	0.005572
260	1367.46	0.006294	285	1367.77	0.005202
261	1366.73	0.014465	286	1367.32	0.008656
262	1367.37	0.007769	287	1367.35	0.016438
263	1366.62	0.007734	288	1367.34	0.009633
264	1367.61	0.004811	289	1367.20	0.006581
265	1367.59	0.006389	290	1367.43	0.004443
266	1368.07	0.006867	291	1367.33	0.005865
267	1367.25	0.036312	292	1367.28	0.005734
268	1367.51	0.015752	293	1367.74	0.006477
269	1368.00	0.009848	294	1367.66	0.004620
270	1367.37	0.006632	295	1367.65	0.006867
271	1366.91	0.009687	296	1368.16	0.006191
272	1366.98	0.008777	297	1367.54	0.005627
273	1367.15	0.007132	298	1367.60	0.004865
274	1367.05	0.006594	299	1367.63	0.008530
275	1367.39	0.010487	300	1367.53	0.006156

SMM ACRIM SUMMARY FOR CHANNEL A SENSOR *** MEAN VALUES FOR DAYS

1982 DAY	1AU SOLAR IRRADIANCE (W/M2)	STATISTICAL UNCERTAINTY (PERCENT)	1982 DAY	1AU SOLAR IRRADIANCE (W/M2)	STATISTICAL UNCERTAINTY (PERCENT)
301	1368.33	0.005823	326	1366.66	0.008775
302	1368.25	0.006708	327	1366.69	0.012223
303	1368.16	0.003442	328	1366.96	0.005426
304	1367.66	0.006650	329	1367.69	0.008002
305	1368.43	0.009666	330	1367.77	0.006924
306	1368.96	0.004381	331	1367.95	0.004547
307	1368.05	0.010599	332	1367.62	0.007872
308	1368.46	0.006953	333	1367.24	0.007566
309	1368.08	0.016262	334	1366.73	0.010578
310	1367.38	0.011580	335	1367.43	0.003385
311	1368.01	0.006271	336	1366.99	0.005729
312	1368.15	0.005394	337	1366.96	0.004403
313	1367.85	0.011266	338	1366.92	0.007124
314	1367.99	0.007143	339	1366.79	0.007703
315	1367.36	0.018098	340	1367.22	0.006924
316	1366.96	0.006544	341	NO DATA	*****
317	1366.60	0.007289	342	1367.84	0.007310
318	NO DATA	*****	343	1367.45	0.004361
319	NO DATA	*****	344	1367.55	0.005321
320	1367.35	0.006496	345	1367.25	0.006094
321	1367.11	0.008679	346	1367.14	0.009464
322	1367.69	0.008542	347	1366.67	0.009701
323	1367.08	0.007442	348	1366.38	0.011750
324	1367.33	0.011020	349	1366.94	0.007304
325	1368.10	0.016956	350	1367.04	0.010190

SMM ACRIM SUMMARY FOR CHANNEL A SENSOR *** MEAN VALUES FOR DAYS

1982 DAY	1AU SOLAR IRRADIANCE (W/M2)	STATISTICAL UNCERTAINTY (PERCENT)	1982 DAY	1AU SOLAR IRRADIANCE (W/M2)	STATISTICAL UNCERTAINTY (PERCENT)
351	1368.15	0.005210	***	* 1983	*****
352	1368.54	0.006235	***	* 1983	*****
353	1368.07	0.004221	***	* 1983	*****
354	1368.16	0.005360	***	* 1983	*****
355	1367.86	0.011915	***	* 1983	*****
356	1367.66	0.013168	***	* 1983	*****
357	1367.53	0.006241	***	* 1983	*****
358	NO DATA	*****	***	* 1983	*****
359	1367.73	0.010803	***	* 1983	*****
360	NO DATA	*****	***	* 1983	*****
361	NO DATA	*****	***	* 1983	*****
362	1367.08	0.009194	***	* 1983	*****
363	1367.57	0.014878	***	* 1983	*****
364	NO DATA	*****	***	* 1983	*****
365	1367.46	0.006377	***	* 1983	*****
***	* 1983	*****	***	* 1983	*****

DISCUSSION OF WILLSON PRESENTATION

MOORE: What are the widely variant points on the plot?

WILLSON: They are improperly corrected for the Earth-Sun distance. Our ephemeris didn't work well near midnight.

HUDSON: Those are the legendary zero hours UT flares.

ZIRIN: (proper guffaw).

SOFIA: Is there anything different in the processing of the February 1981 data?

WILLSON: No.

MOORE: If the 0.04% temporal decrease seen in the pointed-mode data is extrapolated, does it fit the spin-mode data?

WILLSON: Yes.

FOUKAL: Are there any cases where the observed dip in irradiance is larger than the predicted dip?

WILLSON: Yes.

FOUKAL: If the observed dip is less than the prediction, that could be evidence of partial cancellation by facular emission. If the observed dip is greater than the prediction, there would be no obvious explanation.

EDDY: Isn't there a zero level change in the data after day 346 that would produce an arbitrary slope?

WILLSON: Yes, there is a shift of 0.112%, which is a known correction for the difference in timing of the data cycle between pointed and spin modes.

RABIN: Is there a trend in the pointed data alone?

WILLSON: Yes.

FOUKAL: Your confidence in measuring that slope depends on knowing the sources of all instrumental drifts. Flamondon's earlier Mariner data had this problem.

WILLSON: Yes, but we think we have solved the drift problems, and know what affected Flamondon's data. Of course, we can't prove this since we cannot calibrate common drift in all three [ACRIM] channels.

FOUKAL: Is the periodicity at 24 days or 27 days?

WILLSON: Early in 1980 it was 24 days, when we saw the same active area for six rotations.

MOORE: In a large group, new spots may arise in front of the old.

HEATH: Yes, which implies it is not a mass motion.

EDDY: Are there changes in slope over the three years of data?

WILLSON: Many, on short timescales. We see no general change.

SOFIA: We should look for trends in the (observed-predicted) irradiance.

FOUKAL: Can you find irradiance dips associated with the growth of spots on the disk as opposed to the simple transit of spots of constant size?

HUDSON: The April 1980 dip is a good place to look.

Status of Solar Measurements and Data Reduction for ERB-Nimbus 7

J. R. Hickey and B. M. Alton
The Eppley Laboratory Inc.
Newport, RI 02840

INTRODUCTION

This presentation includes the description of the status of the Total Solar Irradiance data obtained using the cavity radiometer aboard the Earth Radiation Budget experiment of the Nimbus 7 satellite. That experiment has been returning data since November 16, 1978 and is still functioning properly as of this time. There are projections that this measurement mission could continue until 1991, based on the condition of the spacecraft and the instrument. The instrument and the measurement method have been described previously (1,2) and the data sets and processing have been presented in the previous workshop proceedings (3). The processing of the ERB data involves many steps and the involvement of many people including, the Nimbus ERB Science (Experiment) Team, the Nimbus Ground Station and Operations Personnel, and the ERB Processing Team. The ERB experiment has a number of sensors which measure the radiative fluxes (both shortwave and infrared) leaving the earth as well as the solar channels. The complexity of the processing of the earth-flux data, both wide and narrow angle has necessitated a reprocessing effort which produces the final data. Since the solar data is embedded in the same data stream and tape product as the earth-flux data, it has not been generally available in a format convenient for analysis as a separate product. In the past, we have periodically released a preliminary product in order to keep the solar community informed of the indicated variability in the extraterrestrial solar flux, within a reasonable time after the measurement. In looking back, this may have been cause for some scepticism regarding the ERB solar data. Here we will present values for the final data product only and provide a few remarks concerning the basic features of the data. There will be no scientific conclusions presented here other than those directly related to the measurement results. A set of tabulated values is appended in accordance with the request of the organizers of the workshop.

DATA AVAILABILITY

While there are a number of products developed for the data from the ERB, the most convenient for use in assessing solar

irradiance is a tape product named the Solar and Earth Flux Data Tape (SEFDT). This tape contains orbital summary records from which the calculated solar irradiance for that orbit's solar measuring period are calculated using the algorithms and constants agreed upon by the ERB Science Team. While there may be further revisions based on the history of the in-flight calibrations or based on more in-depth analysis of the other data products, this data set is the best currently available. There can be up to 14 solar measurements per day, one per orbit. The ERB sensor views the sun as the satellite passes over the terminator at the southern extreme of its polar orbit, just before its northward pass over the sunlit hemisphere of the earth. ERB is on the forward looking surface of the satellite as opposed to the familiar SBUV experiment which views the sun at the northern limit of the orbit.

There are now 3 years of this final data product available. This covers the period from November 16, 1978 through October 31, 1981. With the exception of a few days in July 1981, this set is complete. For purposes of assigning dates to the data presented here November 16, 1978 has been designated as mission day 1.

For a long period of time, it was possible to obtain the "peak" signal from the cavity radiometer from an engineering analysis program output in the Nimbus ground station. This was generally available for one orbit per day on those days when the program was run. This data was delivered to our colleagues at NOAA/NESS (Dr. Herbert Jacobowitz and Paul Pellegrino) who added the necessary ancillary data before forwarding the data to us at Eppley Laboratory. The data released was termed the "engineering level data" (see reference 3). Upon receipt of a sufficient amount of final (SEFDT) data it was found that the engineering level results were yielding irradiance values which were too high by about 0.2%. In subsequent releases the data were adjusted to lower the values by the ratio obtained by comparing the two data sets for days on which both were available. To simplify the identification of the different data sets as they presently stand the terms final and preliminary are used for the SEFDT and the adjusted engineering data sets respectively. The only reason for retaining the preliminary (engineering) level product is to monitor health of the instrument on a near-real-time basis, since there is still some delay in obtaining the final product.

The fourth year of data is presently in the final stages of reprocessing. That is, the data for the period from November of 1981 through October of 1982 will be available in final form in a few months. The preliminary data is available into early July of 1983, only a few weeks behind present.

RESULTS

A table of the daily mean values of the final data is appended. Readers desiring the more detailed values obtained on an orbital basis can obtain these values on tape from the NIMBUS Project Office at NASA, Goddard Space Flight Center (or may contact the authors). Only the final data are tabulated. However, the final data and the preliminary data are plotted in figure 1. The final data covers 1082 days from November 16, 1978 through October 31, 1981. The data was made available by Dr. Richard Willson of JPL (see his presentation in these proceedings) is also plotted on the figure. The simple solar indicators, sunspot number and 2800 MHz flux are also included so that the reader may orient the data sets with the solar activity indicators. No quantitative relationship should be inferred from this plot. The reader is referred to other presentations in these proceedings for detailed analysis of the relationships between total solar flux and the solar activity parameters. There are 815 daily mean values in the final set. There are also 238 data points from the preliminary set covering the period from November 1, 1981 through July 5, 1983. The pertinent statistics are tabulated below.

Table 1. Total Solar Irradiance Results from ERB-Nimbus 7

data set	points	Irradiance in W/m^2			
		mean	minimum	maximum	std.dev.
Final	815	1371.0	1367.8	1372.9	0.765 (0.056%)
Preliminary	238	1370.5	1367.9	1372.3	0.803 (0.059%)

The mean value of the SMM/ACRIM (Willson) results shown here is $1367.7 W/m^2$ with a standard deviation of 0.802 (0.059%). The correlation results with the SMM data are given in table 2.

Table 2. Correlation of ERB results with SMM/ACRIM results for data shown in Figure 1.

data set	corr. points	corr. coeff.	period covered
Final	437	0.776	February 1980-October 1981
Preliminary	175	0.626	November 1981-August 1982

There had been an indication of a small downward trend in the irradiance as a function of time amounting to approximately 0.02 percent per year. As the data set gets longer this slope appears to decrease in magnitude while retaining its negative sign.

FURTHER REMARKS

One of the most significant contributions which the ERB solar irradiance data can make is to correct the existing data base back to 1975. In July 1975, the Nimbus 6 version of the ERB experiment began making total solar irradiance measurements. Unfortunately, there was not a cavity radiometer in that older instrument, but only a simple thermopile device. That sensor is duplicated on Nimbus 7 as channel 3. Both the Nimbus 6 and 7 versions of the channel 3 sensor are identical in every respect including calibration traceability. While the Nimbus 6 presented encouraging results in a relative sense due to the stability of the sensor, the absolute value was apparently high. This result was also obtained on Nimbus 7. However, now we have both the cavity sensor and the SMM results with which to compare. There is a reprocessing effort in progress to obtain the Nimbus 6 results for the period for which both Nimbus 6 and Nimbus 7 were operational (after November 1978 and before March 1980). Plans are to rectify the Nimbus 7 channel 3 data to the cavity results and then to rectify the Nimbus 6 results based on this comparison. Early indications are encouraging, but there are insufficient overlap data to reach a conclusion. Nimbus 6 was continually operational through the solar minimum period between cycles 20 and 21. There were indications of "dips" in the solar irradiance through March 1977 which may have been associated with events near the end of cycle 20. No conclusions were made at that time because of uncertainties in the instrument performance at the low percentage level (especially angular alignment) because the complete final data set relative to orientation was not available. We hope that we will be able to report some progress soon.

Another aspect of the ERB solar measurements which is not discussed here is the spectral measurement capability of the other solar sensing channels. The early measurements from Nimbus 7 were affected by a contamination event, from which the sensors later recovered. Effort in correlating the spectral results with both the total irradiance results and the solar activity indicators is now beginning as the final data sets become available for time periods further into the mission (after April 1979).

SUMMARY

In this brief presentation we have provided a status report on the total irradiance measurements obtained from the ERB instrument aboard Nimbus 7. The final data from the first three years of operation are given in tabular form. A plot of these data plus additional preliminary data through early July 1983 is also presented. The ERB total measured solar irradiance is about 0.2% higher than the comparable measurements by the ACRIM instrument on SMM. This is well within the accuracy stated for the ERB instrument.

ent whose characterization is not known to the degree that is stated for the SMM/ACRIM instrument. Because of the digitization capability of the overall data system, the ERB instrument does not have the instantaneous resolution of the ACRIM, but by averaging over the solar pass the certainty of the measured value increases as the reciprocal of the square root of N ($N=45$ for this analysis) and no drift in either calibration results or voltage calibration levels has been experienced beyond the resolution limit. In terms of temporal comparability the ERB is restricted to one measurement every approximately 104 minutes while the SMM/ACRIM can measure over a more substantial portion of its orbit. This is because of the nature of the Nimbus orbit and not an experiment limitation. Also the ERB is subject to a 3-day-on and 1-day-off operational sequence because of the power distribution requirements of the Nimbus observatory. Despite all of these limitations there is a very good correspondence of the sensed events between ERB and ACRIM. These temporal and resolution limitations may be the reason that the correlation coefficient is only 0.776. However, if one were to have predicted this level of agreement, a few years ago, between independently developed instruments on two different satellites in space, it is an understatement to say he would have been considered a dreamer. While the solar physics community may have more stringent requirements than the ERB results can meet, the ERB instrument more than adequately performs its mission of measuring the input term in the radiation budget equation, the mission for which it was intended.

REFERENCES

1. Jacobowitz, H., L.L. Stowe and J.R. Hickey, The Earth Radiation Budget (ERB) Experiment, The Nimbus 7 Users' Guide, NASA Goddard Space Flight Center, Greenbelt MD, pp33-69, 1978
2. Hickey, J.R., L.L. Stowe, H. Jacobowitz, P. Pellegrino, R.H. Maschhoff, F.B. House and T.H. Vonder Haar, Initial Solar Irradiance Determinations from the Nimbus 7 Cavity Radiometer Measurements, SCIENCE, 208, pp 281-283, April 18, 1980.
3. Hickey, J.R., B.M. Alton, F.J. Griffin, H. Jacobowitz, P. Pellegrino, E.A. Smith, T.H. Vonder Haar and R.H. Maschhoff, Solar Variability - Indications from Nimbus 7 Satellite Data, in NASA Conference Publication 2191, Variations of the Solar Constant, S. Sofia, editor, NASA Goddard Space Flight Center, 1981.

* This work was supported in part by NASA, Goddard Space Flight Center under Contract NAS5-22947 and by NOAA under contract NA81RAC00077

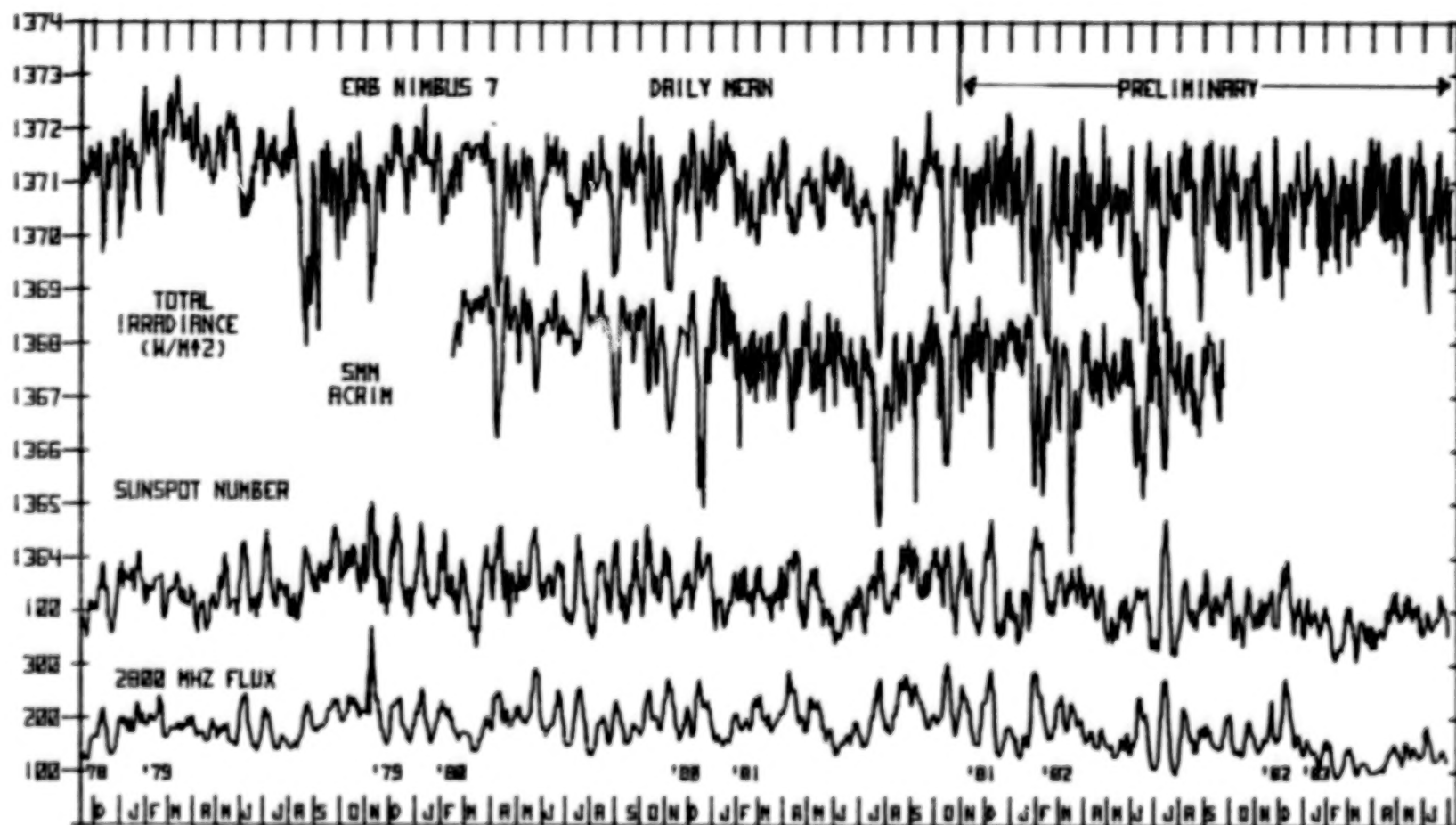


Figure 1. Composite plot vs. time of the total solar irradiance and solar activity indicators. Final, daily mean, ERB/Nimbus 7 results are plotted from November 16, 1978 to October 31, 1981. Preliminary ERB results are plotted from November 1, 1981 to July 5, 1983. The SMM/ACRIM results were supplied by Dr. R. Willson of JPL. The solar activity indicators are included for time orientation purposes and are not intended to denote any quantitative relationship, although the event correspondence is evident.

ERB NIMBUS-7 CHANNEL 10C DATA: SEFDT DAILY MEAN

observation number	mission day	irradiance (W/m ²)	observation number	mission day	irradiance (W/m ²)
1	1	1370.74	51	66	1371.14
2	2	1370.97	52	67	1370.85
3	3	1371.37	53	69	1370.50
4	5	1371.21	54	71	1371.29
5	6	1371.07	55	73	1371.38
6	7	1371.14	56	75	1372.23
7	8	1371.30	57	77	1372.76
8	9	1371.12	58	79	1371.84
9	10	1371.34	59	81	1371.55
10	11	1371.65	60	83	1371.90
11	13	1371.25	61	85	1372.10
12	14	1371.26	62	86	1372.29
13	15	1371.54	63	87	1372.09
14	17	1371.43	64	89	1371.71
15	18	1371.12	65	90	1372.29
16	19	1371.40	66	91	1372.35
17	21	1371.74	67	93	1371.41
18	22	1371.38	68	94	1370.96
19	23	1371.67	69	95	1370.47
20	25	1369.79	70	97	1370.39
21	26	1369.72	71	98	1371.01
22	27	1369.90	72	99	1371.53
23	29	1370.14	73	101	1371.96
24	30	1370.94	74	103	1371.87
25	31	1371.52	75	105	1371.90
26	32	1371.40	76	106	1372.37
27	33	1371.00	77	107	1372.50
28	34	1370.88	78	109	1372.15
29	35	1371.28	79	110	1372.51
30	37	1370.94	80	111	1372.65
31	38	1371.45	81	113	1371.84
32	39	1371.82	82	114	1371.97
33	41	1371.54	83	115	1372.39
34	42	1371.38	84	117	1372.54
35	43	1371.81	85	118	1372.95
36	45	1370.00	86	119	1372.85
37	46	1370.50	87	121	1372.37
38	47	1370.25	88	122	1372.26
39	49	1370.58	89	123	1372.35
40	50	1371.61	90	125	1371.80
41	51	1371.95	91	126	1371.84
42	53	1370.90	92	127	1372.09
43	54	1371.61	93	129	1371.86
44	55	1371.66	94	130	1372.00
45	57	1371.47	95	131	1371.84
46	58	1371.51	96	133	1372.10
47	59	1371.77	97	134	1372.22
48	61	1371.28	98	135	1372.24
49	62	1371.55	99	137	1371.51
50	65	1371.51	100	139	1371.40

ERB NIMBUS-7 CHANNEL 10C DATA: SEFDT DAILY MEAN

observation number	mission day	irradiance (W/m ²)	observation number	mission day	irradiance (W/m ²)
101	141	1371.70	151	209	1370.65
102	143	1372.45	152	210	1370.47
103	145	1371.80	153	211	1370.56
104	146	1371.70	154	213	1371.05
105	147	1371.67	155	214	1370.69
106	149	1371.52	156	215	1371.29
107	150	1371.26	157	217	1371.20
108	151	1371.47	158	218	1371.27
109	152	1371.31	159	219	1371.61
110	153	1371.46	160	221	1371.56
111	154	1371.48	161	222	1371.45
112	155	1371.88	162	223	1371.87
113	157	1371.65	163	224	1372.00
114	158	1371.82	164	225	1371.73
115	159	1371.64	165	226	1371.70
116	161	1371.41	166	227	1371.95
117	162	1371.15	167	229	1371.34
118	163	1371.17	168	230	1370.98
119	164	1371.00	169	231	1371.23
120	165	1371.16	170	233	1371.46
121	167	1371.10	171	234	1371.17
122	169	1371.54	172	235	1371.59
123	170	1371.52	173	236	1371.70
124	171	1371.96	174	237	1371.69
125	173	1372.06	175	238	1371.44
126	174	1371.80	176	239	1371.76
127	175	1371.85	177	241	1371.87
128	177	1371.34	178	242	1371.41
129	179	1371.25	179	243	1371.55
130	180	1371.42	180	245	1371.35
131	181	1371.64	181	246	1371.30
132	183	1372.09	182	247	1371.25
133	185	1372.30	183	249	1371.24
134	186	1372.04	184	250	1371.10
135	187	1372.16	185	251	1371.55
136	189	1372.12	186	252	1371.60
137	190	1372.03	187	253	1371.31
138	191	1372.25	188	254	1371.36
139	193	1371.62	189	255	1371.63
140	194	1371.59	190	257	1371.22
141	195	1372.00	191	258	1371.27
142	196	1371.90	192	259	1371.39
143	198	1371.40	193	261	1372.35
144	199	1371.13	194	262	1371.51
145	201	1370.56	195	263	1371.98
146	202	1370.37	196	265	1371.77
147	203	1370.63	197	266	1371.49
148	205	1370.79	198	267	1371.67
149	206	1370.82	199	268	1371.40
150	207	1370.39	200	269	1370.96

ERB NIMBUS-7 CHANNEL 10C DATA: SEFDT DAILY MEAN

observation number	mission day	irradiance (W/m ²)	observation number	mission day	irradiance (W/m ²)
201	270	1370.66	251	334	1371.40
202	271	1370.74	252	335	1371.37
203	273	1370.20	253	337	1370.43
204	274	1369.47	254	338	1370.65
205	275	1369.42	255	339	1370.93
206	277	1368.64	256	341	1371.42
207	278	1368.43	257	342	1371.18
208	279	1368.42	258	343	1371.92
209	280	1368.00	259	345	1371.47
210	281	1368.70	260	346	1370.92
211	282	1369.60	261	347	1371.13
212	283	1369.15	262	349	1371.22
213	285	1368.77	263	350	1370.67
214	286	1369.08	264	351	1371.19
215	287	1371.36	265	353	1370.91
216	289	1371.05	266	354	1370.64
217	290	1370.33	267	355	1370.95
218	291	1369.71	268	357	1369.88
219	293	1368.74	269	358	1368.82
220	294	1368.29	270	359	1369.17
221	295	1368.27	271	361	1369.65
222	296	1370.70	272	362	1369.49
223	297	1370.62	273	363	1370.00
224	298	1371.57	274	365	1370.90
225	299	1371.62	275	366	1370.98
226	301	1371.31	276	367	1371.29
227	302	1370.98	277	369	1371.29
228	303	1370.60	278	370	1370.83
229	305	1371.75	279	371	1371.13
230	306	1371.29	280	373	1370.90
231	307	1371.57	281	374	1370.49
232	309	1370.96	282	375	1370.95
233	310	1370.41	283	377	1371.52
234	311	1370.84	284	378	1371.33
235	313	1371.24	285	379	1371.42
236	314	1370.90	286	381	1371.36
237	315	1371.13	287	382	1371.16
238	317	1370.12	288	383	1371.19
239	318	1369.60	289	385	1371.35
240	319	1370.54	290	387	1372.06
241	321	1371.30	291	389	1372.00
242	322	1371.11	292	390	1372.02
243	323	1371.43	293	391	1371.58
244	325	1370.48	294	393	1371.98
245	326	1369.98	295	394	1371.53
246	327	1370.24	296	395	1371.69
247	329	1370.66	297	397	1371.33
248	330	1370.35	298	399	1371.23
249	331	1370.64	299	401	1370.83
250	333	1371.72	300	402	1370.45

ERB NIMBUS-7 CHANNEL 10C DATA: SEFDT DAILY MEAN

observation number	mission day	irradiance (W/m ²)	observation number	mission day	irradiance (W/m ²)
301	403	1370.80	351	470	1371.68
302	405	1371.48	352	471	1371.73
303	406	1371.49	353	473	1371.71
304	407	1371.26	354	474	1371.61
305	409	1371.26	355	475	1371.75
306	410	1371.08	356	477	1371.62
307	411	1371.55	357	478	1371.54
308	413	1372.03	358	479	1371.42
309	414	1371.63	359	481	1371.63
310	415	1371.92	360	482	1371.49
311	417	1372.00	361	483	1371.61
312	418	1371.52	362	484	1371.70
313	419	1371.59	363	485	1371.47
314	421	1371.55	364	486	1371.36
315	422	1371.36	365	487	1371.73
316	423	1371.82	366	489	1371.71
317	425	1372.41	367	490	1371.49
318	426	1371.40	368	491	1371.54
319	427	1371.48	369	493	1371.53
320	429	1371.36	370	494	1371.34
321	430	1371.31	371	495	1371.73
322	431	1371.41	372	497	1371.93
323	433	1371.35	373	498	1371.62
324	434	1370.85	374	499	1371.55
325	435	1371.06	375	501	1371.18
326	437	1371.61	376	502	1371.02
327	438	1371.61	377	503	1371.36
328	439	1371.91	378	505	1371.45
329	441	1371.71	379	507	1370.42
330	442	1371.44	380	509	1369.26
331	443	1371.02	381	510	1368.73
332	445	1370.26	382	511	1369.19
333	446	1370.29	383	513	1369.15
334	447	1370.69	384	514	1369.59
335	449	1370.70	385	515	1370.14
336	450	1370.45	386	517	1370.74
337	451	1370.80	387	518	1370.84
338	453	1370.97	388	519	1371.48
339	454	1370.91	389	521	1371.70
340	455	1371.21	390	522	1371.38
341	457	1371.19	391	523	1371.25
342	458	1370.76	392	525	1370.83
343	459	1371.08	393	526	1370.54
344	461	1371.54	394	527	1370.86
345	462	1371.39	395	529	1371.28
346	463	1371.36	396	530	1371.13
347	465	1370.89	397	531	1371.38
348	466	1370.83	398	533	1370.88
349	467	1371.12	399	534	1370.35
350	469	1371.61	400	535	1370.51

ERB NIMBUS-7 CHANNEL 10C DATA: SEFDT DAILY MEAN

observation number	mission day	irradiance (W/m ²)	observation number	mission day	irradiance (W/m ²)
401	537	1370.95	451	603	1370.72
402	538	1370.98	452	605	1370.62
403	539	1371.31	453	606	1370.21
404	541	1371.63	454	607	1370.32
405	542	1371.40	455	609	1370.64
406	543	1371.23	456	610	1370.43
407	545	1371.05	457	611	1370.44
408	546	1370.86	458	613	1370.40
409	547	1371.48	459	614	1370.53
410	549	1371.37	460	615	1370.67
411	550	1371.32	461	617	1371.23
412	551	1371.44	462	618	1371.37
413	553	1371.08	463	619	1371.41
414	554	1370.60	464	621	1370.96
415	555	1370.23	465	622	1370.72
416	557	1369.80	466	623	1370.70
417	558	1369.50	467	625	1371.29
418	559	1369.95	468	626	1371.29
419	560	1370.00	469	627	1371.56
420	561	1370.59	470	629	1371.17
421	562	1370.57	471	630	1370.97
422	565	1370.96	472	631	1370.85
423	566	1370.81	473	633	1370.98
424	567	1371.01	474	634	1370.90
425	569	1371.12	475	635	1371.00
426	570	1370.95	476	637	1371.05
427	571	1371.46	477	638	1371.24
428	572	1371.90	478	639	1371.85
429	573	1371.39	479	641	1371.41
430	574	1371.21	480	642	1371.29
431	575	1371.66	481	643	1371.35
432	577	1371.50	482	645	1371.22
433	578	1371.34	483	646	1370.93
434	579	1371.30	484	647	1370.92
435	581	1371.68	485	649	1371.19
436	582	1371.62	486	650	1370.81
437	583	1371.84	487	651	1370.79
438	585	1371.17	488	653	1370.41
439	589	1371.43	489	654	1369.64
440	590	1371.49	490	655	1369.29
441	591	1371.64	491	657	1369.61
442	593	1371.12	492	658	1369.39
443	594	1371.38	493	659	1369.70
444	595	1371.57	494	661	1370.49
445	597	1370.63	495	662	1370.71
446	598	1370.61	496	663	1371.65
447	599	1370.72	497	665	1371.75
448	600	1370.80	498	666	1371.56
449	601	1370.78	499	667	1371.41
450	602	1370.56	500	669	1370.95

ERB NIMBUS-7 CHANNEL 10C DATA: SEFDT DAILY MEAN

observation number	mission day	irradiance (W/m ²)	observation number	mission day	irradiance (W/m ²)
501	670	1370.91	551	738	1370.84
502	671	1371.32	552	739	1371.12
503	673	1371.65	553	741	1371.46
504	674	1371.17	554	742	1371.22
505	675	1371.11	555	743	1371.50
506	677	1370.86	556	745	1371.00
507	678	1370.64	557	746	1370.48
508	679	1370.97	558	747	1370.70
509	681	1371.40	559	749	1371.25
510	682	1371.20	560	750	1370.94
511	683	1371.28	561	751	1371.30
512	685	1371.55	562	753	1371.97
513	686	1371.34	563	754	1371.83
514	687	1371.50	564	755	1371.91
515	688	1372.20	565	757	1371.57
516	690	1371.41	566	758	1370.53
517	690	1371.21	567	759	1370.65
518	691	1371.51	568	761	1370.31
519	693	1371.37	569	762	1369.96
520	694	1370.69	570	763	1370.48
521	695	1370.44	571	765	1370.90
522	697	1369.90	572	766	1371.01
523	698	1369.76	573	767	1371.62
524	699	1370.76	574	769	1371.38
525	701	1371.87	575	770	1370.90
526	702	1371.59	576	771	1371.29
527	703	1371.55	577	773	1371.20
528	705	1370.70	578	774	1370.64
529	706	1370.17	579	775	1370.77
530	707	1370.17	580	777	1371.56
531	709	1370.77	581	778	1371.74
532	710	1371.04	582	779	1372.14
533	711	1371.49	583	781	1370.83
534	713	1371.20	584	782	1370.53
535	717	1370.58	585	783	1371.21
536	718	1370.15	586	785	1371.02
537	719	1369.92	587	786	1371.05
538	721	1369.33	588	787	1371.22
539	722	1369.04	589	788	1371.80
540	723	1369.11	590	789	1371.74
541	725	1369.08	591	790	1371.21
542	726	1368.99	592	791	1371.61
543	727	1369.15	593	793	1371.63
544	729	1369.75	594	794	1371.28
545	730	1370.03	595	795	1371.58
546	731	1370.53	596	797	1371.93
547	733	1371.02	597	798	1371.54
548	734	1370.67	598	799	1371.71
549	735	1370.69	599	801	1371.64
550	737	1370.77	600	802	1371.36

ERB NIMBUS-7 CHANNEL 10C DATA: SEFDT DAILY MEAN

observation number	mission day	irradiance (W/m ²)	observation number	mission day	irradiance (W/m ²)
601	803	1371.44	651	871	1371.37
602	805	1371.58	652	872	1371.70
603	806	1371.41	653	873	1370.91
604	809	1370.89	654	874	1370.49
605	810	1370.24	655	875	1370.59
606	811	1370.34	656	877	1370.45
607	813	1371.04	657	878	1370.16
608	814	1370.93	658	879	1370.51
609	815	1370.86	659	881	1370.10
610	817	1370.76	660	882	1370.06
611	818	1370.36	661	883	1370.13
612	819	1370.62	662	885	1370.16
613	821	1371.21	663	886	1370.39
614	822	1370.54	664	887	1370.78
615	823	1370.52	665	888	1370.80
616	825	1370.41	666	889	1370.71
617	826	1370.07	667	890	1370.40
618	827	1370.57	668	891	1371.05
619	829	1370.84	669	893	1371.09
620	830	1370.22	670	894	1370.99
621	831	1370.29	671	895	1370.96
622	833	1370.22	672	897	1371.13
623	834	1370.14	673	898	1371.17
624	835	1370.03	674	899	1371.29
625	837	1369.88	675	901	1370.99
626	838	1370.02	676	902	1370.85
627	839	1370.39	677	903	1370.65
628	841	1371.06	678	905	1370.81
629	842	1370.52	679	906	1371.06
630	843	1370.79	680	907	1370.84
631	845	1370.60	681	909	1370.73
632	846	1370.46	682	910	1370.41
633	847	1370.96	683	911	1370.56
634	849	1371.11	684	913	1370.18
635	850	1371.05	685	914	1370.24
636	851	1371.39	686	915	1370.32
637	853	1371.57	687	917	1370.97
638	854	1371.25	688	918	1371.55
639	855	1371.35	689	919	1371.66
640	857	1370.61	690	921	1371.16
641	858	1370.43	691	922	1371.03
642	859	1370.77	692	923	1371.05
643	861	1371.04	693	925	1370.93
644	862	1370.77	694	926	1370.86
645	863	1371.04	695	927	1371.19
646	865	1371.25	696	929	1370.86
647	866	1371.11	697	930	1370.98
648	867	1371.54	698	931	1371.05
649	869	1371.82	699	932	1371.50
650	870	1371.36	700	933	1371.37

ERB NIMBUS-7 CHANNEL 10C DATA: SEFDT DAILY MEAN

observation number	mission day	irradiance (W/m ²)	observation number	mission day	irradiance (W/m ²)
701	934	1371.02	751	1000	1370.30
702	935	1371.34	752	1001	1370.65
703	937	1371.46	753	1002	1370.90
704	938	1371.34	754	1003	1371.84
705	939	1371.34	755	1005	1370.99
706	941	1370.66	756	1006	1370.68
707	942	1370.69	757	1007	1370.60
708	943	1370.59	758	1009	1370.81
709	944	1370.60	759	1010	1370.76
710	945	1370.72	760	1011	1371.11
711	946	1370.87	761	1013	1371.62
712	947	1371.28	762	1014	1371.42
713	949	1371.18	763	1015	1371.09
714	950	1370.96	764	1016	1370.70
715	951	1370.99	765	1017	1370.86
716	953	1370.45	766	1018	1370.72
717	954	1370.57	767	1019	1370.88
718	955	1370.24	768	1021	1371.17
719	957	1370.35	769	1022	1371.04
720	958	1370.22	770	1023	1371.16
721	959	1370.21	771	1025	1370.80
722	960	1370.40	772	1026	1370.16
723	961	1370.58	773	1027	1370.17
724	962	1370.71	774	1029	1370.91
725	963	1370.61	775	1030	1370.64
726	965	1370.56	776	1031	1370.47
727	966	1370.73	777	1033	1370.89
728	967	1370.86	778	1034	1370.71
729	973	1370.29	779	1035	1371.01
730	974	1370.33	780	1037	1371.43
731	975	1370.42	781	1038	1371.02
732	977	1370.44	782	1039	1371.16
733	978	1369.83	783	1041	1371.23
734	979	1369.31	784	1042	1371.72
735	981	1368.29	785	1043	1371.89
736	982	1367.88	786	1044	1372.30
737	983	1367.78	787	1045	1371.73
738	985	1368.03	788	1046	1371.39
739	986	1368.38	789	1047	1371.44
740	987	1368.97	790	1049	1371.39
741	988	1369.60	791	1050	1371.28
742	989	1369.71	792	1051	1371.51
743	990	1370.64	793	1053	1371.62
744	991	1370.89	794	1054	1371.14
745	993	1370.67	795	1055	1370.97
746	994	1370.51	796	1057	1370.95
747	995	1370.47	797	1058	1371.10
748	997	1369.67	798	1059	1371.32
749	998	1369.57	799	1061	1370.29
750	999	1369.93	800	1062	1369.67

ERB NIMBUS-7 CHANNEL 10C DATA: SEFDT DAILY MEAN

observation number	mission day	irradiance (W/m ²)	observation number	mission day	irradiance (W/m ²)
801	1063	1369.23			
802	1065	1369.13			
803	1066	1368.63			
804	1067	1368.67			
805	1069	1369.55			
806	1070	1369.62			
807	1071	1370.29			
808	1072	1370.60			
809	1073	1371.28			
810	1074	1371.24			
811	1075	1371.15			
812	1077	1371.33			
813	1078	1371.52			
814	1079	1371.73			
815	1081	1370.98			

DISCUSSION OF HICKEY PRESENTATION

FOUKAL: With the new data set, what happens to the August 1979 dip?

HICKEY: It gets a little less deep when correction is made for the off-axis pointing.

FOUKAL: What is the slope when you compare the ERB data to SMM?

HICKEY: 0.8.

FOUKAL: Then there is a 20% calibration difference?

HICKEY: If you remove the trends, the residuals show a slope of 0.977.

FOUKAL: How do the dips compare in amplitude between the instruments?

WILLSON: The sampling is too infrequent, so you get a noisy fit.

FOUKAL: The noise looks low to me.

SCHATTEN: When there are errors in both coordinates, the regression line has a slope less than the true one.

MOORE: Yes, you should do the regression both ways and average.

NEWKIRK: Why are there slope differences between the two data sets?

WILLSON: I'll explain that one in the discussion section.

FACULAR LIMB-DARKENING FUNCTIONS FOR IRRADIANCE MODELING

T. Hirayama, T. Okamoto, and H.S. Hudson¹
Tokyo Astronomical Observatory

ABSTRACT

The limb-darkening function of faculae is an important factor in estimating facular contributions to solar irradiance variations. We review the existing photometric data and generate a synthetic limb-darkening function for faculae, which we then compare with the limb-darkening functions currently in use for irradiance modeling. We find that the excess facular flux ranges from 0.017 to 0.0349 of the solar photospheric flux for the various representations. The present limitation appears to be the lack of comprehensive photometric data. The representations are especially varied near the limb, where photometry is most difficult.

Synoptic data on calcium plage areas can be used as a substitute for facular areas in modeling. Based upon the existing data, the present best value for the effect of faculae on the solar constant is given by

$$\Delta S/S = 3.9 \times 10^{-8} A_{\text{plage}},$$

for an active region near disk center, where A_{plage} is the calcium plage area in millionths of a solar hemisphere. Representative data on the development of plage and spot areas in an active region suggests that the respective energy excess and deficit are comparable in magnitude, when integrated over the lifetime of the active region.

INTRODUCTION

The Solar Maximum Mission and Nimbus satellites are now making accurate measurements of variations of the magnitude of the solar constant. The largest of these variations, amounting to at most a few tenths of one percent, are strongly correlated with the presence of sunspots on the visible hemisphere (ref. 1). The presence of sunspot deficits in active regions without appreciable plage areas, as observed by Willson *et al.*, implies that a given active region may store energy for a time comparable to its lifetime. This storage must take place beneath the photosphere and most likely is associated with the magnetic structures that form the spots. At the same time, a correlation with facular regions also exists (ref. 2), and it is clear that effective modeling of the total irradiance variations requires consideration of both sunspot deficits and facular excesses.

¹Permanent address: Center for Astrophysics and Space Sciences, UCSD

The modeling effort consists of an attempt to find an accurate description of the solar irradiance variations in terms of the physical parameters associated with the models, for example the areas and effective temperatures of the sunspots. The model parameter information can then be used to elucidate the physical processes involved in the variations. The ultimate goals of these exercises, as regards solar physics, lie in obtaining observational information on the internal structure of the solar convection zone, the nature of stellar magnetism, and the nature of convection itself. Since these phenomena have heretofore been describable only in terms of their surface effects, any advance in observational capability would be extremely welcome.

The purposes of this paper are to review the empirical limb-darkening functions obtained from existing observations and to explore their implications for irradiance modeling. An accurate representation of the facular limb-darkening function is important not only for this purpose (and for understanding the physical nature of faculae) but also for the interpretation of solar oblateness data (e.g. ref. 3). Finally, we give the present best estimate for the calibration of facular irradiance in terms of calcium plage areas, although a considerable improvement can be made on this relationship with better data.

OBSERVATIONS OF FACULAR LIMB DARKENING

Observations of faculae are greatly hindered by the necessity for excellent angular resolution. The individual facular granules are small, and most observations appear to be at best marginally able to resolve them adequately for a real determination of the specific intensity. Nevertheless ground-based observations (refs. 4,5) have given us some reasonable data with which to supplement the brief observations from above the atmosphere. Several balloon-borne solar telescopes have provided snapshots of individual active regions at different times and with telescopes of differing capabilities. The earliest and some of the best balloon-borne data come from the Stratoscope project (ref. 6), but unfortunately the facular data consisted of only a single region close to the limb. More recently, newer balloon data have been reported (refs. 7, 8). We have considered the problem of representing these heterogeneous data for the purpose of constructing a "best" approximation to the facular limb darkening function. It is easiest to work with the peak intensity observed in a given facular measurement, although this value might vary quite widely even for the same faculae as viewed by the different instruments used, because of variations of the spatial filtering caused by systematic effects of seeing, telescope modulation transfer function, and scattered light. To accomplish the intercomparison in as simple a manner as possible, we have considered only data sources that provide observations at two or more positions on the sun. This allows us to reduce the comparison to results on the shape of the limb-darkening function, rather than its absolute normalization, which must be determined separately. The underlying hypothesis is that the simultaneous observations at two positions on the solar disk will have comparable systematic terms in the photometry. We have included one single-point observation in this procedure, namely the Stratoscope data (ref. 6). All data, except these of Chapman (ref. 9) who did not report original data, are uncorrected for smearing due to

instrumental or seeing effects. The Hirayama (ref. 10) data have been re-evaluated, and have an average wavelength of $5400 \pm 200 \text{ \AA}$.

The observations considered appear in Table 1. We have formed the data into a single composite limb-darkening distribution by adjustments of the normalization of each set to produce a minimum scatter in the plot of Figure 1. Note that the adjustment was performed on the logarithmic representation of the reported facular contrasts. The table shows the values of the factors needed to make these adjustments in the raw photometric data. As can be seen from the figure, a reasonably clean correlation ($\log \Delta I/I \leq 0.1$) exists that traces out a limb-darkening function with a maximum contrast in the vicinity of $\mu = 0.3$, where μ is the usual cosine of the vertical angle of viewing. We have arbitrarily chosen to normalize to the balloon data of Hirayama and Moriyama, although these are not necessarily the definitive data, and a numerical representation of the resulting limb-darkening function appears in Table 2.

The existence of a maximum in the facular contrast in the vicinity of $\mu = 0.3$ seems inescapable. Waldmeier (ref. 11), for example, placed this maximum at 71° , corresponding to $\mu = 0.33$. The lack of a maximum in observations with only moderate angular resolution is at present a puzzle.

REPRESENTATIONS OF FACULAR LIMB DARKENING FOR MODELING

Several authors have provided different analytic forms to represent the limb darkening of facular regions (refs. 12, 14, 15, 25). We summarize these forms in Table 3, including the numerical representation of the plot shown in Figure 1. Figure 2 compares these different analytic forms, which differ considerably. This lack of agreement is one of the main motivations for the present summary of the data. In order to clarify the definitions of the different quantities used to describe the facular radiation, Table 3 gives the different representations and calculates the facular excess flux, $\Delta F/F$, where

$$F = 2 \int_0^1 \mu I d\mu$$

where $I(\mu)$ is the specific intensity. Frequently the photospheric limb-darkening function is represented by

$$I_p/I_o = (3\mu + 2)/5,$$

with the central specific intensity of the quiet photosphere $I_o = 2.55 \times 10^{10} \text{ ergs}(\text{cm}^2\text{sec sr})^{-1}$. The flux F of the quiet photosphere $F = 4\pi/5 I_o = 6.41 \times 10^{10} \text{ erg}(\text{cm}^2\text{sec sr})^{-2}$. Most of the facular observations are monochromatic, and we make use of the tabulations of Kurucz (ref. 17) to obtain a rough bolometric correction to the data. For 5400 \AA , the correction factor is approximately 0.81 (ref. 14), not significantly different from unity in view of the uncertainties in the different representations shown in Figure 1.

The quantity $\Delta F/F$ is the key quantity that allows a comparison between the total energy deficit of a sunspot group and total energy excess of its associated facular region. It gives the angle-integrated total flux per unit area in the facular region in terms of the flux of the quiet photosphere. The

corresponding quantity for sunspot deficits (ref. 18) is

$$\Delta F_{\text{spot}}/F = -\alpha \times A_{\text{spot}}$$

with $\alpha = 0.315$ for the data given in Allen (ref. 16), and the spot area (umbra plus penumbra) measured in millionths of the hemisphere.

Thus for the limb-darkening representation of faculae in Table 2, a facula/spot area ratio of $0.315/0.0301 = 10.5$ is needed to establish exact balance; more precisely this is the ratio of the time integrals of facular and spot areas. The observed ratio of areas is approximately a factor of four on the average for a given spot group, although it varies from group to group and as a function of time within a given group (e.g. ref. 19). The area-time integral ratio may be close to the needed value, but there is uncertainty related to the identification of a plage region with a spot group that may have died several rotations earlier.

It is of interest to note that the integrand for ΔF has its maximum contribution at intermediate values of μ . The uncertainty in the value of $\Delta F/F$ displayed in Table 3 therefore does not depend very strongly on the extreme limb photometry, and there is no reason why improved data should not be readily obtained.

CALIBRATION OF Ca PLAGE AREA FOR REPRESENTATION OF FACULAE

The existing synoptic facular data are very limited in extent and in quality. Hence there is a desire to use alternative better-measured quantities, such as calcium plage reports or 10 cm flux indices to represent the faculae. This can be done provided that an adequate calibration of these proxy data can be made. This is therefore an urgent requirement for any extensive modeling of solar irradiance variations. To date only two initial attempts at such a calibration have been made (refs. 7, 9).

For active regions near disk center, we obtain a calibration of $\Delta S/S$, the fractional variation of total solar irradiance, in terms of the Ca plage area A_{plage} (millionths of the hemisphere):

$$\Delta S/S = 3.9 \times 10^{-8} A_{\text{plage}}.$$

This agrees with the Chapman determination (ref. 9) of the plage calibration, based upon photoelectric photometry.

With this calibration of the facular area in terms of Ca plage, we can estimate the ratio of facular excess to sunspot deficit for representative data. Figure 3 shows the time development of plage and spot areas for a large active region in 1972, taken from the Solar-Geophysical Data. From the above calibration, we find

$$\Delta W_{\text{fac}} = (\Delta F/F) \times F_p \times (1.56 \times 10^{-2}) / (C_f - 1) \int A_{\text{plage}} dt.$$

Here $(\Delta F/F)$ is the photospheric flux excess as tabulated in Table 3 for a given

representation of the facular limb-darkening function, $I_p = 4\pi/5 I_0$, and C_f is the facular contrast. Similarly the sunspot energy deficit²

$$\Delta W = -\alpha \times F_p \times \int A_{\text{spot}} dt.$$

For the representative data in Figure 3, we find

$$\Delta W_{\text{fac}} = 1.1 \times 10^{36} \text{ ergs}$$

$$\Delta W_{\text{spot}} = 0.9 \times 10^{36} \text{ ergs,}$$

so that in this case there was an approximate balance of energy between spots and faculae for the lifetime of this active region. The implied energy storage time would be on the order of one month, although it is interesting to note that Fig. 3 shows an extended period of slower decay of the plage region following its initial rapid decay.

The approximate agreement that we have found does not really prove anything, since it is based upon an approximate calibration of Ca plage and an ill-understood facular limb-darkening function. A conservative estimate of the uncertainties in these areas would be a factor of two; in addition it is known (e.g. ref. 28) that individual active regions do not have the same value of the parameter α , for example. One can conclude, however, that substantial energy does appear in faculae. The circumstantial evidence is compelling that this energy comes from the reservoir filled by the convective flux blocked by the sunspot group. This compensating flux reappears in a non-diffusive manner, quite unlike the prediction of the Spruit thermal model (ref. 29).

CONCLUSION

The facular limb darkening functions used by various authors for modelling of the total irradiance variations show a surprising uncertainty. The last column of Table 3 shows a facular flux excess ranging from 0.0167 to 0.0349, but to achieve even this factor-of-two range required very ill-defined normalizations of the existing photometric data. We have attempted to place these different treatments into a common framework in order to reduce the confusion, and have collected various observations together to make up a synthetic facular limb darkening function for future use. The uncertainty in the relationship between facular contrast and total facular flux, together with great uncertainty about the facular brightness at the extreme limb, are the present limiting factors in using facular data as a component in total-irradiance modeling. The present attempts to calibrate calcium plage areas for use as a representation of facular brightness are only preliminary for the same reason, namely the inadequacy of the present photometric data. One strong conclusion from these considerations is that routine photoelectric photometry with adequate spatial resolution should be carried out in the forthcoming solar minimum period. This photometry should not only provide better white-light data, but also data on chromospheric emission such as the Ca K line or HeI $\lambda 10830 \text{ \AA}$ (ref. 30), so that both deficit and excess components of the active-region energetics can be studied.

The present situation can well be summarized in the words of Wormell (ref. 20), who apparently anticipated in 1936 the need for space-borne observations of the solar constant:

"We are thus led to anticipate a variation in the total radiation of the Sun as an area of disturbance travels across the disc, the radiation being below its normal value when the disturbance was near the center of the disc, and perhaps above its normal value when the disturbance was close to the limb. Such a variation would scarcely be detected by the ordinary methods of determining the solar constant."

After the passage of a half century, this opinion might be reversed. It is now the "ordinary methods" of ground-based synoptic measurement that desperately need improvement.

Acknowledgments. Hudson derived support from the National Science Foundation grant ATM81-17355 and from the U.S.-Japan Cooperative Science Program for travel to Tokyo, where he greatly appreciated the warm hospitality that he received during his stay at the Tokyo Astronomical Observatory.

REFERENCES

1. Willson, R.C., Gulkis, S., Janssen, M., Hudson, H.S., and Chapman, G., 1981, "Observations of Solar Irradiance Variability", *Science*, **211**, 700.
2. Hudson, H.S., and Willson, R.C., 1981, in L. Cram and J. Thomas (eds.), *"The Physics of Sunspots"* (Sunspot, Sacramento Peak Observatory), p. 434.
3. Chapman, G.A., and Klabunde, D.P., 1982, "Measurements of the Limb Darkening of Faculae Near the Solar Limb", *Astrophys. J.*, **261**, 387.
4. Prazier, E.N., 1971, "Multichannel Magnetograph Observations. III. Faculae", *Solar Phys.*, **21**, 42.
5. Muller, R., 1975, "A Model of Photospheric Faculae Deduced from White Light High Resolution Pictures", *Solar Phys.*, **45**, 105.
6. Rogerson, J.B., 1961, "On Photospheric Faculae", *Astrophys. J.*, **134**, 331.
7. Hirayama, T., 1982, "On the Global Energy Balance of Solar Facular Regions", *Proceedings of Hinode Symposium* (Tokyo, ISAS), p. 227.
8. Hirayama, T., and Moriyama, F., 1979, "Center to Limb Variation of the Intensity of the Photospheric Faculae", *Solar Phys.*, **63**, 251.
9. Chapman, G.A., 1980, "Variations in the Solar Constant Due to Solar Active Regions", *Astrophys. J. (Lett.)*, **242**, L45.
10. Hirayama, T., 1978, "A Model of Solar Faculae and Their Lifetime", *Publ. Ast. Soc. Japan*, **30**, 337.
11. Waldmeier, M., 1949, "Die Sichtbarkeitsfunktion der Sonnenfackeln", *Zs. f. Astrophys.*, **26**, 147.
12. Kiepenheuer, K.O., 1953, in G. Kuiper (ed.), *"The Sun"*, p. 322.
14. Foukal, P., 1981, "Sunspots and Changes in the Global Output of the Sun", in L. Cram and J. Thomas (eds.), *"The Physics of Sunspots"* (Sunspot, Sacramento Peak Observatory), p. 391.
15. Sofia, S., Oster, L., and Schatten, K., 1982, "Solar Irradiance Modulation by Active Regions During 1980", *Solar Phys.*, **80**, 87.

16. Allen, C.W., 1973, *Astrophysical Quantities*, (Athlone), ch. 9.
17. Kurucz, R.L., 1979, "Models on Atmospheric G,P,A,B and O Stars", *Astrophys. J. Suppl.*, 40, 1.
18. Hudson, H.S., Silva, S., Woodard, M., and Willson, R.C., 1982, "The Effects of Sunspots on Solar Irradiance", *Solar Phys.*, 76, 211.
19. De Jager, C., 1959, "Structure and Dynamics of the " Solar Atmosphere", *Handbuch der Physik* LII, p.80.
20. Wormell, T.W., 1936, "Effect of Rotating Secondary Mirror of Collostat", *Mon. Not. R. Astr. Soc.*, 96, 736.
21. Schmahl, G., 1967, "Measurements on Sunspots in the Photosphere", *Zs. Astrophys.*, 66, 81.
22. Stellmacher, G., and Wiehr, E., 1973, "Observed Facula Line Profiles and Contrasts, Comparison with Models", *Astron. Astrophys.*, 29, 13.
23. Richardson, R.S., 1933, "A Photometric Study of Sunspots and Faculae", *Publ. Ast. Soc. Pacific*, 45, 195.
24. Chapman, G.A., 1970, "On the Physical Conditions in the Photospheric Network: An Improved Model of Solar Faculae", *Solar Phys.*, 14, 315.
25. Hoyt, D.V., and Eddy, J.A., 1982, "An Atlas of Variations in the Solar Constant Caused by Sunspot Blocking and Facular Emissions from 1874 to 1981", NCAR/TN-194+STR.
26. Eddy, J.A., 1983, these proceedings.
27. Libbrecht, K., and Kuhn, J., 1983, "A New Measurement of the Limb Darkening of Faculae Near the Solar Limb", submitted to Nature.
28. Bray, R.J., 1981, "A Refined Measurement of the Sunspot Radiative Flux Deficit", Solar Phys., 69, 3.
29. Spruit, H.C., 1977, "Heat Flow Near Obstacles in the Solar Convective Zone", Solar Phys., 55, 3.
30. Harvey, J., 1983, these proceedings.

Table 1. Facular Contrast Observations

Authors	Symbol	$\lambda(\text{\AA})$	Type ¹	$\Delta \log$	Comments
Schmahl (ref. 21)	X	4929+5777	C	0.60	
Prazier (ref. 4)	•	5200	C	0.65	100 Gauss
Stellmacher and Wiehr (ref. 22)	•	5780	C	0.55	
Richardson (ref. 23)	■	5780	C+L	0.45	
Rogerson (ref. 6)	■	5940	C+L	0.0	Single point
Chapman (ref. 24)	⊙	5300	C+L	0.30	Corrected data
Muller (ref. 5)	▲	5250+5750	C+L	0.30	
Hirayama (ref. 10)	▽	5300	C+L	0.30	
Hirayama and Moriyama (ref. 8)	⊙	5300	C+L	0.0	Normalization

¹C refers to continuum photoelectric observations; C+L to photographic observations which include lines.

Table 2. Synthetic Facular Contrast at 5200-5600Å
(Table 1 x 0.235)

$\mu = \cos\theta$	$\Delta I(\mu)/I(\mu)$
0.05	≤1.2%
0.1	7.5
0.2	10.3
0.3	10.8
0.4	7.1
0.5	4.0
0.6	2.8
0.7	2.2
0.8	1.7
0.9	1.4
1.0	1.3

Table 3. Representations of Facular Contrast

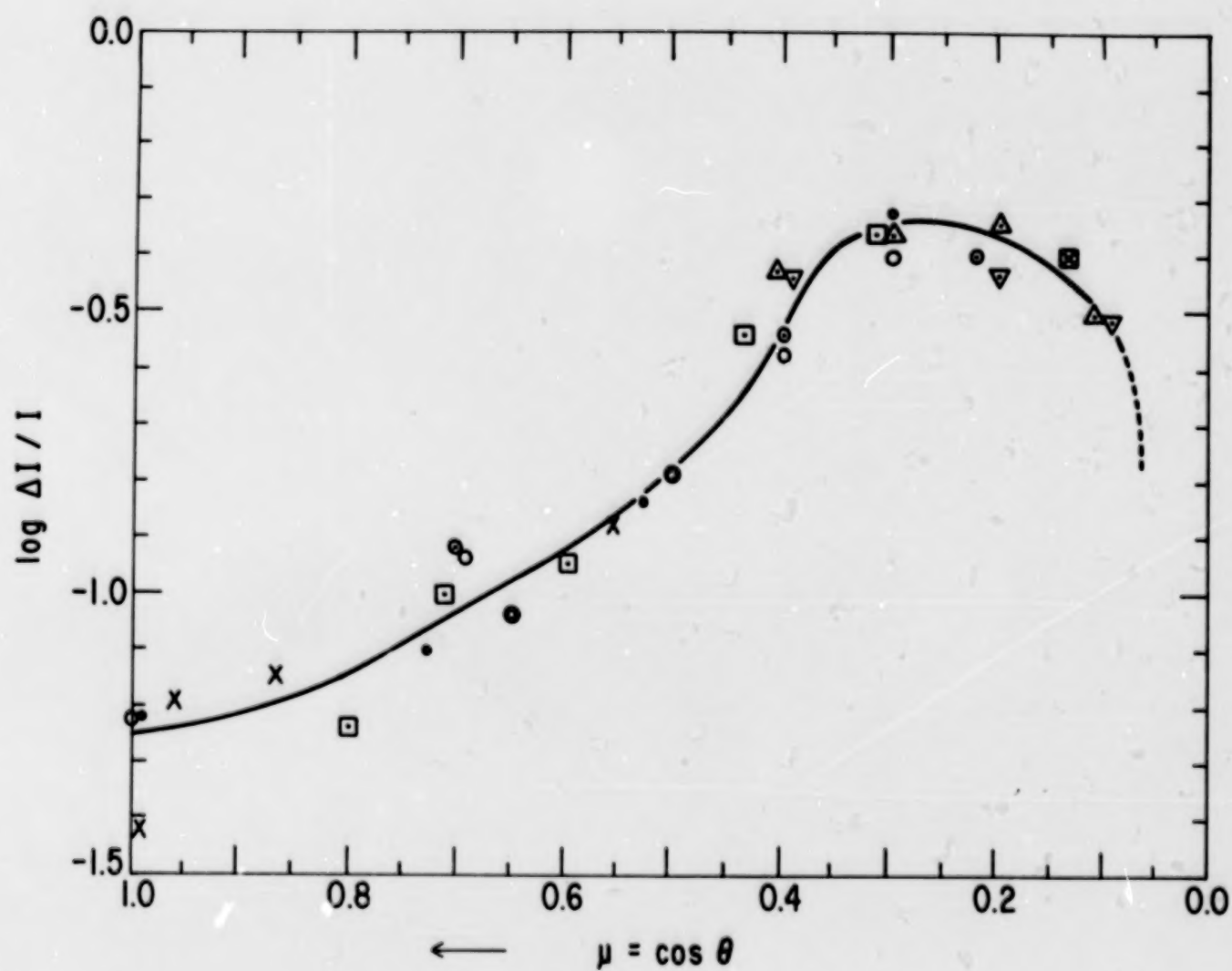
Author	$(I_f - I_p)/I_p$	$\Delta F/F$
Kiepenheuer (ref. 12)	$0.2(1-\mu)/(2+3\mu)$	0.0167
Chapman (ref. 9)	$0.04(1/\mu - 1)$	0.0300
Foukal (ref. 14)	$0.81(a+b\mu+c\mu^2)$	0.0349
	$a = 0.068$ $b = 0.124$ $c = -0.205$	
Sofia et al. (ref. 15)	$a+b\mu+\mu^2$	0.0325
	$a = 0.205$ $b = -0.40$ $c = 0.20$	
	$(I_p = a+b\mu+c\mu^2)$	
	$a = 0.2558$ $b = 0.9732$ $c = -0.2284$	
Hoyt & Eddy (ref. 25)	$0.15/(3\mu+2)$	0.0375
Present compilation	Table 2	0.0301

FIGURE CAPTIONS

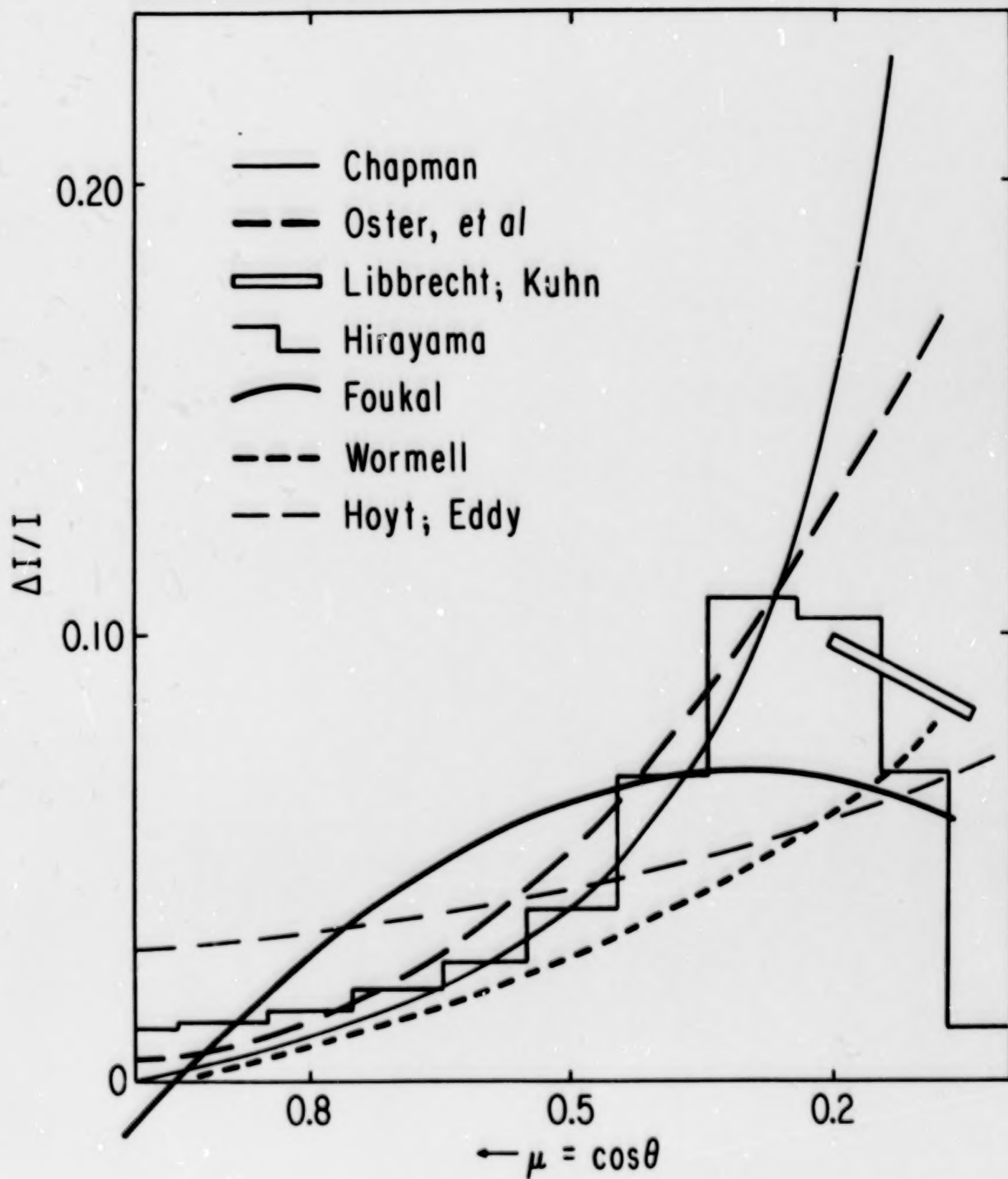
1. Compilation of data on facular contrast, with sources identified in Table 1. The various data have been shifted vertically to provide a best fit, and the corresponding factors are also given in the Table. With the exception of the Stratoscope data, only sources providing observations at two or more values of μ have been considered. Note that the normalization is arbitrary, and that the best fit (Table 2 and Figure 2) has been adjusted by a factor of 0.235.

2. Comparison of the synthetic facular limb-darkening function from Table 2 (dots) with various representations used for modeling solar total irradiance: light line, Chapman (ref. 9); heavy line, Foukal (ref. 14); dashed line, Sofia et al. (ref. 15); dotted line, fit by Kiepenheuer to the early data of Wormell (ref. 20). The modern curves contain multiplicative adjustments to approximate the conversion from high-resolution measurements of contrast to total facular flux, as described in the text and summarized in Table 3.

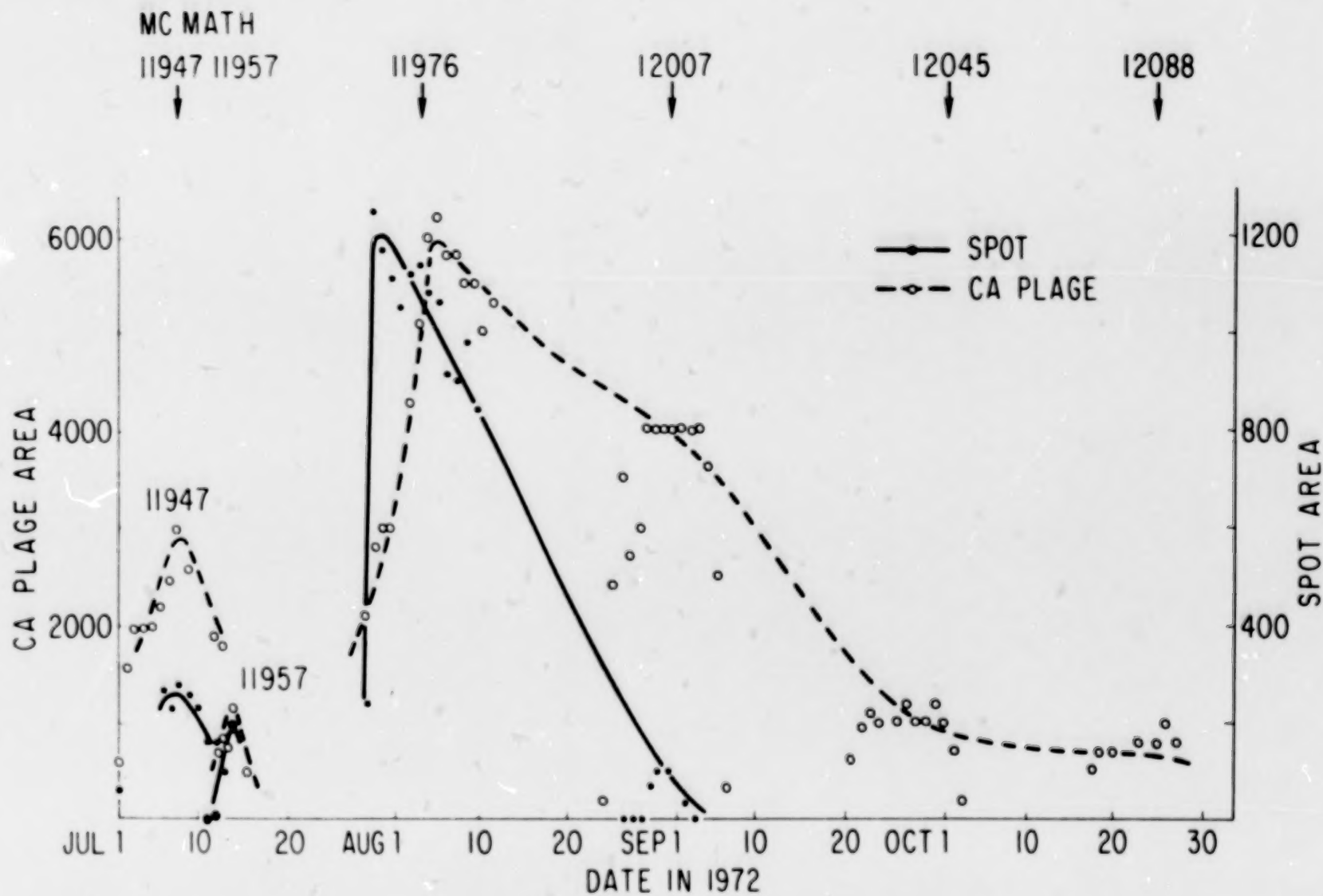
3. Time histories of tabulated synoptic data for plage and sunspot area in a representative active region of 1972, taken from the Solar-Geophysical Data. Areas are plotted in millionths of the solar hemisphere. The time integrals of areas are approximately $6 \times 10^{25} \text{ cm}^2\text{sec}$ for the spots, and $6.4 \times 10^{26} \text{ cm}^2\text{sec}$ for the plage.



BEST COPY AVAILABLE



BEST COPY AVAILABLE



DISCUSSION OF HUDSON PRESENTATION

MOORE: What is the difference between faculae and active network?

ZIRIN: Active network corresponds to dispersed unipolar magnetic regions, faculae corresponds to bipolar active regions.

HEATH: They are not physically different, but are just accounted for differently?

ZIRIN: They are physically different, in that one is old and the other is young.

SOFIA: The facular contrast $\Delta I/I$ near the limb is not important for the solar constant, but is important for the oblateness measurements.

HUDSON: Yes.

SOFIA: The ratio of facular to Ca K plage areas is not known.

HUDSON: Chapman and Hirayama give the ratio as one to four (plus or minus 25%).

SCHATTEN: What facular contrast did Hoyt and Eddy use?

EDDY: We used 3%, independent of the central angle. That value was also varied to see what happens.

GROUND-BASED MEASUREMENTS OF SOLAR IRRADIANCE VARIATIONS

Gary A. Chapman

San Fernando Observatory/CSUN

ABSTRACT

A brief review, is presented, of observing and data analysis programs being carried out at the San Fernando Observatory. A digital analysis of sunspot area from full disk photographs shows an especially good correlation with areas published in the Solar Geophysical Data Bulletin with scale factor near unity. Results are presented from photoelectric photometry of active regions using the Extreme Limb Photometer. These results suggest energy balance between sunspots and faculae. Preliminary results are presented from a new program of photoelectric photometry using a linear array of diodes. Results are presented for the August 1982 passage of a large active region. This active region caused a maximum dip in the quiet sun irradiance of about 800 parts per million.

INTRODUCTION

This review will be concerned with recent attempts to relate solar features to global indicators of solar variability. I will emphasize that work with which I have been associated since other work will be covered by other speakers at this conference. At the San Fernando Observatory/CSUN we have been studying solar activity and its effect on solar variability for several years. Our work is based on photographic and photoelectric work. Photographic work involves the analysis of full disk photographs obtained at SFO or at other observatories. Photoelectric work has been done at SFO with the Extreme Limb Photometer (ELP) as well as diode arrays mounted on the vacuum spectroheliograph. The analysis of the ELP data is the most advanced and I will end my review with some speculations concerning the energy balance of active regions.

ANALYSIS OF PHOTOGRAPHS

Much of the work relating solar activity to spacecraft measurements of solar irradiance variations has been based on estimates of the area of sunspots, published by the National Bureau of Standards, either the Space Environment Services

Center or the World Data Center A. These measurements of sunspot area are incorporated into a fluctuation index such as that due to Hudson, the Photometric Sunspot Index, PSI. The PSI is defined by

$$PSI = a \sum_i S_i \left(\frac{3\mu_i + 2}{5} \right),$$

(ref. 1). The quantity a represents the bolometric effect of the umbra and penumbra of a sunspot, weighted by their relative area.

We have measured the area of selected sunspots during several months during 1980. The photographs were made available from the synoptic program carried out at the Sacramento Peak Observatory. These full disk photographs, on 35mm film are digitized by an Optronics P-1000 with a square spot of 50 μ m spacing. This corresponds to about 6 arc sec on the sky. The data are calibrated assuming a mid-visible limb darkening.

Relative intensities are determined by normalizing with the quiet sun limb darkening. Figures 1a and 1b show the raw digitized image and the calibrated local contrast, $\Delta I/I$, respectively. The computer can then search for sunspot pixels on the "flattened" solar image, count them, and determine their position. In this way we have obtained quantitative measurements of sunspot areas. The position is used to correct for foreshortening in order to obtain sunspot area in millionths of a hemisphere (ref. 2). We have regressed the SESC and SGD areas against the area from our program, FDAP. The results are shown in figures 2 and 3. We find that the data are more complete in the SESC listing than for the SGD listing. For the period of time from 27 February to 15 May 1980, we find that the linear regression $SGD = a + b \cdot FDAP$, gives $a = 4.0 \pm 12.5$ ppm and $b = 0.990 \pm 0.026$ with the linear correlation coefficient $r = 0.975$, where FDAP is the computer-determined area and SGD is the published sunspot area in the Solar-Geophysical Data Bulletin, both areas in millionths of a hemisphere. For this interval the number of data pairs is 78.

For the same period of time, the analysis of SESC data, using $SESC = a + b \cdot FDAP$, gives $a = 30.4 \pm 8.1$ and $b = 0.843 \pm 0.018$ with $r = 0.963$. The number of data pairs is 171. In the case of the SGD data, the mean residual is 81 ppm. For the SESC data, the mean residual is 83 ppm. The distribution of the residuals is not quite gaussian and there may be some nonlinearities in the determination of sunspot areas. There is clearly a significantly different scale factor for the two

sources of data. The SGD data give a slope very near 1.0 but there is more missing data for this compilation. We are performing further statistical tests on the data with large residuals and this aspect will be discussed in ref. 2. These data will also be used to calculate a PSI (ref. 1) to be compared to fluctuations in the ACRIM signal.

Each photograph requires approximately 3 minutes to digitize and approximately 10 minutes of machine time to copy the tape and run the program FDAP. We believe this analysis points to the need and feasibility of providing objective, digital sunspot areas. The determination of facular or plage area may be as important as for spots but more difficult due to the lower contrast and larger area of facular regions. A computer controlled search for faculae will require the highest quality white-light photographs. Several full disk images so far analyzed by the full disk program, FDAP, show significant non-uniformities across the image (figure 1b). These non-uniformities make it very difficult to detect faculae.

ACTIVE REGION PHOTOMETRY WITH THE ELP

Two-dimensional or areal photometry has been carried out with the Extreme Limb Photometer (ELP) of active regions at various disk positions (ref. 3). This photometer has been described in ref. 4 and ref. 5. Measurements reported here were carried out in October 1980 and the summer of 1982. The ELP scans in a circular path using a slit with dimensions 3" by 39". A circular swath across an active region has a resolution given by this slit size. It has been determined that during 1980 and 1982, over 45 active regions were well mapped by one or more swaths with the ELP at a wavelength of 525 nm. The detailed results will be published (ref. 6). The ELP cannot determine the "intrinsic contrast" of sunspots or faculae because of its rather long slit. It can "map" or photometer a complete active region with only a few separate pointings of the telescope. By a knowledge of the position of the swaths, either from a sunspot map, or from the ELP data, the brightness fluctuations of the active region from the separate swaths can be combined into a brightness fluctuation for the entire region, relative to the quiet sun.

An example of several swaths covering an active region is shown in figure 4. This active region was several days from the limb yet the facular emission can be seen to be roughly equal to the sunspot deficit. This effect cannot be explained

by scattered light, since scattering will cause a loss of the positive facular signal as well as the negative sunspot signal. We have found, in general, that sunspots dominate in the central regions of the disk but faculae dominate near the limb.

We have correlated the Photometric Sunspot Index, PSI, (ref. 1), and the Photometric Facular Index, PFI, (ref. 7), with the sunspot and facular signals from the ELP. The PSI and PFI are defined by

$$\text{PSI} = C_S A_S \mu (3\mu + 2)$$

and

$$\text{PFI} = C_P A_P (\mu - 3\mu^2 + 2),$$

where A_S and A_P are the areas of the sunspots and Calcium plage, respectively, in millionths of a hemisphere published in the Solar-Geophysical Data Bulletin. The ELP photometry of an active region has been divided into a sunspot brightness fluctuation, $(\Delta B/B)_S$ and a facular brightness fluctuation, $(\Delta B/B)_F$. The sum of $(\Delta B/B)_F$ and $(\Delta B/B)_S$ gives the net brightness fluctuation of the active region in units of millionths of the quiet sun irradiance, assumed constant.

From an analysis of 45 active regions at various points on the solar disk and at various stages in their lifetime, we find $C_S = 0.164 \pm 0.0083$ and $C_P = 0.0092 \pm 0.0014$. Applying bolometric corrections to these monochromatic contrasts (ref. 4) gives $C_S = 0.143 \pm 0.0073$ and $C_P = 0.0078 \pm 0.0012$.

Integrating PSI and PFI over μ , we find that the flux deficit, per unit area, due to sunspots is 24 times that due to faculae. The area of Ca plage has been found to be approximately 25 times that of sunspots (ref. 8). The near equality of these ratios strongly suggests that there exists energy balance within an active region.

Statistical comparisons with ACRIM data (ref. 9) support the energy balance, which was suggested earlier (ref. 10) from a more extensive statistical analysis of modeled ground-based synoptic data with ACRIM data. Sofia et al. (ref. 10) suggested, implicitly, that the energy balance was rather immediate. The ELP results suggest that there must be energy storage within the active region. I will return to this point in the conclusion.

BEST COPY AVAILABLE

DIODE ARRAY PHOTOMETRY

The use of linear diode arrays allows the photometry of a large area yet with relatively high spatial and spectral resolution. Considerable work with this type of detector has been carried out by Foukal and collaborators (ref. 11,12). The advantages of diode arrays over film are linearity and large dynamic range. At the SFO we are using Reticon S-series arrays. These arrays are reported to have a dynamic range up to $10^4:1$. The results obtained so far from the 1982 data are reported in more detail by Lawrence et al. (ref. 13).

Photometry in 1982 at SFO was carried out, for the most part, in a 1.5A band near 6264A in a continuum region clear of absorption lines in the photospheric and the sunspot spectrum. Placed over the exit port of the vacuum spectroheliograph, the diode array is read out at approximately 5 lines per second. At this speed, we have a dynamic range of about 3000:1 with a signal-to-noise of about 10^3 . The data are converted to a 12-bit binary number and written onto tape for subsequent processing. Some data were also obtained at three other wavelengths, 5245A, 7824A, and 10,000A on some days. These data will be used to determine bolometric corrections.

As a rule, observations were obtained that included the limb and sky. These data will be combined with ELP calibration scans, going out into the sky 2.4 solar radii, to yield corrections for scattered light.

Data for several active regions have been obtained for up to 4 solar rotations. We intend to study the irradiance balance during the disk passage of as many regions as can be identified during the observing season. Analysis procedures have been carried out mainly on one large active region, BBSO no. 18511, from 3-16 August 1982. These data are shown in figure 5. For a more complete discussion see ref. 13. The curve connects daily points from diode array photometry. Several aspects deserve mention: (1) The curve appears to be relatively smooth indicating noise is not overwhelming, (2) the diode array results follow, approximately, the PSI values, indicated by x's, and (3) at both limb transits, there exists a net excess in the irradiance fluctuations, indicating the importance of facular emission. More recent analysis brings the diode array excess up to or higher than the squares, which represent the ELP results.

We see clear evidence, near central meridian passage, for a rapid change in the irradiance deficit, probably indicative

of sunspot evolution. Such changes point out the need for accurate photometry at intervals of less than 1 day, perhaps as little as 6 hours.

CONCLUSION

As discussed, it appears possible that there exists energy balance within an active region between sunspots and faculae. Since there is a considerable difference in the lifetimes of these two phenomena, there must be energy storage. Since sunspots and faculae are, in most cases, magnetically connected it follows that the energy "blocked" by sunspots is stored in the magnetic fields of the active region. Since it is difficult to imagine thermal energy being stored in magnetic flux tubes, I suggest that the energy is converted into magnetic energy (ref. 14) which later is degraded back to heat in the faculae.

The complete understanding of irradiance changes will require improved synoptic ground-based observations, improved in accuracy over current practices and improved in temporal coverage.

REFERENCES

1. Willson, R. C., Gulkis, S., Janssen, M., Hudson, H. S., and Chapman, G. A.: Observations of Solar Irradiance Variability. *Science*, 211, 700, 1981.
2. Chapman, G. A., and Groisman, G.: A Comparison of Published Sunspot Areas with Digitized Full Disk Photographs, in preparation, 1983.
3. Meyer, A. D.: Photometry of Active Regions and Their Relation to the Solar Irradiance Variation, M. S. Thesis, CSUN, August 1983.
4. Chapman, G. A.: Variations in the Solar Constant due to Solar Active Regions. *Ap. J.* 242, L45-L48, 1980.
5. Chapman, G. A., and Klabunde, D. P.: Measurements of the Limb Darkening of Faculae near the Solar Limb. *Ap. J.* 261, 387-395, 1982.
6. Chapman, G. A., and Meyer, A. D.: Photometry of Active Regions and Solar Irradiance Variations, in preparation 1983.
7. Chapman, G. A., and Meyer, A. D.: Comparison of Estimated and Observed Active Region Intensity Balance, *B.A.A.S.*, 14, 573, 1981.
8. Foukal, P., and Vernazza, J.: The Effect of Magnetic Fields on Solar Luminosity. *Ap. J.* 234, 707, 1979.
9. Chapman, G. A.: On the Energy Balance of Solar Active Regions, submitted to *Nature*, 1983.
10. Sofia, S., Oster, L., and Schatten, K.: Solar Irradiance Modulation by Active Regions during 1980. *Solar Phys.* 80, 87-98, 1982.
11. Foukal, P. V., Mack, P. E., and Vernazza, J.E.: The Effect of Sunspots and Faculae on the Solar Constant. *Ap. J.* 234, 707, 1979.
12. Fowler, L. A., Foukal, P., Duvall, Jr., T.: Sunspot Bright Rings and the Thermal Diffusivity of Solar Convection. *Solar Phys.* 84, 33, 1983.

13. Lawrence, J. K., Chapman, G. A., Herzog, A. D. and Shelton, J. C.: Two-Dimensional Photometry of Active Regions. Workshop on Solar Variability on Active Region Time-Scales, NASA CP - _____, 19____. (Paper _____ of this compilation).
14. Wilson, P. R.: Theories of Sunspot Structure and Evolution. The Physics of Sunspots, L. E. Cram and J. H. Thomas, eds., Sunspot, New Mexico, 83-92, 1981.

FIGURE CAPTIONS

Figure 1(a). Printer plot of digitized full disk photograph for 7 April 1980 from Sacramento Peak Observatory (L. Gilliam). The film density is represented by symbols. (b) Printer plot of calibrated contrast relative to published limb darkening (ref. 2).

Figure 2. A linear regression of the published sunspot areas, published in the Solar Geophysical Data Bulletin (SGD) versus the areas from the Full Disk Analysis Program (FDAP) using synoptic "white-light" images from the Sacramento Peak Observatory.

Figure 3. A linear regression of SESC sunspot areas, published in the weekly forecasts of solar activity. The linear regression coefficient is further from unity than in the first case but the number of data pair are twice as great.

Figure 4. Adjacent scans with the Extreme Limb Photometer (ELP) across active region 18474 on 20 July 1982. The scans are displaced for clarity.

Figure 5. Monochromatic brightness fluctuation of active region BBSO #18511. The brightness fluctuation, $\Delta B/B$, is the net fluctuation faculae minus sunspot, in units of millionths of the quiet sun irradiance. The preliminary diode array results are open circles connected by solid lines (the dashed line bridges a missing day). The error bars are ± 1 standard deviation except where only two observations have been examined in which case the error bars are the separation of the two data points from the mean (6 Aug. 82). Where no error bars are shown, they are within the circle (these are formal errors and do not include any systematic errors). The open squares represent results from the ELP corrected to this wavelength, 6264 Å. Recent improvements in the quiet sun limb darkening have raised the diode array results, near the limb, to or above the ELP data points shown here. The other symbols are discussed in ref. 13.



Figure 1(a)

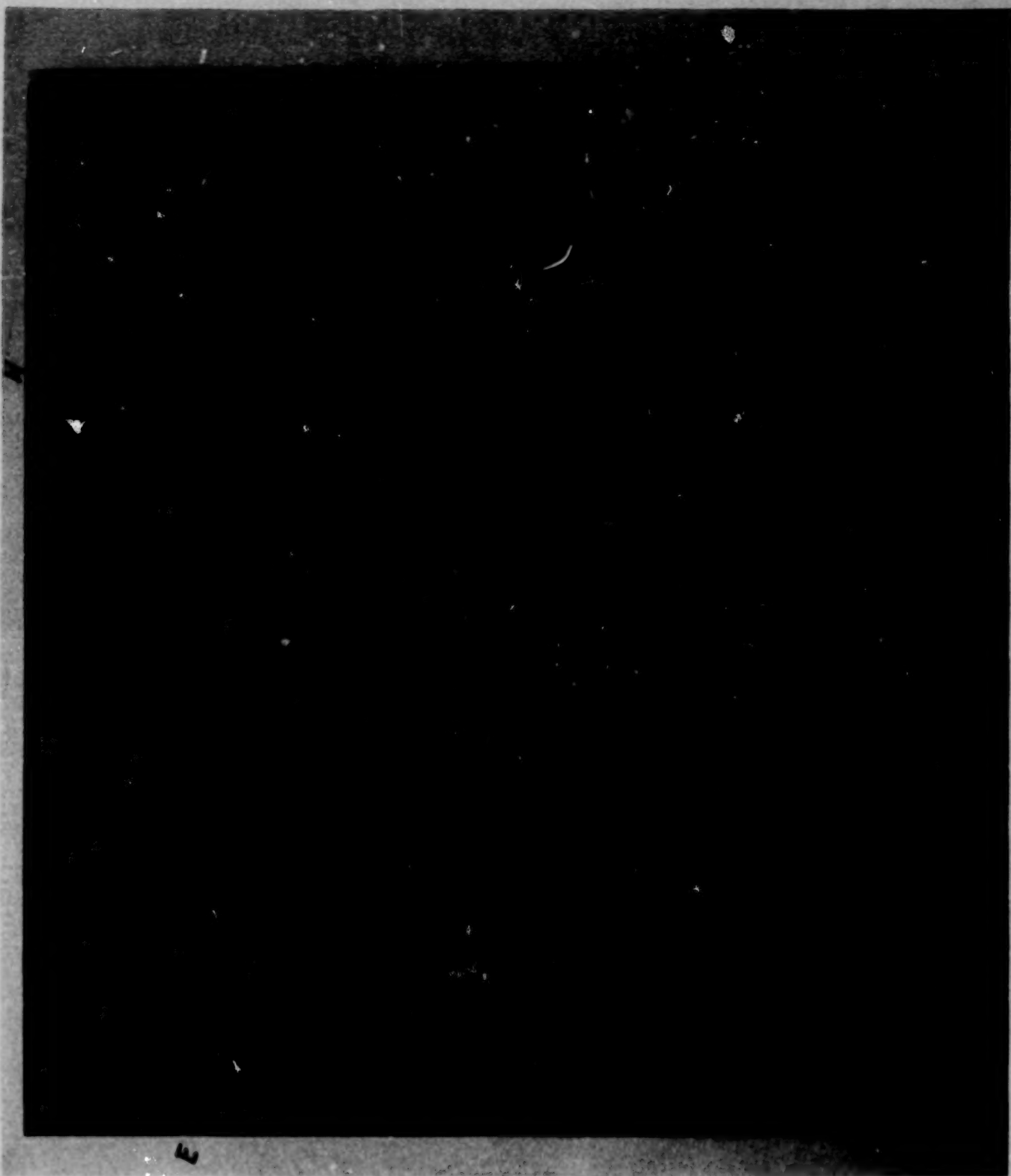


Figure 1(b)

POINTS 78

Y INTERCEPT 3.96

S.D 12.539

SLOPE 0.99

S.D 0.026

LINEAR CORR. 0.9748

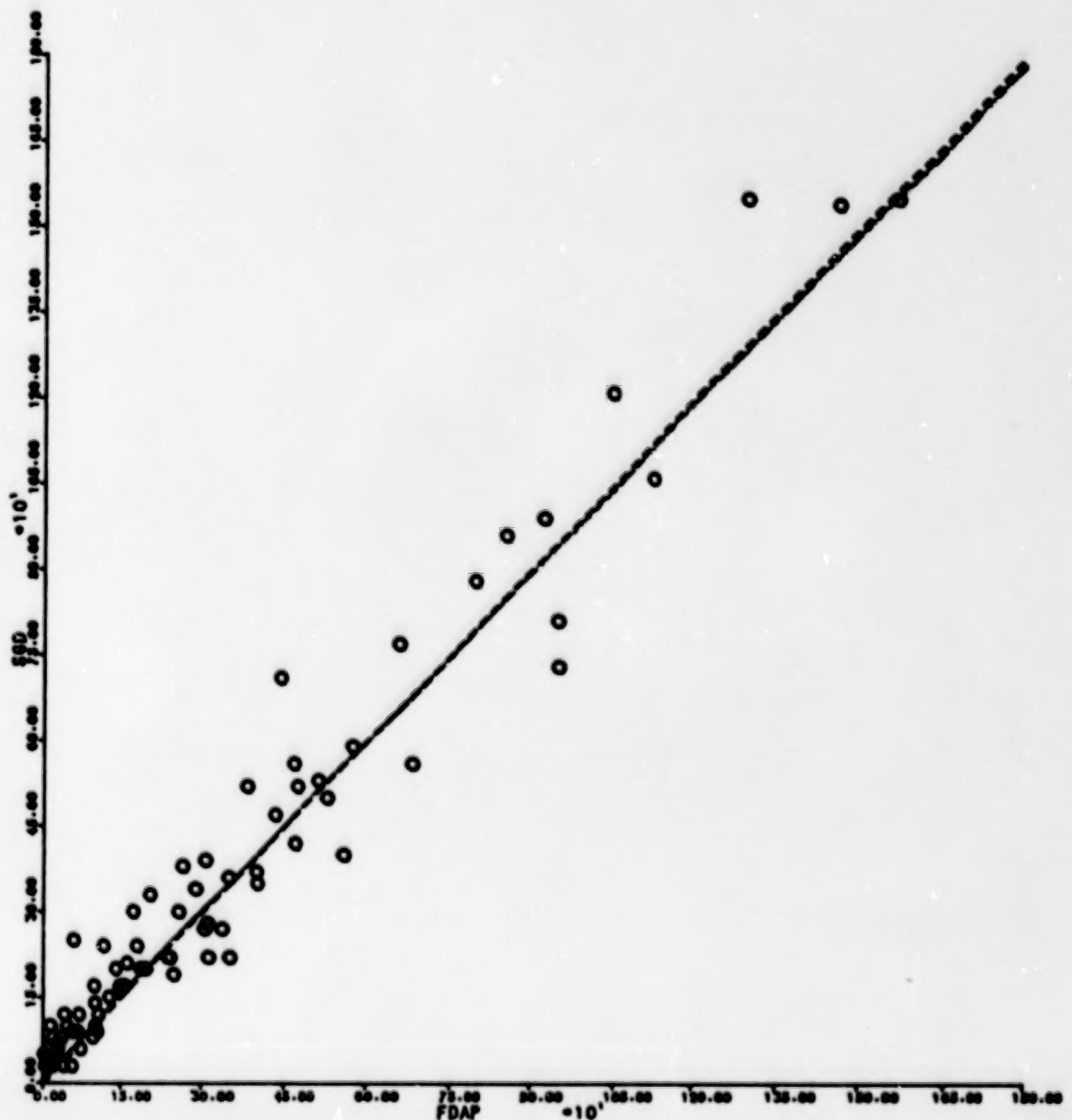


Figure 2

POINTS 171

Y INTERCEPT 30.43

S.D 8.114

SLOPE 0.84

S.D 0.018

LINEAR CORR. 0.9628

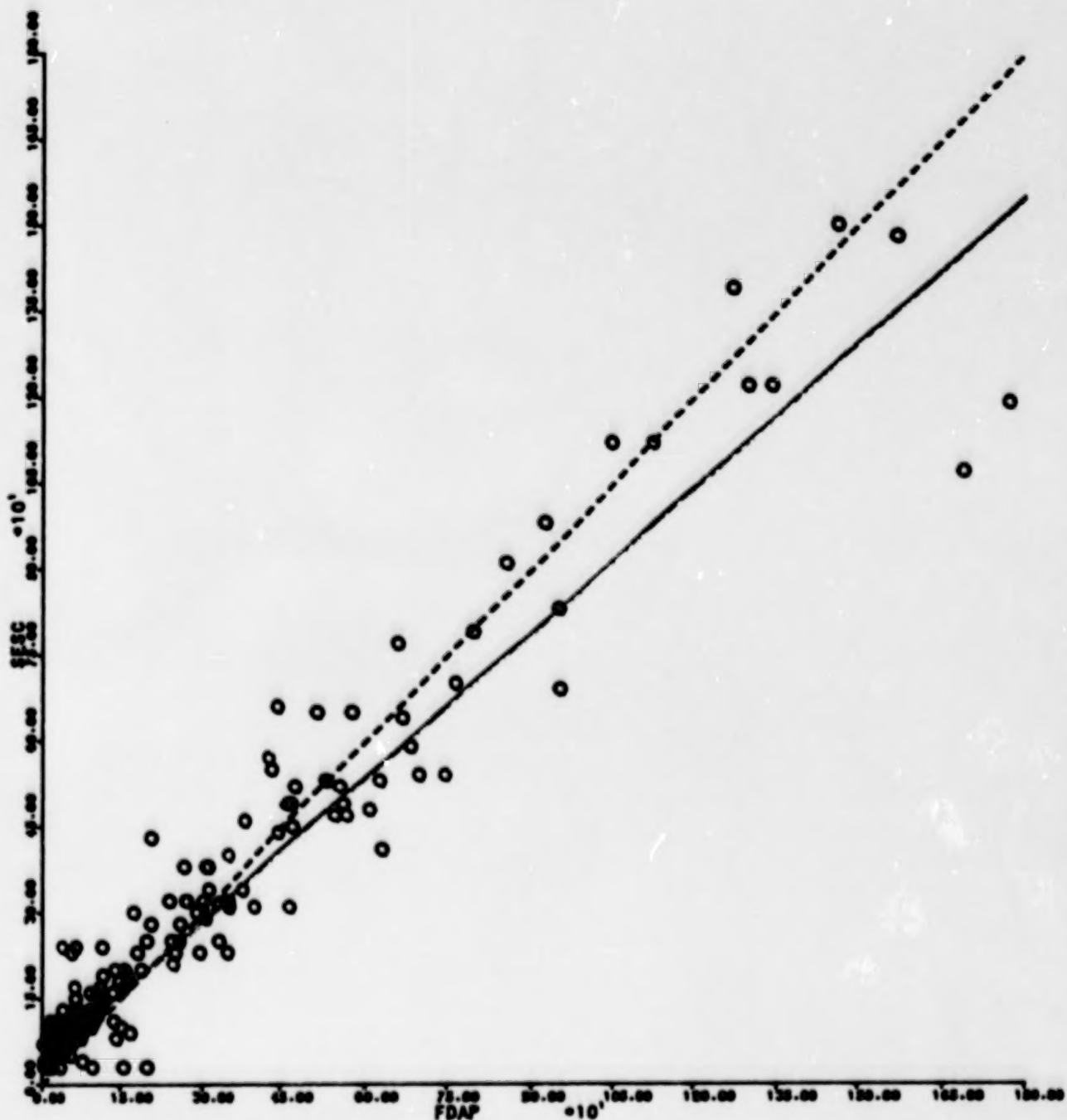


Figure 3

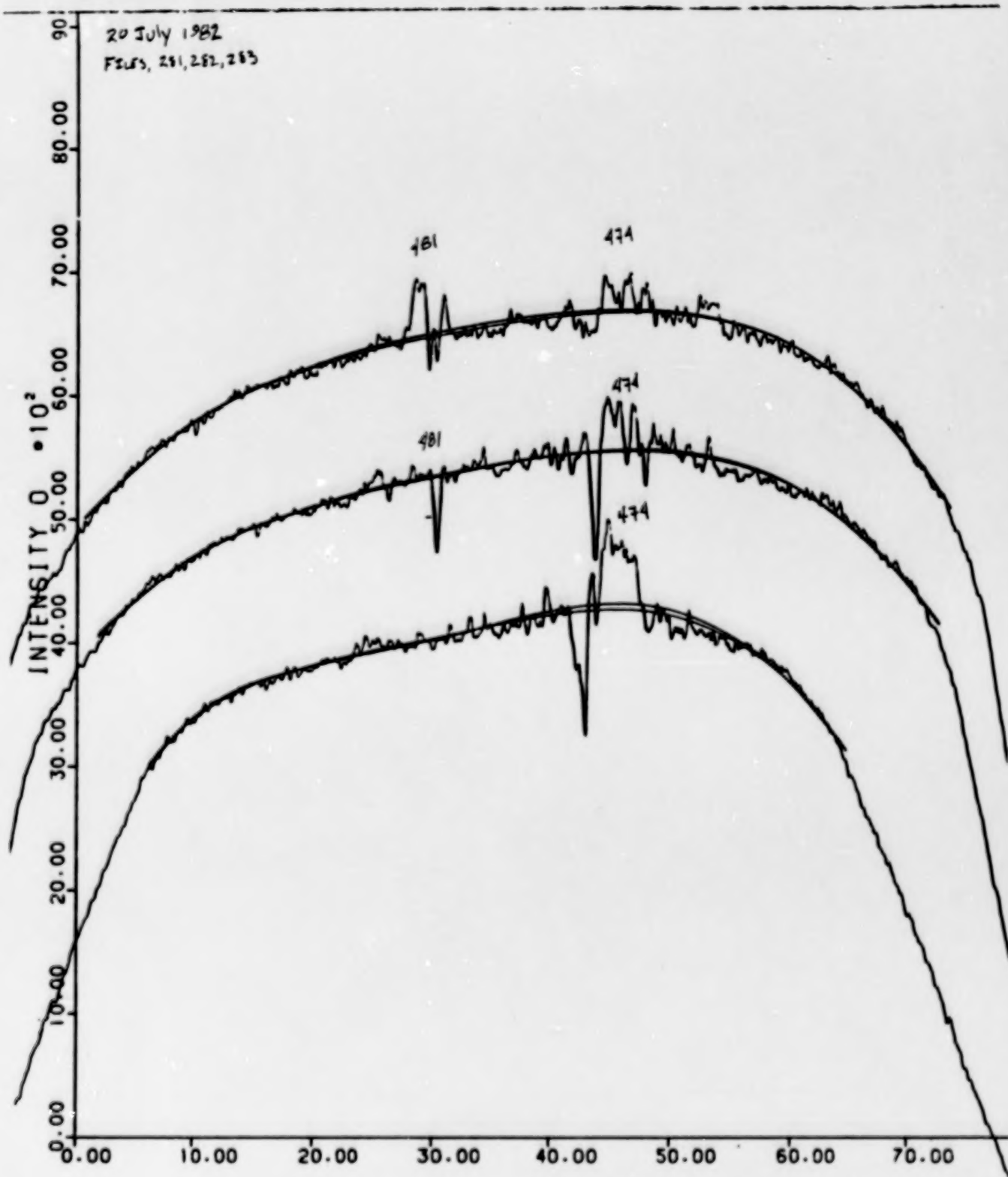


Figure 4

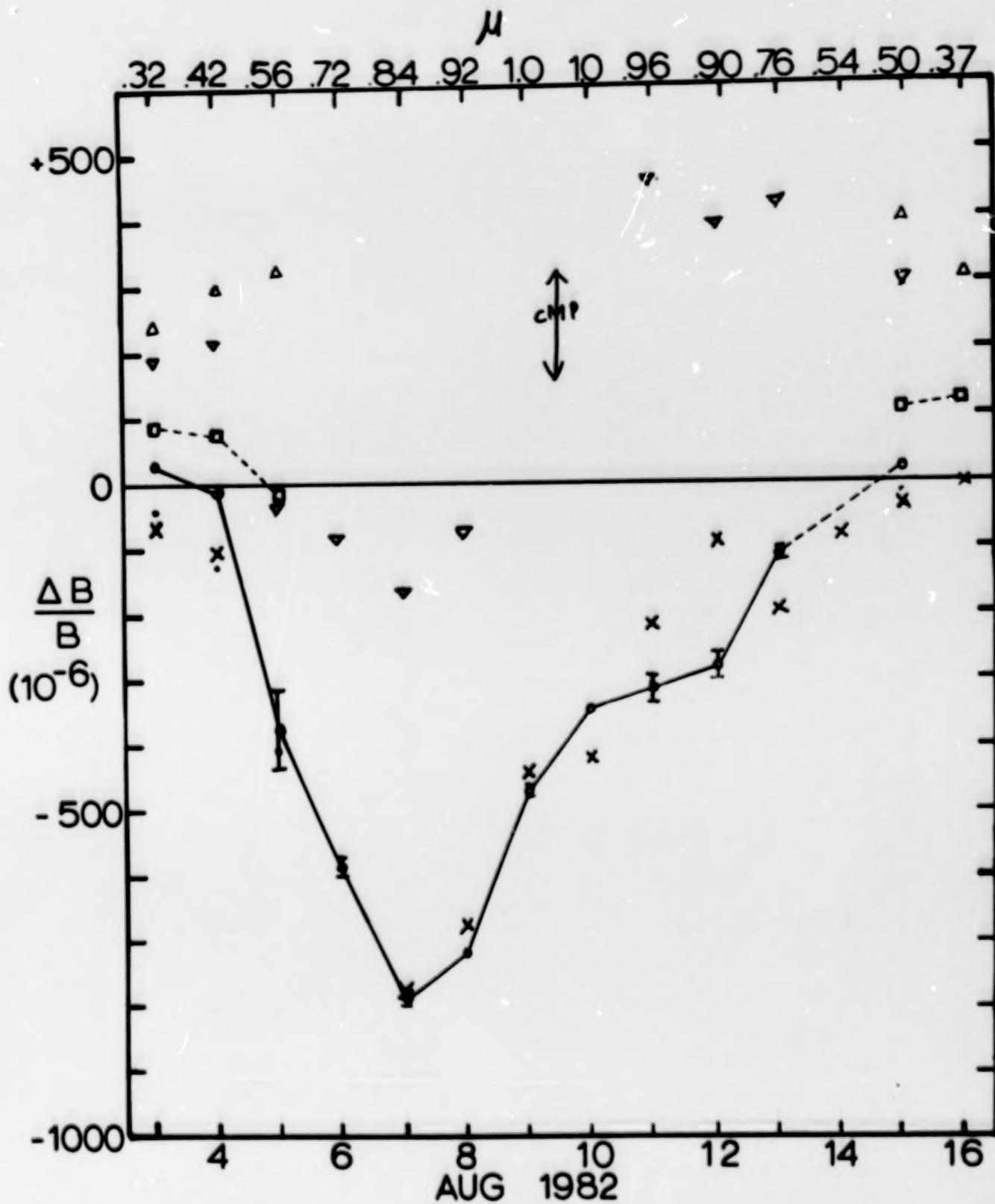


Figure 5

DISCUSSION OF CHAPMAN PRESENTATION

RABIN: How large are the photographic density gradients across the image?

CHAPMAN: Seven percent.

SKUMANICH: Does scattered light affect the conclusion that the facular emission outweighs the spot deficit?

CHAPMAN: No.

MOORE: But this is only true very near the limb.

CHAPMAN: The spot wins out three to four days from the limb. The spot loses at one day from the limb.

FOUKAL: Scattered light and seeing will change this result by a factor of two.

CHAPMAN: No, the measured intensity is an integral over the 38 arc second slit length, so we do a set of scans and just sum. We use an area of 200 by 200 arc seconds, so nearby scattering doesn't matter.

FOUKAL: It depends on the measured area of the spots and faculae.

CHAPMAN: We don't measure the areas, just sum the intensities.

FOUKAL: Then it depends upon the zero level.

CHAPMAN: The zero level is unknown to a few percent.

FOUKAL: Then you can't know the true total well.

MOORE: Do faculae look dark at disk center in the continuum?

CHAPMAN: No, but the data aren't good enough.

FOUKAL: How deep is the spot if magnetic energy is to match the energy not emitted?

CHAPMAN: The depth of the convection zone.

FOUKAL: That's pretty large!

HUDSON: It depends on the variation of the field strength with depth.

HEATH: Since an observer at the poles can see faculae in the active latitudes better than the spots, there is a net excess of emission from the Sun toward the polar directions, which must affect the spot-faculae balance.

HUDSON: The angular dependence of the emission is included in the integrals.

NEWKIRK: What bandpasses do you use?

CHAPMAN: We have three or four filters from UV to the near IR.

SCHATTEN: I don't see how kinetic energy gets transformed into magnetic energy.

CHAPMAN: There is no model, but it is inferred from the balance of the spot and facular emission.

SCHATTEN: Why don't the spots just keep growing bigger and bigger?

CHAPMAN: I don't know.

BLANK PAGE

TWO-DIMENSIONAL PHOTOMETRY OF ACTIVE REGIONS*

J. K. Lawrence, G. A. Chapman and A. D. Herzog
San Fernando Observatory
Department of Physics and Astronomy
California State University, Northridge

J. C. Shelton
TRW, Inc.

ABSTRACT

We describe a set of two-dimensional photometric images of solar active regions (AR's). Preliminary analysis of the data is described, and estimates are presented of the contribution of an AR to total solar irradiance variations during its 1982 August 3 - 16 disk passage. Results indicate an excess contribution near the limb and a deficit away from the limb. Also apparent is an evolutionary change in the AR which can be represented as a decrease in sunspot area. Future plans are also discussed.

OBSERVATIONS

Our purpose in this contribution is to characterize two-dimensional photometric data we have taken with the San Fernando Observatory (SFO) Reticon, a 512 element linear diode array system, and to describe the results we are now beginning to achieve on the contributions of active regions (AR's) to variations in the total solar irradiance.

The observations are carried out with the SFO 28 cm vacuum solar telescope and vacuum spectroheliograph (SHG). The SHG exit slit is set on a clean continuum portion of the solar spectrum at 6264 \AA with a bandwidth of 1.5 \AA . This wavelength band was selected for its freedom from both photospheric and sunspot absorption lines. It is also conveniently close to the 6303 \AA line used for other studies. The diode array, mounted at the exit slit, produces 512×512 pixel images as the entrance slit is swept across an AR. The images are stored on magnetic tape using one of SFO's two Varian 620i computers with 12 bit precision per pixel. With this arrangement the pixel spacing is $0.94''$ allowing pictures with resolution $> 2''$ and a field of view of $480''$. The scanning time per picture is 104 sec, and scans can be repeated at intervals as short as 2 min. Typically intervals greater than 20 min were used between scans of a given region, to randomize the signal from granulation patterns. The observations were repeated for up to 4 hours near local noon so that later digital averaging could suppress the effect of transient features and enhance the signal-to-noise ratio of subtle brightness structures. Short calibration scans were included frequently to record both the dark current response of the diodes and sunspot-free photosphere near disk center. The solar limb and nearby sky were observed periodically. Occasionally, observations were made of

* This work was supported in part by NSF Grant No. AST-8121863.

sunspot fine structure with the SFO 61 cm vacuum telescope, which provided a pixel spacing of 0.42". A few observations were made at other wavelengths to obtain color/temperature information on various AR components. These observations were made in the IR at 10000 Å, in the red at 7824 Å, and in the green at 5254 Å. Some AR scans were also made in the Ca II line at 8662 Å.

Except when interrupted by bad weather or equipment failure, observations were made continuously from 1982 July 8 to October 23, a period including 5 solar rotations. Coverage during the full interval was 80/112 days or 71%. Better weather earlier in the summer permitted 87% coverage from July 8 to September 12. On the average, observations were made of ~5 AR's per day (range 0 - 9) with an average of ~5 scans/AR/day. Note that AR's near the limb require fewer scans because of their greater facular contrast coupled with a somewhat lower granulation contrast. Several regions have been observed on as many as four disk passages.

An example of a 512 x 512 digital picture of an AR is shown in Fig. 1.

DATA REDUCTION

Reduction of a digital picture like that in Fig. 1 to a value for the AR's contribution to a solar irradiance deficit or excess requires several steps, not all of which have yet been carried out. For example, no corrections have yet been applied for scattered light or for color differences between AR components. The results presented here must therefore be regarded as preliminary.

Raw data are first corrected for differing responses of the individual array diodes by means of dark (shutter closed) and bright (spot-free, disk center) calibration scans. The quantity (observed - dark)/(bright - dark) is normalized to an arbitrary value of 200 units at hypothetical disk center. Then data are square averaged down to make a 256 x 256 pixel array.

The next series of steps corrects the data for limb darkening. Using Mt. Wilson sunspot drawings a first estimate is made of the location of solar disk center in pixel coordinates. Then each pixel is divided by a calibrated quiet sun (QS) brightness obtained from a Pierce and Slaughter 5th-order polynomial limb-darkening curve (Ref. 1) which has been interpolated to our wavelength (6264 Å). Disk center coordinates are then re-adjusted to give the best fit (flat background), and, if necessary, the zero level is adjusted to bring this level to the arbitrary 200 unit value. After this, pixels with values below, within, or above the range 193 - 207 units ($\pm 3.5\%$ of the average value) are assigned to "sunspot", "photosphere", or "faculae" categories, respectively. This offers a number of quality-of-fit parameters, such as the relative numbers of pixels assigned to the three categories, or the standard deviations of the pixel values within each of the categories. Also, a correction factor is determined to bring the average of the "photosphere" pixels back to 200 units.

At this point it is possible to subtract the theoretical limb darkening from the calibrated data pixels. The residual values are then summed and the result expressed in parts per million (ppm) of the total QS brightness. The process is repeated for up to four same-day pictures of the AR, and an average of the results is obtained.

RESULTS

The procedure we have described was carried out during the passage of Big Bear AR No. 18511 across the solar disk from 1982 August 3 to 16. The results are shown in Fig. 2. The average deficits and excesses are plotted as circles with error bars (Φ) signifying the standard deviations of the means of these averages, in ppm of QS. No results are available for August 14 or 16. In cases where no error bar appears, the formal error is smaller than the plotted circle.

Also plotted in Fig. 2 are a number of other measures of the effect of ARs on solar irradiance. All are in the same units. Plotted as small squares (\square) are irradiance deficits and excesses for AR 18511 as measured by the SFO extreme limb photometer (ELP) described in (Ref. 2). Plotted as dots (\cdot) are the sunspots-only (faculae ignored) contributions measured by the ELP. Plotted as x's (x) are daily values of the AR photometric sunspot index (PSI) based on sunspot areas A, in ppm of the solar hemisphere, published in Solar Geophysical Data and corrected for limb darkening according to

$$\text{PSI} = -0.164 A_{\mu}(3\mu + 2), \quad (1)$$

where $\mu = \cos \theta = (0,1)$ at (limb, disk center). See Ref. 3. Inverted triangles (∇) in Fig. 2 represent differences between the diode array results and a PSI figure based on a constant area sunspot with its area normalized to fit the central meridian data. Right-side-up triangles (Δ) represent the difference between the ELP results and the constant-area PSI values.

DISCUSSION

As can be seen in Fig. 2, the diode array results show contributions to an excess irradiance when the AR is near the limb ($\mu \lesssim 0.5$) and a deficit when it is away from the limb ($\mu \gtrsim 0.5$). This is expected because of the known enhancement of facular contrast near the limb. The ELP results show greater excesses than do the diode array results. This may be caused in part by the fact that the diode array calculations have been stopped several arc seconds from the limb, so some facular contributions have been left out. We are currently trying to improve limb darkening fits so that this situation may be improved. The ELP - diode array discrepancy on August 5 ($\mu = 0.56$) may be more difficult to reconcile.

Our belief in the reliability of the diode array results is increased by their reasonable agreement with the PSI values from published sunspot areas. It should be kept in mind, of course, that, by definition, PSI can never show an excess irradiance. Note, however, the close agreement of the PSI values with the ELP results with faculae excluded. This indicates that in reconciling results near the limb we will more probably end up adjusting the diode array calculations.

The asymmetry of the diode array deficit about central meridian passage can be interpreted as a decrease with time in the AR sunspot area. Values near the limb appear to be influenced by facular effects, so to study AR

evolution we here consider only values for August 5 - 13. The deficits are converted to effective sunspot areas by inverting the equivalent of Eq. (1). These areas show a decreasing trend that can be approximated as linear. A regression analysis gives a slope for this of $dA/dt = -137 \text{ ppm/day} = -5 \times 10^9 \text{ m}^2/\text{s}$. Note that this is about an order of magnitude faster than published decay rates for long-lived sunspots (Ref. 4). This effect, together with the fact that sunspots alone can not show irradiance excesses, is also illustrated by the plot of differences between diode array values (V) and ELP values (Δ) on the one hand versus the constant disk sunspot model on the other. The asymmetry illustrates the convolution of AR evolution effects with projection effects in our observations.

Our hope is to be able to separate these effects so that we will be able to determine the dependence of the brightness and color of the various components (e.g., sunspots, faculae) of ARs. We would then hope to be able to determine the contribution of ARs to solar irradiance as a function of their full evolution. We may then be able to determine the relative contributions to energy balance of sunspots vs faculae over the complete lifetime of an AR.

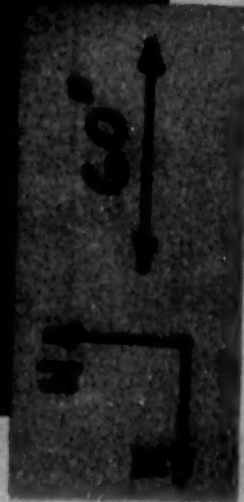
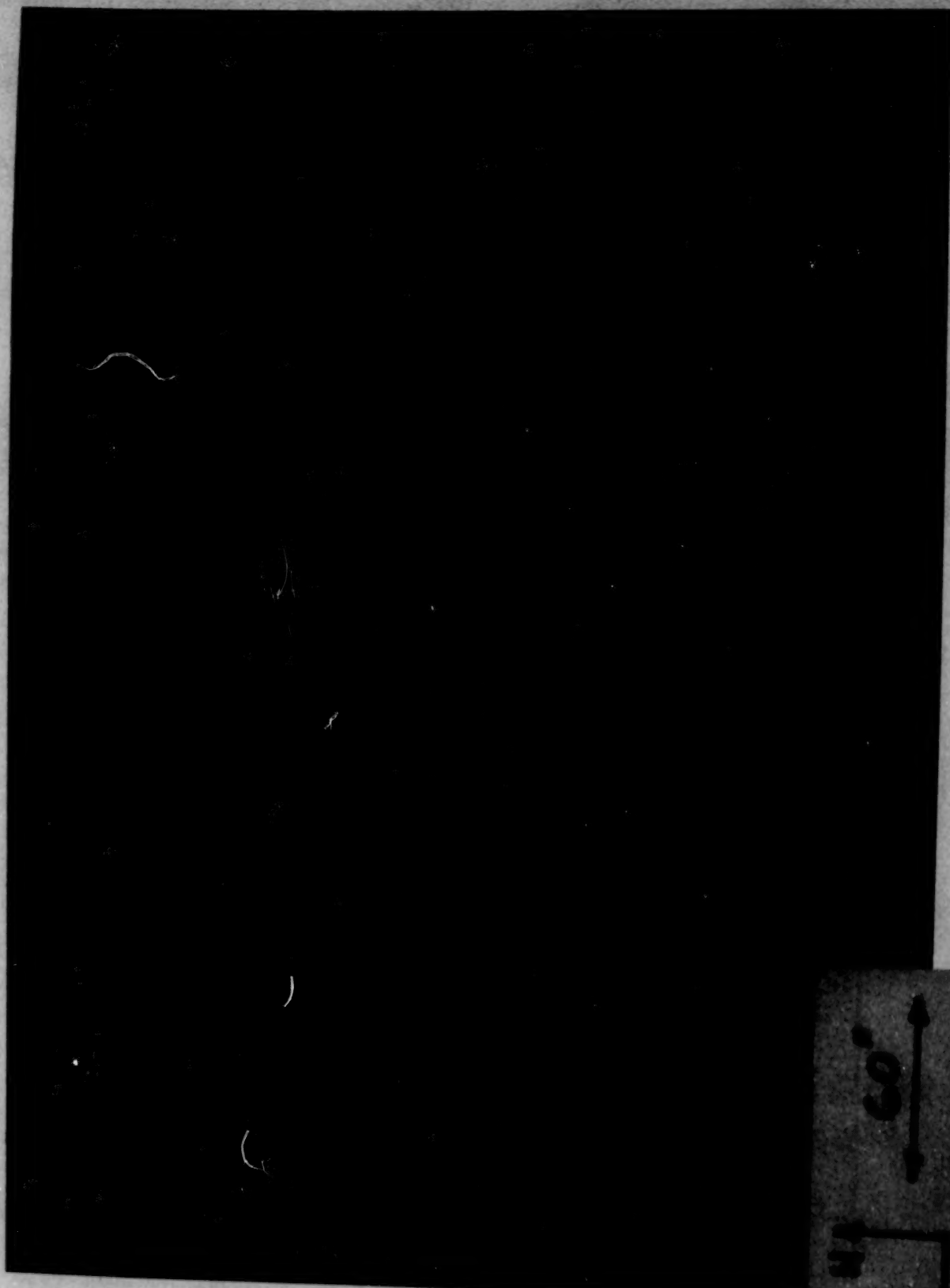
As stated above, we have observations of ARs like 18511 on 4 disk passages, and we have observed regions where ARs have recently disappeared to search for residual faculae. On the other hand, it will be necessary to acquire further multi-color data, and the formidable problems of fitting darkening near the limb and of corrections for stray light have not yet been fully faced.

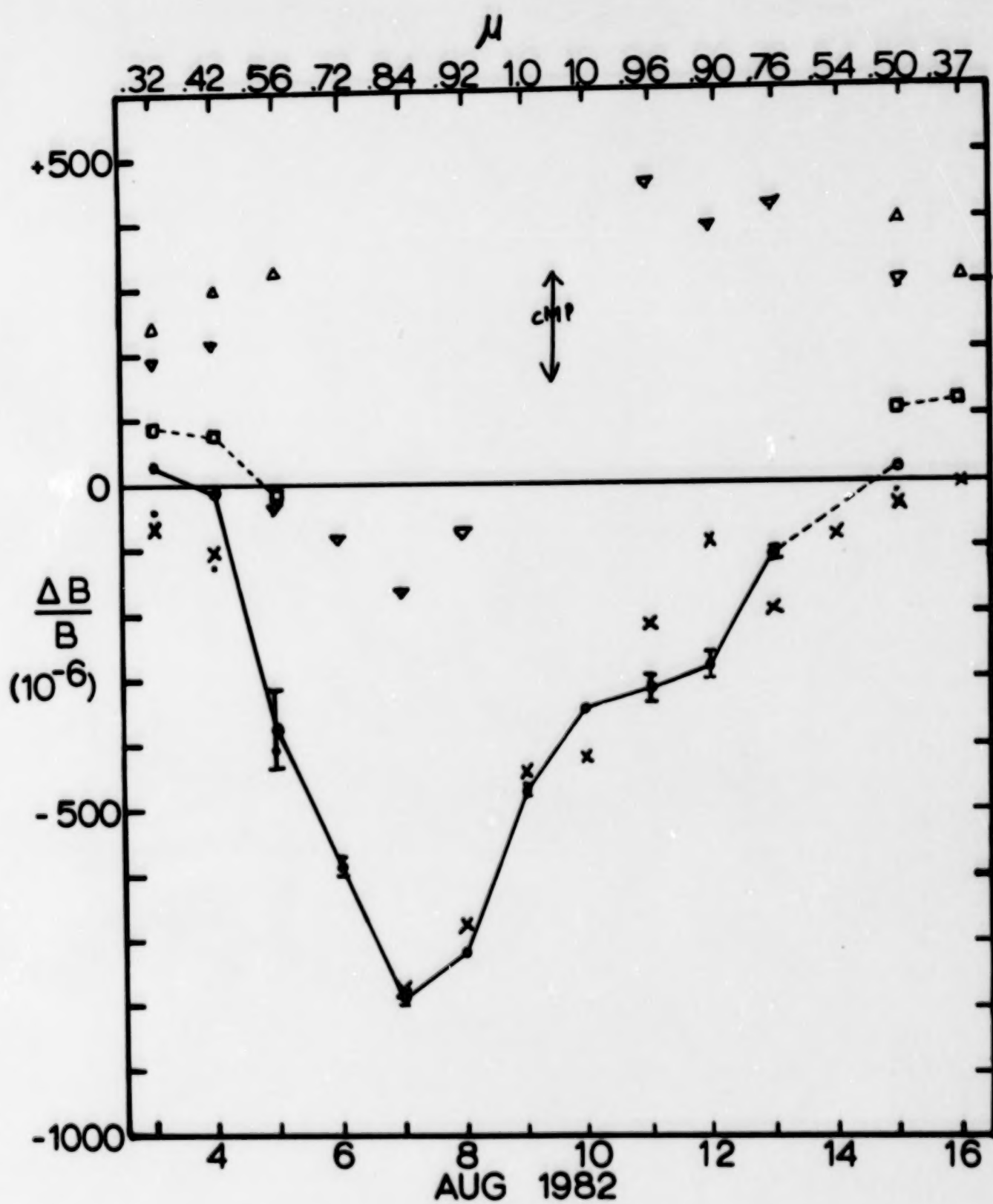
REFERENCES

1. Pierce, A. K. and Slaughter, C. D.: Solar Limb Darkening I: $\lambda\lambda(3033-7297)$. Solar Physics, vol. 51, no. 1, Jan./Feb. 1977, pp. 25.
2. Chapman, G. A.: Ground-Based Active Region Photometry. Workshop on Solar Irradiance Variation on Active Region Timescales NASA CP _____, 19 _____. (Paper _____ of this compilation.)
3. Willson, R. C., Gulkis, S., Janssen, M., Hudson, H. S. and Chapman, G. A.: Observations of Solar Irradiance Variability, Science, vol. 211, no. 4483, 13 Feb. 1981, pp. 700.
4. Cowling, T. G.: The Growth and Decay of the Sunspot Magnetic Field. M.N.R.A.S., vol. 106, 1946, pp. 218.

FIGURE CAPTIONS

1. Diode array digital image of Big Bear AR No. 18511 made 1982 August 8 with the SFO 28 cm vacuum telescope.
2. Contributions to irradiance deficit or excess in ppm due to Big Bear AR No. 18511 during the disk passage of 1982 August 3 - 16. Details are described in the text.





PHOTOMETRIC STUDIES OF HEAT FLOW AT THE PHOTOSPHERE

Peter Foukal
Atmospheric and Environmental Research, Inc.
840 Memorial Drive
Cambridge, Massachusetts 02139

Abstract

This paper summarizes three years of continuum photometry carried out at KPNO, and the results of comparing these observations with models of photospheric heat flow developed at AER. The main results so far are; a) a possible detection of weak ($\sim 0.2\%$) bright rings around some spot penumbrae implying that the eddy thermal conductivity K near the photosphere calculated from mixing length models might be significantly too large, b) no evidence is found for large scale ($5 \times 10^4 \text{ km} < L < 2.5 \times 10^5 \text{ km}$) photospheric brightness inhomogeneities exceeding 2-3 K; this appears to place tighter constraints on models of global scale convection than do previous observational limits on a pole-equator temperature difference, c) supergranular-scale continuum structures observed across the photosphere appear mainly due to random clumping of granules, but the spatial structure of 5-minute brightness oscillations may also contribute to this pattern, d) the one case observed of a sunspot emergence shows no "thermal shadow" exceeding 1.5 K rms one day prior to umbra appearance; rough calculations on the depth and scale of the spot at that time suggest values of K consistent with those predicted by Spruit's (1974) convection zone model, and higher than the Baker and Temesvary (1966) model, e) network and faculae are found to show a small ($\sim 0.1\%$) excess brightness even at $\mu = 1$, so our earlier detection of faculae at $\mu = 1$ by differential photometry seems to indicate a gentler temperature gradient near $\tau = 1$ in the facular (relative to cell) atmosphere. It does not mean that T_{eff} is lower in faculae in clean continuum as we originally believed, f) our limb-darkening study shows no significant global variations to within 0.1% rms over $0.2 < \mu < 1$ between 1980 and 1982. Earlier variations we reported (Rosen et al. 1982) were caused by facular noise. This lack of variation between 1980-82 rules out a change in ∇T near $\tau = 1$ as large as that reported by Livingston and Holweger between 1976-1980 from line strength variations.

1. Introduction

The main subject of this overview is the photospheric photometry we have been carrying out at KPNO since 1980. I will also mention some results obtained from comparison of the photometry with a time-dependent model of heat flow developed at AER for interpretation of sunspot effects on solar luminosity.

The observations divide naturally into two areas; two-dimensional photometry of the solar active latitudes, and one-dimensional photometric scans to study possible slow changes of the solar limb-darkening function. The two dimensional photometry has been carried out with L. Fowler at AER, and in collaboration with T. Duvall and B. Gillespie at KPNO. Some of the solar structures we have investigated or searched for in continuum radiation include faculae and network, bright rings around spots, thermal shadows preceeding sunspot formation, large convective cells and supergranular convection.

The one-dimensional photometry has been carried out for the past 3 years at the McMath telescope in collaboration with W. Rosen of Vassar and AER, K. Pierce at KPNO, R. Kurucz at SAO, and L. Petro at AER. This paper is intended to review some published results, correct and extend these in the light of recent findings, and suggest some future directions we intend to pursue. Two papers in preparation (Foukal and Fowler 1983, and Petro et al. 1983) describe our recent work in the 2-D photometry and limb-darkening respectively. The reader is referred to these for a more detailed account of the procedures and results summarized here.

2. Two-Dimensional Photometry

a) Instrumentation

The KPNO vacuum telescope and 512-channel magnetograph have been used to generate continuum raster pictures of the solar active latitudes at a scale of one arc-sec per pixel. Each raster picture covers 512×2048 arc sec and requires roughly 10 minutes. The spectrograph is used to isolate a narrow (~ 0.25 Å) passband of clean continuum, most frequently at $\lambda 5256$. Details of the instrumentation and procedures have been given by Foukal, Duvall and Gillespie (1981) and Foukal and Fowler (1983). Some recent runs have been performed via long-distance telephone link between the KPNO vacuum telescope and AER in Cambridge.

b) Reduction

The first step in reduction of the photometric raster pictures is removal of limb-darkening to the level of 0.1%. This is a difficult task; the best scheme we have found is based on generating a limb darkening template from all the data in a run of typically 5 days length. Sunspots and bright faculae are removed from the data a priori. This template removes the need to approximate the shape of photospheric limb-darkening with polynomial fits, which tend to produce low-amplitude rings after subtraction from individual scans.

Subsequent steps involve i) correction of successive scans spaced by 10 mins for mean solid-body solar rotation, ii) summation of up to 10 successive scans of the N or S active latitude belt on a given day, iii) final de-streaking to remove diode variations across the 512-element array.

c) Summary of Results

Fig. 1 shows a photometric raster picture of the active latitudes on May 22, 1982. The 1 arc sec data have been degraded to 4 arc sec, and ten successive scans have been summed to generate this picture. The grey-scale has been adjusted to cover a dynamic range of $\Delta I/I = 2.6\%$, or $\Delta T/T = 40$ K. On this highly expanded brightness scale, sunspots are completely saturated dark, and the brightest limb faculae lie outside the upper limit of the scale.

Continuum Mottles

The most conspicuous feature is a pattern of mottles of scale and shape reminiscent of the CaK network. However, investigation (Foukal and Fowler 1983) of the poor spatial correlation with magnetic network near sun center, and of the temporal autocorrelation of these mottles (yielding a time-scale of 5-10 mins) shows that this resemblance is illusory. In fact, numerical simulations we have performed show that a field of spatially independent random brightness oscillators might reproduce the basic morphology of the large-scale mottles through spatial smoothing of granules by a plausible instrumental profile. This indicates that the supergranule-sized mottles we see in Fig. 1 do not necessarily require any physical mechanisms (beyond instrumental smoothing) that would act to correlate granular brightness fields over larger scales.

Nevertheless, we note that some of the observed pattern may be due to a real 5-minute oscillatory component in the continuum. Isolation of this component would be of some interest in revealing the spatial structure of the 5-minute oscillation and in studying its interaction with granular convection.

Large-Scale Convection

Fig. 2 shows a photometric raster sum of 10 scans covering the active latitudes, but now with the data spatially averaged to 64×64 arc sec spatial resolution. The full range of the temperature scale in this picture is 5 K. When the variations due to active regions are discounted, inspection of coarse-grid rasters such as Fig. 2 indicates few large scale convective structures in the range of dimensions $5 \times 10^4 \text{ km} < L < 2 \times 10^5 \text{ km}$, above an amplitude of $\Delta T \sim 2\text{--}3 \text{ K}$. Structures at this level are occasionally seen, but their symmetry about sun center and/or their reluctance to rotate at the solar rate from day to day indicates they are most likely residual imperfections in our limb-darkening correction scheme.

The limit of 2-3 K for large-convective cell temperature amplitudes might be compared with the predicted amplitudes of $\Delta T = 10\text{--}100 \text{ K}$ estimated theoretically by Glatzmaier and Gilman (1981). Although this cell-center to edge variation of ΔT is comparable to the pole-equator ΔT predicted by the same models, the cell variation may prove a more useful constraint on the models. The reason lies in the fact that ΔT (pole-equator) is predicted to be quasi-steady, while the cells are expected to change on turn-over times of order 10^6 secs. Thus the cell variation is less likely to be smoothed by the lateral heat diffusivity of surface layers (Foukal and Fowler 1983).

Sunspot Bright Rings

Fig. 3 (Fowler, Foukal and Duvall 1983) illustrates the procedure used to analyze possible continuum bright rings around spot penumbrae. After time averaging of up to 10 rasters around a spot, the area outside the penumbra was divided radially into annular regions extending to roughly 120 arc sec from the spot center. The mean intensity in each annulus could then be plotted against radius. In practice, this plot was constructed separately by 4 quadrants or by octants, so that the effect of asymmetrically distributed faculae could be evaluated. Fig. 3b illustrates $I(r)$ for these quadrants individually, and Fig. 3c shows the grand average for the spot.

The main result of this study was that we detected no evidence of continuum bright rings exceeding 0.2-0.3% in observations of 10 different spots on 18 days. The extended bright areas of $\Delta I/I = 1\text{--}2\%$ reported by Hirayama and Okamoto (1981) seem to be faculae rather than the diffuse bright rings expected from heat diffusion calculations.

A second result was that 6 of the 10 spots observed showed some evidence for a weak 0.2-0.3% bright ring, visible in all quadrants. Fig. 4 shows this evidence. One must be cautious since bright rings as weak as this might be caused by a slight excess continuum brightness of small facular points sometimes distributed around the penumbral perimeter. This needs to be checked with near-simultaneous scans made in continuum and a line such as MgIb. On the other hand our observations (see Fowler, Foukal and Duvall 1983, Table II) show no correlation between the presence of a bright ring and the limb-distance of the spot. This argues against a magnetic point explanation, since it is well known that magnetic faculae show marked continuum limb-brightening.

We have compared the peak amplitude and shape of these weak bright rings with calculated values computed from a time-dependent numerical model of heat flow around thermal obstructions. This model has been described in detail by Foukal, Fowler and Livshits (1983), and is illustrated schematically in Fig. 5. Heat flow near the photosphere is assumed to be an eddy diffusive process on the length and time scales of interest near the spot. The "spot" is represented as a thermal plug inside which the eddy thermal conductivity $K = 0$.

Fig. 6 shows the bright rings of excess heat flux $\Delta F/F$ computed around "deep" and "shallow" spots immersed in a standard model convection zone. The comparison indicates that even a very shallow spot barely produces the weak rings of 0.2-0.3% amplitude. The influence of incorporating inevitable radiative leak from the ring into the cool umbra (see Spruit 1977a) is to further reduce the calculated $\Delta F/F$ for a given spot depth and convection-zone profile of K .

The main conclusion is that bright rings even as weak as 0.2-0.3% require a substantially lower eddy thermal conductivity near the top of the convection zone, than calculated from conventional mixing-length models.

Thermal Shadows

Models of heat flow as described above predict "thermal shadows" (see Spruit 1977) at the photosphere, caused by submerged magnetic active regions. Fig. 7 shows the decreased photospheric heat flux computed for a standard convection zone model above a "spot" obstruction submerged 6×10^4 km below the surface (from Foukal, Fowler and Livshits 1983).

Our photometric observations include a set taken over 4 successive days before and after emergence of a spot group in previously quiet photosphere. We

are able to place an upper limit of $\Delta T \leq 1.5$ K rms on any thermal shadow over the area of the active region, one day before its emergence. Comparison with the calculated ΔT expected for an obstruction of the estimated scale and depth indicates closer agreement with the depth-profile of K given by the mixing length model of Spruit (1977b) than with that of Baker and Temesvary (1966).

More observations (or limits) on thermal shadows associated with larger spots are desirable. But in principle the lack of observable thermal shadow implies a lower limit on K , to be compared with the upper limit on K (in somewhat shallower layers) implied by the observation of bright rings described above. Some observational constraints on the effective value of K near the photosphere would be useful for improvements in mixing-length theories of the solar convection zone (see e.g., Mullan 1971) and for dynamical models of solar convection, whose results depend upon the uncertain ratio of eddy diffusivity and viscosity - the Prandtl number.

Faculae and Network

Recent photometry indicates a correction is required in our earlier claim (Foukal, Duvall and Gillespie 1981) that the sun-center appearance (Fig. 8) of faculae in our differential continuum photometry probably implies a temperature deficit near $\tau = 1$ in those magnetic tubes. Plots of continuum intensity vs. magnetic flux show that even at sun center, network and faculae are slightly ($\sim 0.1\%$) brighter in clean continuum than are non-magnetic areas (i.e., cells). This indicates that the high visibility of faculae near sun center in pictures formed from the difference of two widely separated continuum passbands is probably due to formation of the two continuum passbands at substantially different heights in both the facular and quiet atmospheres. In particular, as suggested in the Foukal, Duvall and Gillespie paper, the visibility of faculae near sun center could be caused by a difference in temperature gradient in the facular atmosphere from that in the photosphere, between the formation heights of $\lambda 5256$ and $\lambda 7009$ continuum. The sense of the difference is consistent with the temperature gradient in faculae above $\tau_{5000} = 1$ being gentler than in the quiet photosphere.

We plan to test this interpretation by carrying out further two-wavelength observations at continuum points to either side of the H^- opacity peak. If this interpretation is correct, the facular signal at sun center should disappear when the two intensities at widely separated wavelengths of equal H^- opacity are used in the subtraction.

3. Limb-Darkening Variations

Measurement of limb-darkening variations might serve as a useful (and inexpensive) ground-based technique for studying slow (months to decades) global changes in the temperature structure of the solar photosphere (Abbot 1922; Rosen, Foukal, Kurucz and Pierce 1982). Any changes (or lack of variation) would be useful in placing constraints on variations of the solar luminosity and uv flux over the solar cycle through global processes not directly connected to active regions.

a) Instrumentation

Our limb-darkening scans have been obtained at the main spectrograph of the KPNO McMath telescope. A narrow (0.2 Å) continuum passband at $\lambda 4451$ has been used for most of the observations, but about three hundred profiles have been taken at $\lambda 8902$ also. The scans are obtained by allowing the sun's diameter to drift across a 25×2.5 arc sec entrance slit. This simple one-dimensional solar-rate scanning has the advantages of obviating vignetting or air mass corrections and the scan rate is highly stable. Some disadvantages that we are seeking to remove are discussed below.

b) Reduction

Fig. 9 shows daily averages of the typically 10-100 scans taken on a given day for our runs between June 1980 and November 1982. Three more runs have since been obtained in 1983, and are being reduced. Aside from spots and large faculae which are easily recognized and rejected, the rms noise of granulation and scintillation in an n -scan average is reduced to the level of roughly $1\%/\sqrt{n}$.

Other sources of error in comparing runs taken months apart are variations in atmospheric and instrumental scattering and residual facular noise at $\mu < 0.5$. Early difficulties with photomultiplier hysteresis have been eliminated by using a blue-sensitive diode as a detector, and seeing variations have negligible effect over the range of $\mu > 0.2$ of interest here.

A careful study of scattered light variations at the McMath telescope has been carried out (Petro et al. 1983). A satisfactory fit to the aureole can be made on a day-to-day basis, and the scattered light contribution across the disc can be corrected to the 0.1% error level. Faculae contribute to error closer to the limb than $\mu \sim 0.5$ in our scans taken near solar activity maximum.

However, it is now clear that even in this range of μ , the error can be significantly reduced by rejecting parts of scans where facular features are quite easily recognized.

c) Results

Fig. 10 shows the residuals of averaged limb-darkening curves for 4 days. The residuals are obtained by subtracting an arbitrary "standard" limb-darkening curve from the data, so that small-amplitude variations are more easily seen. In the case shown here, the subtracted standard was the Pierce and Slaughter (1977) limb-darkening curve at $\lambda 4451$.

The upper left curve shows a pronounced slope due to the asymmetric effect of detector (PMT) hysteresis on the preceeding and following limbs. About 30% of the data were rejected altogether on grounds of such a clear asymmetry of instrumental origin. The other three curves illustrate typical behavior before scattered light, spots and faculae are removed. The dashed curves show the size of the scattered light correction to be made across the disc.

All the residuals show a tendency to rise near the limb; this excess has been identified as an error in the Pierce and Slaughter curve (Petro et al. 1983), which is based on only 1 scan at $\lambda 4451$. The largest limb residuals are due to faculae which had not been removed when this figure was made.

Fig. 11 shows the the change of limb-darkening at $\lambda 4451$ as a function of μ that would be expected if the photospheric temperature gradient near $\tau = 1$ had changed between 1980-1982 as much as reported by Livingston and Holweger from observations of line equivalent widths made between 1976-1980. A change of some 0.7% would be required near $\mu = 0.5$. This size of change is easily ruled out by our limb-darkening data whose rms variation over the 3 years lies between 0.06% at $\mu = 0.9$ and 0.13% at $\mu = 0.2$. Since our observations do not extend before 1980, and Livingston's more recent data do not show the clear trend reported between 1976-1980 (private communication), it is not clear that there is any contradiction between the two techniques of studying changes in global photospheric structure. In principle, the two techniques should be nicely complementary, since the lines studied by Livingston are formed somewhat above our continuum which originates deeper, between $0.2 < \tau < 1$.

This work is supported at AER under NSF grants ATM-8112339 and ATM-8200763.

References

- Abbot, C., 1922, Ann. Smithsonian Ap. Obs. 4, 217.
- Baker, N. and Temesvary, S., 1966, "Tables of Convective Stellar Envelope Models. Goddard Space Center.
- Foukal, P. and Fowler, L., 1983, submitted to Ap. J.
- Foukal, P., Duvall, T and Gilliespie, B., 1981, Ap. J., 249, 394.
- Foukal, P., Fowler, L. and Livshits, M., 1983, Ap. J., 267, 863.
- Fowler, L., Foukal, P. and Duvall, T., 1983, Solar Phys., 84, 33.
- Glatzmaier, G. and Gilman, P., 1981, Ap. J. Suppl., 47, 103.
- Hirayama, T. and Okamoto, T., 1981, Solar Phys., 73, 37.
- Livingston, W. and Holweger, H., 1982, Ap. J., 252, 375.
- Mullan, D., 1971, Mon. Not. Roy. Ast. Soc., 154, 467.
- Petro, L., Foukal, P., Rosen, W. and Pierce, K., 1983, submitted to Ap. J.
- Pierce, K. and Slaughter, C., 1977, Solar Phys., 51, 25.
- Rosen, W., Foukal, P., Kurucz, R. and Pierce, K., 1982, Ap. J. Lett., 253, 89.
- Spruit, H., 1974, Solar Phys., 30, 277.
- Spruit, H., 1977a, Solar Phys., 55, 3.
- Spruit, H., 1977b, Astr. Ap., 55, 151.

Captions

- Figure 1 Photometric raster sum at $\lambda 5256$ on May 22, 1982, 4 arc sec resolution (from Foukal and Fowler 1983).
- Figure 2 Photometric raster sum at $\lambda 5256$, with 64 x 64 arc sec resolution (from Foukal and Fowler 1983).
- Figure 3 Photometric raster sum of area around a spot showing annular areas and quadrant subdivisions used for analysis of bright rings (from Fowler, Foukal and Duvall 1983).
- Figure 4 Evidence for weak bright rings around 3 spots showing for each spot the 4 quadrants separately, and the average curve (from Fowler, Foukal and Duvall 1983).
- Figure 5 Schematic diagram illustrating the thermal blocking model (from Foukal, Fowler and Livshits 1983).
- Figure 6 Plot of bright ring excess flux $\Delta F/F$ against distance from spot center for a shallow spot of depth 1000 km (curve a) and a deep spot (curve b) of depth 10^4 km. The dashed line represents the shallow spot curve at a time before an equilibrium heat flow pattern has been established (from Fowler, Foukal and Duvall 1983).
- Figure 7 The decrease in spatially integrated heat flux Φ as a function of time t after an obstruction of radius 4×10^4 km is placed at a depth 6×10^4 km below a planar photosphere of radius 2×10^5 km (from Foukal, Fowler and Livshits 1983).
- Figure 8 Photometric rasters near sun center; (a) is the sum of intensities at $\lambda 5256$, 7009, (b) is the difference of the two intensities, (c) is a magnetogram of the same area (from Foukal, Duvall and Gillespie 1981).
- Figure 9 Limb darkening scans (daily averages) at $\lambda 4451$ taken between June 1980 and November 1982.
- Figure 10 Residuals of daily-average limb-darkening curves for 4 days.
- Figure 11 The change in limb-darkening at $\lambda 4451$ calculated by R. Kurucz using the change in photospheric temperature structure reported by Livingston and Holweger (1982) between 1976-1980.

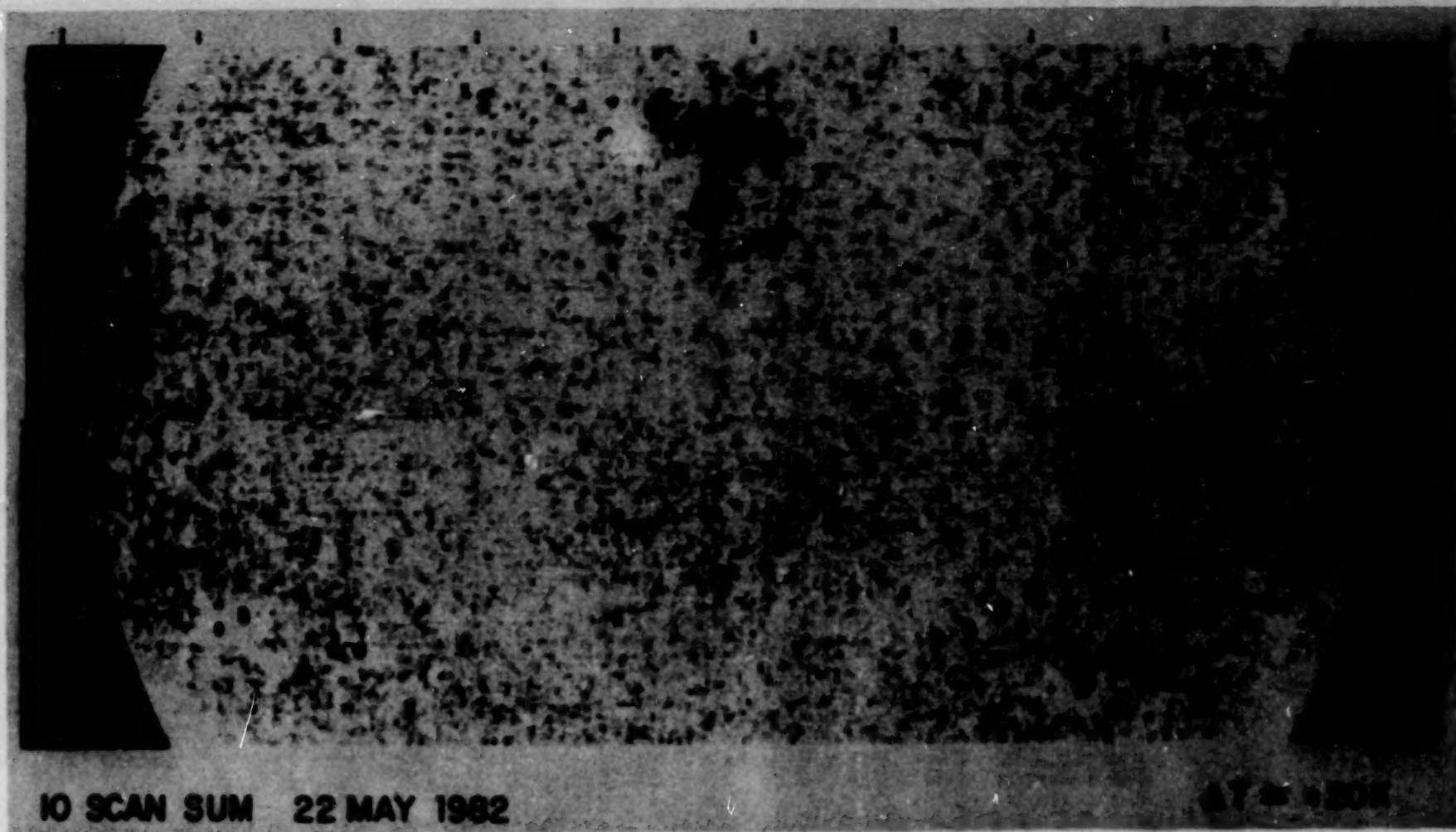


Figure 1

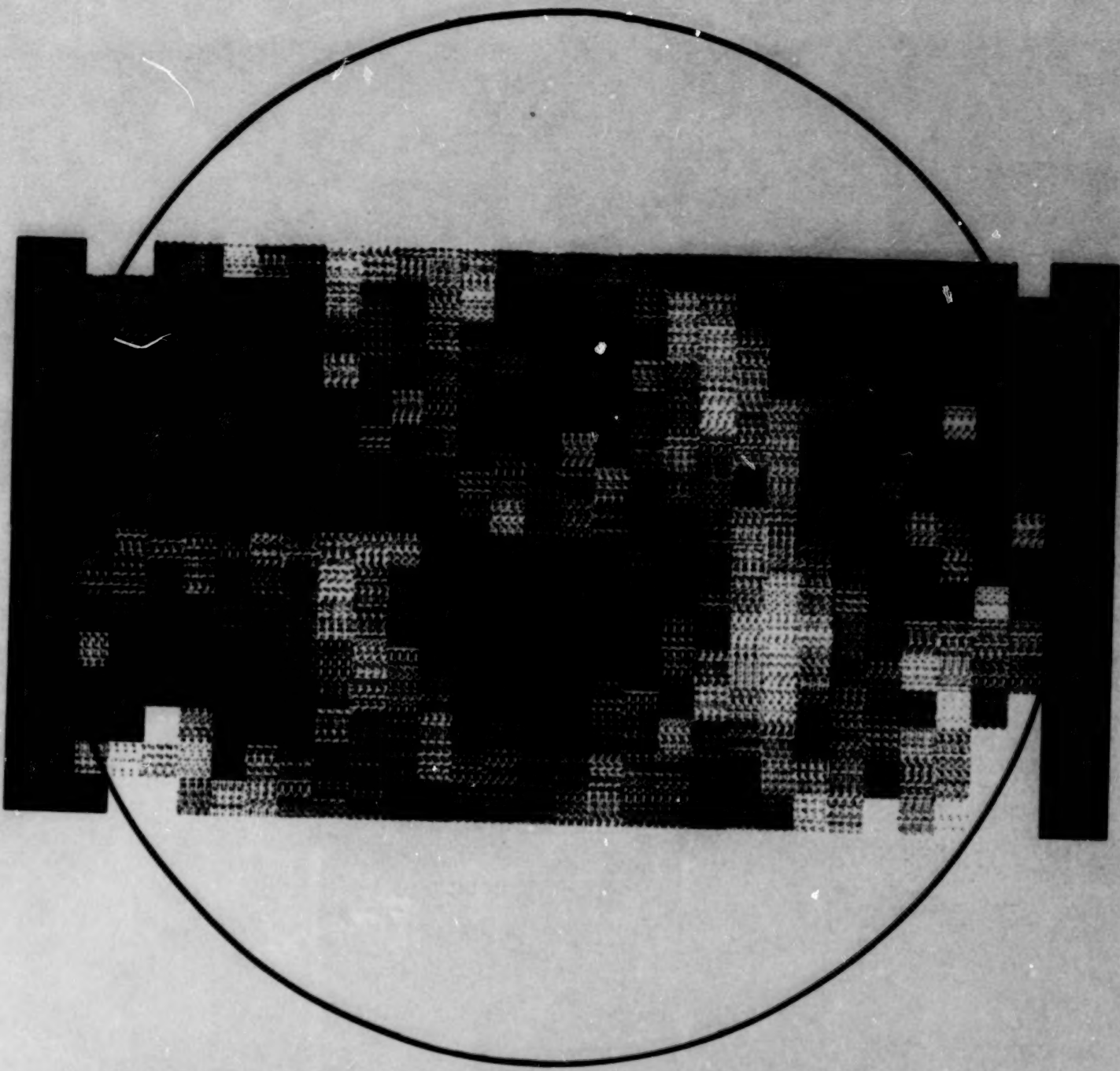
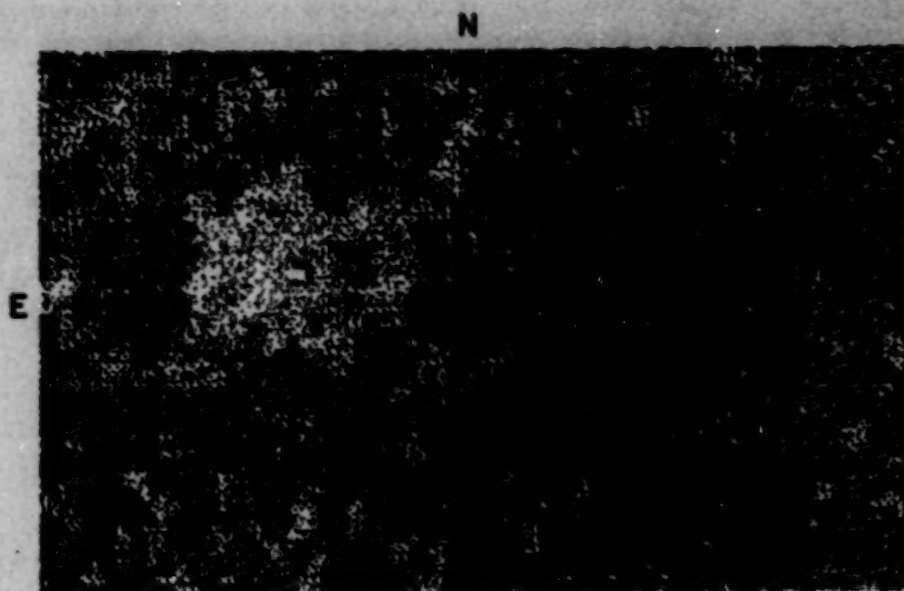
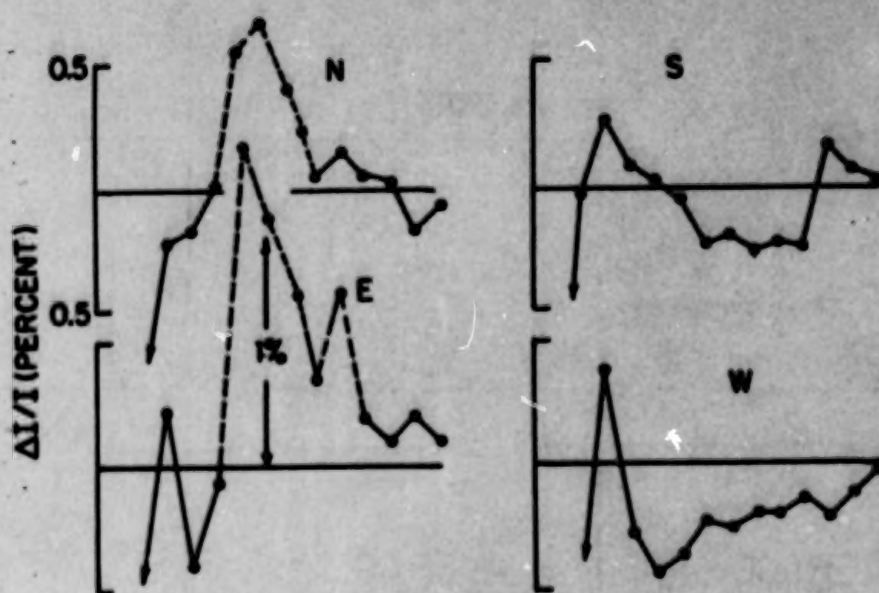


Figure 2

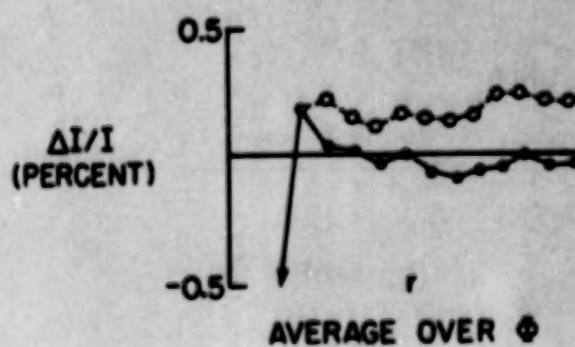
108



(a)



(b)



(c)

Figure 3

QUADRANT RADIAL INTENSITY PROFILES

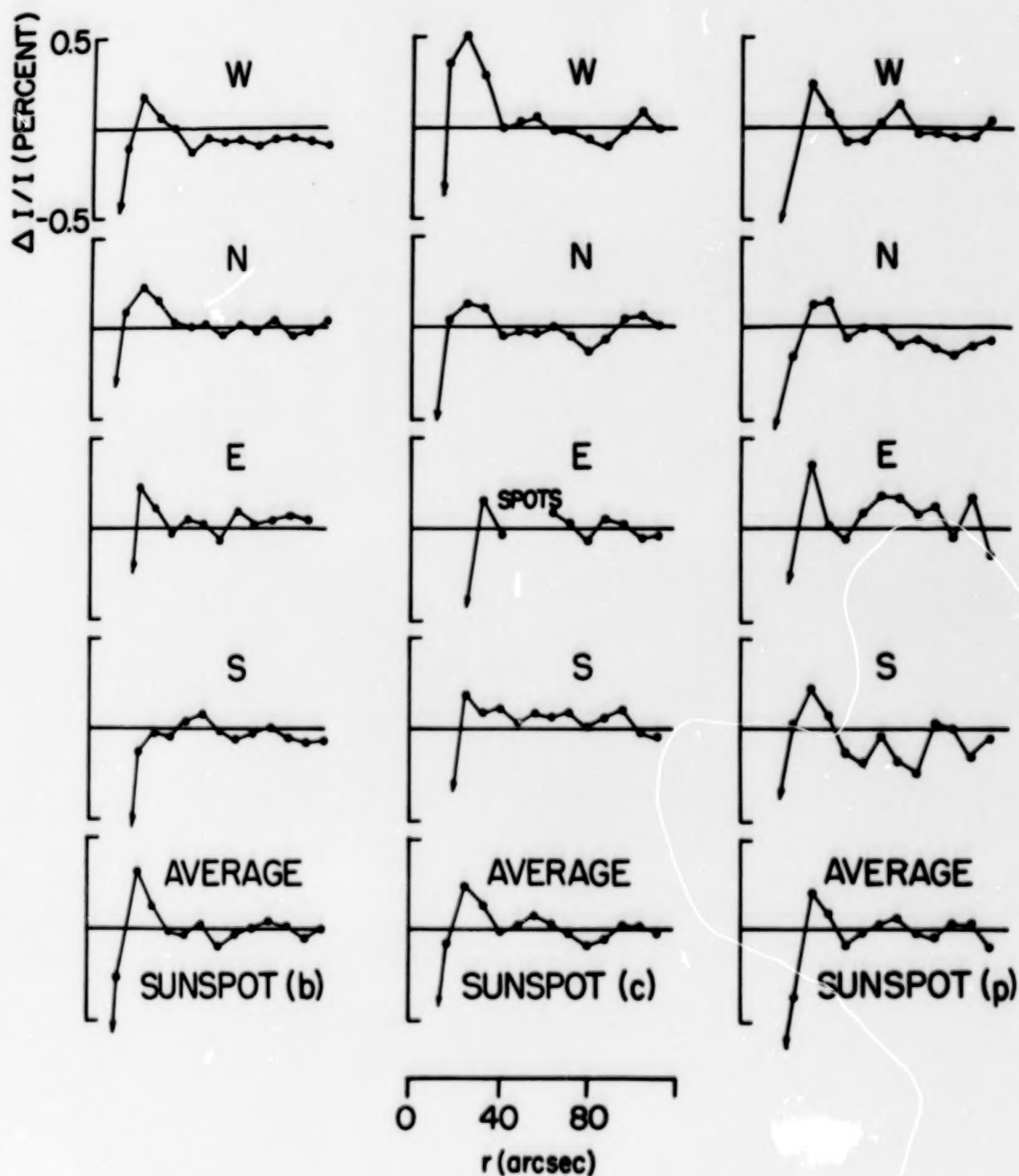


Figure 4

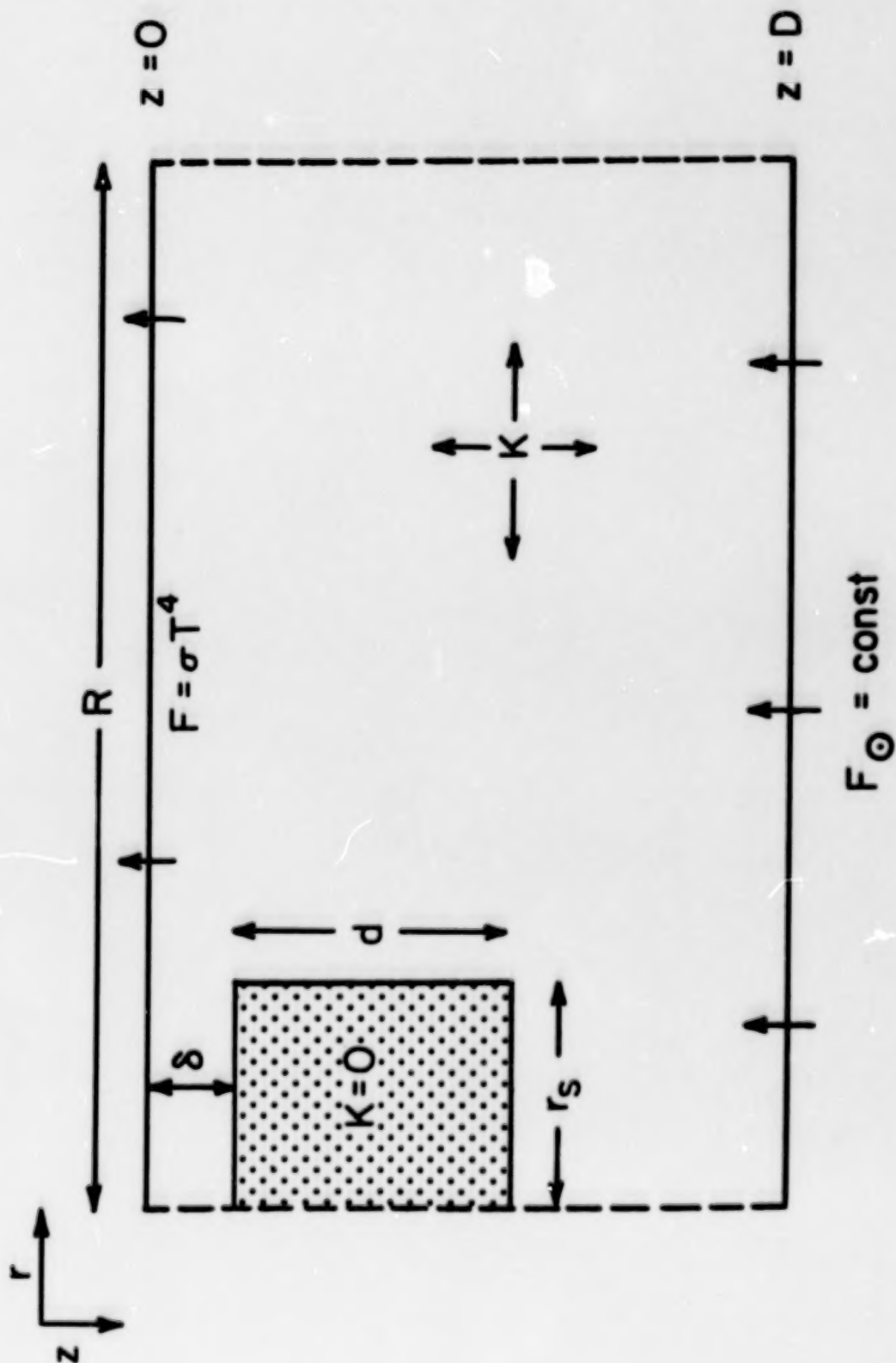


Figure 5

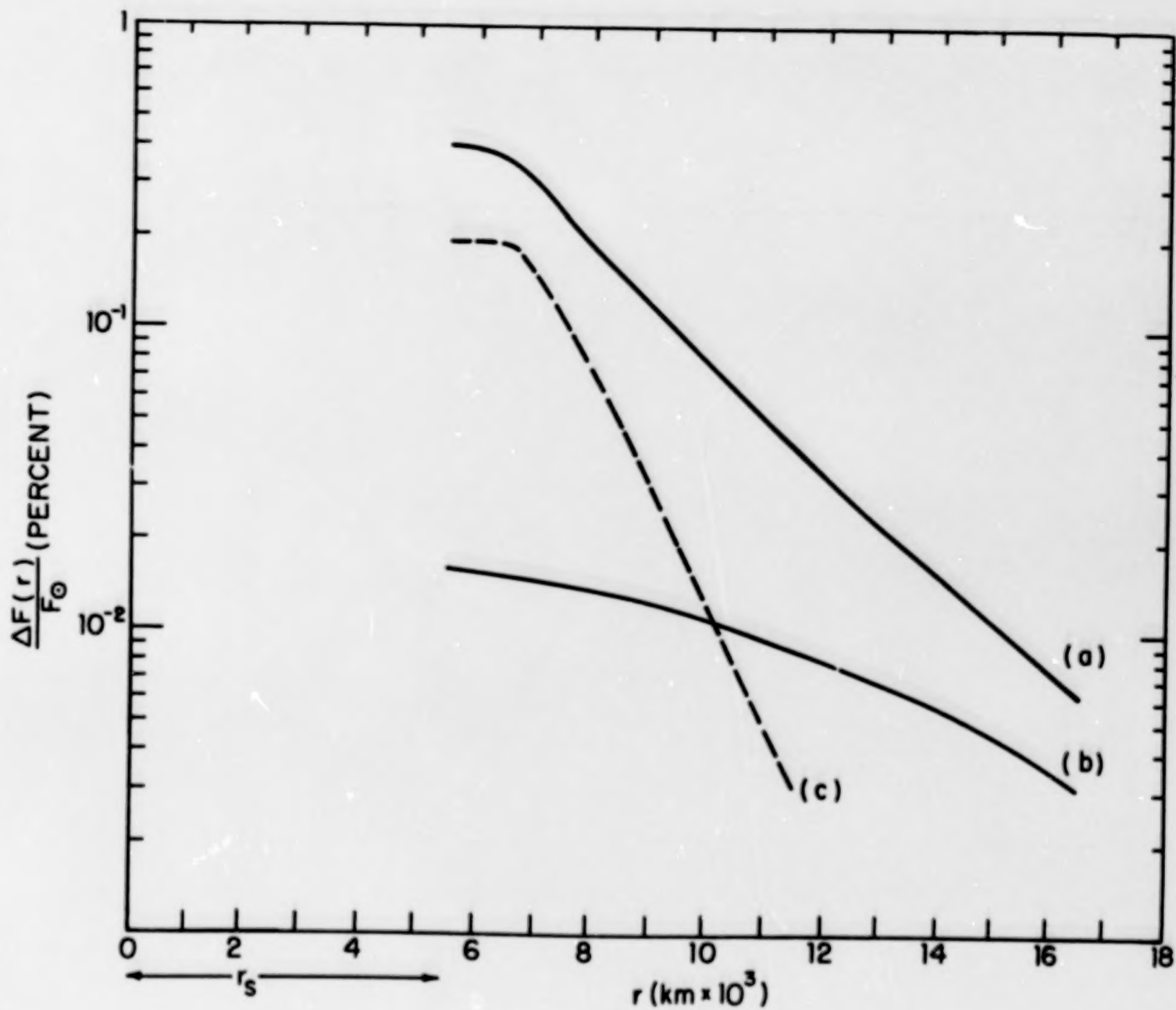


Figure 6

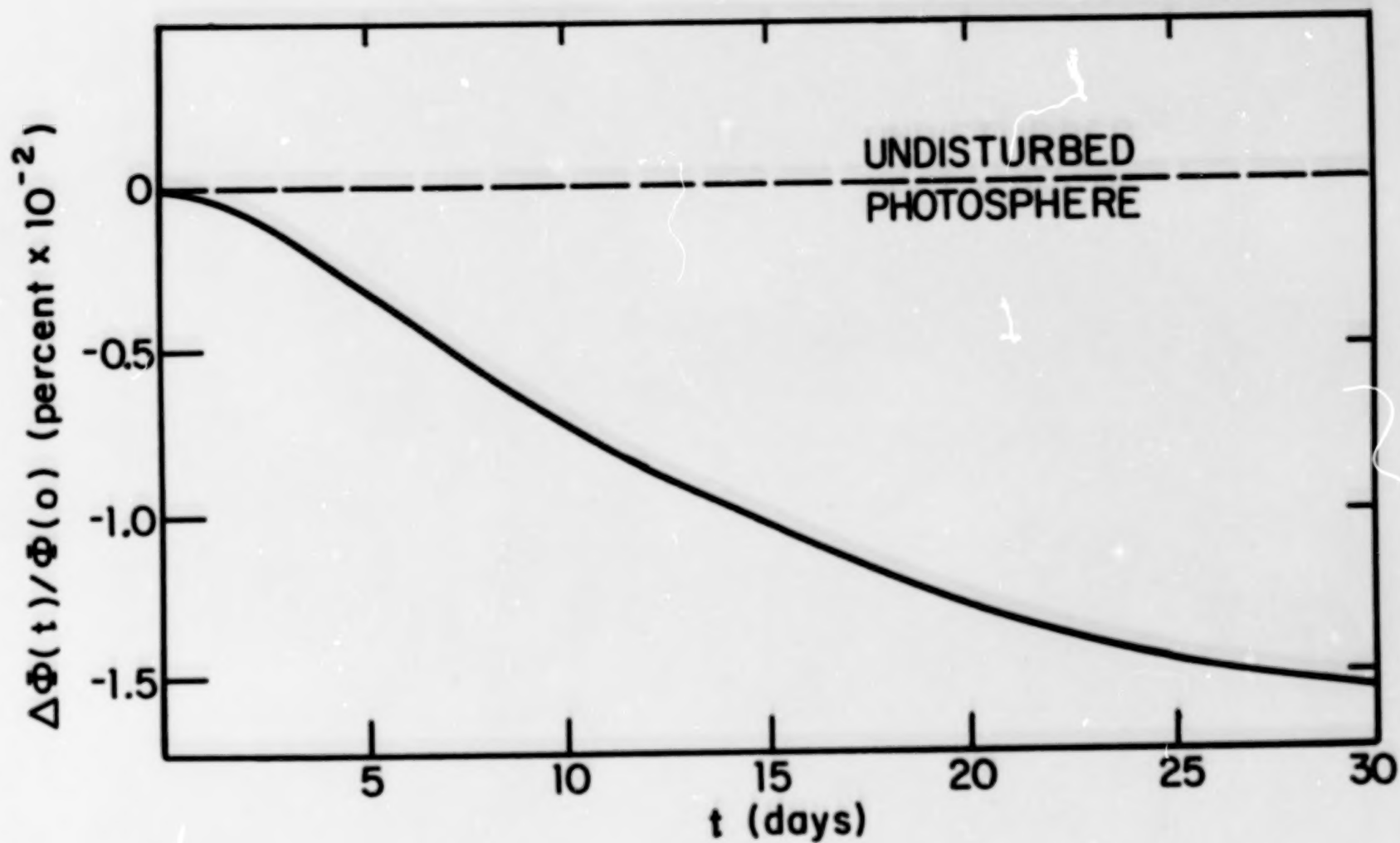
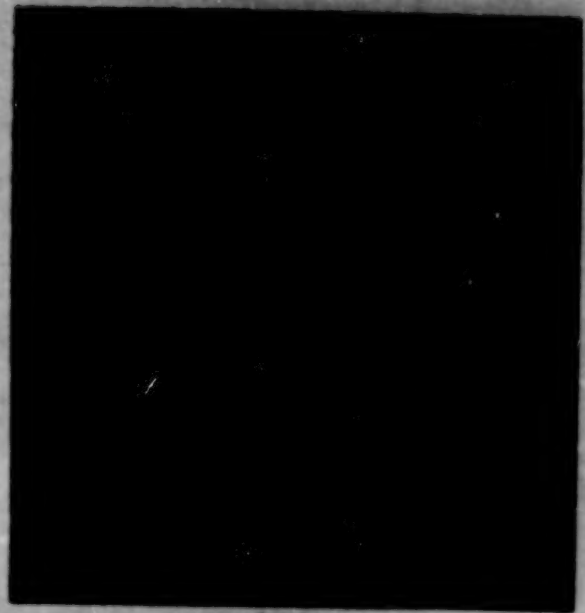


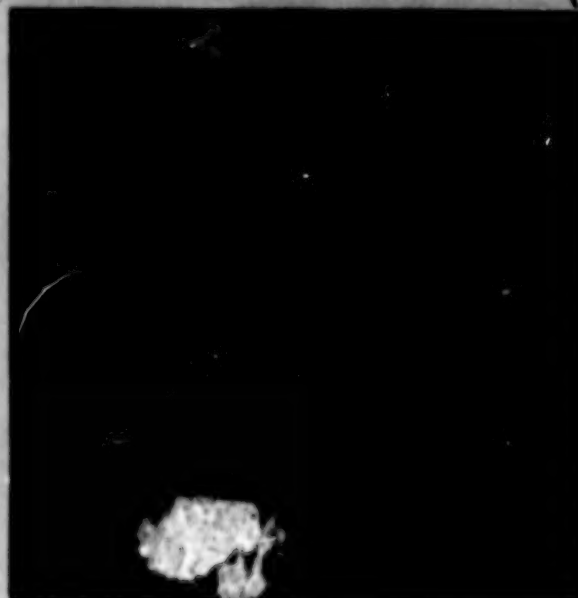
Figure 7



(a)



(b)



(c)

Figure 8

LIMB DARKENING SCANS
DAILY SUMS
 $\lambda 4451 \text{ \AA}$

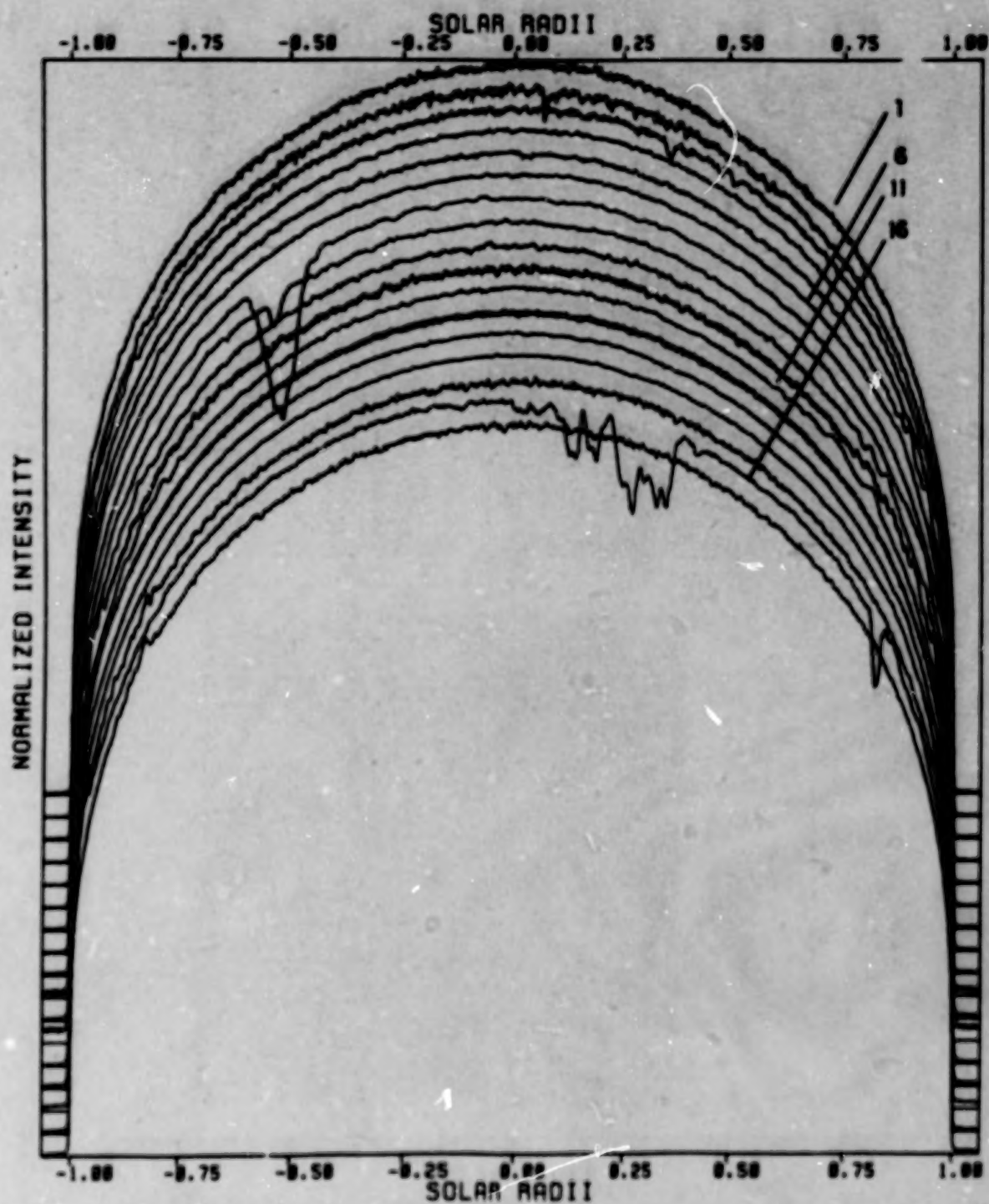


Figure 9

LIMB DARKENING RESIDUALS

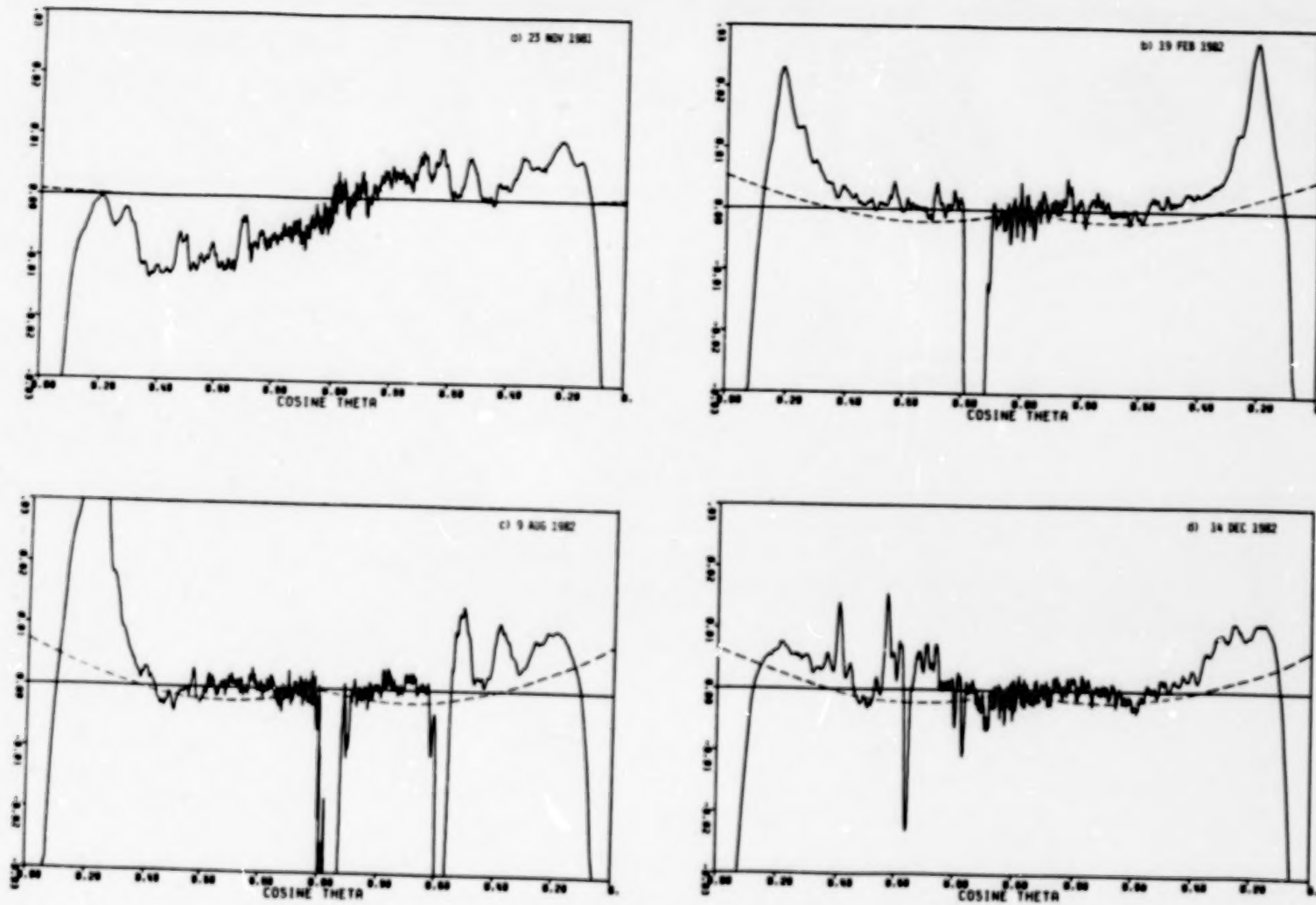


Figure 10

116

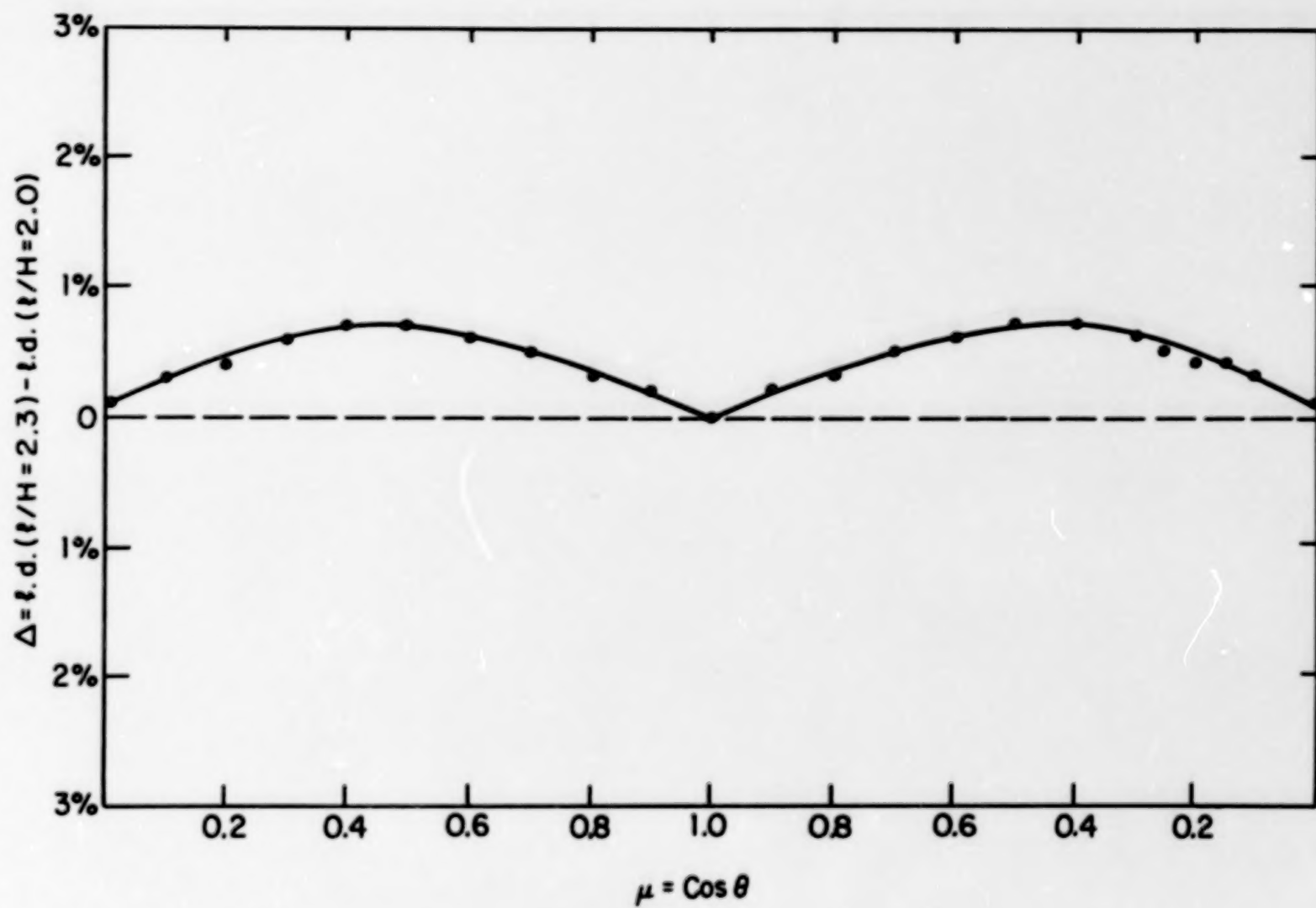


Figure 11

117

DISCUSSION OF FOUKAL PRESENTATION

HUDSON: Why don't you see stronger leftover contrast from the granulation?

FOUKAL: It depends on the instrumental broadening.

HUDSON: What is the radiative leak in the heat flow models?

FOUKAL: Emission into the spot.

ZIRIN: What is the amplitude of the temperature difference between λ 5200 Å and λ 7000 Å?

FOUKAL: The calibration is relative, there is no temperature scale.

EDDY: How do you reconcile these results with the Japanese observations of bright rings around sunspots?

HUDSON: It may be a language problem. I think that they also believe that their excess brightness is in faculae.

EDDY: What are the giant bright rings in the data?

FOUKAL: If they do not rotate with the Sun, then there is just an error in the analysis.

ZIRIN: If the large bright rings around spots existed you could see them.

HUDSON: Power spectra of the ACRIM data have a lot of power in periods longer than five minutes, but shorter than 27 days, probably due to larger convective motions. You should see them rotating in a sequence of data.

FOUKAL: We're trying!

HUDSON: Don't those models say that the mixing-length theory is way off?

FOUKAL: They argue for a high lateral diffusivity or that the Prandtl number is off by an order of magnitude. You get the wrong differential rotation if the Prandtl number is changed that much in a convective-zone model.

MOORE: Why do you assume isotropic thermal diffusion?

FOUKAL: The diffusivity K is estimated, so it's not well determined. We just use the simplest physics.

MOORE: What if it were really anisotropic?

FOUKAL: That may work better.

SKUMANICH: If the scales are about the size of supergranules, then it may well be anisotropic.

POUKAL: Since there is no temperature signal observed in supergranulation, they may not be convective cells. The only convection we see is granulation.

MOORE: Doesn't the contradiction of the bright ring and the spot shadow results tell us about this issue?

POUKAL: The magnetic fine structure has been ignored and it shouldn't have been.

BLANK PAGE

INTERACTION OF CONVECTION AND SMALL-SCALE MAGNETIC FIELDS: INFLUENCE ON THE SOLAR LUMINOSITY

Åke Nordlund¹

High Altitude Observatory/National Center for Atmospheric Research²

ABSTRACT

This contribution discussed changes in the local solar luminosity due to the presence of a small-scale structured (facular) magnetic field in the photosphere. The discussion was based on three-dimensional numerical simulations of the magneto-hydrodynamics of the top of the convection zone, and the adjacent stable photosphere (Nordlund, 1983). The simulations demonstrate that practically all of the magnetic flux present is concentrated into intense magnetic flux structures with flux densities of the order of 100 to 150 mT (1 to 1.5 kG), such that the magnetic field pressure is balanced by the gas pressure of the surrounding plasma. The flux concentration is caused by the convectively unstable stratification, as discussed in detail by Spruit (1977, 1979). In this situation, the average luminosity of the area is influenced by three effects: 1) The brightness of the flux concentrations, 2) their filling factor, and 3) the average luminosity of the surrounding (field-free) plasma.

The interior of the flux concentrations have a brightness that depends strongly on the degree of evacuation; i.e., on the Wilson depression. The flux concentrations are brighter than the average photosphere for large Wilson depressions, and darker than the average photosphere for small Wilson depression (Spruit, 1976). Observations of these flux concentrations ("solar filigree") in the photospheric continuum (Mehlretter, 1974; Muller, 1983) suggest that they are brighter than the average photosphere only part of the time. The strong limb-brightening of these (facular) structures was explained by Spruit (1976) as due to the increased visibility of the hot, very thin "walls" of the flux concentrations. This can, as yet, not be directly verified from the numerical simulations, because the horizontal resolution is insufficient to describe the wall structure accurately.

The filling factor of the flux concentrations is, because of their well defined flux density, just a measure of the horizontally averaged flux

¹Visitor from the University of Copenhagen

²NCAR is sponsored by the National Science Foundation

density of the area.

The average luminosity of the field-free plasma is probably not influenced by the presence of the magnetic flux concentrations. Because of the short duration of the numerical simulation (16 solar minutes), this cannot be directly inferred from the numerical simulations. However, the presence of the flux concentrations in the intergranular lanes restricts the horizontal flow of the granules, and this is likely to change the efficiency of the convection. The recently observed variation of the number density of granules with the phase of the solar cycle (Rösch, 1983) may be observational evidence of this.

At a depth of only some 1500 to 2000 km below the photosphere, the temperature stratification is already very nearly adiabatic (cf. Spruit, 1974). The local surface luminosity is determined by how efficiently the last 1500 to 2000 km of the convection zone can transport energy to the photosphere, *given this constant entropy* ("potential temperature") *at the bottom of this layer*. The presence of a magnetic field changes this efficiency in the three ways discussed above. These are *local* effects, and depend in no way on the presence of sunspots elsewhere on the sun, or locally at earlier times. The presently popular conjecture (cf. this volume) that there is a detailed balance between luminosity deficit in sunspots and luminosity excess in facular areas must therefore be rejected as unphysical.

ACKNOWLEDGEMENTS

Financial support by the Danish Space Board and the Danish Natural Science Research Council is gratefully acknowledged. Part of this work was done while I was a visitor at the High Altitude Observatory / National Center for Atmospheric Research. I am grateful to HAO and the Copenhagen University for making this stay possible.

REFERENCES

- Mehlertretter, J.P. 1974, *Solar Physics* **38**, 43.
Muller, R. 1983, *Solar Physics* **85**, 113.
Nordlund, Å. 1983, in *Solar and Stellar magnetic fields: Origin and Coronal Effects*, Stenflo, J.O. (ed.), Reidel, Dordrecht.
Rösch, J. 1983, in *Small-Scale Dynamical Processes in Quiet Stellar Atmospheres*, Keil, S. (ed.), Sac-Peak.
Spruit, H. 1974, *Solar Physics* **34**, 277.
Spruit, H. 1976, *Solar Physics* **50**, 269.
Spruit, H. 1977, *Solar Physics* **55**, 3.
Spruit, H. 1979, *Solar Physics* **61**, 363.

DISCUSSION OF NORDLUND PRESENTATION

FOUKAL: What is the signature of convective changes in the bisector?

NORDLUND: An absolute lineshift.

FOUKAL: Do the models reproduce the velocity contrast?

NORDLUND: Yes, it comes out when we fit the bisectors, with no fudge factors.

HUDSON: Does this work imply the lifetime of an active region in terms of the Kelvin-Helmholtz time scale?

NORDLUND: No one knows the depth of the spot.

CHAPMAN: Do you assume Spitzer conductivity?

NORDLUND: Yes. It doesn't matter since different resistivities do not alter the topology, but only the sharpness of the magnetic boundaries, and add some Joule heating.

CHAPMAN: But we see discrete magnetic points in the K-line.

NORDLUND: But they are much larger than the modeled scales.

SKUMANICH: From Herse's data with one to two arc second resolution, the lifetimes of points at the temperature minimum are minutes.

BLANK PAGE

7

ENERGY FLOW CONTINUITY IN SOLAR ACTIVE REGIONS

K. H. Schatten

NASA/Goddard Space Flight Center

ABSTRACT

The models for sunspots of Parker and faculae by Spruit are combined into an active region model with consideration for the energy flow beneath active regions. In our active region irradiance modelling, there is an apparent average energy balance between the sunspot deficit and the facular excess, i.e. - no 11-year variations in solar luminosity associated with the activity centers. This is seen as a consequence of the upper convection zone's inability to store these significant amounts of energy for periods greatly in excess of weeks. This view is supported by observed active region behavior and detailed numerical modelling. Bray and Loughhead and Brandt review the development of activity centers and find that increases in facular and spot brightness are nearly commensurate, with the faculae outlasting the spots on time scales of the order of weeks to a couple of months. Foukal finds "the radiation (deficit from a sunspot blocking model) recovers slowly on a timescale of approximately 83 days."

ACTIVE REGION ENERGY FLOW CONTINUITY

The brightness of faculae has been studied by Spruit (ref. 1), and a reasonable model for them suggests that they consist of many (usually) unresolved flux tubes. Spruit (ref. 1) shows that the inner hot wall of a thin flux tube can yield an intensity contrast increase when the faculae are viewed at large angles. Differing size flux tubes can yield either a central bright or dark structure, consistent with the bright filigree and the dark pores. Some emission from a hot gas above the faculae can also explain this chromospheric behavior. We incorporate Spruit's facular model with Parker's sunspot model into a combined active region model, which provides a consistent picture for the active region average energy conservation found in our total irradiance modelling.

Figure 1 shows the Parker (refs. 2,3,4) spot model and the Spruit (ref. 1) facular model (not to scale) for a young active region. In the young active region the sunspot fields are large with only a few facular flux tubes having "peeled off" of their associated spot group. Thus the downdraft of the sunspots predominate with less emission of energy leaving the active region area (compared with a quiet region) as shown in the figure. Heat builds up below the active region, causing a gradient in temperature and pressure. This contributes an outward pressure gradient force which may lead to the gradual dispersal of the sunspot flux tubes (after Parker's model).

Figure 2 shows the active region in a later stage of development. Now the temperature enhancement is more widespread, but the spots are nearly decayed (or all decayed), and the faculae are more numerous. The extra thermal energy below the surface increases the convection and the faculae emit more energy than the quiet sun until a return to normal conditions occurs.

The appearance of faculae may not necessarily be associated with the diffused magnetic field of sunspots, but perhaps the need to remove the heat excess. McIntosh (ref. 5) discusses the decaying plage and sunspot fields and points out there "are no dispersive proper motions among decaying sunspots" and plage elements. The spreading and weakening of active region plage elements seem to occur by the formation of new elements more distant from the center of the region. These observations have the appearance of a diffusive phenomenon.

The approximate timescale for the above phenomena to occur may be estimated using both experimental and theoretical values. Choosing a moderately large active region, we take a sunspot with an umbral radius of 20,000 km (400 millionths of a solar hemisphere). We allow the subsurface energy storage region associated with the sunspot to be comparable in area to the surrounding plage region size. This has an area ten times larger than the sunspot area (see Allen, (ref. 6)). The depths to which the sunspot flow energy can prevent the upward convection heat transport must be considered. Parker has calculated his flow models to depths of order of a few thousand kilometers. Foukal (ref. 7) has chosen a sunspot blocking depth of 7,500 km. We choose a range of depths from 2,100 km to 7,000 km. Significantly greater values appear to be unrealistic, insofar as the sunspot magnetic fields break up into flux tubes which decrease in areas markedly with depth, and thereby lose the ability to interact significantly with the surrounding fluid. Spruit has shown that the horizontal convective transport of heat is so effective at these depths as to obliterate any bright ring around the sunspot. Foukal's model also allows for horizontal transport of heat to occur thereby enabling the heat to flow to the surface at several thousand kilometers distance. The intensity of the spot umbra is near 24% of the photosphere (ref. 6), and with a solar emission of $F = 6.27 \times 10^{10} \text{ erg cm}^{-2} \text{ s}^{-1}$, we find an energy flux deficit of $\Delta F = 4.7 \times 10^{10} \text{ erg cm}^{-2} \text{ s}^{-1}$, which does not leave the photosphere due to the spot umbra, or a total power of near $5.9 \times 10^{29} \text{ erg s}^{-1}$. Allowing this energy to heat the gaseous regions beneath the active region in accordance with the above model, we calculate the approximate time scale, τ , for energy storage as follows. We assume that the surface gases can only be heated to increases in temperature, ΔT , of order of the standard convection zone model temperature, T , although this is clearly an upper limit. We let the deficit in energy output, ΔE , heat the gases as follows:

$$\Delta E = P\tau = Nk\Delta T = NkT = kT \int A n dh \quad (1)$$

where P is the power deficit, N is total number of particles, ΔT is the temperature increase, which we assume is of order of standard convection zone model temperatures, T , at depths, h ; with particle number density, n , in an active region area, A . Choosing solar structure densities and temperatures from standard models (ref. 6), we obtain a timescale, τ of 2 days, 5 days 10 days, and 100 days, for depths of 2,100 km; 2,800 km; 3,500 km, and 7,000 km, respectively. The modelling of Foukal (ref. 7), where he chose a sunspot blocking depth of 7750 km, gave a comparable transport timescale of 83 days. Both timescales are comparable to the times by which active region faculae outlast their sunspot compatriots.

The model of Foukal appears to be an accurate computer model for the rectangular sunspot structure chosen, however, this geometry leads to an overestimation of the sunspot's ability to store energy. This is due to the

increasing field strength and decreasing area of a sunspot field with depth (see Parker (ref. 2) and Spruit (ref. 1). For example, if a sunspot completely occupies an area A at the photosphere, owing to flux conservation and pressure balance, at a depth of 700 km, it will occupy only $1/3 A$; at 3,500 km, $6\% A$; and at 7,000 km $2\% A$. Thus at moderate depths in the convection zone, the sunspot fields are considered to be thin "fibril" fields moving with the fluid motion.

The timescales just calculated for energy storage appear to be comparable to the sunspot and facular aspects of active region development. Some aspects of Bray and Loughhead's (ref. 8) review of a representative history is as follows. The sunspots increase in area until, on average, day 6-13. At that point the faculae brightness is still increasing. On days 14-30 all the spots, except the western (following) group, have disappeared but the faculae are now "very extensive". They continue to decrease from days 30-60 and at 60-100 they resume the "form of a bright network". This is similar to Brandt's (ref. 9) active region review where spots and faculae originate on day 1, and grow until maximum development for the spots on day 11, with the magnetic flux growing until day 27, while the faculae still increase until about day 54-81. On day 54, the facular brightness decreases and on day 81 the faculae are dissolved. This appears to be consistent with the model of Sofia et al. (ref. 10) where it states "there is no evidence that the active region does anymore than redistribute the out-flowing energy, with no storage beyond the fact that the reemitted energy for faculae is spread over a longer time interval than the energy deficit of spots,...".

Thus the present view, which draws together existing ideas for the energy flow in and below an active region is summarized, as follows. A sunspot magnetic field floats to the photospheric surface. Associated with the hydrodynamics involved, to conserve fluid, a downdraft occurs. This prevents the entire heat flow from reaching the surface and causes a sunspot. Consequently heat builds up at several thousand kilometers depth. The associated pressure and horizontal transport near the surface gradually destroy the sunspot's magnetic flux tubes and pores are formed in the surrounding supergranular network. Horizontal heat flow (and/or Alfvén waves) transports the energy to surrounding regions many thousands of kilometers distant, where it emerges as facular enhancements. The spot dies and the last remaining heat is dissipated in weeks to months timescales.

There does not appear, on average, to be any net deficit within our present observational and calculational uncertainties. At any average time, the average spot deficit is closely matched by the facular excess over the whole sun. There is only a brief period (much less than 11 years) for storage. The thin layers of the upper convection zone cannot store energy for more than a few weeks. The top 3,500 km of the sun has a base density of $2 \times 10^{-5} \text{ gm/cm}^3$. Storing a single sunspot's energy flux deficit of $6 \times 10^{29} \text{ erg s}^{-1}$ for a few days in a layer 3,500 km thick, with the above density, over the entire surface of the sun, could raise the level, 1,000 km against gravity. Thus, the heat energy of the sun, unless stored much deeper, must leave the sun in near real time. That is, the luminous flux deficit associated with sunspots cannot be stored for a solar cycle in the upper convection zone. If any secular variational trends exist in the solar constant, we suggest they are not due to the surface manifestations of solar activity, but a more deep rooted and global phenomenon.

REFERENCES

1. Spruit, H. C.: 1981, The Physics of Sunspots, ed. Cram and Thomas, Proc. of a conference at Sacramento Peak, p. 98.
2. Parker, E. N.: 1979a, Cosmical Magnetic Fields, Clarendon Press, Oxford.
3. Parker, E. N.: 1979b, Astrophys. J., 232, 291.
4. Parker, E. N.: 1979c, ibid., 234, 333.
5. McIntosh, P. S.: 1981, The Physics of Sunspots, ed. Cram and Thomas, Proc. of a conference at Sacramento Peak, p. 7.
6. Allen, C. W.: 1973, Astrophysical Quantities, Athlone Press, London.
7. Foukal, P.: 1981, The Physics of Sunspots, ed. Cram and Thomas, Proc. of a conference at Sacramento Peak, p. 391.
8. Bray, R. C. and Loughhead, R. E.: 1964, Sunspots, London, Chapman and Hall.
9. Brandt, J. C.: 1966, The Physics and Astronomy of the Sun and Stars, McGraw-Hill Book Co., New York.
10. Sofia, S., Oster, L. and Schatten, K. H., Solar Phys., 80, 87.

Figure Captions

- Figure 1. A sketch of the magnetic field configuration near a young active region. The sunspot field divides into individual flux tubes some distance below the visible surface. The dashed arrows represent the presumed convective downdraft which helps to hold the separate flux tubes together in the tight cluster that constitutes the sunspot. The downdraft inhibits the upward transport of heat and the temperature increases below the active region, shown by the isotherm. The energy flux, ΔF , is negative from the spot and faculae lag the spot development. Thus the net flux difference is negative.
- Figure 2. The field and energy flow around an older active region is shown. The faculae emit more energy than the small spot deficit and the net energy flux, ΔF , is greater than average. The isotherm enhancement is returning to undisturbed conditions.

YOUNG SOLAR ACTIVE REGION

OUTWARD
ENERGY FLUX VARIATIONS

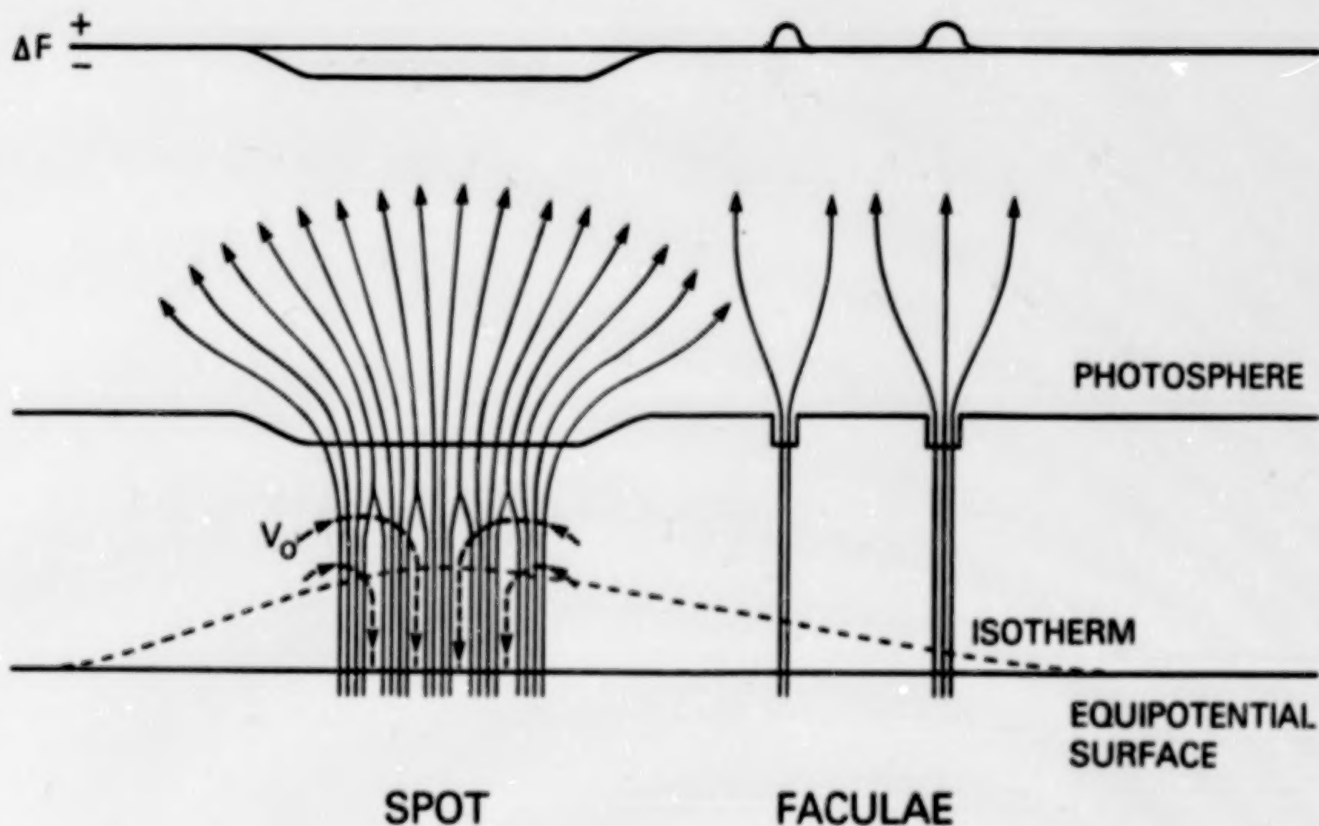


Figure 1

OLD SOLAR ACTIVE REGION

OUTWARD
ENERGY FLUX VARIATIONS

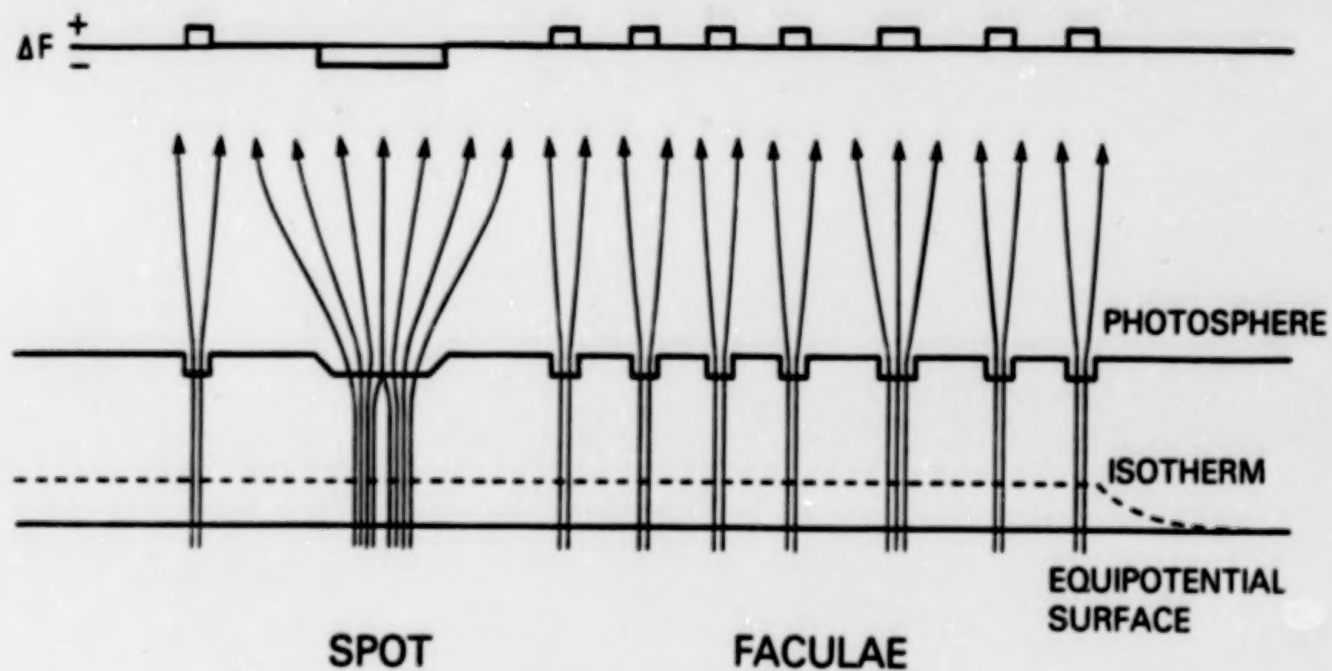


Figure 2

BLANK PAGE

ACTIVE REGION CONTRIBUTIONS TO SOLAR IRRADIANCE VARIATION,

DISCUSSION, AFTERNOON 20 JUNE 1983

INTRODUCTORY REMARKS

Gordon Newkirk, Jr.

High Altitude Observatory

Perhaps, we might begin by restating some of the questions that are on everybody's minds to establish the perspective for this afternoon's discussion. It seems an accepted fact that sunspot blocking is the principal cause of short-term variations in the total solar irradiance. This major advance in our understanding is recent: a little more than three years ago many would have placed the question of the reduction of total irradiance by sunspots in the "yet to be demonstrated" category although hints of a sunspot modulation had emerged from the reanalysis of the historic ground-based data assembled during the Smithsonian solar constant program. However, this advance immediately brings us to the first series of questions.

Is there *any* short-term release of the blocked flux either in the immediate locality of the active region or on a global scale?

What fraction of the blocked flux is released?

What is its temporal behavior?

Also relevant to the question of short-term energy balance, is the role played by active region faculae. Is there any evidence that active region faculae are different from their counterparts far from active regions in their temperature structure, brightness, and limb darkening? Or are active region faculae simply packed together more tightly? We must also inquire more deeply about the photosphere in the neighborhood of an active region that is *unoccupied* by faculae. We heard this morning that *some* active regions show evidence of a bright ring, which accounts for a small fraction of the blocked flux but is still much larger than predicted by the theoretical models. Is such a ring a general feature of all active regions in a certain stage of their development? It appears that the tools for precision photometry of the solar disk now available can go a long way towards answering many of these questions.

We can ask yet other questions regarding active region faculae. The faculae and sunspots in an active region show a similar temporal behavior, both are magnetic structures, and both inhibit convection. Is there any reason to believe that thermal processes play *any* role in coupling the growth and decay of these two phenomena? If active region faculae even partly balance the flux blocked by sunspots, what physical processes are responsible for channeling this excess from the neighborhood of the spot into the faculae and how do the latter respond? Earlier we heard theoretical reasons why *no* such channeling is to be expected; yet not everyone at this symposium is convinced that faculae do *not* play a compensating role.

Turning to much larger spatial and temporal scales, we note that the total magnetic flux of the sun changes by a factor of 3 or 4 during the solar cycle. The magnetic field which appears in such macroscopic forms as sunspots varies by two orders of magnitude over the cycle. Is there any influence of this

dispersed, large-scale magnetic field upon the radiant flux?

Is there any long-term storage of the blocked flux? Certain theoretical models suggest that storage should persist for a very, very long time compared to the lifetime of an active region. What precision measurements over what time-scales are required to yield empirical answers to the questions of long-term storage?

Although the last few years have brought us exciting discoveries, serious roadblocks to further progress still exist. Since the late 1970's we have had elegant and precise measurements of the bolometric solar irradiance from spacecraft made by Hickey, Willson, and their collaborators. The ACRIM observations made during the first nine months of SMM operation achieved a relative precision of 3×10^{-5} . Still higher precisions of better than 10^{-6} are apparently feasible. The interpretation of such observations is crucially dependent upon knowledge of the radiometric properties of sunspots and faculae. Yet our methods of measurement of sunspots and faculae have been, with a couple of exceptions, little different from the techniques pioneered by Galileo and Scheiner. In fact, they are the same--the 17th century technology of drawing sketches from which areas are estimated! It is rather amazing that this antique method has allowed us to explain even half the variance in the fluctuations in total irradiance. Papers and plans presented at this meeting are very encouraging in demonstrating a rapid move into the 20th century with plans to measure the *bolometric* contributions of sunspots, faculae, and limb darkening as essential ingredients in the interpretation of the precise, space-based measures of total irradiance.

These thoughts raise another question. Suppose the precision of the next satellite-based observations of irradiance is 10^{-6} or somewhat better and that a temporal resolution of about one minute is obtained. What are we going to do with such observations? Now is the time to consider what subsidiary ground-based observations will be needed to interpret improved, second-generation measurements of the solar constant.

Let us turn for a minute to theory. Two significant theoretic models--those by Spruit and by Foukal, Livshits, and Fowler--describe the influence of sunspots on the radiant flux. Both models predict that there should be essentially no short-term release of the blocked flux and that this flux is stored almost indefinitely in the convection zone. My personal reaction to these models is that they are really fun. Solar physics has become so complicated that it is rare that a simple model can so richly illustrate the basic physics behind the phenomena and also guide the practical interpretation of new data. However, present sunspot blocking models have limitations that cannot be overlooked. The most serious limitation arises from the fact that these are pure, diffusive transport models. They might be thought of as describing a Sun of solid copper covered by a thin insulating skin. The diffusion coefficient is taken to be uninfluenced by the heat flow around the sunspot. Yet the models predict a superadiabatic temperature distribution with a distinct horizontal gradient due to the buildup of heat below the sunspot. Such gradients will inevitably lead to large-scale organized flow, which will also transport heat. The models developed thus far are simple approximations of unknown accuracy to a complex dynamical problem. The dynamical problem must be solved before we can have confidence that we have a theoretical understanding of the thermal response of the sun to the presence of sunspots and faculae.

I wish to close with one final remark. Most of us are now intent on interpreting very specific phenomena on the Sun. However, the interpretation of these phenomena have the potential for leading to fundamental contributions

to the understanding of the physics of turbulent convection. Our models of turbulent convection on the sun are extremely crude. The entire spectrum of turbulent eddies which doubtless occur within the convection zone are commonly characterized by a single number--the mixing length ratio. Yet the most casual observation of our own atmosphere, which should be no more complex than the convection zone of the sun, reveals a broad spectrum of turbulent eddies. A more detailed analysis of the thermal response of the Sun to sunspot blocking will surely reveal some of the failures of the simple mixing-length theory of the solar convection zone. We may even hope that our analyses will point the way towards more realistic descriptions of these fundamental processes.

BLANK PAGE

SABATINO SOFIA: The Goddard Model of ACRIM Data

SOFIA: I'll begin with the conclusion. We have modeled the total ACRIM data set. The model is the Goddard standard, except we no longer assume that the spots and faculae do not evolve. We use the daily observed values and interpolate the missing days.

The difference (observed-predicted) jumps after one year, or about when the satellite changed modes of operation. There is no temporal drift in the residuals in the first year, but there is after that time. Or, one could represent this as a change in level. I can't tell the difference. If we did not include faculae in the model, the departure would be greater. A model without facular emission should go up (because of the reduced spot contribution) but the data is going down.

The drift or jump is important because either we have the wrong model, or, as some have suggested, there is modulation of the irradiance by something other than active regions.

The ACRIM and the ERB experiments have shown there is anisotropy in the solar radiation, and one should talk about the luminosity and the irradiance as separate entities, since the latter is directional while the former is a total over all directions. If one imagines a fictitious zero level as an integral over a hemisphere of quiet sun, variations in irradiance have two components. One is active regions, and the other is from this background, what I believe to be a structural readjustment of the Sun.

One question is whether the presence of solar activity modifies the quiet sun background and if so, on what timescale? There are two separate ways to answer this question. One is theoretical, analogous to Peter Foukal's work. This is a complicated problem. The other solution is to look empirically. If we assume the background variation is zero, we just plot the residuals from the active-region model and see if it is so.

The basis of the model is straightforward. The area of the spot, with appropriate geometric factors, is multiplied by the contrast as a function of limb distance. The faculae are treated similarly. What can be in error?

- The contrast may vary with the area.

- The limb darkening may vary with the area.

We have assumed the area of the faculae equals the area of the plages. This is not a significant problem as long as the ratio of one to the other is a constant. We must make this assumption because the plage areas are available while the facular areas are not.

DISCUSSION

HUDSON: Is the limb contrast law for faculae based upon the facular photometry or on a fit to the ACRIM data?

SOFIA: It is based upon the facular photometry. The difference in the limb contrast curves look large near the limb, but when you weight by area ($\cos\theta$) it is not important.

EDDY: How does it affect the model if the ratio of facular and plage areas is not unity?

SOFIA: The facular contribution could be changed by a factor of two and still be within the uncertainties of the data.

Also, the area values for the same spot on the same day differ by a factor of two among different observers.

EDDY: I don't agree.

SOFIA: Most of the irradiance variation is represented by the spot signal. In the first year of ACRIM the residuals oscillate around zero, but after that there is a trend.

RABIN: If most of the variation is in spots, is the correlation with faculae significant? When you add more parameters, you always get a better fit.

SOFIA: The significance of the fit goes from 120 to 140.

HUDSON: But is that significant?

SOFIA: We are not free to discard the faculae, we know they are present and bright. Further, the high-frequency variation of the irradiance comes from the faculae, because at each disk passage you get two maxima, one at each limb.

FOUKAL: I distrust these models which try to show a detailed balance of spots and faculae. We know these phenomena have lifetimes of several months, and spend half their time on the invisible hemisphere. Even if you know completely the properties during the visible disk passage, there still is an uncertainty of order 50% in the question of the time-averaged energy liberation. We are spending a large effort, but will it answer the question?

SOFIA: The burden of proof lies with those who propose that the sun does not conserve energy!

FOUKAL: If we just want to know whether facular emission balances spots, since the timescales are several rotations, you always will have the uncertainty of not knowing what the faculae were doing when you could not observe them.

CHAPMAN: The purpose of the model is to match the observations from the satellite.

FOUKAL: We know from some extreme cases when the Sun has spots and insufficient faculae to balance them that there must be storage.

SOFIA: The model has storage because faculae outlive spots.

FOUKAL: And in specifying that storage over the lifetime of the object you have a 50% uncertainty right away.

SOFIA: The purpose of the model was simply to compare the data with the known

spots and faculae. When the fit appeared very good, we asked what the average contribution over several months was. I expected there would be a difference (spots-faculae), because when you look at the pole, there is more of an excess. There is no reason why there is a balance in the ecliptic plane. But, we found there was no difference to 20 or 30%. That is within the uncertainty of the data. Our statement is there is no evidence for energy storage beyond the lifetime of the faculae. If someone thinks the timescale is 10^5 years, let him prove it.

FOUKAL: That is not an educational statement.

SCHATTEN: Do you believe the back side of the Sun is different from the one we see?

FOUKAL: No. But as Helen Dodson-Prince points out, strange things happen on the other side of the Sun.

WILLSON: Just because you cannot see it half the time does not give you a 50% error.

FOUKAL: You get an error at least as large as the one for the visible hemisphere, which is claimed to be 20 or 30%.

SOFIA: Rather than argue over whether there is detailed balance, we should reduce the error by improving the observations.

LAWRENCE: One way is to take an ensemble average by studying many active regions. The uncertainty of the regions on the unseen hemisphere can be reduced to a negligible size.

SOFIA: The points I wanted to make are:

(1) The measures of spots and faculae are very poor. If we get better data, one product is the residuals (observed minus predicted), with much reduced error. Any trend would then be easily seen.

(2) We assume the intensity of all faculae are the same, independent of size. An uncalibrated Brightness Class is given for each plage; perhaps we should calibrate it.

ZIRIN: In the new data being reported, the brightness is calibrated.

SOFIA: Good. Once we get the residuals down, I would be surprised if we did not see trends. Trends can come from horizontal redistribution of energy or structural changes (for example, the radius). It is probably just such long term changes, or timescales longer than active regions, that have the most significant consequences.

FOUKAL: We have talked about faculae as though they only perturb the thermal behavior of the photosphere at $\tau=1$. But they also are major perturbers of the nonthermal heating of the atmosphere. I have a hard time understanding why the Sun would want to keep the sum of the thermal perturbations due to spots and faculae, plus the nonthermal perturbations due to faculae constant. The

nonthermal heating is due to wave or joule heating - what keeps the sum constant?

SOFIA: The balance is over all spots and faculae present, of varying ages, when you average over a few months.

HUDSON: I side with Sabatino. You do not have to have a model to accept the observations. We should be able to count the energy fluxes from spots and faculae, using the areas and brightnesses. It is a simple question to ask if the two numbers are comparable.

POUKAL: You have to produce a physical model that explains why such a balance occurs.

NORDLUND: If there were a physical model that explained the energy flow from one place to another, then an uncertainty of 20 or 30% would be consistent. But when there is no model, just saying they are of the same order of magnitude is not significant.

LABONTE: The spot blocking causes the storage of heat in some upper layer of the convection zone. The lower opacity in faculae causes a somewhat thinner layer at the top of the convection zone to leak energy faster than it would otherwise. In some sense both structures influence the same reservoir.

CHAPMAN: If the total lifetime energy deficit of a spot is roughly balanced by the lifetime excess of its faculae, then there must be a (magnetic?) connection. Why would it occur in case after case, if it is an accident?

POUKAL: We seem to polarize into those who want thermal models and those who want detailed balance. There are lots of models which are neither, and this early it is not useful to get locked into one viewpoint. Perhaps most of the spot energy goes into Alfvén waves and deposited at depth - this fits neither side. It concerns me that we are going off to do photometry to prove the detailed balance, which I find to be a low probability situation.

NEWKIRK: Generally, rather wild theories accompany poor observations.

RABIN: Is there evidence for a rough balance of spot and facular signal independent of the ACRIM comparisons?

SOFIA: Our model was constructed just from the optical data. The comparison with ACRIM comes later.

HUDSON: Given all the uncertainties of areas, lifetimes, etc. we seem to be about where we started 2 years ago. During the lifetime of the spots the faculae cancel some 15 or 20%. After the spots go away, the cancellation may go to 50%, (\pm 50% just due to observation error).

JACK EDDY: The Quality of Existing Spot and Facular Data

EDDY: I want to limit my remarks to the sunspot and facular data. I agree with Sofia that better measurements are needed. I disagree with their statements about how bad the data are, or that we are limited with what we can do. I do not think the comparison of model with data have been conclusive.

It is usually said the spot data are no good to a factor of two, particularly the SEL data commonly used. We have done a comparison of several stations that report a daily measure of the total spot area, some by the 17th century method, but some by photography. They are SEL, that reports a daily value - there are no gaps in the data set; Catania; Rome; Taiwan; and a string of data from Lee, in Peking. So there are data from around the world that report on sunspot area. Now, how much improvement do we need to make; How much can it be affecting the model?

I will show 70 days from 1980 which are picked at random to compare the data.

HUDSON: Are there political reasons for choosing the particular colors?

EDDY: Red for China, for sure. These are projected areas in millionths of the solar disk. The SEL data run more or less through the middle of the others. There are periods when it is low. This time interval was chosen because it has peaks and valleys in it. You can see that when the spot number got low, there was a big divergence. This is what Sofia would point to for his factor of two.

SOFIA: Yes.

EDDY: There is at least a factor of two between Taiwan and SEL. I think that is unusual. If you look at the rest of the interval, the measures all cluster together. If we could not get better data, I would suggest we just take the mean of all these datasets. You find the standard deviation of the mean is quite small, much better than using a single station's data.

LABONTE: Why are the data as noisy as they are? There are many days on which you can find a range of 1000 millionths, which is a big area.

EDDY: Yes. I suspect it is seeing. Another problem is, how much are we losing in all these measures due to loss in visibility at the limb? That is emphasized in the Goddard model, which assumes you lose so much that you should not trust the observations. Perhaps that's an overstatement. I think you can recover the limb loss. We looked at the SEL data for one year. Assuming that in the year there is no preference for spots to be on any particular longitude, you expect the corrected areas to be distributed uniformly in longitude. We derive a limb visibility function, which shows as a function of central meridian distance how the areas sum in the course of the year. One expects this to be a cosine in longitude. You can see where you are losing area at the limb of the Sun. If you assume you see all the spots there are at disk center, by this method you can measure the loss. The total loss is 13%. This is for the SEL, that I suspect is typical of the other observatories. Maybe that is part of the answer - different stations have different visibility functions, with 10 to 15% loss in total.

ZIRIN: For years there was an east-west asymmetry of spot areas, that was explained by saying the growing new regions were followed better. You have the opposite asymmetry.

EDDY: I do not think you can say much from one year's data.

POUKAL: Maunder's old result was that you see more spots on the east limb than on the west. The explanation was the west spots are masked by faculae in the following parts of regions.

ZIRIN: Yes, you are right. But another explanation is that you see the growing spots from the east on later days, while those on the west rotate out of sight.

EDDY: It is probably accidental that this year of data come out that way. In any case, you only miss 13% of the spots in one year, and that is a lot less than the Goddard correction.

SOFIA: We overestimated the correction. We assumed that if you take the spot area at central meridian passage and assume no evolution, the errors should balance out. But occasionally, because of data gaps, the spot area used was not from the central meridian but some distance off. That systematically would increase the correction, by 10 or 15%. We have done away with that assumption, and just take the observations.

EDDY: Not just the central meridian areas?

SOFIA: We do not do that any more. Do you see any systematic difference between photographically determined areas and the others?

EDDY: No, and that is surprising.

The other issue is the facular areas. We all agree that a large improvement is needed. What is the facular to sunspot area ratio? There have been complaints that in our model we used a ratio which is too small, and I suspect that is true. But the models that suggest detailed balance use a ratio which is much too large.

There is one source of data that has not been discussed - the long series from the Greenwich Observatory. Between 1874 and 1976 they made daily measures from photographs of the Sun.

First, we see there is not a simple relationship between the sunspot and facular areas. The ratio changes with time and activity. As the sunspot areas have increased during the 20th century, the facular areas have not increased as much. Further, when the sunspot area is highest, the facular to spot area ratio is lowest. From a biased view, that is another argument against detailed balance. If the faculae dutifully radiate the energy trapped by spots, you would expect their areas to track, with some constant ratio. But they do not. A plot of the ratio of corrected facular to spot areas falls with increasing spot number. When the spot number is as high as it was in 1980, about 150, the expected area ratio is nearly 1, rather than 10. Were the Greenwich observers missing 90% of the faculae?

MOORE: Perhaps when the spots were most numerous the observers were so fatigued from counting them all that they did a poor job on the faculae.

EDDY: They measured them the same way they do sunspots. They look at the pictures with a grid.

ZIRIN: All the faculae are near the limb?

LA BONTE: That's a big point. The spots are seen at all central distances but the faculae are only near the edge.

FOUKAL: We did a power spectrum of the rotation of the Sun using the Greenwich data on faculae and sunspots. We came out with this marvelous 28-day peak plus there was this booming peak at 9 days. We concluded that they only see faculae on the east and west limbs. We asked the people at Greenwich and they said that is the case. They see no faculae within $\pm 60^\circ$ of Sun center.

EDDY: They do not look for polar faculae?

FOUKAL: I do not know. They are not seeing faculae as they track across the Sun.

ZIRIN: It is impossible to see them near the center of the disk.

LA BONTE: So the facular areas need to be multiplied by 3 to get the total area on the disk, since they only measure in 1/3rd of all longitudes.

SOFIA: We put the faculae where they are, and when they are near the center the contrast is zero.

EDDY: If we multiply by 3 we have to divide by 2, which is the correction for projected to corrected areas. Again, the ratio of faculae to spot area falls the more spot areas there are. When the spot area is as high as it was in 1980, the projected facular area, which is what counts for modulating the irradiance, that is about equal to the spot area.

CHIPMAN:(?) Can you get to the point where the amount of facular area is a sizeable fraction of the total area they can detect them in? This would set a limit to the total area.

EDDY: You mean all the real estate is taken up by sunspots and faculae?

CHIPMAN: Yes. They fill up the area.

ZIRIN: I think the large spot areas come when you have big spots near the center of the Sun, but the faculae are always restricted to the limbs. You just do not get big increases in the facular area. But for 9 days the spot area counts heavily, when no faculae are visible. The most interesting thing is the facular areas are 2 to 3 times the spot areas, and the contrast is only a few percent, while the spots knock out 50% of the light. There is no way you can ever balance them.

EDDY: I agree.

CHAPMAN: The faculae are down in contrast by an order of magnitude. Jack pointed out they are already missing 13% of the spots and if you knock down the contrast,

you could lose much more of the faculae in the measurements.

ZIRIN: They are measuring what they are seeing. If the faculae are down so low you have to have so many of them.

SCHATTEN: One reason why the spots give large irradiance dips and faculae do not is the lighthouse effect. Faculae spread their excess brightness over a large solid angle. Spots appear dark only if you view them directly.

ZIRIN: We should consider what the Sun looks like from the solar poles? But that only adds a factor of 2, and you are off by a factor of 5 or 10.

SCHATTEN: No, we are not off that much.

EDDY: Yes, you are.

KEN SCHATTEN: A Model for Balancing Spot and Facular Emission

SCHATTEN: While Jack has raised doubts about whether there is energy conservation in active regions, we have found evidence experimentally that there is. I will talk about how this might happen theoretically.

I have looked at a combined Parker and Spruit model for faculae and sunspots. In a young spot region, with spots and faculae, in Parker's model you get a downflow in this region. Below the surface the spot breaks into a lot of little flux tubes and the downflow makes it stable, and also prevents the heat from going upward. You get a buildup of heat, so the isotherm, which used to be on an equipotential surface, changes, becoming slightly elevated. In the faculae in Spruit's model, you see the inner walls of a hot fluxtube at large angles. In the young active region there are few faculae, and the net effect is a lower heat output. Remember, the heat flows only out of the Sun, not into it.

We are talking only about changes in heat flow. You cannot take the energy from the relatively cool shallow layer of the active region and send it back into the center of the Sun. The key factor in determining how long the energy can be stored is the depth of this region. Foukal has this about 7000 km in his sunspot blocking model. Parker has suggested this depth is 2000 to 7000 km.

In a young active region there is a net deficit irradiance because you have large spots and relatively few faculae. As the region ages, the spot decays and more faculae are produced in the breakup. A large amount of energy has been stored below the surface and the isotherms are slightly higher. The faculae continue to emit until eventually all the excess heat has been liberated, and the initial state is reached.

I have done some simple calculations of the timescale by redistributing the energy to different depths and asking how long it takes to be released. For 2000 km depth the storage time is 2 days; 2800 km gives 5 days; 3500 km, 10 days; and 7000 km, 100 days. Foukal's model with a spot depth of 7700 km gave a timescale of 83 days.

DISCUSSION

HUDSON: What is the mechanism of energy transport in your calculations?

SCHATTEN: This is Parker's idea that there is a downflow in the spot which inhibits the upward flux. He has shallow sunspots.

HUDSON: Is it diffusive or is it convective?

SCHATTEN: The upward transport of convection is inhibited because you have a downflow.

Foukal's value may be a little overestimated but is still of the right order of magnitude. The spot will not have a square cross-section as his does. If you conserve magnetic pressure and flux with depth, the fields are compressed to a small area. At 3500 km depth, the area is only 6% of its surface value, and at 7000 km, only 2%.

The important point is that once the energy gets to these shallow depths,

there is no way to stop it from coming out. It's like trying to dam the Mississippi. You may temporarily store the energy, but there is large horizontal heat transport, so it will go around obstructions. There will not be storage for anything like 11 years, which would be needed to get solar cycle variations.

NEWKIRK: Why do the magnetic faculae act as preferential transporters of heat outwards? The usual picture is that vertical magnetic fields are inhibitors.

SCHATTEN: I have mostly taken other people's models. Spruit's faculae have an evacuated region in the high field. At large angles you see the hot inner walls. The faculae just sit around cooling the Sun.

NEWKIRK: Why do faculae anchored in the region of stored heat radiate more than ones anchored elsewhere?

LABONTE: I want to ask Foukal a question. Why is the time delay so large? Convection is very efficient and the difference from the adiabatic gradient is so small. If you put in a small temperature perturbation it should just drive all the energy out. Why is the timescale for storage longer than the turnover timescale?

FOUKAL: It goes back to the analogy with the Mississippi, which is wrong. If you build a dam, the water continues to flow downstream, but the elevation of the water propagates upstream. That is what happens with a thermal plug. The heat flows outwards, but the thermal signal propagates downward fast. The heat flow right down to the bottom of the convection zone is perturbed in such a way as to store energy. The product of the difference in temperature and the specific heat gives you the stored energy.

SCHATTEN: After a very short time the sunspot is gone and then it all comes out.

FOUKAL: The propagation time downwards is $\leq 10\%$ of the lifetime of a spot. Once you have perturbed the whole convection zone, the timescale that comes into play is the time it takes to radiate the stored heat from the photosphere. The amount of heat stored is enormous because the specific heat is very high. The amount of temperature excess you generate at the photosphere is extremely small. So that gives you a timescale that is long.

ZIRIN: One should not use sunspots as interchangeable with plages. While they are associated, the recent work of Wallenhorst and Topka tried to study what happened when the sunspot decayed. It does not leave a puddle of plage behind. We also gave some examples in our paper on naked sunspots, where the existence of naked sunspots shows you that spots and plage do not always match up. It is not clear what the difference between them is.

HUDSON: The thermal diffusion models have not been done completely because the hydrodynamic expansion has not been included, which should be a major element in the response of the Sun to the blocking of heat.

FOUKAL: Spruit has done that.

HUDSON: Is it published?

FOUKAL: In his paper it is a non-issue because the amount is small. The increase in potential energy due to the expansion you can get from the virial theorem and it will be about 3 to 1.

NEWKIRK: He has done the buoyancy calculation but he has not done the dynamical calculation, for the heliostrophic wind. Nobody has, it is a mess.

HUDSON: What is a heliostrophic wind?

NEWKIRK: That is because you have a horizontal temperature gradient which means a horizontal pressure gradient which means a flow. It is a nonlinear problem.

FOUKAL: I agree, but I do not think that is going to change qualitatively what is going on. The answer you get will be model-dependent since the calculations will be as uncertain as the mixing-length approximation. They have to be because they are parametrized by things like the eddy viscosity. But the answer most likely will be the efficiency of the heat transfer upward from the bottom of the sunspot versus the heat transfer downward will change. There will be a slightly different correspondence of the observed dips and the calculated ones.

NEWKIRK: It may supply the amplitude of the few bright rings you see.

SCHATTEN: As you go down, the area of the spot gets smaller and smaller. The root is like a fibril. They are not going to affect the heat transport in those regions.

FOUKAL: The sunspot blocks all but 10% of the heat flow. The heat flow coming up against its bottom knows that it is there. Parker's model is meant to explain how as much as 10% gets through what is supposed to be a monolithic block of field. To get the model to work he hypothesizes a downflow which is not observed.

SCHATTEN: Meyer et al. originally hypothesized the downflow to make the spots stable.

FOUKAL: Why do you focus on this uncertain downflow to provide the blocking when there is a much simpler explanation?

SCHATTEN: We do not need the downflow. It is irrelevant to the area vs. depth argument.

HUDSON: A second point about the thermal models is that they do not do one thing that we know is happening. They do not put energy into the faculae. It is clear that in active regions energy comes out of spots and goes into faculae.

NEWKIRK: I do not think that is clear. We know both spots and faculae occur; one of them is bright, the other dark. Whether there is a physical coupling has not been established.

FOUKAL: The angular sizes of the Moon and the Sun are the same as seen from the Earth, but you better be careful what you conclude from that.

BLANK PAGE

GARY CHAPMAN: What are Faculae?

CHAPMAN: There are some observational characteristics of faculae that we should keep in mind. In the upper photosphere, between $\tau = 1$ in the quiet sun and the temperature minimum, these are bright structures that are magnetically associated. This is above the level where the hot wall effect is seen. This is evidence that there is dissipation of energy in that location. The energy is then radiated to space. There is energy transport of some form in the photosphere and chromosphere in and above faculae. One wonders where that energy comes from.

Recent observations by Bonnet and Acton show there is not a clear division between pores and faculae. There are beautiful cases of pores in the continuum that disappear in the ultraviolet bands. This has been known for some time. Frazier and Stenflo worked on it. In a couple papers they showed there is a relation between the magnetic flux in a feature and its behavior as a pore or facular. So there is a distribution of properties. There is a flux $\approx 10^{18}$ Mx above which the feature will be recognized generally as a pore, and below which it will be seen as a facula.

We do not know whether these objects are a single flux tube or a collection of even smaller tubes.

DISCUSSION

FOUKAL: Is there a sharp cutoff between what you call faculae and the network?

CHAPMAN: Not very sharp, but in magnetic flux a factor of 5 ± 2 .

FOUKAL: Is there a qualitative cutoff in the physics?

CHAPMAN: There is a change in the physics. As you go to smaller flux tubes, you get heating at lower heights. Parker's idea was wrong about Alfvén wave heating upward. The energy missing from the spot does not go up. But at certain wavelengths, the sunspot is the brightest thing in the transition zone. As you decrease the flux, the heat being deposited in the atmosphere drops to lower levels.

FOUKAL: If you go to the observational evidence I do not see any discontinuity either in the continuum or in the UV.

CHAPMAN: Yes, there is no discontinuity.

FOUKAL: They are just smaller versions of the same thing.

CHAPMAN: They are not the same thing.

FOUKAL: Can you give an observational reason why they are different?

CHAPMAN: From Stenflo's articles, there is a clear distinction between spots and pores on the one hand and faculae on the other.

POUKAL: But I am asking about the difference of faculae from even smaller faculae and network. What this leads to is, if there is no distinction, then all the energy coming out of the network is the relic of missing sunspots. I do not see any observational distinction besides size, which is not a qualitative distinction.

CHAPMAN: I think that is possible. There is not a distinction between network or faculae. The magnetic field is still 1.5 KG. The size of the flux tubes is the only difference.

HARVEY: Just remember that flux does come up in forms other than sunspots. That flux does produce faculae. There are lots of faculae that cannot be traced back to a spot.

CHAPMAN: That's a good point; it's not quite as clear cut.

POUKAL: That would seem even more fatal to the argument of detailed balance. There are self-contained flux tubes that never contained sunspots.

SCHATTEN: When we talk about detailed balance we mean roughly equal, within 10 or 20%.

CHAPMAN: I am not interested with the doctrinaire view of detailed balance. It's a tool to get at how energy might be stored or transported. If you come close, you already have a problem - how do you transport heat from sunspots to faculae? If there is 10 or 20% leak it is interesting but not pivotal.

POUKAL: If you believe the network at high latitudes is being fueled by missing energy from sunspots, you have to have a good mechanism.

ZIRIN: The observations show big irradiance dips that match the sunspots. Is the idea that the loss is made up in between over some long period of time?

NEWKIRK: That is the irradiance, not the luminosity. The question is, does the luminosity change with the appearance and disappearance of sunspots, or is it compensated either locally or globally?

RECENT GROUND-BASED OBSERVATIONS
OF THE GLOBAL PROPERTIES OF THE SUN

Barry J. LaBonte
Institute for Astronomy
University of Hawaii

ABSTRACT

Ground-based observations have achieved sufficient sensitivity and duration to scrutinize many global properties of the Sun. Variations in the properties of granular and supergranular convection have been measured. The surface rotation measurements continue to present contradictory results. A spectrum of torsional motions has been detected. A variety of oscillation measurements now are available for nearly direct probing of the solar interior.

INTRODUCTION

At every workshop I give a paper with the same title. Fortunately, the contents change.

In talking about the global properties of the Sun, you must keep in mind that we only measure the surface. The only large-scale phenomena we can study directly are those of large horizontal scale. Any information about the depth variation of properties is inferred in the context of a model. Indeed, some of the so-called global properties are actually quite local, but must be measured by comparing distant areas on the Sun, such as disk center and limb. We thus assume the phenomena are uniform on a large spatial scale.

The topics I discuss are roughly in order of the "depths" that we believe we are sampling. These are surface convection, surface rotation, torsional motions, and interior structure.

SURFACE CONVECTION

GRANULATION

The granular convection at the surface is not a global phenomenon in the sense of being deep-seated. However, it is the only directly observable convection in the Sun, and as such is critical for testing theoretical models. In addition, the small apparent angular size of the individual cells prohibits accurate fine-scale measurements, so it is necessary to use comparisons of averaged properties from distant regions on the Sun to characterize the convection.

Livingston, the foremost worker in this area, has devised two different programs. The first measures the equivalent widths of a variety of spectral lines of different temperature sensitivities (1). Over the interval 1976-1980, the widths of the individual lines decreased by amounts in the range 0-2.3% in a way uncorrelated on an instantaneous basis with surface magnetic activity. Considering the different excitation properties of the observed spectral lines, the pattern of equivalent width changes is best modeled by a decrease in the photospheric temperature gradient with time.

A change in the photospheric temperature gradient is only accomplished by changing the heat flow in and out of that layer. The radiative losses at the surface are controlled by excitation and radiation processes that are well understood and should be sensitive only to physical conditions in a very local volume. Thus, a change in the temperature gradient ought to directly reflect a change in the photospheric convection. Livingston and Holweger (1) claim that the observed variation can be accounted for by a change in granular convection equivalent to a 15% increase in the standard convective-mixing length. The solar luminosity would remain constant if this change is restricted to a thin surface layer. No physical mechanism is readily apparent to induce such a change.

The second area of Livingston's work is in measurement of disk-integrated line profiles (2). In convective cells, hot bright gas rises and cool dark gas falls, so there is a net line asymmetry and line shift due to the intensity weighting of the profile. A systematic decrease in the asymmetry and in the convective blueshift is observed over 1976-1981. It is inferred that the "strength," that is, the intensity-velocity correlation, of the convection has similarly decreased. Livingston shows that a similar change in line shift and asymmetry is seen in magnetic plages, and suggests the increasing surface magnetic activity in the interval is responsible for the disk integrated line changes. He points out that although the sunspot number peaked in late 1979, he sees no equivalent turnover in the line profile changes.

Several comments must be made about this result. First, the entire change in the disk-integrated profile cannot be caused by the surface fields. By comparing the shifts shown by Livingston, I find that about one-fourth to one-third of the Sun would have to be covered by plage strength fields. This is not observed. Second, at least part (and perhaps most) of the lineshift observed in magnetic regions is a true material inflow. Howard (3) and Beckers and Taylor (4) used a variety of spectrum lines with different convective shifts to show the presence of true mass flow and the absence of gross convective changes. I would also note that in H α and the Ca infrared triplet we see clear evidence of mass inflow in plages, although the mass flux in the chromosphere is much less than what is inferred in the photosphere. In Hawaii I have been working on repeating and extending the work of Beckers and Taylor, and I've finally figured out how to do it correctly.

As far as the failure to see turnover in the line asymmetry at

the time of maximum spot number, it must be noted that other activity indicators show a more prolonged maximum than the spot number. In each of the last two 11-year cycles the magnetic flux had a broad peak that centered 1 to 1-1/2 years after the maximum in spot number. In each of the last three cycles, the 2.8 GHz radio emission also had a broader, later activity maximum. If the phenomenon that Livingston observes is truly correlated with the surface activity, I would expect it to reverse its trend only in the last year.

There does exist another data-set that could be compared with Livingston's, namely, the Mount Wilson velocity maps. Although a Babcock magnetograph with wide exit slits is used, the center-to-limb variation of the convective lineshift is measured with high precision. We know that time variations are present in the data, but the presence of radial inflow (or convective distortion) in magnetic regions disturbs the simple measurement of the quiet Sun velocity limbshift (5). Herschel Snodgrass is now reanalyzing the Mount Wilson data, taking explicit account of the surface magnetic fields.

SUPERGRANULATION

The supergranulation represents another kind of cellular structure at the solar surface. Although the supergranulation has no temperature structure, and so does not carry convective energy at the surface, it may do so at depth. The supergranular scale is most important in the organization of surface magnetic fields.

At the last solar constant workshop at Goddard, it was frequently suggested that some variation in the "character" of large-scale convection might be expected during the 11-year activity cycle. The Mount Wilson velocity maps resolve supergranules, and I tried to search for pole-equator or temporal differences in the supergranular velocities. Unfortunately, the products of the standard reduction program are organized in latitude-longitude bins, so there is possible bias at the 10-20% level. The raw velocity data should be analyzed to look for possible changes in the supergranulation.

The supergranulation can be studied by mapping the Ca K emission network, which lies around the edges of supergranules. Brune and Wohl (6) used this method to look for a pole-equator difference in supergranule size. They found no difference, with an upper limit of ~10%. A problem in this kind of measurement is the increasing confusion as one looks closer to the limb, that is, nearer to the pole. Singh and Bappu (7) measured the Ca K network at disk center and claim to have found a variation of supergranular cell size anticorrelated with activity. The effect they see is a 10% decrease over the range of Zurich sunspot number $R_z = 0$ to 180. Their quoted error is ~1%. This measurement could be contaminated by systematic effects; at low activity levels, the network is less completely defined, and the pairs of small supergranules may be erroneously identified as single large cells. Additional measurements of this type are needed to test Singh and Bappu's results, as it is potentially of great importance.

SURFACE ROTATION

During the last couple years it seemed that the major controversies in solar rotation measurements were being resolved. Most recently, however, new results have thrown us back into confusion. The basic methods of rotation measurement remain (a) the observation of Doppler velocity shifts of spectrum lines and (b) the proper motion of identifiable features (tracers) across the disk.

The basic issues are defined by the difference between the Mount Wilson and Stanford Doppler rotation measurements. Both observatories study velocity fields using the Fe I 5250 Å line with pit spectro-graph-Doppler compensator instruments, and use similar data analysis procedures. Mount Wilson finds a mean rotation rate ~2-4% below the rate measured for recurrent sunspots by Newton and Nunn (43), and also finds variation in the rate by $\pm 2\%$ on all timescales. Stanford (42) finds a mean rate within 0.5% that of the sunspots, with no time variations above the measurement noise level (~0.5% for a single day's measurement).

As corrections were made for several systematic effects (8) the Mount Wilson rotation rate was increased, nearer to the spot rate. Also, the variations in the Mount Wilson rotation rate on short timescales were found to be instrumental (9). A constant, high rotation rate has been confirmed by Snodgrass (10). He has measured the rotation rate by using magnetic fields as tracers. He finds a differential rotation curve that matches the sunspot rate near the equator and the Mount Wilson Doppler rate near the poles (?). He also finds no measurable variation with time above a noise level of ~1% (for a one-solar-rotation interval).

This seeming unification of rotation results has now stopped. First, a new systematic error has been found in the dispersion of the Doppler spectrographs. The problem is that the lines used for the dispersion measurements are only ~400 mÅ apart, but have wavelength uncertainties of ~4 mÅ. Correction for this error lowers both the Mount Wilson and Stanford Doppler rates by 0.5% (11), increasing the difference relative to the sunspot rate.

Second, an independent Doppler rotation measurement by Snider (12) gives a rate ~3% below the spot rate. Snider's instrument is a resonant scattering cell, similar to the ones used by Fossat and Isaak for their very precise 5-minute oscillation observations. This machine is intrinsically more stable and precise than the pit spectrograph-Doppler compensator instruments used by both Mount Wilson and Stanford. It should also have quite different systematic errors, although all such bias seems to be much smaller than the few percent level that we are considering.

Finally, Gilman and Howard (13) have presented the first results from a program that measured 60 years of sunspot positions from the Mount Wilson plate collection. They have measured the day-to-day rotation of individual spots rather than rotation-to-rotation recur-

rences. They have found a cycle-related variation in the spot rotation rate with an amplitude of 2% peak-to-peak. Thus, at least part of the long-term variations in the Doppler rate are probably real solar effects, not just instrumental effects. The constancy of the Stanford Doppler rate is less easily understood in this context.

TORSIONAL MOTIONS

In discussing the solar rotation, we blithely talk about its variation over latitude and time. The only reasonable assumption, however, is that the total angular momentum of the Sun is conserved, and that we simply measure redistribution of that total by internal flows. Thus, the solar rotation rate should properly refer to the time averaged velocity field, and all temporal variations should be considered as torsional motions.

A whole spectrum of torsional motions is now known and is summarized in Table I. The latest addition ($l = 0$ mode) is the observation by Gilman and Howard (13) of a variation of the sunspot rotation rate that shows two peaks during the 11-year activity cycle. The data are averaged over a latitude range of 15° on each side of the equator. This motion is caused by a redistribution of angular momentum in depth; the upper limit on a 5.5-year, $l = 2$ torsional mode, which would represent latitudinal redistribution, is $\sim 2 \text{ m s}^{-1}$. This motion makes the surface rotation appear fast at sunspot maximum and just before minimum.

The other torsional motion discovered since the last solar constant workshop is the $l = 1$ mode (14). This is a difference in the low-latitude Doppler rotation rate between the north and south hemispheres. The amplitude is so small that it is probably premature to consider this a true periodic oscillation. This motion makes the northern hemisphere rotation appear fast during the rising phase of the activity cycle.

The $l = 2$ mode that is observed (15) has an 11-year period. This motion is presumably caused by latitudinal redistribution of angular momentum. This torsional motion was first observed by Livingston and Duvall (16) but not so identified. The phase of this motion causes the ratio of polar to equatorial rotation rates to maximize at activity maximum.

The last motion listed in Table I is the only one intimately related to the surface magnetic activity in latitude position, as opposed to the period alone. The eastward and westward velocity phases of this traveling wave straddle the equatorward-moving zone of magnetic activity. However, the torsional wave is seen for a full 22-year interval as it travels from pole to equator. The amplitude of the torsional wave is nearly constant over the whole interval, but we have found a small increase in amplitude occurs 1 year before the rising phase of the magnetic activity (14).

TABLE I
OBSERVED TORSIONAL MOTIONS

Latitudinal wavenumber ℓ	Period (1) (yr)	Peak-to-Peak Amplitude (m s^{-1})	Observed Character	Reference
0	5.5	40	low latitude spot rotation	(13)
1	11	4	north-south low latitude Doppler rotation	(14)
2	11	20	pole/equator Doppler rotation	(15)
6	11	10	activity related traveling wave	(15)

Notes: (1) The Doppler observations cover an interval of ~ 15 years; the periods of the $\ell = 1$ and $\ell = 2$ modes are thus provisional.

There have been attempts to observe this activity related wave by measuring the motions of tracers. These have not yet succeeded, either because the noise level was too high (10) or because the tracer data were incorrectly binned (17).

INTERIOR STRUCTURE

There are several recent observational results that (we think) have recently probed the interior structure of the Sun. Their interpretation is necessarily uncertain, but the potential for the relatively direct tests of solar models is large.

FIVE-MINUTE OSCILLATIONS

The frequencies of the resonant pressure-mode oscillations are directly related to the variation of sound speed (and thus temperature) with depth (e.g., 18). Ulrich and Rhodes (19) have shown that the observed frequencies do not match those predicted by the standard interior models. They point out that nonstandard models developed to explain the observed solar neutrino flux still provide worse fits to the p-mode frequencies. Most remarkably, the discrepancy between observation and theory occurs for low-degree modes formed deep in the radiative core, and disappears for high-degree modes concentrated higher, in the convection zone (20). This contradicts the standard belief that convection is poorly modeled in stellar structure calculations.

The Birmingham group has gone beyond simple measurement of the low-degree mode frequencies. They additionally claim to observe frequency-splitting of the modes, which they believe is evidence that the solar core rotates more rapidly than the surface (44). One problem with a simple interpretation of the data is that more frequency components are observed ($2\ell + 1$, ℓ the longitudinal degree) than should be present ($\ell + 1$ only). Isaak (21), Gough (22), and Dicke (23) have all tried to explain the observations by postulating that the core is distorted from a purely spherical shape by a strong magnetic field ($B \sim 10^8$ G); such a distortion alters the p-mode patterns and permits more components to be observed. This seems to hang a large hat on a small hook, and I will be happier when more observational results are available. The splitting could simply be due to systematic effects in the time-series analysis (32).

One result that is clear from all the comparisons of observed and predicted p-mode frequencies is that the solar convection zone is deeper than originally thought (19, 24, 25, 26). Current estimates all fall near one-third of the solar radius, compared with earlier estimates of about one-fifth. In crude terms, the increased depth corresponds to a ratio of mixing length to pressure scale height ~ 2 , rather than ~ 1 as commonly used. This result has been suggested for several years (41), but the new data place it beyond question.

MEAN VELOCITY OSCILLATION

The Birmingham group also has measured an apparent 13^d oscillation of the disk-integrated solar velocity (27). The resonance-scattering cell they use is effectively an absolute velocity instrument, and comparison of the mean observed solar velocity from day-to-day is possible. The amplitude of the velocity oscillation is $\sim 12 \text{ m s}^{-1}$ peak to peak, and is clearly seen for most of a 90^d observing run. They suggest the oscillation is caused by the rotation of a distorted solar core with a 13^d period.

However, several analyses have shown that the likely source of this variation in the apparent solar velocity is the asymmetric distribution about the central meridian of dark sunspots and bright faculae (28, 29, 30). The asymmetry, coupled with the projection of the 2000 m s^{-1} rotational velocity across the disk, produces net variations of the disk-integrated solar velocity. The apparent period is 13^d rather than the 27^d rotation period because active regions happened to cluster near longitudes $\sim 180^\circ$ apart. This distribution of activity is not unique (45).

Even though this velocity signal is uninteresting for solar physics, it may be of great importance in the search for planetary systems around other stars. One method proposed for such a search is to monitor the radial velocity of stars to detect period variation as the star orbits the center of mass of the star-planet system. For example, the Sun should show a $\pm 10 \text{ m s}^{-1}$ velocity oscillation with a 12-year period as it orbits the Sun-Jupiter barycenter. The presence

of spots and faculae on other stars is known; thus this additional noise source must be considered.

LIMB INTENSITY OSCILLATIONS

Hill (31) has continued to observe intensity variations at the extreme limb, which he identifies with internal p- and g-mode oscillations. In addition, he has observed splitting of the mode frequencies, which he has interpreted as evidence for a rapidly rotating core. Unfortunately, confirming observations of the modes are not yet available, unlike the situation for the Doppler p-mode oscillations. As a true hidebound astronomer, I want to see more observations, and some unification of the limb and p-mode oscillation results. Indeed, comparison of the two data-sets ought to resolve issues of mode identification, since different properties of the same modes ought to be observed.

MERIDIONAL FLOW

Observations of meridional flow are presently at the limit of sensitivity of Doppler velocity instruments. The measurements indicate a poleward flow $\sim 20 \text{ m s}^{-1}$, but a major complication is the presence of apparent inflow in magnetic regions (33). Since both inflow, meridional flow, and the convective limbshift are all symmetric about the central meridian, small errors in fitting the much larger limbshift and inflow velocities can distort meridional flow measures. Magnetic field patterns have been used as tracers to measure a poleward meridional flow of the same order as the Doppler results (34), but the diffusion of fields can produce a similar effect, and work is in progress to model diffusion and meridional flow in a unified way (35).

Meridional flow is produced in the convection zone by the same convection-rotation interactions that generate the differential rotation. However, since the meridional flow velocity is more than one order of magnitude smaller, it is probable that any model of the solar interior that matches the differential rotation will need only minor adjustments to also match the meridional flow.

RADIUS VARIATIONS

At the Goddard Solar Constant Workshop the issue of using variations in the solar radius to probe the interior structure or to infer the solar constant was one of the dominant topics. This has become much less interesting, for several reasons. Theoretically, it appears that arbitrary combinations of radius and luminosity variations are possible, depending on what change in the internal structure is postulated. Thus, there is no clear target for observations to focus on.

Observationally, several promising programs have failed to produce definitive results. The Mount Wilson photoelectric (36) and photographic (37) measures have some presently irreducible systematic effects, as does the project started by Duvall at Kitt Peak (38). The limit on radius variations is "stuck" at ~ 0.1 arc second over the span of a few years. Analysis of historical radius measures from transit instruments appear to show long-term variations near the 0.1 arcsecond level (39), but the issue of systematic effects is difficult to put to rest. However, one positive outcome of the flurry of activity on the solar radius has been the construction and operation of a dedicated instrument at High Altitude Observatory (40). Perhaps this will provide definitive answers in the future.

This work was supported by NASA grant NGL 12-001-011.

REFERENCES

1. Livingston, W. C. and Holweger, H.: 1982, Ap. J., 252, 375.
2. Livingston, W. C.: 1982, Nature, 297, 208.
3. Howard, R.: 1972, Solar Phys., 24, 123.
4. Beckers, J. M. and Taylor, W. R.: 1980, Solar Phys., 68, 41.
5. LaBonte, B. J. and Howard, R.: 1982, Solar Phys., 80, 361.
6. Brune, R. and Wohl, H.: 1982, Solar Phys., 75, 75.
7. Singh, J. and Bappu, M. K. V.: 1981, Solar Phys., 71, 161.
8. LaBonte, B. J. and Howard, R.: 1981, Solar Phys., 73, 3.
9. LaBonte, B. J., Howard, R. and Gilman, P. A.: 1981, Ap. J., 250, 796.
10. Snodgrass, H. B.: 1983, Ap. J., 270, 288.
11. Snodgrass, H. B.: 1983, private communication.
12. Snider, J. L.: 1983, Solar Phys., 84, 377.
13. Gilman, P. A. and Howard, R.: 1983, Ap. J. Submitted.
14. Howard, R. and LaBonte, B. J.: 1983 in J. Stenflo, ed., IAU Symp. 102, Solar and Stellar Magnetic Fields, in press.
15. LaBonte, B. J. and Howard, R.: 1982, Solar Phys., 75, 161.
16. Livingston, W. and Duvall, T. L.: 1979, Solar Phys., 61, 219.
17. Godoli, G. and Mazzuconni, F.: 1982, Astr. Ap., 116, 188.

18. Leibacher, J. W., and Stein, R. F.: 1981, in S. Jordon, ed.,
The Sun as a Star, NASA SP-450, p. 263.
19. Ulrich, R. K. and Rhodes, E. J.: 1983, *Ap. J.* 265, 551.
20. Duvall, T. L. and Harvey, J. W.: 1983, *Nature*, 302, 24.
21. Isaak, G. R.: 1982, *Nature*, 296, 130.
22. Gough, D. O.: 1982, *Nature*, 298, 350.
23. Dicke, R. H.: 1982, *Nature*, 300, 693.
24. Scherrer, P. H., Wilcox, J. M., Christensen-Dalsgaard, J., and
Gough, D. O.: 1982, *Nature*, 297, 312.
25. Gabriel, M., Scuflaire, R. and Noels, A.: 1982, *Astr. Ap.*, 110,
50.
26. Scuflaire, R., Gabriel, M. and Noels, A.: 1982, *Astr. Ap.* 113,
219.
27. Claverie, A., Isaak, G. R., McLeod, C. P. and Van der Raay, H.
B.: 1982, *Nature*, 299, 704.
28. Durrant, C. J. and Schroter, E. H.: 1983, *Nature*, 301, 589.
29. Nyborg Anderson, B. and Maltby, P.: 1983, *Nature*, 302, 808.
30. Edmunds, M. G. and Gough, D. O.: 1983, *Nature*, 302, 810.
31. Bos, R. J. and Hill, H. A.: 1983, *Solar Phys.*, 82, 89.
32. Woodard, M., and Hudson, H.: 1983, *Solar Phys.*, 82, 67.
33. LaBonte, B. J. and Howard, R.: 1982, *Solar Phys.*, 80, 361.
34. Topka, K., Moore, R., LaBonte, B. J., and Howard, R.: 1982,
Solar Phys., 79, 231.
35. Sheeley, N. R., Boris, J. P., Young, T. R., DeVore, C. R., and
Harvey, K. L.: 1982, in J. Stenflo, ed., IAU Symp. 102,
Solar and Stellar Magnetic Fields.
36. LaBonte, B. J. and Howard, R.: 1981, *Science*, 214, 907.
37. Howard, R. private communication.
38. Duvall, T. and Jones, H. P.: 1981, in S. Sofia, ed., Variations
of the Solar Constant, NASA Conference Publication 2191,
p. 129.
39. Gilliland, R.: 1981, *Ap. J.*, 248, 1144.

40. Brown, T. M., Elmore, D. F., Lacey, L. and Hull, H.: 1982, Appl. Optics, 21, 3588.
41. Gilman, P. A.: 1979, Ap.J., 231, 284.
42. Scherrer, P. H., Wilcox, J. M., and Svalgaard, L.: 1980, Ap. J., 241, 811.
43. Newton, H. W., and Nunn, M. L.: 1951, M.N.R.A.S., 111, 413.
44. Claverie, A., and Isaak, G. R., McLeod, C. P. and van der Raay, H. B.: 1981, Nature, 293, 443.
45. Dcnnelly, R. F., Heath, D. F., Lean, J. L., and Rottman, G. J.: Paper in this proceedings.

DISCUSSION OF LABONTE PRESENTATION

[long discussion between Bruning and LaBonte]

Question: What was the time base over which the correlation analysis was done?

LABONTE: That was about fifteen years or so of Mt. Wilson data.

CHAPMAN: I don't understand how the resonance cells get you away from the scattered light problem.

LABONTE: No, he's still got a scattered light problem. The issue always has been about whether there's a difference between the spectrographs at Mt. Wilson and Stanford, and at Kitt Peak where a lot of work has been done. They are all using pit spectrographs, long focal lengths. The resonance cell is a different kind of spectral analyzer, basically, and it has a great deal of intrinsic stability. It does these p-mode observations that you can't really hope to do with a conventional grating spectrometer. I think the spot result is interesting, but there's a real question.

Question: I'm expecting a comment on how fair do we have to be in accepting sunspot rotation rates? ...?

LABONTE: That's right, they're very different, there are large individual proper motions. I think the new spot results are interesting, but we will have to check very carefully.

SCHATTEN: A good way of thinking about the radius variations, with respect to the other kinds of observations we have been talking about - p-mode oscillations and so forth - is that perhaps these other kinds of observations are better probes of the solar interior. They might let us understand the average structure of the sun better, but I don't think that we are expecting them to be sensitive to variations in time, particularly secular changes. The radius variations would be very sensitive to those things, but perhaps aren't going to tell us a tremendous amount about the solar interior structure.

CHAPMAN: But the radius of the sun is supposed to change rapidly, isn't it? With flux blocking, for example.

LABONTE: You mean, does it? No, you don't expect it to change much. For many common sorts of things the radius isn't expected to change much; you get more of a luminosity variation, and since we have some limits on that, they tend to limit the radius variations to very small values.

NEWKIRK: I can't quite agree with the statement you made about the radius variations; that if one had concomitant, I'm not saying over what time-scales, radius and luminosity measurements, the combination between the two can form a useful diagnostic as to what process is causing both.

LABONTE: Yes. It would diagnose it in that sense, but I think the problem is that there are enough postulated processes that any ratio between the luminosity and

radius could be achieved.

SOFIA: Surely the situation is a lot clearer. It appears that the relationship between radius and luminosity depends upon one parameter, and that is the depth at which the perturbing mechanism operates. If it is very shallow, like a Doppler observation, then then the response of the radius is very small. The fact that (probably) radius changes have been observed implies that that is not the mechanism. If on the other hand you use any kind of mechanism - you mix the core or whatever - you have a unique relationship between the radius and the luminosity. So as long as the origin of the perturbation is below 95% of the radius there is a unique number, very well defined, that brings very sensible values. It is not a "quickie." We are carrying out a very exhaustive perturbation analysis by mixing the core, by magnetic perturbations, on different time scales, etc., and it is taking years to get the answers. It is not that there are no answers. What everybody has done is the "alpha" perturbations, to get a small result and then drop it. That is only a very tiny portion of the question and indeed, whenever you perturb anything very shallow, in the superadiabatic zone, there is no appreciable radius change. But if you do anything else, then there is an appreciable change.

CHAPMAN: Doesn't that involve a much larger heat content?

SOFIA: Not necessarily, it turns out that the magnitude of the process is never really overwhelmingly large. It is primarily the adjustment simply if you want to find the adiabat. The problem is more under control and meaningful than you give credit. But on the other hand it is not [yet] published. that signal will be anticorrelated?

SKUMANICH: I can answer your question; what you have here is ACRIM plotted upside down, also plotted in repeated upper and lower panels, a plage signal solely from plage models that Judith Lean and I computed, and the actual K flux measured [photometrically] by Livingston.

QUESTION: What time period is this?

SKUMANICH: This is the middle of '81 to July '82.

MOORE: So the answer to the question is yes?

SKUMANICH: The amplitudes there's a factor of 10 difference between the ACRIM range of 1-3 mmag and the K-line range is 30 mmag or so. They are definitely anticorrelated.

[general grumbling and complaints about low correlation]

CHAPMAN: So at least paper 1 seems to go along with this, right? As the continuum flux in the star goes down, although the data are very spotty (sic), the calcium goes up.

GIAMPAPA: Yes, but that's paper 2.

HUDSON: Are we at the limits of ground-based photometry here?

BLANK PAGE

LIMB DARKENING VARIATIONS

David H. Bruning
Mount Wilson and Las Campanas Observatories
of the Carnegie Institution of Washington

ABSTRACT

Variations of the solar limb darkening as measured in the line wing of the Fe I line at $\lambda 5250$ have been observed at Mount Wilson Observatory. The measurements were made over the visible solar disk excluding those points where the magnetic field strength exceeded 5 Gauss. This exclusion of magnetic points should reduce the effects of faculae upon the derived limb darkening curve. The observations cover 160 days during 1980 and show evidence of variations of $0.002 I_0$ over timescales of thirty days.

INTRODUCTION

Variations of the solar limb darkening were first noticed by Abbott in 1922 (ref. 1). At that time, it was noticed that the solar limb darkening varied from day to day, and from year to year, with an amplitude of $0.003 I_0$. In 1982, Rosen, Foukal, Kurucz, and Pierce (ref. 2) presented observations that also suggested that the limb darkening varies and that the variations might be positively correlated with the ACRIM solar irradiance variations. These variations might have been due to the presence of large facular regions near the solar limb; however, examination of the intensity at points far from the limb suggests that the limb darkening variations were indeed observed. This conclusion is reinforced by the work of Rosen, Foukal, Petro, and Pierce (ref. 3) which also shows limb darkening variations.

The Rosen *et al.* papers may be criticized because their observations cover such a limited period of time, the limb darkening curves are derived from drift curves which represent only a single scan line across the sun and, as that mentioned above, their data is affected by facular regions near the limb. This paper describes an attempt to produce a daily set of limb darkening data obtained from the entire visible disk of the sun. The effects of faculae have been minimized by excluding from the analysis all points where the magnetic field strength is greater than 5 Gauss.

OBSERVATIONS

As part of the daily magnetogram observation at Mount Wilson Observatory, the intensity of each point on the sun as measured in the wing of the Fe I $\lambda 5250$ line is recorded. These intensities are used to form a least squares

solution to the limb darkening formula used by Pierce and Waddell (ref. 4).

$$I(\mu) = A + B \mu + C \mu [1 + \log (1 + 1/\mu)] + \\ D t + E t^2 + F x/R$$

where the additional terms D and E account for variations in atmospheric transparency and F for vignetting by the telescope. Each observation consists of roughly 22000 points and takes one hour to complete. The data sets comprising the present study are those deemed of highest quality by Bruning and LaBonte (ref. 5), which amounts to 160 days during 1980.

The limb darkening curve as written above uses all of the data over the surface of the sun, but it is of interest to investigate the quiet sun limb darkening curve separately. It is commonly assumed that the solar irradiance variations are due entirely to the effects of active regions and that the background quiet sun remains constant. However, this may not be the case and it is therefore of interest to investigate the nature of the quiet sun irradiance. To do this, we omit all points on the surface of the sun whose magnetic field strength is greater than 5 Gauss in the magnetogram obtained simultaneously with the intensity data.

RESULTS

The average values for the limb darkening coefficients for 1980 are

A =	0.674	σ =	0.0016
B =	0.501		0.0010
C =	-0.571		0.0023
mean intensity =	0.775		0.0019.

From days with two observations, we find the standard deviation for the mean intensity to be 0.0012. The difference between the two values for the standard deviation suggests that part of the scatter of the observations is due to systematic variations of the mean intensity. A plot of the mean intensity for each day is shown in Figure 1. If we use only the data obtained during periods of high sky transparency, we obtain the plot shown in Figure 2. The mean intensity is seen to vary in both figures on timescales of roughly 30 days.

It might be suggested that the variations are related to scattered light in the telescope. Figure 3 shows a scatter plot of the mean intensity versus the scattered light as measured for each observation. There is no apparent relationship between the two quantities suggesting that scattered light does not seriously affect our observations.

Rosen *et al.* found for their data around day number 275 of 1980, that the mean intensity rose in tandem with the increase seen by the ACRIM experiment. Comparison of our mean intensity values with the residual irradiance obtained by Hoyt and Eddy (ref. 6) and Sofia, Oster, and Schatten (ref. 7) by subtracting their model predictions from the ACRIM data values for each day indicates that there is no correlation between the limb darkening variations and the irradiance residuals.

CONCLUSIONS

There appears to be a variation in the quiet sun limb darkening curve as measured in the Fe I $\lambda 5250$ line wing. This results in a variation of the mean solar intensity of amplitude 0.2 with timescales of roughly 30 days. These variations do not appear to be the result of instrumental scattered light and do not correlate with ACRIM irradiance measurements. More observations of the solar limb darkening need to be made before the existence of the variations can be established. These observations would best be made at several different wavelengths to better probe the temperature response of the photosphere as per the studies by Livingston and Holweger (ref. 8).

REFERENCES

1. Abbott, C. G.: Ann. Astrophys. Obs. Smithsonian Inst., 4, 217, 1922.
2. Rosen, W.; Foukal, P. F.; Kurucz, R.; and Pierce, A. K.: Astrophys. J. Letters, 253, 89, 1982.
3. Rosen, W.; Foukal, P. F.; Petro, L.; and Pierce, A. K.: Bull. A. A. S., 14, 922, 1982.
4. Pierce, A. K.; and Waddell, J.: Memoirs R. A. S., 68, 89, 1961.
5. Bruning, D. H.; and LaBonte, B. J.: Astrophys. J., 1983, (in press).
6. Hoyt, D. V.; and Eddy, J. A.: NCAR Tech Note TN-194+STR, pp. 106, 1982.
7. Sofia, S.; Oster, L.; and Schatten, K.: Solar Phys., 80, 87, 1982.
8. Livingston, W. C.; and Holweger, H.: Astrophys. J., 252, 375, 1982.

FIGURE CAPTIONS

Fig. 1. Mean intensity of the sun for 1980 as derived from the limb darkening curve for the Fe I line at $\lambda 5250$.

Fig. 2. Mean intensity as in Fig. 1 but for those days of high sky transparency.

Fig. 3. Scatter plot of the mean intensity versus instrumental scattered light. No correlation is seen to exist suggesting that our observations are not seriously affected by scattered light.

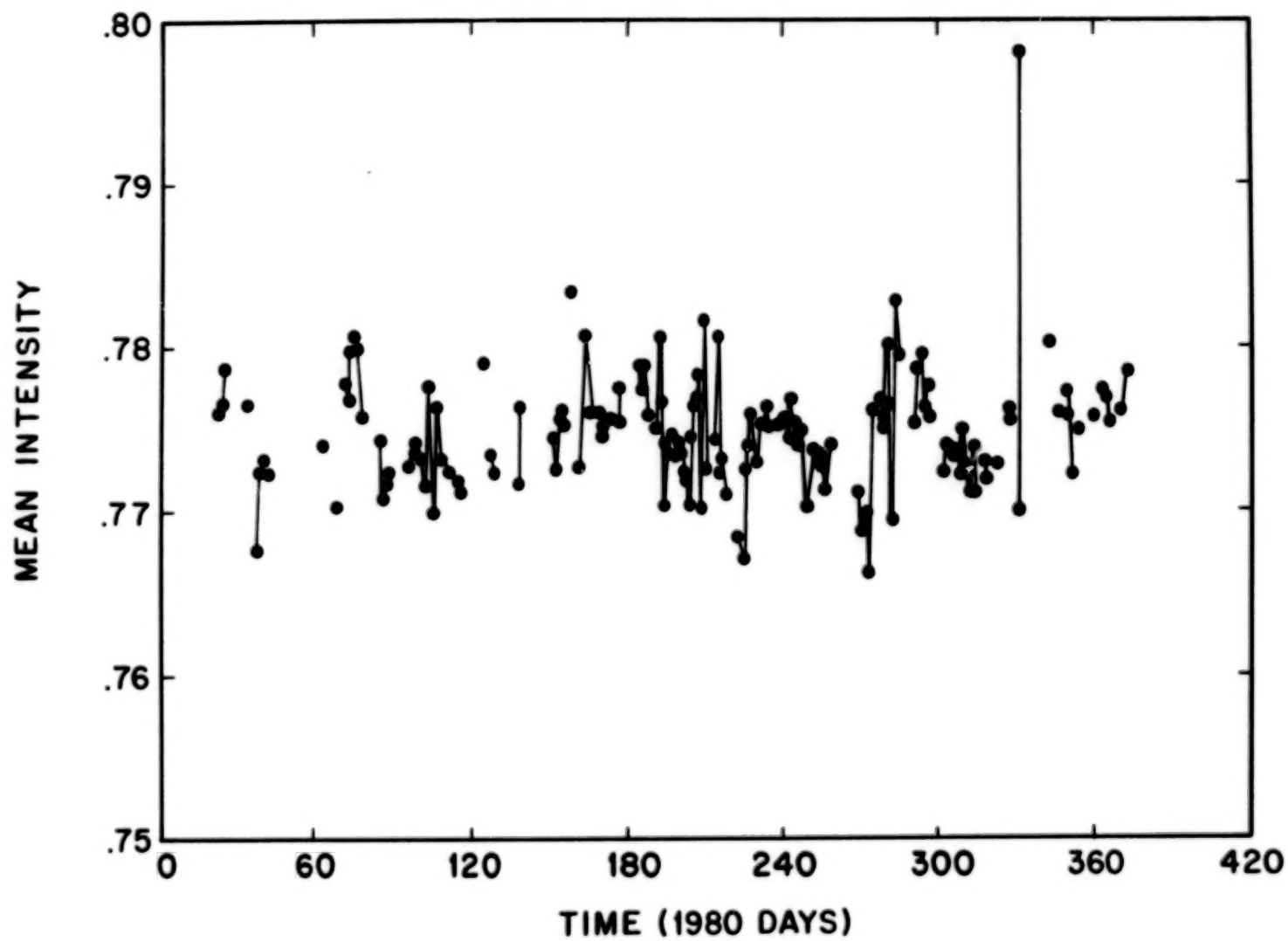


Figure 1

169

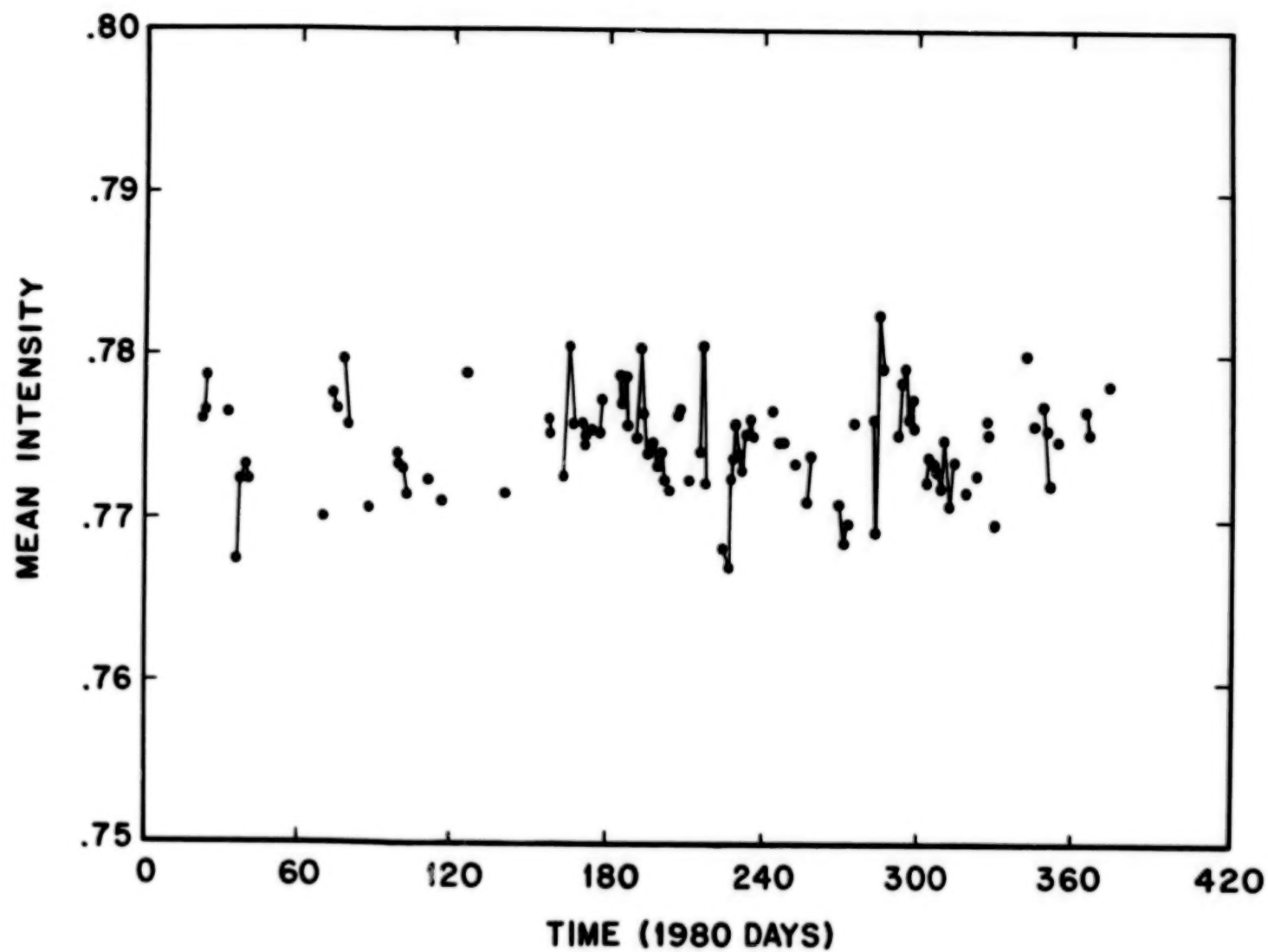


Figure 2

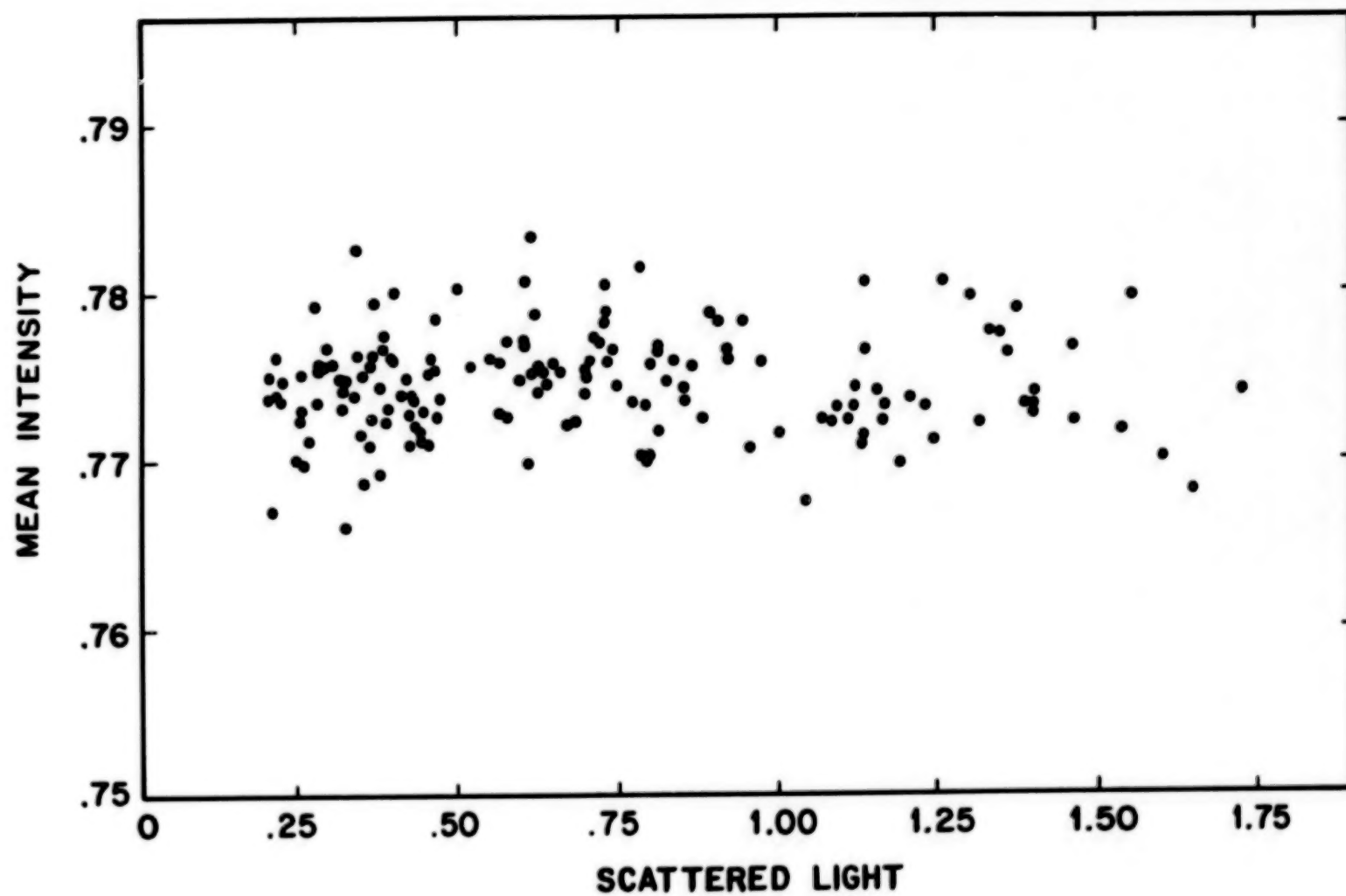


Figure 3

171

DISCUSSION OF BRUNING PRESENTATION

POUKAL: Actually, what are you plotting on the y-axis?

BRUNING: This is the mean intensity now derived from the limb darkening curve. Standard deviation is probably on the order of one or two units here.

SKUMANICH: Have you weighted the ... it's the mean flux, in other words...

BRUNING: Yes.

HUDSON: The point is, that's the limb darkening change ...

BRUNING: No, what I do is I use that curve, that general μ -dependence, to derive what the limb darkening is for each day, and take that limb darkening curve that I derive and compute what the mean intensity is for that day. If the limb darkening has changed, then that's telling you then that the quiet Sun background that are assumed constant is not constant, and that you have some kind of global variation in the solar irradiance.

SKUMANICH: This is in units of the center of the disk?

BRUNING: Right.

PHOTOMETRIC VARIATIONS OF
SOLAR-TYPE STARS: RESULTS OF
THE CLOUDCROFT SURVEY

Mark S. Giampapa
National Solar Observatory

ABSTRACT

I summarize the results of a synoptic program conducted at the Cloudcroft Observatory to search for the occurrence of photometric variability in solar-type stars as seen in continuum band photometry. The survey disclosed the existence of photometric variability in solar-type stars that is, in turn, related to the presence of spots on the stellar surface. Moreover, the observed variability detected in solar-type stars is at enhanced levels (~1%) compared to that observed for the Sun.

INTRODUCTION

In general terms, stellar observations provide the means of comparing the chromospheres and coronae of stars with varying levels of activity. Given the fact that solar activity represents but one data point, our ignorance in this regard reflects itself crucially in our comprehension of solar atmospheric activity, its causes, and its influence on solar structure. From this perspective the study of stellar atmospheres becomes an integral part of solar physics.

The results of the ACRIM experiment on board the Solar Maximum Mission (SMM) spacecraft indicate that the disk passage of sunspots can produce irradiance variations at the level of a few tenths of a percent. This result stimulated the search for the occurrence of photometric (continuum) variability in solar-type stars that is analogous to that detected for the Sun. The occurrence of spot-related variability on dMe and RS CVn stars has been well established. Thus the principle objectives of the Cloudcroft survey were to (1) monitor a relatively large sample of more nearly solar-type stars in an effort to detect photometric variability, and (2) ascertain if a relationship exists between any detected continuum variability and fundamental stellar characteristics. Such stellar characteristics include rotation rate, age, spectral type and atmospheric activity (i.e. chromospheric and coronal emission).

The observational constraints on the program were implied by the ACRIM results and the previously described objectives. In particular, the ACRIM results indicated that a photometric precision of better than 1% was required. Moreover, a large sample of stars had to be monitored to attain statistical confidence in the results. Finally, the chosen sample of stars had to represent a range of stellar characteristics. The requirements were satisfied as described in detail in three papers by R. R. Radick and collaborators (refs. 1, 2, 3; hereafter Paper I, Paper II and Paper III, respectively). The observational procedures and data analysis techniques are extensively discussed in these papers. In brief summary, the photometry was

referred to an ensemble average for each field. In this way, high photometric precision ($< 1\%$) was achieved combined with high observing efficiency. The fields chosen were within the Hyades, Pleiades, and a Malmquist field. These fields offered a range in stellar age that is, in turn, empirically related to mean rotation rate and chromospheric/coronal emission for the stellar fields considered in these investigations.

The observational strategy in Paper II departed somewhat from the aforementioned approach. In particular, a small sample (11 stars) of solar-type field stars were selected from Wilson's survey of chromospheric activity (ref. 4). This sample represented a range of a factor ~ 5 in mean Ca II emission flux. The observational program utilized differential photometry involving standard stars. Hence Paper II more directly addressed the topic of the relationship between stellar continuum variability and chromospheric activity. In the following I will summarize the main results of each paper.

RESULTS

The segment of the Cloudcroft survey program described in Paper I involved synoptic observations of a Malmquist field and fields in the Hyades and Pleiades. The main conclusions of this study include:

I. The solar-age main sequence F-K stars in the Malmquist field were not observed to be variable at the 0.5% level; variability at the 1% level was typically detected for the late FV-early KV stars in the two cluster fields. Interestingly, none of the B, A, or early F main sequence stars exhibited detectable variability.

II. The extreme time scales of variability were weeks to months; typical variability time scales were days to weeks.

III. An examination of available Ca II, X-ray and photometric variability data for the Hyades stars revealed no correlation between observed continuum stellar variability and chromospheric/coronal activity. However, no correlation between Ca II emission and X-ray luminosity was found for the sample of Hyades objects discussed in this investigation. Hence the lack of any correlation is likely due to the fact that none of the CaII-X-ray-Cloudcroft variability data sets were acquired simultaneously.

IV. The typical time scales (\sim a few days) of variability detected in the Hyades and Pleiades fields is compatible with the typical rotational periods for these stars. This is suggestive that the origin of the continuum variability is related to the rotational modulation of spots combined with the emergence and decay of active regions.

The segment of the Cloudcroft survey discussed in Paper III is a continuation of the previously described program (Paper I) with the addition of parallel observations of 36 Hyades stars obtained by G. W. Lockwood at the Lowell Observatory 0.5m telescope. The results of Paper III confirmed and extended those of Paper I. In particular:

I. The two Cloudcroft lists of variable candidates between the observing seasons of Paper I and III were completely disjoint thus implying that the amplitude of variability can change substantially over a time scale of 1

year. There was acceptable agreement between the Cloudcroft and Lowell lists of variable candidates given in Paper III.

II. As in Paper I, no stars earlier than F7 were found to be variable. The late F stars exhibited variability only at relatively low amplitudes.

III. An analysis of the seasonal mean magnitudes for the program stars (as referred to the ensemble average for a field) revealed variability on time scales ~ 1 year.

IV. An examination of the correlation between variability in seasonal mean brightness, Δm , and b-y color displayed a qualitative dependence on spectral type. More specifically, the distribution of Δm vs. b-y was tighter for the early B and A stars than for the later spectral types. The outliers in this distribution tended to be candidates for variability.

V. Analysis of Δm vs. changes in short-term variability, $\Delta \sigma$, revealed a positive correlation for the Hyades stars. That is, as mean brightness declines, short term variability increases and vice-versa.

In Paper II, the association of photometric variability with chromospheric activity, as suggested by the solar ACRIM results, was directly addressed through the inclusion of Ca II H & K chromospheric emission data obtained (fortuitously) nearly simultaneously at Mt. Wilson. The results of Paper II were:

I. Correlated variability in the Stromgren u,v,b bands was observed in main sequence solar-type stars at the 1% level. The characteristic time scales were days to weeks.

II. The continuum variability was of higher amplitude in the shorter wavelength u and v bands. This is corroborative evidence for spots as the cause of the variability. Since spots are cooler than the surrounding photosphere the flux deficit would be greater at shorter wavelengths.

III. The addition of the Mt. Wilson Ca II data revealed that the continuum variability is associated with chromospheric activity. In particular, continua minima are correlated with maxima in chromospheric emission (see Figure 1) which presumably arises from plage associated with the spots.

IV. As in the case of the Sun, these centers of activity are localized but characterized by filling factors of a few percent on the visible stellar surface. By contrast, solar filling factors are a few tenths of a percent.

CONCLUSIONS

The principal result of the Cloudcroft survey is that photometric variations in continuum bands analogous to solar irradiance variability, as detected by the SMM-ACRIM experiment, is present in solar-type stars. The variability can be attributed to the rotational modulation (disk passage) of spots, as with the Sun. The stellar continuum variability, however, can be an order of magnitude greater in amplitude than solar variability, but an order of magnitude less than that detected in dMe stars and RS CVn systems.

The fact that continuum band photometry reveals the presence of spots on solar-type stars implies that this kind of photometric technique can be utilized to measure stellar rotation periods and, potentially, differential rotation. This technique may be more suitable than synoptic observations of stellar Ca II emission arising from plage for the measurement of differential rotation. In particular, integrated synoptic solar Ca II K line observations did not exhibit solar differential rotation because of the wide distribution in latitude of plage and the solar Ca II network (ref. 5). However, I must note the caveat that sunspots (and perhaps starspots) evolve more rapidly than plage (ref. 8). Hence, a localized spot region may not be present for as many stellar rotation periods as plage. Nevertheless, the results of Papers I and II reveal that coordinated, synoptic observations are necessary in order to relate stellar photometric (continuum) variability with stellar chromospheric/coronal activity.

Finally, I am particularly intrigued by the results for the main sequence F stars. The Mt. Wilson Ca II surveys (refs. 4 and 6) show no or low amplitude cycles (analogous to a solar cycle) for F stars. Furthermore, little or no rotational modulation of Ca II emission is detected in the F stars. As noted herein, continuum variability is not detected or is detected at relatively low amplitudes in F stars. These observations imply either a low level of activity, a uniform distribution of spots, or no spots on the surfaces of F stars. However, the X-ray luminosities of F stars are typically 10-100 times the X-ray luminosity of the quiet Sun (ref. 7). I therefore hypothesize that the main sequence F stars are characterized by a uniform distribution of rapidly emerging magnetic flux that is not sufficiently concentrated to produce spots. Thus the F stars would have only "network" uniformly distributed over their surfaces. Perhaps there is insufficient time for the amplification via the ω -dynamo of interior magnetic flux before it emerges on the stellar surface. Consequently spots are not formed on these stars characterized by shallow convection zones.

REFERENCES

1. Radick, R. R. et al. 1982, P.A.S.P., 94, 934, Paper I.
2. Radick, R. R. et al. 1983, P.A.S.P., 95, 300, Paper II.
3. Radick, R. R. et al. 1983, P.A.S.P., in press, Paper III.
4. Wilson, O. C. 1978, Ap. J., 226, 379.
5. Keil, S. L. and Worden, S. P. 1983, Ap. J., in press.
6. Vaughan, A. H. et al. 1981, Ap. J., 250, 276.
7. Vaiana, G. S. et al. 1981, Ap. J. (Letters), 245, 163.
8. LaBonte, B. 1984, Ap. J., in press, January 1 issue.

FIGURE CAPTIONS

Figure 1: CaII H & K emission flux (S) and averaged photometric data (mag), plotted against Julian Date for HD 152391. Observations separated by 4 days or less are connected in both panels. Continuum light and Ca II emission both increase upward.

BLANK PAGE

BLANK PAGE

BLANK PAGE

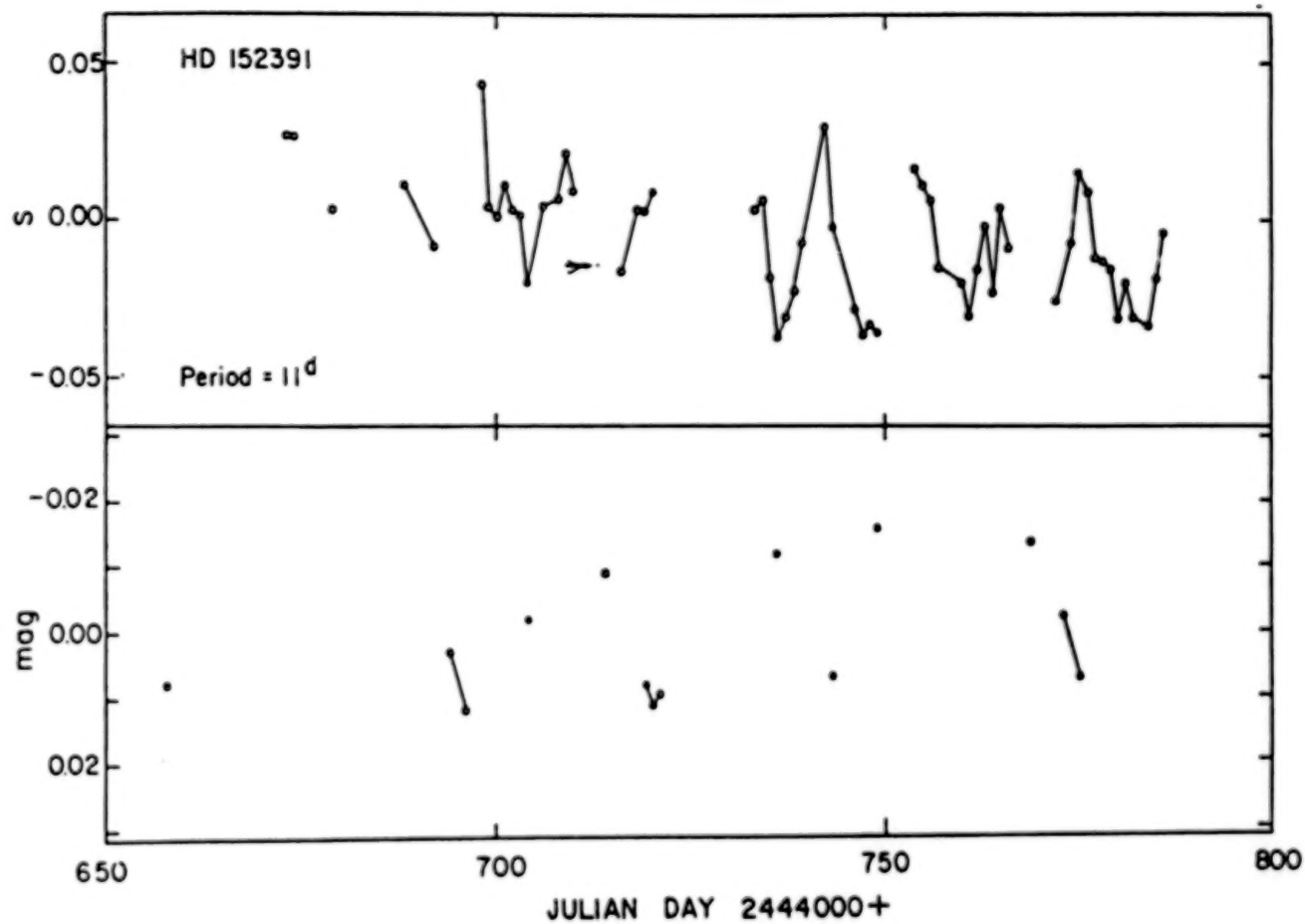


Figure 1

179

DISCUSSION OF GIAMPAPA PRESENTATION

GIAMPAPA: -----the calcium is low the star brightness is high, and again if the calcium is high the brightness of the star decreases.

COOK: There's a slight shift on the sun too, so as long as it's a couple of days it's not bad.

GIAMPAPA: Now, this was convincing to me anyway and it agreed with my prejudices. But the basic conclusions were that the continued variability at the 1% level, timescales of days and weeks on solar type stars was present, and was more pronounced in shorter wavelengths; knowing that spots are cooler you might expect the flux deficit therefore to be more pronounced at the blue wavelengths. That was more solid evidence for the variability being ascribed to activity, ...

NEWKIRK: I don't think you can make the statement you made regarding the asymmetry of these sorts of stars in comparing them with the sun. You basically have a selection thing, you've selected out those stars in which there's a large collection, or maybe one big spot on one hemisphere. If things were sprinkled around more or less uniformly in longitude on the star, you simply wouldn't see the fluctuation, since most of your stars are really at the edge of your detectability of variability anyway.

GIAMPAPA: Yes. That's correct. That was also the point of the solar paper by Keil and Worden, that plage is distributed in such a way that you don't see the differential rotation. You can pick out the mean rotation of the Sun. In the stars that behavior is manifested at an enhanced scale and so, by looking at stars like that you are looking at different stellar characteristics such as differential rotation for example, and that may thereby provide a better handle on the parameters involved in this. The observations of variability will of course show up in those kinds of stars, and the question is how representative are they? Or do you think the sun is a very peculiar case? Is that your opinion?

NEWKIRK: I'm not quite sure what the question is!

GIAMPAPA: You seem to be implying that somehow in the stellar observations you may not be addressing the problems of magnetic field generation in stars in general, and that we are looking mainly at special cases.

NEWKIRK: If you have stars with an entire distribution let's say in the clustering of spots, all the way from ones which you might regard as pathological situations where activity lasts for a very long time on one hemisphere; others perhaps of the same general magnetic activity may distribute the activity in longitude. The first type are going to be easier to detect.

GIAMPAPA: That's right. But your second point is not correct anyway. You don't see stars with high activity that do not exhibit that kind of behavior. With the exception of the F stars, you don't see solar-type stars with high X-ray luminosity, or with strong calcium emission, that do not show rotational modulation. So you're right, but the facts don't support the premise of your second statement.

NEWKIRK: If you had lots of little spots, my claim is you wouldn't detect them.

GIAMPAPA: That's right, but you don't see stars at high levels of activity that have lots of little spots.

CHAPMAN: You're saying it's not uniform. If it's a high level of activity it tends to be non-uniform in time.

HUDSON: Based upon the solar example, as you know very well, there's nothing that says that the occurrence of active regions has anything to do with solar rotation. It's not correlated with the rotation of the sun past the earth; so the more activity you've got, the more variability you're likely to have (you do have on the sun). So why should we have

CHAPMAN: I think the one point, if I may interject myself, that might be pertinent here is based on the solar example; that Gordon may be wrong on his second point but you're basing that on the assumption that the sun represents a good model, are you not?

GIAMPAPA: Well, in the sense that I have a phenomenon like spots that I know about on the sun.

CHAPMAN: ... but if you had distributed activity that was really well mixed in longitude then indeed you might not see it. But the sun doesn't work that way ...

GIAMPAPA: Well it's not just the sun but many stars don't work that way either, although with that possible exception ...

HUDSON: In general more activity should lead to more variability, since the appearance of active regions should never be correlated with the direction to the Earth.

CHAPMAN: If I make one point, if I may interject myself here... You are basing everything on the solar model, but Gordon may be wrong here; is the sun really a good model here? Yes, but if you had distributed activity that was well mixed in longitude, you might not even see it except as a fluctuation.

GIAMPAPA: It's not just the sun; many stars don't work that way either.

COOK: I'd just like to mention another paper in the second Cambridge cool stars workshop... some stars showing a faster rise to maximum...(inaudible)

CHAPMAN: His example of what, stars being similar to the Sun?

COOK: No, of applying solar-type ideas.

CHAPMAN: Does it seem to work or not?

COOK: Yes.

MOORE: Has anyone shown that if you look at the sun as a star in the K-line, that

that signal will be anticorrelated?

SKUMANICH: I can answer your question; what you have here is ACRIM plotted upside down, also plotted in repeated upper and lower panels, a plage signal solely from plage models that Judith Lean and I computed, and the actual K flux measured by the valley photometer by Livingston.

QUESTION: What time period is this?

SKUMANICH: This is the middle of '81 to July '82.

MOORE: So the answer to the question is yes?

SKUMANICH: The amplitudes there's a factor of 10 difference between the ACRIM range of 1-3 mmag and the K-line range is 30 mmag or so. They are definitely anticorrelated.

[general grumbling and complaints about low correlation]

CHAPMAN: So at least paper 1 seems to go along with this, right? As the continuum flux in the star goes down, although the data are very spotty (sic), the calcium goes up.

GIAMPAPA: Yes, but that's paper 2.

HUDSON: Are we at the limits of ground-based photometry here?

GIAMPAPA: Yes, we might be in fact, if they've correctly identified sources

HUDSON: An error of 0.003 mag is the goal?

GIAMPAPA: Yes, if they've correctly identified the sources of errors, it looks like we are limited to a half of percent level by the atmosphere.

LaBONTE: Doesn't that mean that you just have to observe the whole subset of stars in a shorter time?

GIAMPAPA: It would be ideal to get the synoptic observations of the large telescope and a fast detector [... a multichannel, chopping, a CCD might be good... brief, confused discussion].

FOUKAL: You could probably do a bit better than that by cross-correlating results from different observatories.

GIAMPAPA: Yes, that was tried in Paper III; there was acceptable agreement, but there were some discrepancies which I can't account for.

CHAPMAN: But the errors were about the same, right?

GIAMPAPA: Right. I think that the future for this kind of program looks rather bleak. As you know, the Cloudcroft facility was shut down by AURA and the telescope has been mothballed.

HUDSON: Aren't you being rather pessimistic about what ground-based photometry might be able to do? For rapid variations, for example, we have the excellent photometry of Kurtz on Ap stars. He seems to have a value of σ about a factor of ten better than this 0.3 mmag level.

GIAMPAPA: I see. Of course, they are bright A stars. But of course the brightness shouldn't matter unless you are photon limited.

NEWKIRK: Although it hasn't worked yet, or hasn't been put on the air yet, the hope is that McGraw's meridian telescope at Kitt Peak will be delivering magnitude observations with precisions of about a thousandth of a magnitude.

GIAMPAPA: Yes, that's like the scintillation noise. I'd be surprised...

NEWKIRK: His advantage is that he measures a large number of stars in a very short period of time.

GIAMPAPA: That is true, but as we heard at the Santa Fe meeting, only faint stars. I would encourage that kind of program, but it's very difficult. They won't even know what they are looking at. There should be a follow-up program to find the spectral types of the stars they observe.

QUESTION: ?

GIAMPAPA: I'd say that's a real compromise compared to having a synoptic telescope devoted to this problem

CHAPMAN: If we got the real errors down by a factor of five, we would really start to see things.

BLANK PAGE

THE K2-DWARF V 471 TAU:
A STELLAR VERSION OF SOLAR VARIABILITY

A. Skumanich¹

A. Young²

High Altitude Observatory
National Center for Atmospheric Research³
Boulder, Colorado 80307

ABSTRACT

Simultaneous observations of the rotational modulation with a 1/2 day period of chromospheric H α emission and of broadband irradiance for the K2-dwarf in V471 Tau are presented. The observations cover eight rotation periods but do not cover the full surface of the dwarf because of timing constraints. Our preliminary results show a phase relation between enhanced chromospheric emission and continuum darkening similar to that observed on the sun. A comparison with chromospheric Mg II resonance emission modulation observed about 2 1/4 years earlier by Guinan and Sion shows that the same active longitude is involved. This is either coincidental due to lucky phasing or signifies, as we believe, a stable longitude that has persisted for hundreds of rotations.

INTRODUCTION

The issue of solar variability on active region time scales can not but benefit from being placed in context with similar phenomena in other solar-like stars. The point here is that such stars represent different states of rotation (and presumably differential rotation), convective strength and other parameters that enter into the underlying magnetic driver of such activity. We present a preliminary report here on our simultaneous observations of the continuum and the H α line in the rotating K2-dwarf in the Hyades eclipsing binary V471 Tau. This dwarf represents a case of rapid rotation ($P = 0.52$ days) driven by tidal locking to a white dwarf companion, located at 5 stellar radii from the center of the K2-dwarf.

¹Visiting Astronomer, Kitt Peak National Observatory, which is operated by the Association of Universities for Research in Astronomy, Inc., under contract with the National Science Foundation. The authors have contributed equally to this work.

²Visiting scientist from San Diego State University.

³Sponsored by the National Science Foundation.

The H α observations were obtained at Kitt Peak National Observatory during early January 1983 with the Coudé Feed with a $\sim 1\text{\AA}$ resolution. The exposure times were sufficiently long (~ 0.7 hr) as to cause undesirable rotational phase smearing. Simultaneous broadband irradiance measurements at two colors were made at the Mt. Laguna Observatory of San Diego State University. In all, eight rotation periods were covered distributed in phase from 0.0 to 0.7. Extinction effects did not allow irradiance measurements past 0.43 in phase. Timing constraints prevented observations of the entire surface of the dwarf, since its period is nearly a half-integral day.

H-ALPHA LINE PROFILE VARIATION

Figure 1 presents a comparison of the H α line at phase 0.01 with that of a normal non-chromospherically active K2-dwarf (HR 6806) of matching spectral type. It is obvious that the lines in V471 are rotationally broadened and that H α is diluted. We take this to mean that it is partially filled by emission, so that this face, 180° opposite the white dwarf, has some areas of general magnetic activity. We presume that, like the sun (cf. ref. 1), this residual activity is distributed over 180° in longitude. We take the H α profile at this phase to be our "zero-point" for identifying plage-like active regions which are more intense and/or more compact in extent elsewhere on the star.

Figure 2 compares the H α profile at phase 0.36 with our zero-point profile (phase 0.01). At this phase the line is filled with active region (AR) emission which rises above the continuum. The "excess emission" is the difference of these two profiles and is given in Figure 3. We note that differences in the continuum at the different phases are ignored here. The area under the "emission line", in units of the continuum (hence in Angstroms), represents the radiative loss from the active region. We find that the "emission line" exhibits doppler shifts in wavelength relative to the photospheric lines appropriate to the appearance of the active region on the approaching limb and its movement by rotation across the visible face.

ROTATIONAL LIGHT VARIATIONS

Applying the above procedure to the H α profiles that have been reduced for other phases one obtains a time sequence of active region excess emission that is plotted as phase grouped mean points in Figure 4 modulo the rotational period. Also plotted as a solid line is the mean irradiance light curve corrected for ellipsoidal distortion. The observing and reduction procedure used is described in ref. 2. The error bars indicate the precision of the 5 day mean (8 rotations) light curve. Guinan's (ref. 4) ellipsoidal correction was used. The curve is inverted so that the magnitude increase (1 millimag = 0.001 magnitudes $\approx 0.09\%$) or degree of darkening increases upward. We have marked the location of two "spotted" regions at SP1 and SP2. The location of the latter is uncertain but it is clear that a second spot exists.

To compare with the solar case we present in Figure 5b the rotation modulation of the solar white light irradiance (in magnitudes increasing upward) as a solid line (ref. 3) along with the associated chromospheric modulation in the Ca II K resonance line ($\lambda 3933\text{\AA}$), dotted line, observed for the same period by Livingston (ref. 4) at Tucson. In Figure 5a the predicted modulation due

only to Ca II plages, dotted line, based on the model of Skumanich et al. (ref. 1), is plotted with the white light irradiance modulation.

It is apparent that in both stars a good correlation exists between chromospheric active regions--plage--and "spottedness" and that the chromospheric signal is broader in phase than the continuum signal. We defer the discussion of phasing differences to a more careful analysis of the data. The sun appears to yield a noisier correlation than V471 Tau, suggesting that on V471 Tau spot and plage regions occur in active longitudes that are fewer in number but larger in relative size.

ACTIVE REGION TIME SCALES AND LONGITUDES

A comparison with the 1979 observations of V471 Tau by Guinan and Sion (ref. 5) allows one to make some comment about active region time scales. The continuum darkening curve observed by them indicated two "spotted" regions, a weak one at phase 0.12 and a stronger one at 0.63. The phase of at least one of the "spotted" regions is somewhat different between the two epochs. The localization to similar hemispheres is either coincidental, due to lucky phasing if differential rotation drift occurs, or indicates relatively stable active longitudes. Figure 6 illustrates the Mg II resonance emission ($\lambda 2800\text{\AA}$) rotational modulation found by Guinan and Sion in 1980 (private communication). The chromospheric Mg II emission bears a very close resemblance to our current epoch chromospheric H α emission. We would interpret this as possibly indicating a stable active longitude over the 2.2 year period. In the case of the sun such persistent active longitudes have been identified, but their lifetime was found to be 3 to 6 rotations (ref. 6). However, our result is in agreement with the observation of Ca II chromospheric rotational modulation in other main-sequence dwarfs (ref. 7) as well as in the "spotted" dMe stars (ref. 8).

Whether the fact that the activity in V471 Tau is most pronounced at phase 0.5, i.e., centered on the face directly below the companion, is coincidental or indicative of some kind of tidal locking of activity is unclear at this time. A similar sub-secondary longitude effect has been found in the "spotted" dMe binary CC Eri (ref. 8). If tidal locking is causal, then binary stars such as V471 Tau may be poor solar analogues; but instead they may shed considerable insight into fundamental questions concerning the physics of convective dynamos and differential rotation and that is the purpose of comparing and contrasting their properties with those of the sun.

A more detailed analysis of our observations is currently in progress. Photometric observations at Mt. Laguna were made by Victoria Paylor.

The authors are grateful to D. Mihalas for a careful reading of the manuscript and his suggestions.

REFERENCES

1. Skumanich, A.; Lean, J. L.; White, W. C.; and Livingston, W. C.:
The Sun as a Star: Three Component Analyses of Chromospheric Variability
in the Calcium K Line. *Astrophys. J.* (in press) 1983.
2. Young, A.; and Nelson, B.: Analysis of the White-Dwarf Eclipsing Binary
BD + 16°516, *Astrophys. J.*, Vol. 173, p. 653, 1972.
3. Willson, R. C.; Gulkis, S.; Janssen, M.; Hudson, H.S.; and Chapman, G. A.:
Observations of Solar Irradiance Variability. *Science*, Vol. 211, p. 700,
1981.
4. Lean, J. L.; Livingston, W. C.; White, O. R.; and Skumanich, A.: Modeling
Solar Spectral Irradiance Variations at Ultraviolet Wavelengths.
Workshop on Variations of the Solar Irradiance on Active-Region Time
Scales. NASA CP-____, 19____. (Paper ____ of this compilation.)
5. Guinan, E.; and Sion, E.: *International Bull. Var. Stars*. No. 1922,
1980.
6. Gaizauskas, V.; Harvey, K. L.; Harvey, J. W.; and Zwaan, C.: Large-Scale
Patterns Formed by Solar Active Regions During the Ascending Phase of
Cycle 21. *Astrophys. J.*, Vol. 265, p. 1056, 1983.
7. Baliunas, S. L.; Vaughan, A. M.; Hartmann, L.; Middlekoop, F.; Mihalas,
D.; Noyes, R. W.; Preston, G. W.; Frazer, J.; and Lanning, M.: Stellar
Rotation in Lower Main-Sequence Stars Measured from Time Variations in H
and K Emission Line Fluxes: II. Detailed Analyses of the 1980
Observing-Season Data. *Astrophys. J.* (submitted) 1983.
8. Busko, I. C.; Quast, G. R.; and Torres, C. A. O.: H α . Variability
in CC Eri. *Astron. Astrophys.*, Vol. 60, p. L27, 1977.

FIGURE CAPTIONS

Figure 1. Comparison of $H\alpha$ spectral line for V471 Tau at phase 0.01 with that in a normal K-dwarf. The spectra have been continuum matched.

Figure 2. Comparison of $H\alpha$ spectrum at phase 0.36 and phase 0.01, continuum matched.

Figure 3. Difference spectrum of $H\alpha$ at phase 0.36 relative to phase 0.01.

Figure 4. $H\alpha$ emission equivalent width relative to phase 0.01 (dots) compared to photometric darkening (solid curve). The reduced irradiance at phase 0.2 is real and signifies the location of spot SP1. The existence of spot SP2 is conjectured since the star must eventually brighten, but its location in phase is indeterminant.

Figure 5. Comparison of solar photometric darkening with: a) calculated Ca II 1.0 Angstrom index for plage component only b) observed Ca II index. (cf. Ref. 3).

Figure 6. Mg II light curve as observed by Guinon and Sion with the International Ultraviolet Explorer.

HR6806 AND V471 TAU (Phase 0.01)

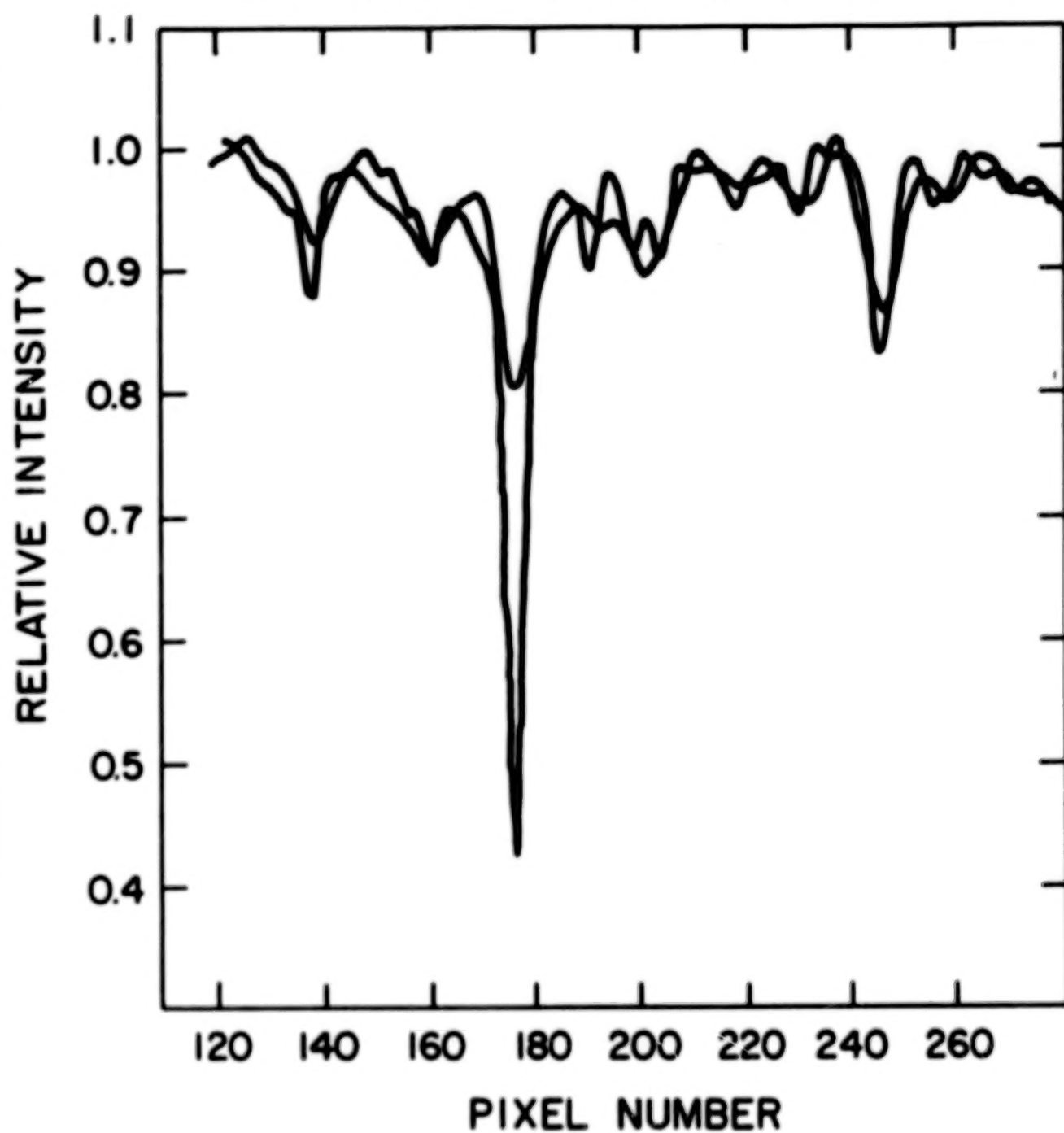


Figure 1

V471 TAU H α (Phases 0.36 and 0.01)

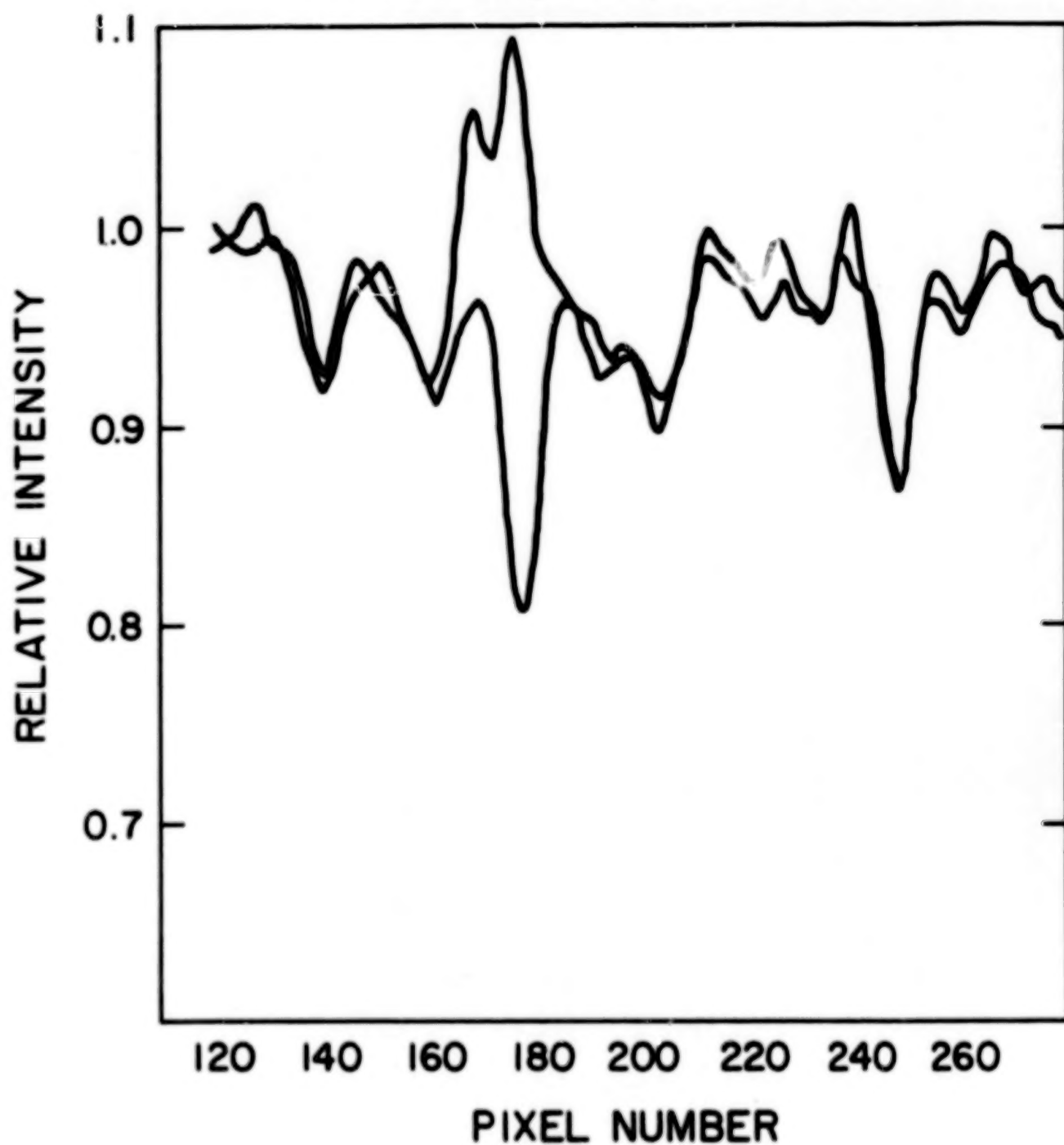


Figure 2

V471 TAU H α (Phase 0.36)

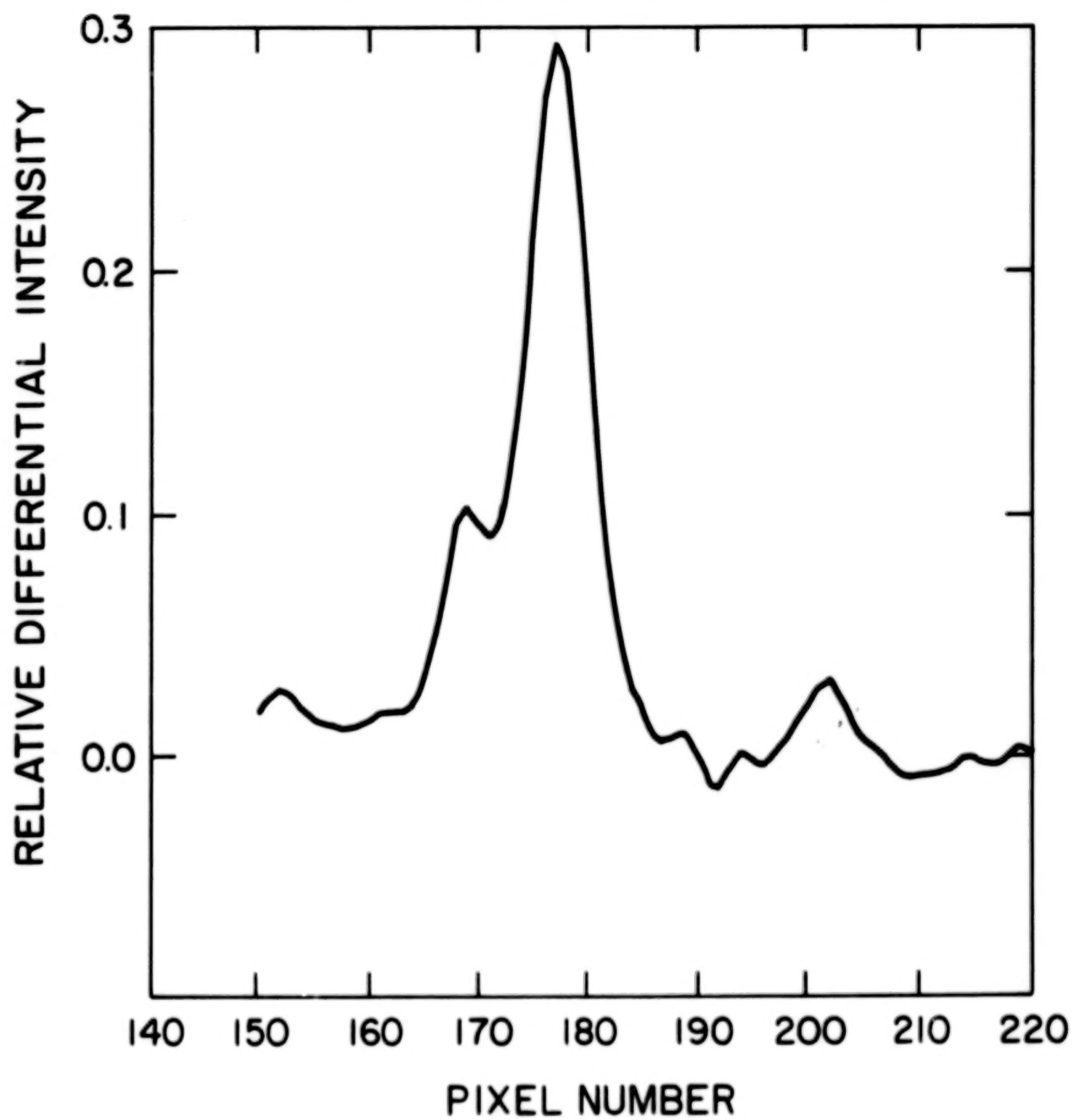


Figure 3

V471 TAU

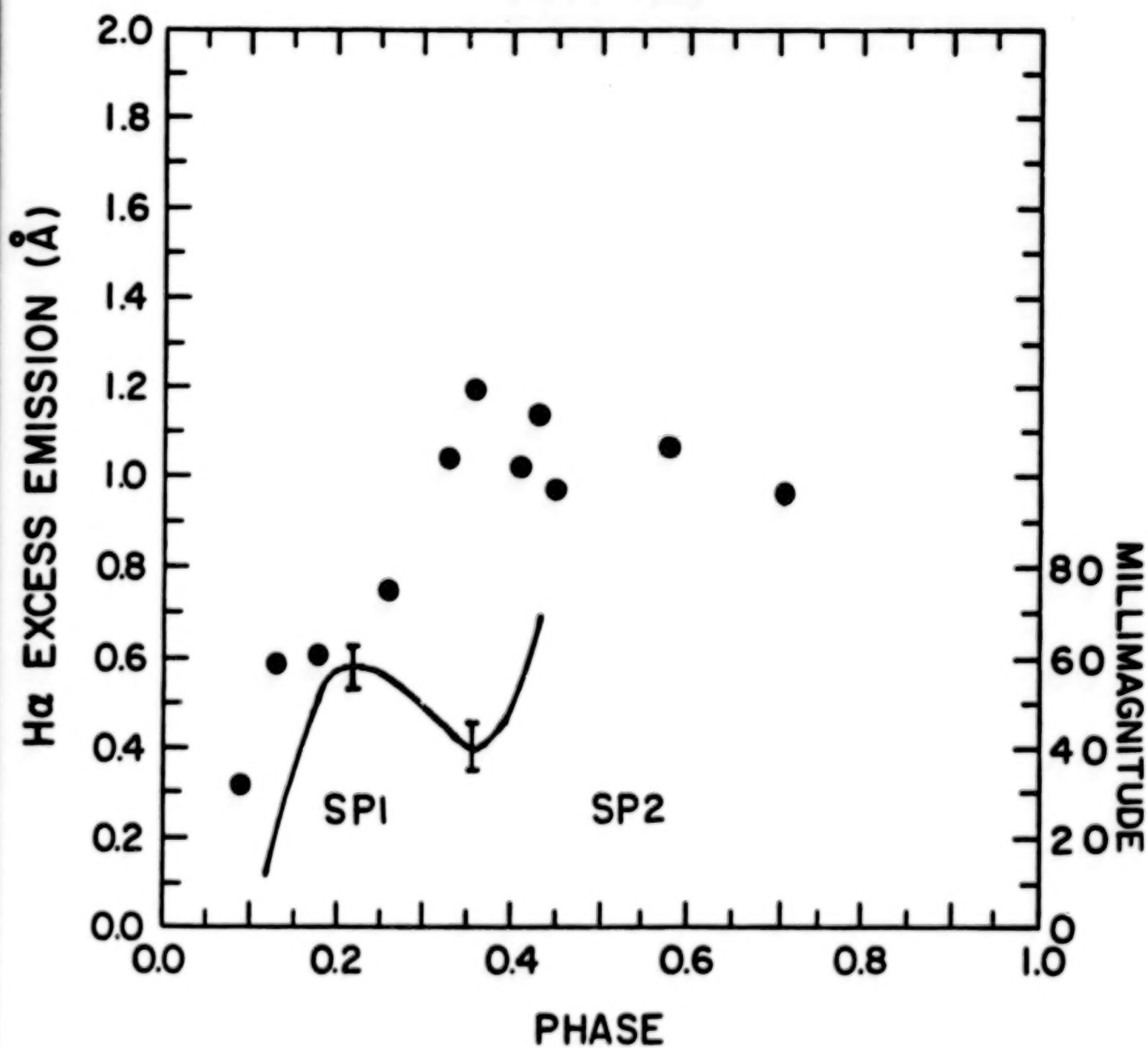


Figure 4

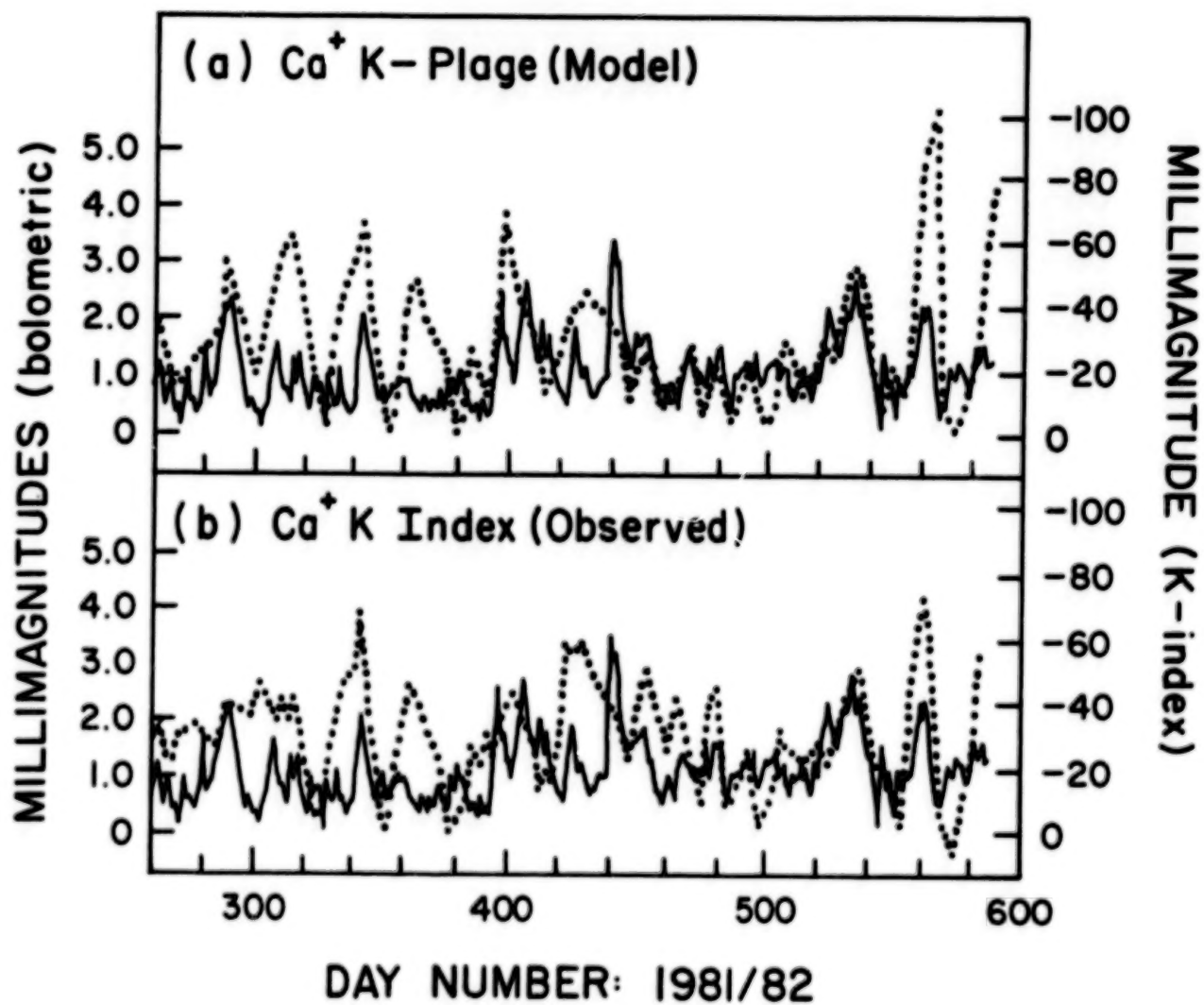


Figure 5

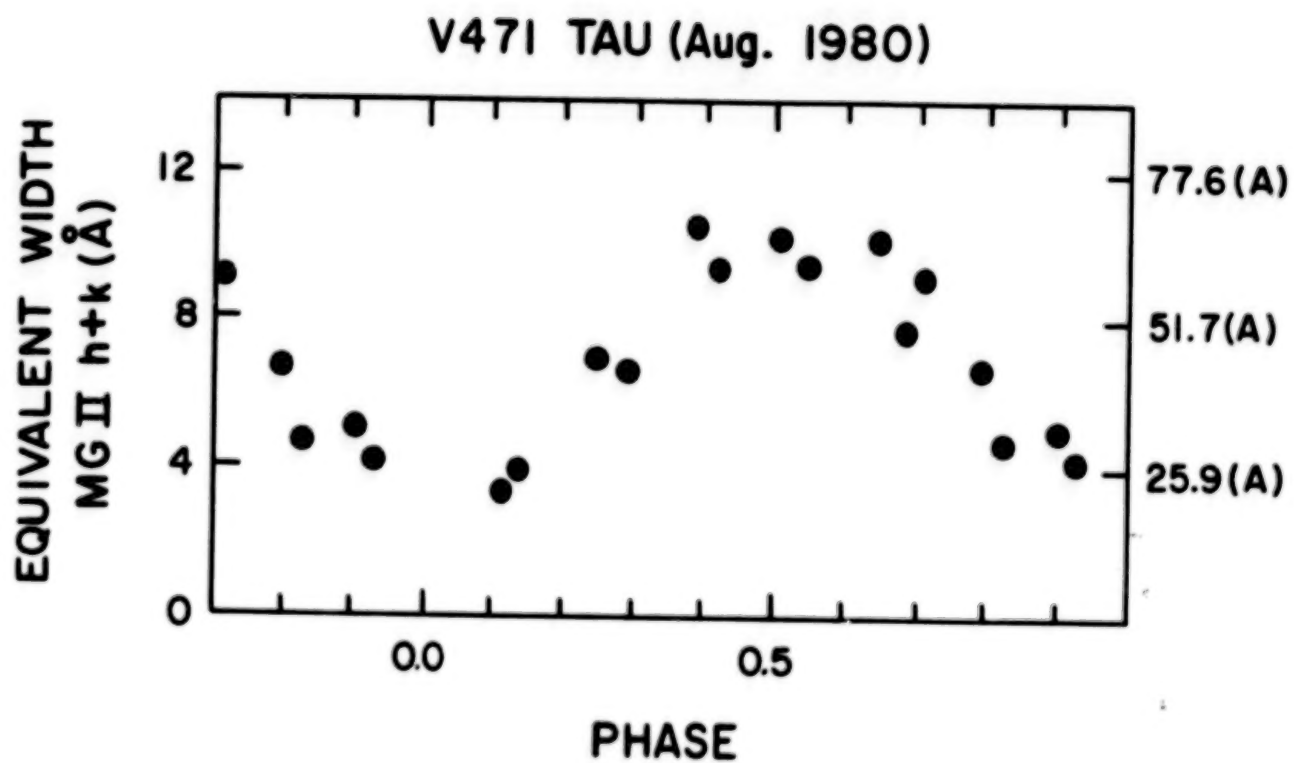


Figure 6

DISCUSSION OF SKUMANICH PRESENTATION

CHAPMAN: Could you pose that question once again? About the packing fraction of spots in active regions?

SKUMANICH: Yes, what is the ratio of spot area to active-region area? Can that change when you go to a K-star from a solar-type star? In the average active region, we know that there's an asymmetry, we know that the spots tend to occur at the leading part; the field tends to be concentrated in spots, the following part of the field tends to be more spread out in plage. Can we detect or infer that kind of asymmetry from stellar observations?

GIAMPAPA: What about other causes of variability in the M dwarfs? Do you need to have an accretion disk?

SKUMANICH: I think Occam's Razor ought to apply and that we have magnetic activity on these stars.

HELIUM 10830Å IRRADIANCE: 1975-1983

J. W. Harvey
Kitt Peak National Observatory*

ABSTRACT

Digital spectroheliograms made daily at Kitt Peak are processed to determine values of the equivalent width of the He I 10830Å chromospheric spectrum line averaged over the visible solar disk. A fairly complete time series from late-1974 to mid-1983 is available. A solar-cycle variation from about 28 mÅ in 1975 to about 80 mÅ in late 1981 is the major component of the signal. The 10830 variation reaches minimum about a year before the sunspot minimum and reaches maximum about a year after sunspot maximum. Superposed on the solar cycle variation is a modulation of up to ± 13 mÅ due to the passage of active regions across the disk. Power spectral analysis of the time series shows a major peak at a synodic rotation period of 27.42 days and smaller peaks at $1/2$, $1/4$ and $1/8$ of this period. The spectrum is well modeled by a basic fluctuating component with an exponentially-decaying autocovariance function of scale time of 43 days. The spectrum also shows signals at periods of one year and one-half year which can be attributed to an annual variation in water vapor at Kitt Peak and the semi-annual change in the sub-earth, heliocentric latitude respectively. An analytic signal analysis of the data indicates that the rotational modulation occurs in episodes that last from 4 to 10 rotations. Spatially resolved images show that these episodes arise when active regions tend to occur in a limited longitude range. The analysis also shows that the apparent rotation period increased from 1977 to 1981. The apparent rotation period since 1981 has been markedly shorter. This behavior is contrary to what one might expect from the decreasing latitude of active regions during the course of the sunspot cycle and is due to systematic trends in the longitude at which activity occurs.

INTRODUCTION

The 10830Å line of He I presents a unique view of the sun. This spectrum line is sensitive to coronal radiation (ref. 1) and is readily observed against the disk from the ground (ref. 2). Spectroheliograms show absorption features consisting of active regions, filaments, ephemeral regions, the quiet network and coronal holes in order of decreasing visibility (ref 3). To some degree, observations of 10830 should serve as a proxy for ultraviolet observations obtainable only from space. This spectrum line can be observed in a wide range of stars (ref. 4) and ought to be a good activity diagnostic somewhat distinct from the usual H and K and Balmer lines once its behavior in the sun is understood. One major advantage of the 10830 line compared with other chromospheric lines is that it is almost entirely formed in the chromosphere and has very little photospheric contribution (ref. 5). The presence of a photospheric component in

*Kitt Peak National Observatory is operated by the Association of Universities for Research in Astronomy, Inc. under contract with the National Science Foundation.

lines such as H and K degrades their value as indicators of chromospheric activity (ref. 8). Unfortunately, the details of helium line formation in the sun are still not well understood (refs. 7,8). A preliminary study of the variation of 10830 in the sun was presented earlier (ref. 9).

OBSERVATIONS

Spectroheliograms using the He I 10830Å line have been made with the 512-channel magnetograph at Kitt Peak since February 1974 (ref. 2). Except for a substantial portion of 1976, the coverage has been fairly complete, averaging about 85% of all possible days. The observations consist of digitized full-disk images with a spatial sampling of one arc second. One of the products of processing the observations is a number which represents the strength of the He I line averaged over the visible disk, i.e. the sun seen as a star. These numbers have been calibrated in terms of equivalent width of the He I line by comparison of 107 suitable corresponding direct observations of the equivalent width kindly provided by W. Livingston. Based on this calibration, the internal rms noise of the derived equivalent widths is about ± 2 mÅ and systematic errors appear to be less than 10 mÅ.

In preparing the time series for analysis, observations which did not cover the full disk of the sun were excluded as were a few anomalously noisy observations after these were justified by examination of the original images. The amount of data removed in this way amounted to a few per cent. Figure 1 is a plot of the edited and calibrated time series. Figure 2 is a plot of the same data but with all fluctuations having periods less than 53 days removed by a sharp cut filter in the Fourier transform domain.

We see that the 10830 minimum occurred in mid-1975 at a level of 24 mÅ. Although much of 1976 is not available, it appears that the trend in 1976 was an increasing equivalent width and that the 10830 minimum therefore occurred about a year before the sunspot minimum. This can be understood if small-scale activity, not producing sunspots, was already increasing in 1976 as part of the rise of the new sunspot cycle. These data support previous reports that a minimum in the solar EUV flux occurred in mid-1975 (refs. 10,11). In the smoothed plot, the 10830 maximum is reached in late 1981 at a level of about 83 mÅ. The sunspot record shows a clear maximum in 1979, nearly two years earlier. Although it is dangerous to generalize on the basis of observations of part of one solar cycle, these observations suggest that chromospheric activity reaches a minimum prior to the minimum of sunspot activity (as indicated by sunspot number R_s) and the maximum of chromospheric activity is delayed from the sunspot maximum.

The range of the smoothed 10830 solar-cycle variation, from about 28 to about 70 mÅ or 1:2.5, can be compared with the range of total magnetic flux on the sun during the same time period (2 to 7×10^{23} Mx or 1:3.5 from KPNO measurements) and the range of the 1 Å K-line index, 87 to about 100 mÅ or about 1:1.15 (ref. 12). One might conclude from the much larger range of the 10830 line variation compared with the K line variation that the former would be a superior indicator of activity. For some stellar spectral types this may be true, but for the sun, assuming perfect detectors, the high photon noise associated with the background on which the 10830 line appears cancels its apparent advantage. It is easy to show that the variation to photon-noise-level ratio is nearly identical for the 10830 and K-lines in the sun.

Superposed on the slow variation of the signal is a modulation with an apparent period of about 27 days and an amplitude of up to 15%. Resolved

images show that this is due to the rotation of active regions, filaments and coronal structures across the disk. On occasion (e.g. just before mid-1980) the dominant 27-day period is replaced by a harmonic (in this case a 13-day period). To study the high frequency variations of the 10830 signal, we turn to frequency analyses.

A FOURIER ANALYSIS

The first step in this Fourier analysis was to subtract a single function which fits the major solar-cycle variation of the time series. The form of this function, which was estimated by eye, was

$$50 - 22 \cos[2\pi(d - \text{Nov.25,1974})/3900] \text{ m}\text{\AA} \quad (1)$$

where d is measured in days. The next step was to multiply the first and last 100 days of the time series by cosine bell functions to reduce end effects. Since the time series has many gaps, a standard fast Fourier transform program could not be used. In a case like this, the procedure discussed by Deeming (ref. 13) is appropriate. Essentially one does a brute force integration of the data multiplied by sines and cosines of selected frequencies. The frequencies used here ranged from 0 to 999 in units of $1/4096$ cycles per day. This choice of frequency step slightly overresolved the frequency spectrum but was required for a later analysis.

The power spectral density of the time series is shown in figure 3. The power spectrum of the data window function falls below 1% within 4 frequency steps of the peak and seldom exceeds 0.1% at other frequency steps. Thus the power spectrum of the data is not significantly corrupted by the irregular sampling of the original data. As the data spectrum is quite noisy, it was filtered (in power) by a crude 11-point running mean to produce the smoothed power spectrum in figure 4. The spectrum shows a low-frequency rise together with substantial peaks at frequencies that correspond to one synodic rotation period and its even harmonics, all on top of a significant background level. This type of spectrum looks very much like what one would expect from a basic fluctuation (at low frequency) that is modulated by a periodic function having a significant amount of harmonic content (producing the high-frequency heterodynes). To test this idea, we assume that the basic fluctuation is characterized by an exponentially-decaying, autocovariance function in time, t ,

$$R(t) = \sigma^2 e^{-\alpha|t|} \quad (2)$$

where σ is the standard deviation of the fluctuation and α is the reciprocal of the scale time of the fluctuation. The one-sided power spectral density of this function is

$$P(f) = \frac{4\alpha\sigma^2}{\alpha^2 + 4\pi^2 f^2} \quad (3)$$

where f is frequency. We also assume that the basic fluctuation can be modulated by a cosine function of frequency f_0 to yield an autocovariance function

$$R_0(t) = \sigma^2 e^{-\alpha|t|} \cos(2\pi f_0 t) \quad (4)$$

which has an associated power spectrum,

$$P_0(f) = 2\alpha\sigma^2 \left[\frac{1}{\alpha^2 + 4\pi^2(f + f_0)^2} + \frac{1}{\alpha^2 + 4\pi^2(f - f_0)^2} \right] \quad (5)$$

The proposed model for the power spectrum then consists of a constant background plus $P(f)$ plus four functions $P_i(f)$, one for each major peak. A least-squares fit of this model to the power spectrum gave the smooth curve shown in figure 4. Evidently this simple model fits the data quite well. The value of α corresponds to a scale time of 43 days which seems reasonable for the growth and decay of the activity complexes that produce the bulk of the 10830 signal. However, this value is very likely to be an underestimate because the spectral peaks at the rotation period and its harmonics are not produced by pure cosine modulation of a basic fluctuation. For example, the rotation rate is not constant for all 10830 features and this will lead to a broadening of the observed peaks and a corresponding artificial increase of the basic fluctuation frequency (i.e., a decrease of its period or scale time).

The synodic periods for the peaks are 27.42, 13.56, 6.77 and 4.21 days. The first of these is not significantly different from the Carrington rotation rate. The other periods correspond to rotation rates that are very slightly faster than harmonics of the basic frequency, for reasons that are not clear. The rms noise implied by the background level of the model is about ± 8 mÅ which is a factor of 3 larger than the estimated instrumental noise. One can attribute 2 mÅ of the background to observational noise and 4 mÅ to a high frequency, aliased component of the solar 10830 signal, the most likely solar source being the changing network pattern with a scale time of about 1 day. It would be useful in a future investigation to determine the high frequency spectrum of the solar 10830 signal to test the explanation of the background spectrum proposed here.

There are two narrow spikes in the spectrum at frequencies that correspond to one year and one-half year with respective amplitudes of 1.5 and 0.5 mÅ. The annual variation is probably due to a weak water vapor line within the instrumental passband together with the well-known annual variation of water vapor at Kitt Peak. The semi-annual variation is probably due to the semi-annual change in the absolute value of the heliocentric latitude of the sub-earth point and the resulting changing visibility of polar coronal holes.

One may ask about the fine structure of the spectrum, for example around the frequency of the 27-day peak. There is a great deal of fine structure but it is probably caused by modulation of the basic rotational frequency by changing amplitude, phase and frequency. The result does not convey useful information about rotation rates in the simple spectrum form. There is a more appropriate analysis procedure discussed in the next section.

AN ANALYTIC SIGNAL ANALYSIS

The preceding Fourier transform analysis eliminates phases which may contain physically interesting information. To recover some of this information we construct an analytic signal version of the original time series (ref. 14). This is a complex function which is band-limited to the frequency range containing most of the power around the 27-day peak (specifically, periods from 23.01 to 34.42 days). The real part of the function corresponds to the original signal and the imaginary part is the Hilbert transform of the original signal. The amplitude of the analytic signal is the instantaneous amplitude of the original (band-pass-limited) signal and the time derivative of the phase of the analytic signal is the instantaneous frequency of the original signal. These functions are illustrated in figure 5.

The analytic signal is characterized by episodes of duration 4 to 10 rotations in both amplitude and frequency. A completely different type of analysis,

applied to soft X-ray emission (ref. 15), shows an episodic nature of solar rotational modulation. Unfortunately, the episodes of that analysis do not coincide with the present analysis, probably because the correlation between 10830 and soft X-ray emission is not very good. Examination of spatially resolved images shows that the 10830 episodes are times during which one major complex of activity dominates the 10830 signal or when one longitude tends to be particularly active. The instantaneous amplitude ranges from 0 to 13 mÅ with 4 or 5 a typical value. In other words, the rotational modulation of the 10830 signal is typically 10% of the mean. The behavior of the instantaneous frequency (here plotted as instantaneous period) is very interesting. Each episode seems to be unique which suggests that each complex behaves independently. Examination of resolved images shows that many of the episodes can be attributed to activity around Carrington longitude 180°. The distinguishing characteristic between episodes is the longitude evolution of activity. For example, in mid-1979 the western part of the major activity complex around 180° died, causing an apparent decrease in rotation rate. This only lasted for a few months to be followed by a rebirth of the western part of the complex and an apparent increase in rotation rate. In early 1980, a strong complex of activity developed near 0° which nearly equaled the strength of the 180° complex. The result was a shift of signal away from a 27-day period to a 13-day period for a few months. After the 0° complex died, the 180° complex grew at its eastern edge leading to a decreasing rotation period.

One surprising characteristic is the tendency for the rotation period to increase from 1977 to 1981. Since the average latitude of activity is decreasing, one might expect the period to decrease according to some differential rotation law. A major decrease only occurred starting in mid-1982. Evidently, the evolution of activity swamps the effect of differential rotation. This result argues against simple interpretations of similar observations of other stars. Such warnings have been issued previously (refs. 9,16). It may be worth noting that a sustained decline of activity together with the formation of large, long-lived coronal holes began in mid-1982 at the same time as the change in rotation rate. It will be interesting to see what the rotation rate does during the remainder of the current solar cycle.

CONCLUSIONS

The He I 10830Å line equivalent width integrated over the visible solar disk is a useful indicator of global chromospheric activity. It shows a solar-cycle modulation of a factor of 2.5 and rotational modulation of order 10%. A simple model fits the observed power spectrum. It consists of an aliased high-frequency background due to network evolution, and a strong basic fluctuation due to complexes of active regions that have a characteristic scale time of at least 43 days. The basic fluctuation is modulated by solar rotation to produce heterodynes of the basic fluctuation at periods of the rotation and its even harmonics. An analytic signal analysis shows that activity can be attributed to episodes of 4 to 10 solar rotations. The behavior of the signal during these episodes is controlled by the evolution of active regions within large complexes. This evolution swamps differential rotation effects.

REFERENCES

1. Goldberg, L.: The Temperature of the Solar Chromosphere. *Ap. J.*, 89, 1939, pp. 673-678.
2. Livingston, W. C.; Harvey, J.; Pierce, A. K.; Schrage, D.; Gillespie, B.; Simmons, J.; and Slaughter, C.: Kitt Peak 60-cm Vacuum Telescope. *Appl. Opt.*, 15, 1976, pp. 33-39.
3. Harvey, J. W. and Sheeley, N. R., Jr.: A Comparison of He II 304Å and He I 10830Å Spectroheliograms. *Sol. Phys.*, 54, 1977, pp. 343-351.
4. Zirin, H.: λ 10830 He I Observations of 455 Stars. *Ap. J.*, 260, 1982, pp. 655-669.
5. Livshits, M. A.; Akimov, L. A.; Belkina, I. L. and Dyatel, N. P.: Helium Emission in the Middle Chromosphere. *Sol. Phys.*, 49, 1976, pp. 315-327.
6. Hartmann, L.; Soderblom, D.; Noyes, R. W.; Burnham, N. and Vaughan, A. H.: An Analysis of the Vaughan-Preston Survey of Chromospheric Emission. *Ap. J.*, 1983, in press.
7. Giovanelli, R. G. and Hall, D.: The Helium 10830 Å Line in the Undisturbed Chromosphere. *Sol. Phys.*, 52, 1977, pp. 211-228.
8. Avrett, E. H.; Vernazza, J. E. and Linsky, J. L.: Excitation and Ionization of Helium in the Solar Atmosphere. *Ap. J.*, 207, 1976, pp. L199-L204.
9. Harvey, J. W.: Variation of the Solar He I 10830 Å Line: 1977-1980. Variations of the Solar Constant, NASA CP-2191, 1980, pp. 265-272.
10. Hinteregger, H. E.: EUV Flux Variation during End of Solar Cycle 20 and Beginning Cycle 21, Observed from AE-C Satellite. *Geophys. Res. Letters*, 4, 1977, pp. 231-235.
11. Simon, P. C.: Solar Irradiance between 120 and 400 nm and Its Variations. *Sol. Phys.*, 74, 1981, pp. 273-291.
12. White, O. R. and Livingston, W. C.: Solar Luminosity Variation. III. Calcium K Variation from Solar Minimum to Maximum in Cycle 21. *Ap. J.*, 249, 1981, pp. 798-816.
13. Deeming, T. J.: Fourier Analysis with Unequally-Spaced Data. *Astrophys. Space Sci.*, 36, 1975, pp. 137-158.
14. Bracewell, R. N.: The Fourier Transform and Its Applications. Second ed., 1978, McGraw-Hill, New York.
15. Bouwer, S. D.: Intermediate-Term Epochs in Solar Soft X-Ray Emission. *J. Geophys. Res.*, 1983, submitted.
16. LaBonte, B. J.: Solar Calibration of Stellar Rotation Tracers. *Ap. J.*, 260, 1982, pp. 847-854.

Figure 1. Equivalent width of the He I 10830 Å line averaged over the visible solar disk as a function of time. Each daily measurement is plotted as a cross and is connected by lines if gaps do not exceed 3 days. Estimated random observational noise is ± 2 mÅ. Systematic errors in the ordinate should be smaller than 10 mÅ.

Figure 2. Same as figure 1 but all fluctuations with a period shorter than 53 days have been eliminated by a sharp-cut Fourier filter.

Figure 3. Power spectral density (one-sided) of the 10830 observations from 1975 to mid-1983. The ordinate is a linear scale and the peaks around 400 nHz result from solar rotation.

Figure 4. Same as figure 3 but the power spectrum has been smoothed by an 11-point running mean. The smooth curve is a simple model of the power spectrum (see text).

Figure 5. The 10830 signal was filtered to pass fluctuations from 23 to 34 days period and then converted to an analytic signal form shown here. The upper panel is the instantaneous amplitude of the signal. The lower panel is the instantaneous period of the signal. Symbol size in the lower panel is proportional to the amplitude of the signal. Note the trend toward increasing period from 1977 through 1981.

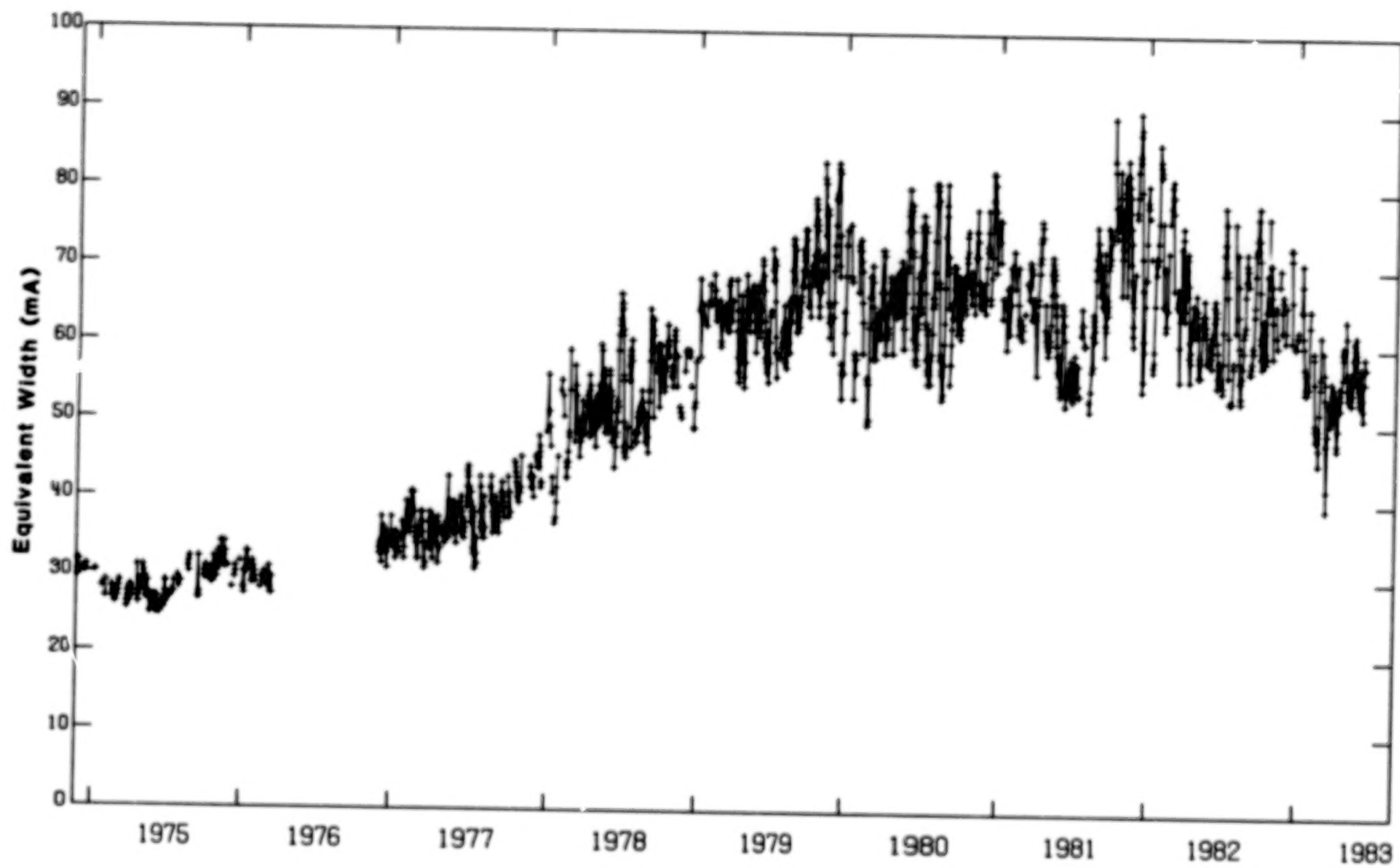


Figure 1

204

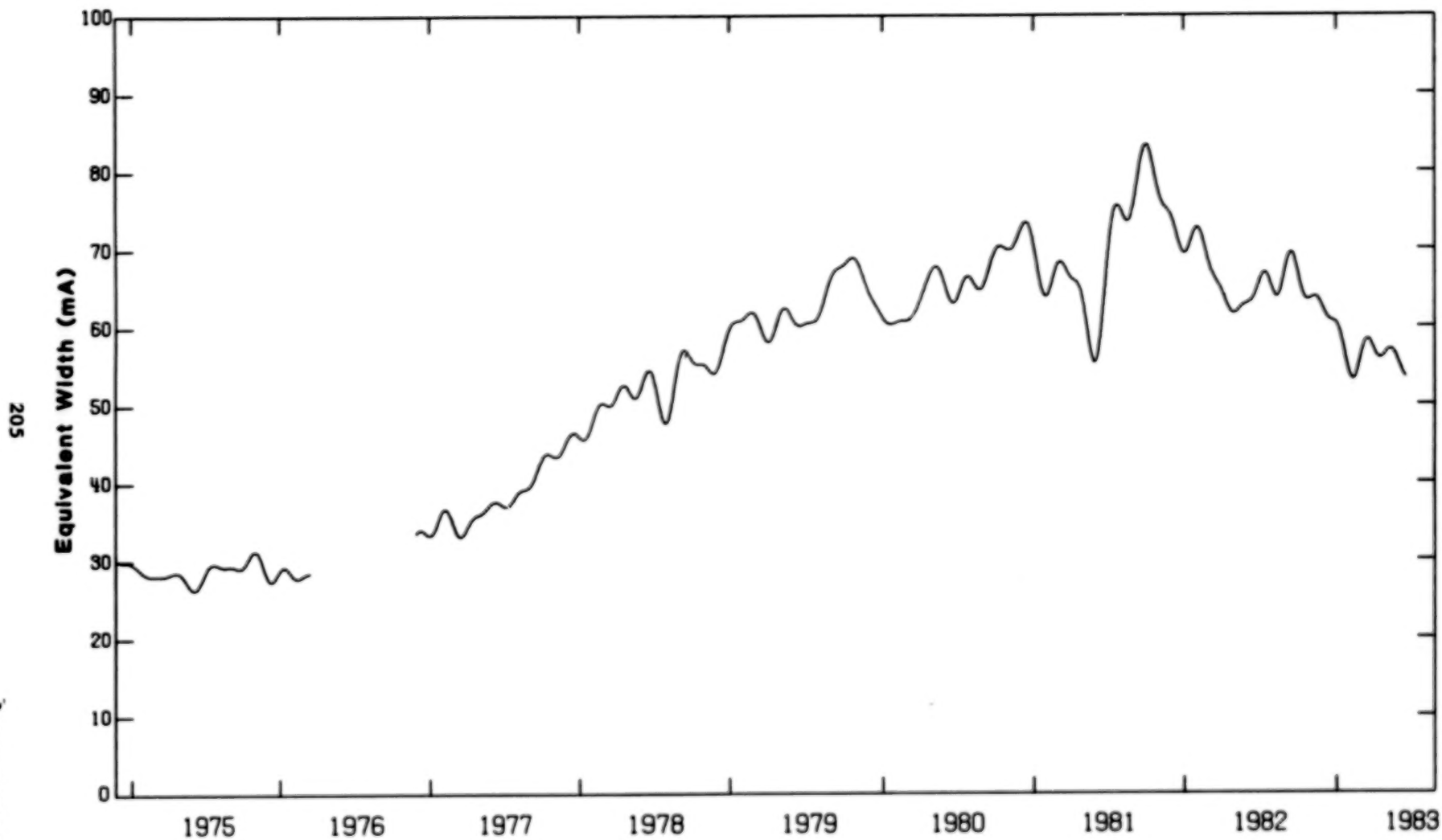


Figure 2

205

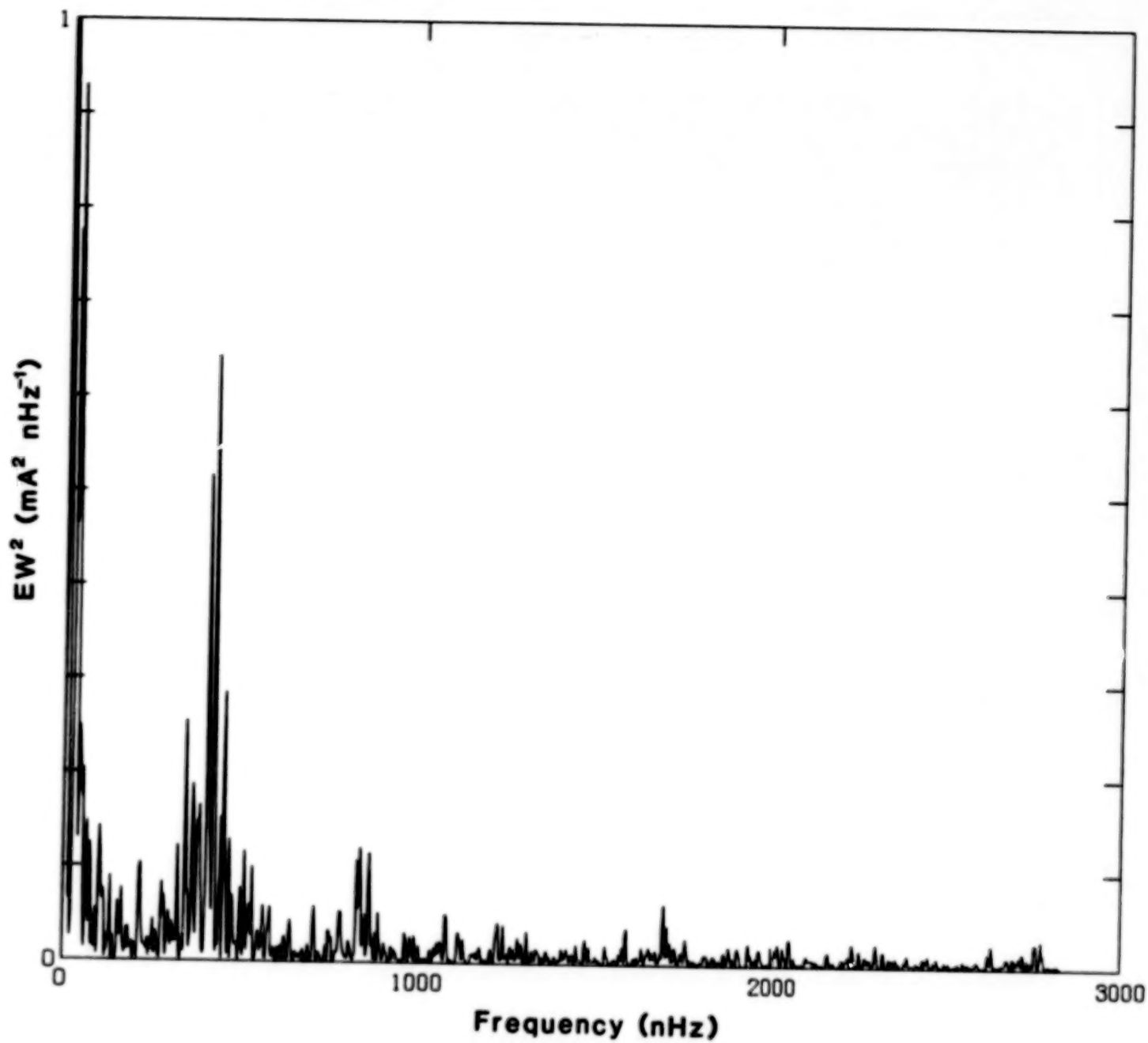


Figure 3

206

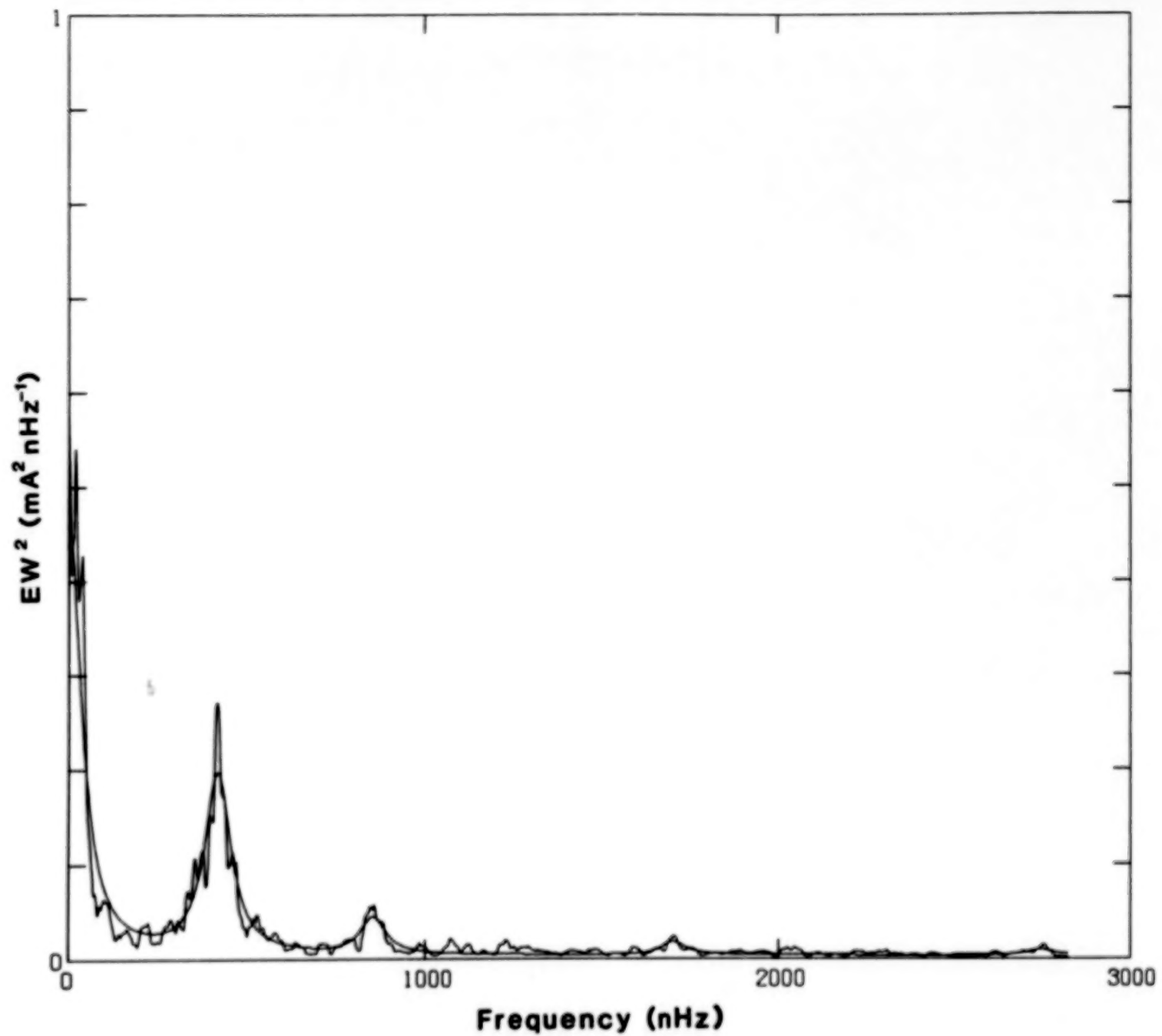


Figure 4

207

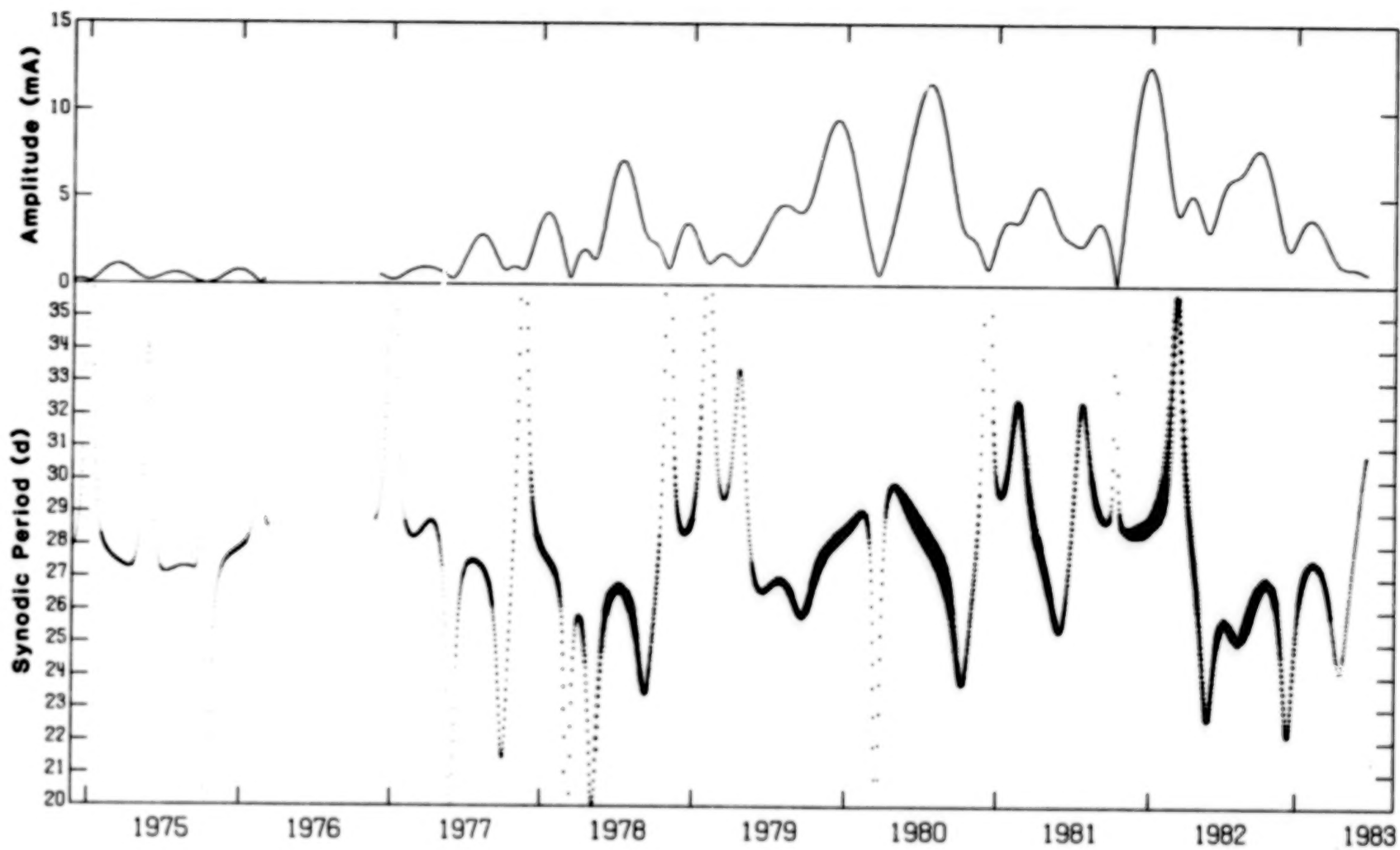


Figure 5

DISCUSSION OF HARVEY PRESENTATION

COOK: What is the affect of coronal holes? It should vary at different phases of the cycle.

HARVEY: I can only give you a crude answer, we haven't done it quantitatively; in essence you are asking how much of this variance might be due to coronal holes. Sorry to say that the coronal hole signal is practically negligible compared to active regions. We'd love to be able to pull out a strong coronal hole signature especially for comparing with other stars, but it's negligible on this scale.

SCHATTEN: The 10830 signal is correlated with spots, but it is just one-to-one.

HARVEY: There is a degree of correlation, which I have not worked out. But my point was that the minimum of the sunspot and 10830 curves is not the same in time, it is a year different than the maxima of this curve and, [for] the sunspot curve there's two years difference, and I consider that as a significant discrepancy. I presume that is mainly due to the fact that the signal in 10830 is primarily due to plages and not sunspots: sunspots are negligible.

GIAMPAPA: Do you have X-ray data?

HARVEY: I just received, courtesy of Dick Donnelly, some nice X-ray data, which I intend to correlate with this. I tried this before but the correlation was extremely bad; it was very hard for me to remove the effects of transient activity in the X-ray signal. Somebody has done a good job on that now.

COOK: [The EUV flux reaches a minimum before the sunspot number.]

HARVEY: To the extent that this is a proxy for what's happening in the EUV, I guess I would tend to agree with Hinteregger's result in that; it looks like it's about a year before.

CHAPMAN: What about sunspot area? Does that peak in '81, or does it peak in '79? Sunspot number is a different thing.

EDDY: I'll show this afternoon that it peaks at the same time, about two years after sunspot [number].

CHAPMAN: That's significant because before you draw conclusions, from the lag, make sure you're talking about the right kind of thing.

HARVEY: I think sunspot numbers are a 17th-century invention! Ephemeral regions reach minimum numbers one year before spots.

ZIRIN: 1974 was one of the most active years; is there a linewidth change?

HARVEY: We do have '74 data, as yet unprocessed, but Livingston is measuring that.

K. HARVEY: I know that there's a bit of controversy on ephemeral regions [but] we

have some data from ... and we also show that for small active regions when they are lifetimes, we get a minimum in the count... flux eruption... slightly out of phase 1 year before.

HARVEY: I had not compared this curve with (say) the total magnetic flux on the sun. I suspect they will be pretty well correlated. That hasn't been done yet.

LEAN: If you take an active component which you say lasts maybe 1 or 2 [rotations] and [compare it with] calcium areas, do you account for all of the change in intensity from the active component ...?

HARVEY: I don't know, I haven't done that; could be.

CHAPMAN: I have a nasty question. Are you missing any of the line in your slit?

HARVEY: Well, undoubtedly we are missing a part of the multiplet, and this may be a function of the position on the disk or the degree of activity.

CHAPMAN: Does the amount of miss change with position on the disk; with the type of activity?

HARVEY: Yes, I'm sure that our fixed slit on a rotating sun is causing some noise, but we use a very standard alignment procedure every day and it ought to be some sort of systematic error which I hope is taken out by calibration comparison with Bill Livingston's stuff. It does provide a source of noise - perhaps that's some of the background noise. I doubt if it's a serious problem, because our slit is quite wide.

ZIRIN: You can't see coronal holes in the K-line, at least not very well, can you?

HARVEY: We have processed the individual images in 10830 to reveal just the coronal holes. One could make a butterfly diagram or the like, but in these integrated 10830 signals, the coronal holes are a negligible source of fluctuation compared to the active regions.

ZIRIN: You could just subtract the integrated K-line from 10830 to see the coronal holes.

CHAPMAN: If the correlation is tight enough.

HARVEY: Well, that's an interesting possibility.

ZIRIN: That would mean, then, that if you look at stars, and subtract the K-line variation from the 10830 variation ...

HARVEY: Well, even with solar data that's going to be a marginal operation. Quite difficult with stellar [data], I would think.

COOK: [Are the plage areas the same in K and 10830?]

HARVEY: Roughly, yes. But, in detail, the plages seen in 10830 don't look like

places seen in any other line. It's kind of a mixture of H α and K, [that's] the best way I can describe it for you. Everything is in absorption and there is strong fibril structure.

MOORE: It looks like Lyman α ?

HARVEY: No. Lyman α looks more like K to me than 10830 does; 10830 is weird. The filamentary structure is very strong in 10830.

BLANK PAGE

THE SOLAR CONSTANT, CLIMATE, AND SOME TESTS OF THE STORAGE HYPOTHESIS

John A. Eddy
High Altitude Observatory
National Center for Atmospheric Research*
Boulder, Colorado 80307

ABSTRACT

Activity-related modulation of the solar constant (S) will have practical consequences for climate only if storage is involved, as opposed to a detailed balance between sunspot blocking and facular re-emission. Four empirical tests are considered that might distinguish between these opposing interpretations: monochromatic measurements of positive and negative flux, comparison of modelled and measured irradiance variations, the interpretation of secular trends in irradiance data, and the direct test of an anticipated signal in climatic records of surface air temperature. The yet-unanswered question of the role of faculae as possible re-emitters of blocked radiation precludes a definitive answer, although other tests suggest their role to be minor, and that storage and an 11-year modulation is implicated. A crucial test is the behavior of the secular trend in irradiance in the declining years of the present activity cycle.

INTRODUCTION

The solar constant is the only strong force in the Sun-weather problem, sufficient to perturb the lower atmosphere directly; any inconstancy, however slight, is certain to alter the surface temperature of the Earth. Is our new knowledge of real variations in the solar constant an advance of practical significance for meteorologists, or only an academic one? A key question, for climatology as for solar physics, is the one so vigorously debated at this Workshop: whether or not observed variations in total irradiance imply any change in the luminosity of the Sun (ref.1). Are the fluctuations more than a directional redistribution? Is there storage beyond the trivial delay between sunspot blocking and facular re-emission?

The day-to-day and hour-to-hour variations in total irradiance detected by the ACRIM and ERB instruments must also be felt in the lower atmosphere of the Earth, where the bulk radiation from the Sun is the principal source of energy input. Moreover, at the level of only 0.1% they exceed by orders of magnitude any other direct effect of solar activity on meteorological processes. Nevertheless, the SMM and Nimbus fluctuations that excite some of us so much are of little or no interest to modellers of global circulation, both because of their small amplitude and their brief duration. A fluctuation of 1 part in 1000 in S lasting but a week is to the climatologist only a jitter when compared to common modulations of mesoscale insolation by cloud

* The National Center for Atmospheric Research is sponsored by the National Science Foundation.

cover, for example. To zeroth order, and ignoring thermal inertia, a change of 0.1% in S implies a direct response of perhaps 0.1 degrees centigrade in surface temperature (ref.2). By contrast, diurnal high and low surface temperatures here in Los Angeles are typically separated by about 10 degrees C --- 100 times the maximum possible impact from the largest, short-term dips in the ACRIM record.

A year-to-year modulation, or trend, of 0.1% in S (which appears to be a matter of record in the Nimbus and the SMM data) is still 70 times smaller than the variation in the same parameter that ensues every year from the eccentricity of the Earth's orbit: an annual modulation of about 7%, full-scale, that is widely unappreciated since in the present era in the northern hemisphere it operates almost exactly out of phase with the more dominant effect of the seasons.

The climatologists' interest in the ACRIM or ERB results is slightly enhanced if the day-to-day fluctuations may be presumed to be cumulative --- that is, if the blocked energy is stored for months or longer (refs.3,4,5). In that case the jitter implies a persistent trend: a predictable, 11-year variation in S (Figure 1) with an amplitude of about 0.1%, which might invoke in inland areas a similar modulation of about 0.1C in surface temperature (ref.6). That is about 5 times smaller than the temperature change attributed by some to the recent El Chichon eruption or the Northern hemisphere warming that characterized the period between the late 1800's and World War II (ref.7). And it is 30 times smaller than the canonical warming of about 3 degrees C that some climatologists anticipate in the next 100 years due to the progressive buildup of carbon dioxide (ref.8).

POSSIBLE TESTS BETWEEN STORAGE AND DETAILED BALANCE

Can we expect an 11-year modulation based on what has been so far observed in spaceborne measurements of S ? How can we determine whether the solar luminosity varies or only the solar irradiance? Is there storage beyond that of facular lifetimes? Four preliminary tests have been applied that might distinguish between the extreme possibilities of storage and detailed balance. As of June, 1983, all are probably inconclusive --- as we might expect, given the limited span of reliable data from the SMM and Nimbus radiometers and our own proclivity for controversy.

MONOCHROMATIC MEASUREMENTS OF POSITIVE AND NEGATIVE FLUX

Bruning and LaBonte (ref.9) have measured full-disk photoelectric images of the Sun in the wings of the 5250 A absorption line of FeI to test how the negative flux of sunspots compares with the positive flux of photospheric faculae in a year of high activity. Specifically they test how the product of contrast and area of dark features in spectroheliograms (made near the maximum of solar spectral emission) compares with that of bright features. Were there a detailed balance between sunspots and faculae --- that is, as suggested in a series of papers by Sofia et al., (refs.10,11,12) a directional redistribution of radiation only --- we would expect the two to be roughly equal over periods long enough to average out the effects of active region evolution. One year seems long enough for that. Bruning and LaBonte conclude that in the year 1980 the bright component (or "positive flux") was nearly constant while the

dark (sunspot) component fluctuated in a way that was highly correlated with the SMM ACRIM measurements. In that year of maximum solar activity they find, however, not dominant blocking but a net positive flux--- implying that if this monochromatic measurement can be taken as a bolometric indicator the effect of solar activity in 1980 was a net increase in the solar constant. Extrapolation would then suggest that in the course of the 11-year activity cycle the solar constant might vary in phase with sunspot number with an amplitude of at most 0.12%. This is of similar magnitude but exactly opposite to the out-of-phase modulation employed in the reconstructions that Hoyt and I published (refs.13,14), where years of maximum sunspot area were taken as times of minimum luminosity. Nor do Bruning and LaBonte find evidence for detailed balance, or the directional redistribution of radiation predicted by the Sofia et al. model. It would seem to confirm, in sense, but not in magnitude, the first finding of Foukal, Mack, and Vernazza (ref.15) in their initial analysis of the Abbot Smithsonian measurements of S, where a weak facular signal was marginally detected, with no discernible sunspot effect.

A crucial assumption in the 5250 analysis, however, is the relevance of monochromatic photometry to bolometry, a step that seems particularly questionable given the strong wavelength dependence of facular contrast. At the heart of the question is the unknown extent of facular emission in the continuum over the whole disk. Chapman has recently estimated that facular areas are 25-30 times those for sunspots (ref.16), supporting the notion of detailed balance, or possibly a net positive effect of solar activity on luminosity. Yet the long series of historical, broad-band photographs of the disk would seem to disallow such a possibility. In 103 years of daily, white-light, full-disk photographs made and analyzed at the Royal Greenwich Observatory (ref.17) the ratio of projected facular area to projected whole spot area is, on average, less than two (Figures 2 and 3), more than ten times smaller than Chapman's more recent photoelectric estimate. Since the positive facular contrast is roughly 10 times smaller than the negative whole spot contrast the historical photographic evidence argues that the effect of solar activity on continuum radiance must be a predominantly negative effect. This would still hold were the Greenwich photographic measurements of facular areas systematically low by a factor of five. This unresolved, order-of-magnitude discrepancy in a basic parameter of the radiating surface of the Sun now clouds the clear resolution of the question of storage or detailed balance.

COMPARISONS OF MODELLED AND MEASURED IRRADIANCE VARIATIONS

A second test, applied by Hudson and Willson (ref.18), by Sofia, Oster, and Schatten (refs.10,11,12), and others (refs.13,14) endeavors to rank the relative roles of sunspots and bright regions by fitting the more precise period of ACRIM data with models that employ measured (or deduced) sunspot and facular areas and contrasts as an input. The goodness of fit is then used as a figure of merit to evaluate the relative roles of negative and positive influences, whether there is obvious re-emission following sunspot blocking, and whether there is evidence of a detailed balance or some form of long-term storage.

Here there is sharp disagreement and opposite conclusions. In my opinion neither the models nor the input data used in any of these attempts has been sufficiently exact to allow any significant improvement on what was done in

1981 by Willson, Gulkis, Janssen, Hudson, and Chapman in their seminal paper in Science (ref.19). A difficulty in all of these attempts is that a certain amount of vertical sliding is allowed in fitting modeled and observed data strings; that is, in each the absolute value of the so-called "quiet-sun" irradiance is unspecified. Thus a deep excursion of obvious sunspot blockage can be interpreted by some as originating at the true "quiet sun" level and by others as notched out from a preceding or coincident facular increase. It is much like the problem of identifying the continuum in a dense spectrum of Fraunhofer absorption lines.

Another source of contention and some confusion is the use of quite different values of daily sunspot and facular areas as inputs to the models. What should surely concern us is that competing models based on grossly different values of sunspot and facular data seem, like stretch socks, equally able to fit the ACRIM data. The number of free input parameters, and the uncertainties in them, severely limit the significance of any conclusions based on goodness of fit. Hoyt and Hudson and I (ref.20) have endeavored to quantify the limits of error in the more-easily measured parameter of sunspot area, including the anticipated loss in visibility at the limbs. But the equivalent and intrinsically more complex question of continuum facular areas seems yet wholly unresolved and ill-defined, in spite of sampled measurements reported at this Workshop.

Hudson and Willson (ref.18) used synoptic sunspot data in a two-parameter model with faculae a free parameter and concluded that sunspot blocking clearly dominated the ACRIM record, with only a small fraction of the "missing flux" balanced by facular or other local or global re-emission. Their analysis would seem to refute the possibility of detailed balance, at least on time scales of weeks to months, and argue in favor of intrinsic solar storage and luminosity modulation.

Hoyt and I came to the same conclusion with similar experiments at varying the facular component (refs.13,14). Since the whole spot contrast is nearly 10 times greater than that of faculae it would require a facula-to-spot area ratio for the whole disk of about 10 to make them balance. While such a ratio has been suggested (ref.16), it is at variance, as noted above, with the long history of routine, continuum photographic measurements of the white-light disk. Chromospheric plages are coarser, higher-lying structures of greater contrast that are more extensive on the disk and, in narrow-band filtergrams, far more easily measured, but we cannot assume them to be a direct proxy of the areal coverage of more filamentary, photospheric faculae. At this symposium Chapman and Lawrence have reported recent, limb-photometer measurements that suggest that the facular area may more nearly approach that of chromospheric plages. Were this the case these unseen faculae might be adequate to reradiate, by processes as yet unknown, the blocked energy of sunspots. But until a more extensive series of broad-band, full disk measurements of faculae demonstrate conclusively that the areal extent of photospheric faculae is indeed five to ten times greater than previously measured the case is unresolved.

The present state of confusion in model fitting is illustrated by the fact that in fitting the same ACRIM data that Hudson and Willson and Hoyt and I did, Sofia, Oster, and Schatten (refs.10,11,12) came to an exactly opposite conclusion: that there is an "almost complete balance of energy deficit due to spots and excess due to faculae." They find that the excess emission

averaged over direction cancels out the integrated deficit produced by sunspots, within an uncertainty of about 10% of the sunspot blocking term. This would impose an upper limit on possible luminosity variations of about 10^{-4} .

The reason behind the discrepant conclusions lies in the gross differences in input values of sunspot and facular areas that have been used to fit the ACRIM data. For example, most interpreters of S variations have employed daily, measured values of sunspot areas taken from standard NOAA SEL compilations. Sofia *et al.* (refs.10,11,12), however, used analytically generated values of sunspot areas in an attempt to compensate for discrepancies in published, measured values and for the loss in visibility of a spot as it moves away from disk center. They also assumed that every spot endures, with constant area, for at least 14 days. The generated sunspot areas that were used in the Sofia *et al.* model were systematically 47% greater than the daily measured values published by the Space Environment Laboratory (ref.20 and Figure 4). This is a large and unsubstantiated correction to observed data.

The presently-observed sunspot area data are indeed imprecise and we need better ones if we are to extract all we can from the more precise solar constant data. But one can show that the loss in visibility of sunspot area at the limb in the SEL data in 1980 was less than 15%, and that the standard deviation in mean daily sunspot area from measurements of 5 independent stations that reported daily values is less than that (ref.20 and Figure 4). Thus Sofia *et al.* heavily overcompensated for suspected errors of measurement and based their conclusion of detailed balance in part on sunspot areas more appropriate for RS CVn stars than for the Sun.

That is only half of the story, however, for, as noted earlier, there are even larger discrepancies in estimates of facular areas. There were no published, daily measurements of facular area or contrast for the SMM period so all of the interpreters were obliged to use proxy ones. Hoyt and I (refs.13,14) based our estimates of facular areas on the long-term average of projected facula to sunspot areas in the 103 years of published Greenwich observations (discontinued after 1976), for which the average value was 1.6. Moreover, annual averages of the ratio of whole-disk facula to sunspot area in the Greenwich data are a distinct function of solar activity; in years of high sunspot number or area, like 1980, the ratio drops to more nearly unity (Figures 2 and 3).

Sofia *et al.* generated facular areas based on Calcium II plage measurements at the center of the disk, equating chromospheric plage area to facular area, but tapering the emission to maximize near the limbs of the Sun. With this approximation they found the ratio of effective facular area to sunspot area in 1980 to be about 10:1; from this they must expect a detailed balance between positive and negative flux since that ratio is roughly the inverse of the ratio of contrasts of the two phenomena.

As stated earlier, this order-of-magnitude discrepancy in estimates of the whole-disk, facula to sunspot area surely illustrates the need for improved disk photometry in the continuum, if we are to interpret precision measurements of the solar constant properly.

SECULAR TRENDS IN THE ACRIM AND ERB RECORDS

We may hope to distinguish between detailed balance and storage directly, through the identification of different secular trends in the string of solar constant measurements already at hand: these are now 4 1/2 years long for Nimbus 7 and more than three years for the SMM. Each set includes the period of maximum activity in solar cycle #21 when we might expect an extremum in slope were there cumulative storage or other cycle-related modulation of S . In this sense the apparent downward, secular trend noted in both the SMM (ref.21) and Nimbus (refs.22,23) data provides important tests between options of storage, detailed balance, or a dominance of facular brightening. If long-term storage applies --- and is the dominant modulator of luminosity on time scales of years--- then we should have expected S to maximize (undetected) at the activity minimum in 1976 and then gradually decline until the maximum of the present cycle #21. That is, when the Nimbus 7 ERB instrument began its measurements, in late 1978, it should have detected a secularly-declining total irradiance, were storage in effect. The notion of storage would also imply that at the cycle peak in sunspot area the declining trend should flatten, reverse sign, and then gradually increase with declining sunspot areas.

Were there detailed balance between sunspot blocking and facular emission, on the other hand, we would expect no 11-year modulation and, if these were the only mechanisms that modulated S , no secular trend. Sofia, Oster, and Schatten (ref.10) have pointed out another possible 11-year modulation that might be called the "butterfly effect", arising from the systematic shift in latitude of active regions in the course of the 11-year activity cycle. The postulated effect is more subtle, and presumably of smaller amplitude than that anticipated from simple storage. When active regions are at higher latitudes, early in the cycle, the contrast of faculae is enhanced, relative to that of spots, diminishing the relative effect of sunspot blocking. If there were no storage and detailed balance applied, one might still expect a subtle 11-year modulation of S due to this latitude effect alone, with S increasing slightly but abruptly with the first activity of the new cycle and diminishing thereafter, in sawtooth fashion, until the end of the cycle when it would abruptly rise again. A "butterfly effect" combined with storage, on the other hand, would act to delay, by perhaps a year or so, the phase of the anticipated luminosity variation. The 11-year behavior of S suggested by the monochromatic measurements of Bruning and LaBonte (ref.9) would follow the phase of the sunspot number curve, with maximum luminosity at the peak of the cycle and a decline thereafter.

Does the secular trend so far noted in the ACRIM and ERB data allow us to discriminate between any of these predictions?

What seems clear, in both the Nimbus and the SMM data, is a persistent downward trend that was in effect when the Nimbus ERB radiometer began measurements in late 1978 (Figure 5). The trend toward lower values of S continued with about the same slope through the end of 1981 and, in 1982 seemed to flatten. The slope before 1981 is somewhat steeper in the ACRIM data than in the ERB data, but as a continuous record the former data are vitiated by the adjustments made necessary by the drastic change in operational mode of the SMM in late 1980. In any case, for the point of this test, the difference in slope between ACRIM and ERB records is unimportant. What is important is whether the secular decrease is real or instrumental, whether the apparent flattening in 1982 is more than a misleading pause, and what happens next.

The secular behavior of S in the ACRIM and ERB records available to us thus far is consistent, in both phase and amplitude, with the 11-year modulation expected from the storage hypothesis (refs.6,13,14)--- but only if the slow flattening in S suggested in the 1982 data proves to be the mark of a real turnaround. The fact that the irradiance continued to fall well after the peak of solar activity cycle #21 (December 1979) is also expected since the maximum in sunspot area was not achieved until late in 1981, nearly two years later (Figure 6). If the secular trend is indeed an 11-year modulation its negative slope in the 1978-1980 Nimbus-7 data is inconsistent with Bruning and LaBonte's conclusion of dominant facular emission (ref.9) and the extrapolated prediction of a solar constant that tracks the phase of the solar activity cycle. A downward trend through 1981 would also be expected from the "butterfly effect", suggested by Sofia et al. (ref.10), although we would expect that fall to continue monotonically through the end of the present cycle, in late 1986 or 1987.

The crucial test, is whether in 1983 and 1984 S will turn up, or continue to decline. It seems to me something we should all want to watch.

IDENTIFICATION OF A POSSIBLE SOLAR CONSTANT MODULATION IN CLIMATE DATA

A fourth test between storage and detailed balance seeks to identify the expected consequences of an 11-year modulation in S in terrestrial records of surface temperature. Needless to say such a test is fraught with all the dangers of Sun-weather correlation studies.

Storage models imply a weak 11-year modulation of surface temperature in the sense of lower temperatures at times of maximum sunspot area, when S should minimize. Systematically higher temperatures should follow at minima in sunspot area. If the prevailing estimates of climate sensitivity are correct, the amplitude of the expected modulation should be about 0.1 degrees C, with an uncertainty of about a factor of two (ref.2).

The identification of the predicted, subtle modulation in surface temperature is of course insufficient proof of the storage hypothesis, since it could well result from other solar or non-solar forcing mechanisms. Still, if such a signal is statistically present, with the appropriate period, amplitude and phase, the simplest climatic explanation would be this very sort of solar constant modulation.

Such a signal is not found in hemisphere-averaged temperatures of the last 100 years. Nor is it particularly expected, when land and near-ocean areas are in this way averaged together. Simple climate models suggest that a 10-year surface temperature modulation induced by changes in bulk solar heating will be severely damped in oceanic regions, and may be more likely to be noted in areas of mid-continental land mass, where the thermal inertia is smaller.

It may be significant that the expected signal was found, by earlier work of Currie (ref.24), in the 80-years of available surface temperature data in North America. Moreover, Currie found the 11-year modulation systematically limited to roughly the anticipated area --- specifically, the northern states east of the Rockies, and southern Canada. There, from Kansas to the eastern seaboard, he found station records of surface air temperature systematically depressed by roughly 0.1 degree C in years of maximum solar activity, as

theory would predict, with higher temperatures at minimum sunspot number. Hanson and Cotton have found a strong spring-summer enhancement of the same effect in a more detailed analysis of North American temperature data (ref.25).

SUMMARY

The 0.1% changes thus far observed in spaceborne measurements of S will have significant climatic impact only if they reflect real changes in solar luminosity. The practical question of whether the luminosity varies now seems embedded in the deeper issue of whether the energy blocked by sunspots is stored for periods of months or more or whether, as some have suggested, the blocked energy is re-emitted by contemporaneous bright faculae, fulfilling a detailed balance of flux on intermediate time scales.

Four tests shed light on the question, but as yet without resolving it. Monochromatic measurements of the relative contributions of bright faculae and dark sunspots, over the disk, suggest that at sunspot maximum faculae seem to dominate. If this is extrapolated as an 11-year, cyclic effect, we might expect a cyclic modulation of S , in phase with the solar activity cycle. Such an extrapolation depends, however, on a questioned equivalence of monochromatic measurements with radiometry. Attempts to distinguish between storage and detailed balance on the basis of fitting observed records of S with measured values of sunspot and facular areas and contrasts have produced conflicting results, as a result of our limited knowledge of the actual values of the latter parameters. Facular area is particularly poorly known, with estimates differing by fully an order of magnitude. The secular trend noted in the ERB and ACRIM data (a persistent decrease between 1978 and 1981) dictates against the notion of dominant facular emission with solar activity; the trend through 1982 in ERB and ACRIM data is wholly consistent with the presence of an 11-year, out-of-phase modulation of S that is predicted by the storage hypothesis. Here, however, the behavior of the trend in the next year or two promises to be a critical discriminator: specifically, whether the downward trend of 1978-1981 undergoes a reversal in 1983 and after, to slowly increase until the end of the cycle in about 1987. Finally, tests of terrestrial surface temperature data reveal the presence of a subtle, 11-year modulation that fits both the phase and amplitude predicted by the storage hypothesis, as well as the geographical distribution required by simple climate models.

REFERENCES

1. Newkirk, G., Jr., Variations in solar luminosity, *Ann.Rev.Astron.Astrophys*, 21, (in press), 1983.
2. Schneider, S. H. and C. Mass, Volcanic dust, sunspots, and temperature trends, *Science*, 190, 741, 1975.
3. Spruit, H .C., Effect of spots on a star's radius and luminosity, in *The Physics of Sunspots* (Cram, L. E. and J. H. Thomas, eds.), Sacramento Peak Obsvty., 480, 1981.
4. Spruit, H .C., Effect of spots on a star's radius and luminosity, *Astron. and Astrophys.*, 108, 348, 1982.
5. Foukal, P., Fowler, L. A. and M. Livshits, A thermal model of sunspot influence on solar luminosity, *Astrophys.J.*, 267, 863, 1983.
6. Eddy, J. A., Gilliland, R. L. and D. V. Hoyt, Changes in the solar constant and climatic effects, *Nature*, 300, 689, 1982.
7. Jones, P. D., Wigley, T. M. L. and P. M. Kelly, Variations in surface air temperatures: Part 1. Northern hemisphere, 1881-1980. *Mon.Weath.Rev.*, 110, 59, 1982.
8. Gilliland, R. L., Schneider, S. H. and L. D. D. Harvey, Volcanic, carbon dioxide, and solar forcing of northern and southern hemisphere surface air temperature, *Nature*, submitted, 1983.
9. Bruning, D. and B. J. LaBonte, Interpretation of solar irradiance variations using ground-based observations, *Astrophys. J.*, 271, 853, 1983.
10. Sofia, S., Oster, L. and K. Schatten, Solar irradiance modulation by active regions during 1980, *Solar Phys.*, 80, 87, 1982.
11. Oster, L., Schatten, K. H. and S. Sofia, Solar irradiance variations due to active regions, *Astrophys.J.*, 256, 768, 1982.
12. Schatten, K. H., Miller, N., Sofia, S. and L. Oster, Solar irradiance modulation by active regions from 1969 through 1980, *Geophys.Res.Letters*, 9, 49, 1982.

13. Hoyt, D. V. and J. A. Eddy, An atlas of variations in the solar constant caused by sunspot blocking and facular emissions from 1874 to 1981, NCAR/TN-194+STR, 106pp, 1982.
14. Hoyt, D. V. and J. A. Eddy, Solar irradiance modulation by active regions from 1969 through 1981, *Geophys.Res.Letters*, 10, 509, 1983.
15. Foukal, P. V., Mack, P. E. and J. E. Vernazza, The effect of sunspots and faculae on the solar constant, *Astrophys.J.*, 215, 952, 1977.
16. Chapman, G.A., Variations in the solar constant due to solar active regions, *Astrophys.J.*, 242, L45, 1980.
17. Royal Greenwich Observatory, Photo-heliographic Results, London, H.M. Stationery Office, 1874-1976.
18. Hudson, H. S. and R. C. Willson, Sunspots and solar variability, in *The Physics of Sunspots* (Cram, L. E. and J. H. Thomas, eds.), Sacramento Peak Obsvty., 434, 1981.
19. Willson, R. C., Gulkis, S., Janssen, M., Hudson, H. S. and G. A. Chapman, Observations of solar irradiance variability, *Science*, 211, 700, 1981.
20. Hoyt, D. V., Eddy, J. A. and H. S. Hudson, Sunspot areas and solar irradiance variations during 1980, *Astrophys.J.*, 275, (in press), 1983.
21. Willson, R. C., Solar irradiance variations and solar activity, *J.Geophys.Res.*, 87, 4319, 1982.
22. Smith, E. A., Von der Haar, T. H. and Hickey, J. R., The nature of the short period fluctuations in solar irradiance received by the earth, *Climatic Change*, 5, (in press), 1983.
23. Hickey, J. R., Updated ERB/Nimbus 7 total solar irradiation results, Eppley Laboratory, Inc., April, 1983.
24. Currie, R. G., Solar cycle signal in air temperature in North America: amplitude, gradient, phase and distribution. *J.Atmos.Sci.*, 38, 808, 1981.
25. Hanson, K. and G. Cotton, Temperature variation in the United States during June: a search for causes and mechanisms, *Weather and Climate Responses to Solar Variations*, (R. M. McCormac, ed.) Colo.Assoc.Univ.Press, Boulder, (in press), 1983.

LIST OF FIGURES

1. Modelled, reconstructed, relative monthly average S based on Royal Greenwich Observatory (1872-1974) and NOAA-ERL (1975-1982) measurements of projected sunspot and facular areas, with an assumed storage time of 10 years (from ref.13).
2. Annual averages (open circles) of the observed ratio of hemisphere facular area to sunspot area (each corrected for foreshortening) from daily measurements of the Royal Greenwich Observatory, 1872-1974 (ref.17). Five outlying values (dotted circles) are annual average ratios for years of extreme minima for which the annual sunspot number was 6 or less.
3. The ratio of observed (projected) facular area to projected sunspot area for the period 1872-1974, as a function of projected sunspot area. Shown are annual averages fit with a linear regression line, from daily measurements of the Royal Greenwich Observatory (ref.17). Whole-disk facula to sunspot area systematically falls with increasing sunspot number or area; the 103-year average is 1.6. The projected area ratio is systematically smaller than the corrected area ratio shown in Figure 2 as a result of the different limb visibility functions of sunspots and faculae.
4. Daily projected sunspot area measurements, in millionths of the visible disk, from 5 reporting stations for 70 days sampling periods of high and low solar activity during 1980 (solid lines, from ref.20; stations listed at top). Simulated values of the same parameter used by Sofia et al. in their modelled fitting of the SMM ACRIM measurements are shown as open circles.
5. Adjusted Engineering Level measurements of S from Nimbus 7, November 1978 through 1982 (ref.23, courtesy J. R. Hickey). As in the SMM ACRIM measurements, the downward secular trend changes slope in late 1981 and after.
6. Monthly averages (continuous lines) and 13-month smoothed monthly means (open circles) of sunspot number R (upper figure, scale at right) and projected whole sunspot area A (lower figure, scale at left in millionths of the visible disk) for November 1978 (Nimbus 7 commencement) through May 1983. Cycle #21 peak of smoothed R , shown with arrow, preceded peak of A (estimated late 1981) by about two years.

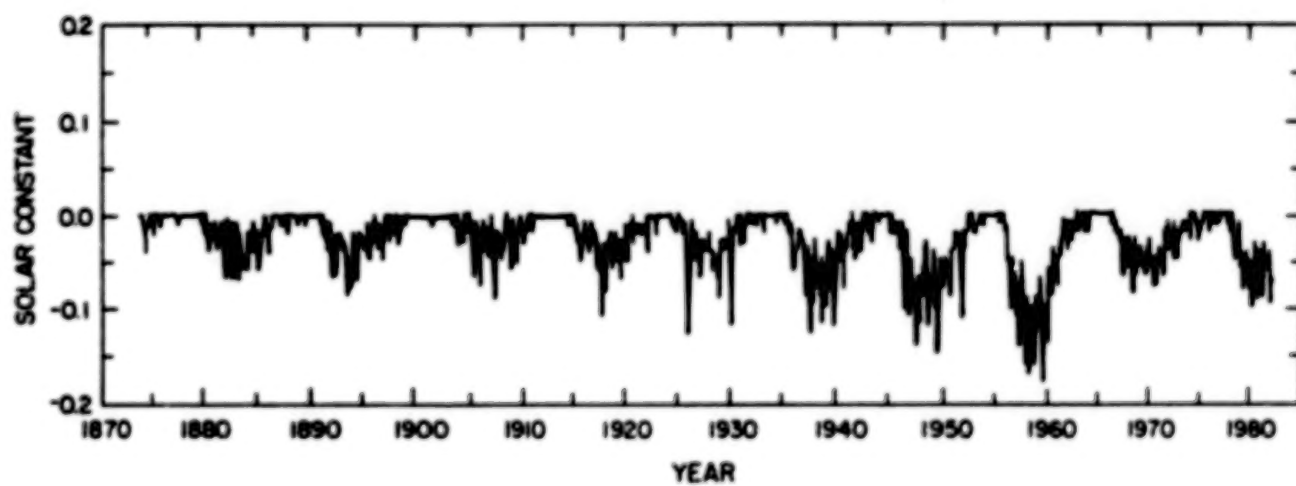


Figure 1

224

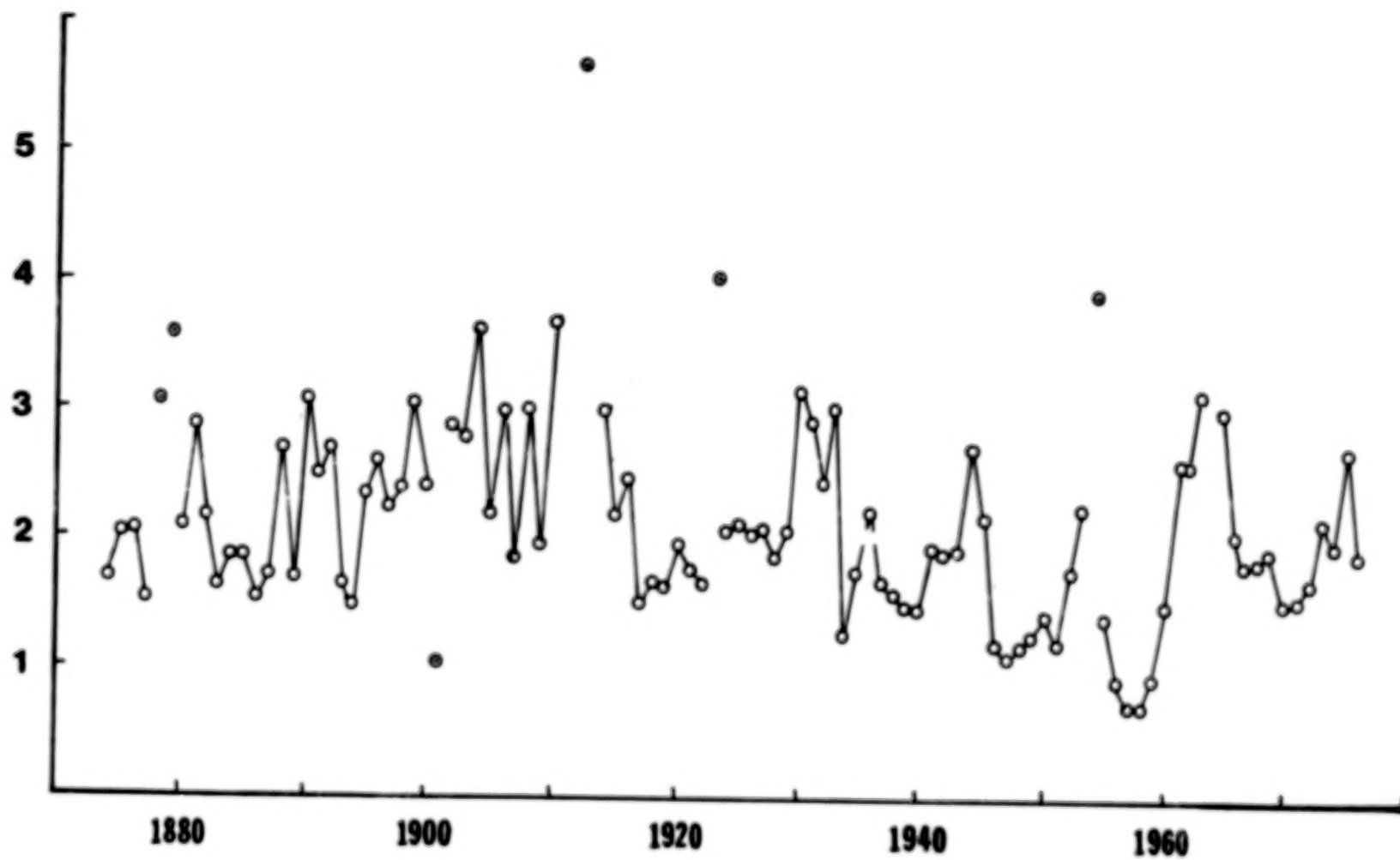


Figure 2

225

BLANK PAGE

BLANK PAGE

BLANK PAGE

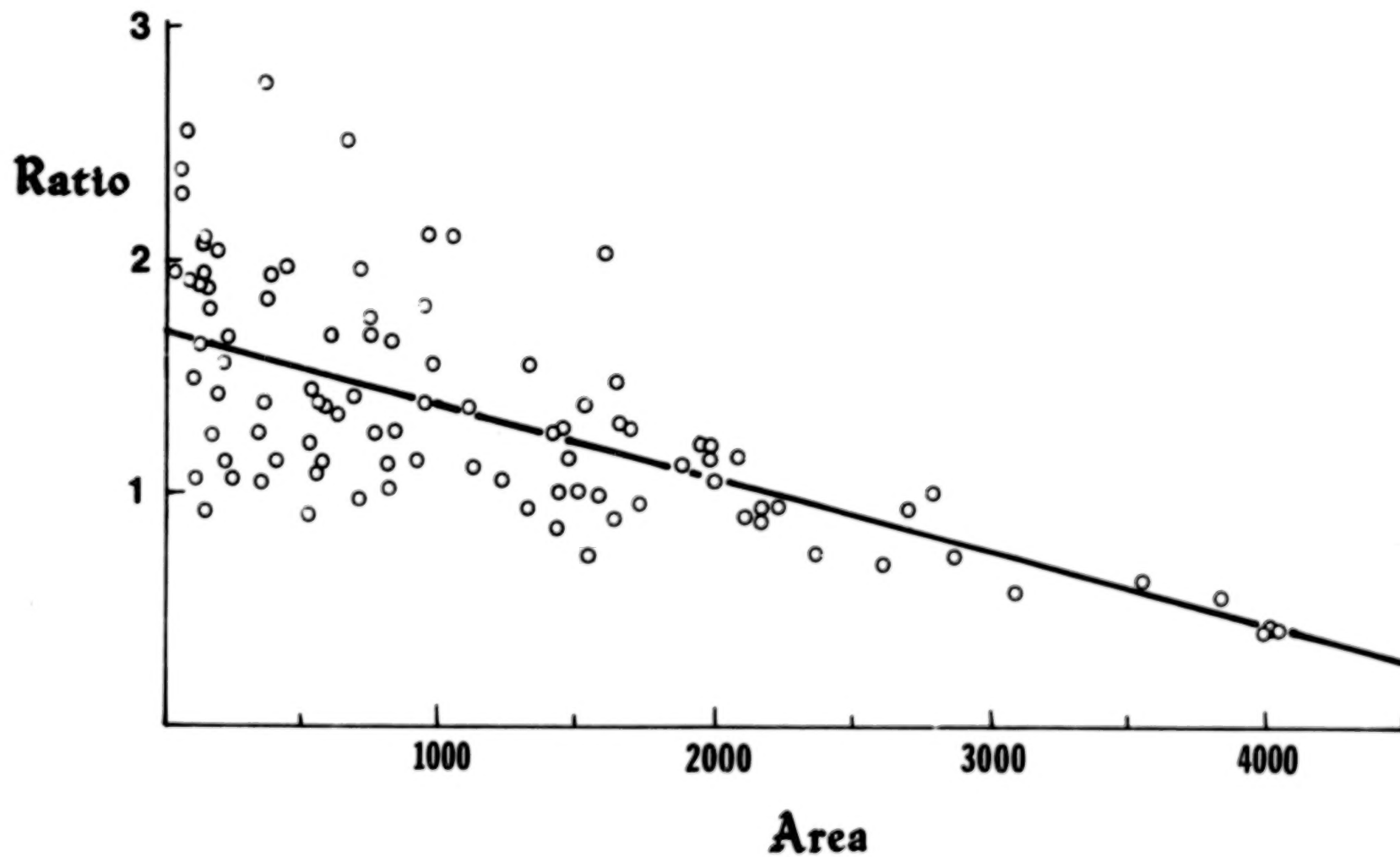


Figure 3

296

DAILY PROJECTED SUNSPOT AREA

NOAA SEL
Taiwan

Catania
Beijing

Rome

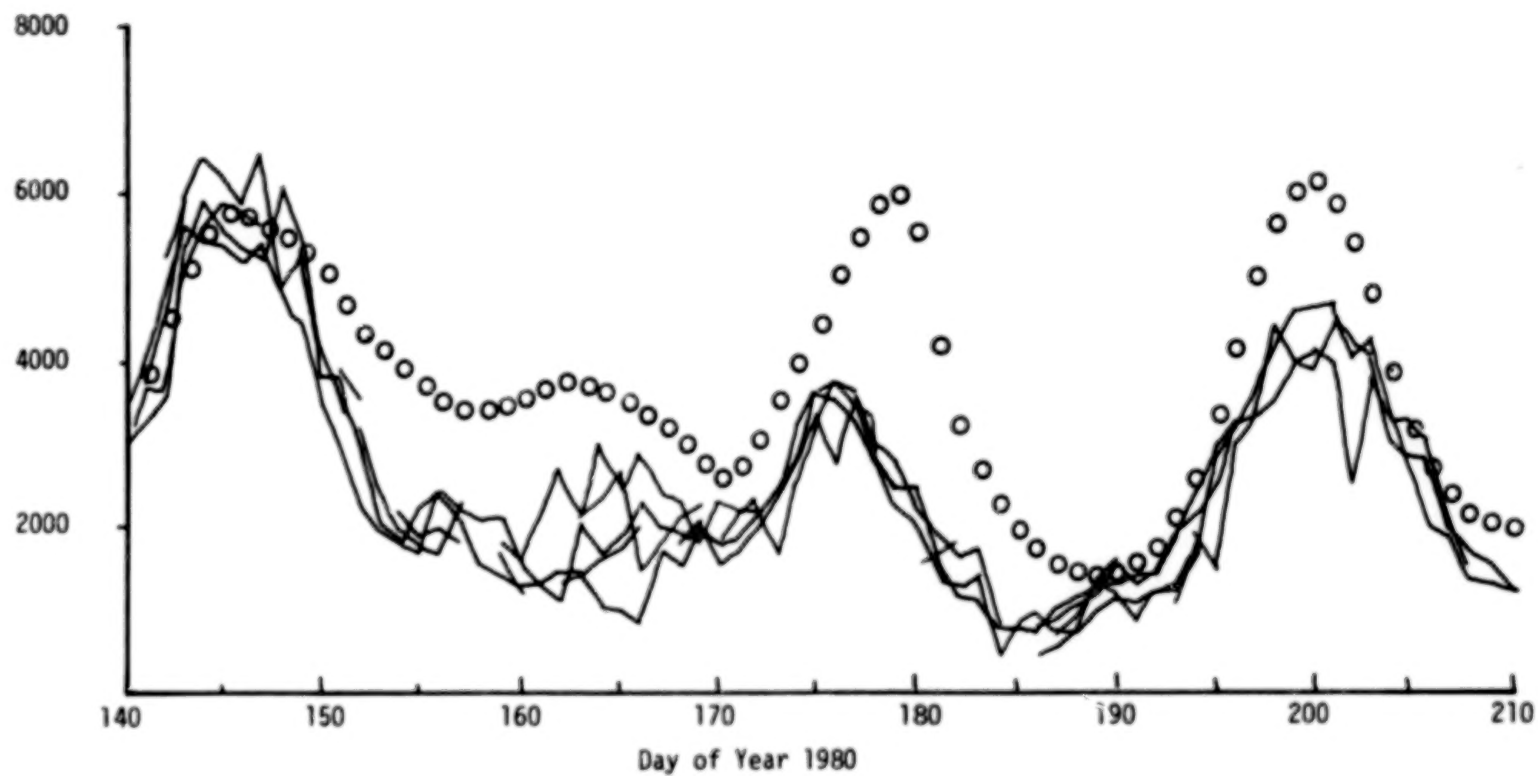


Figure 4

227

ERF, NIMBUS 7 CAVITY PYRHELIOMETER SOLAR IRRADIANCE VS. TIME

EPLAB/NDAA-NESS UPDATE OF MARCH 2, 1983

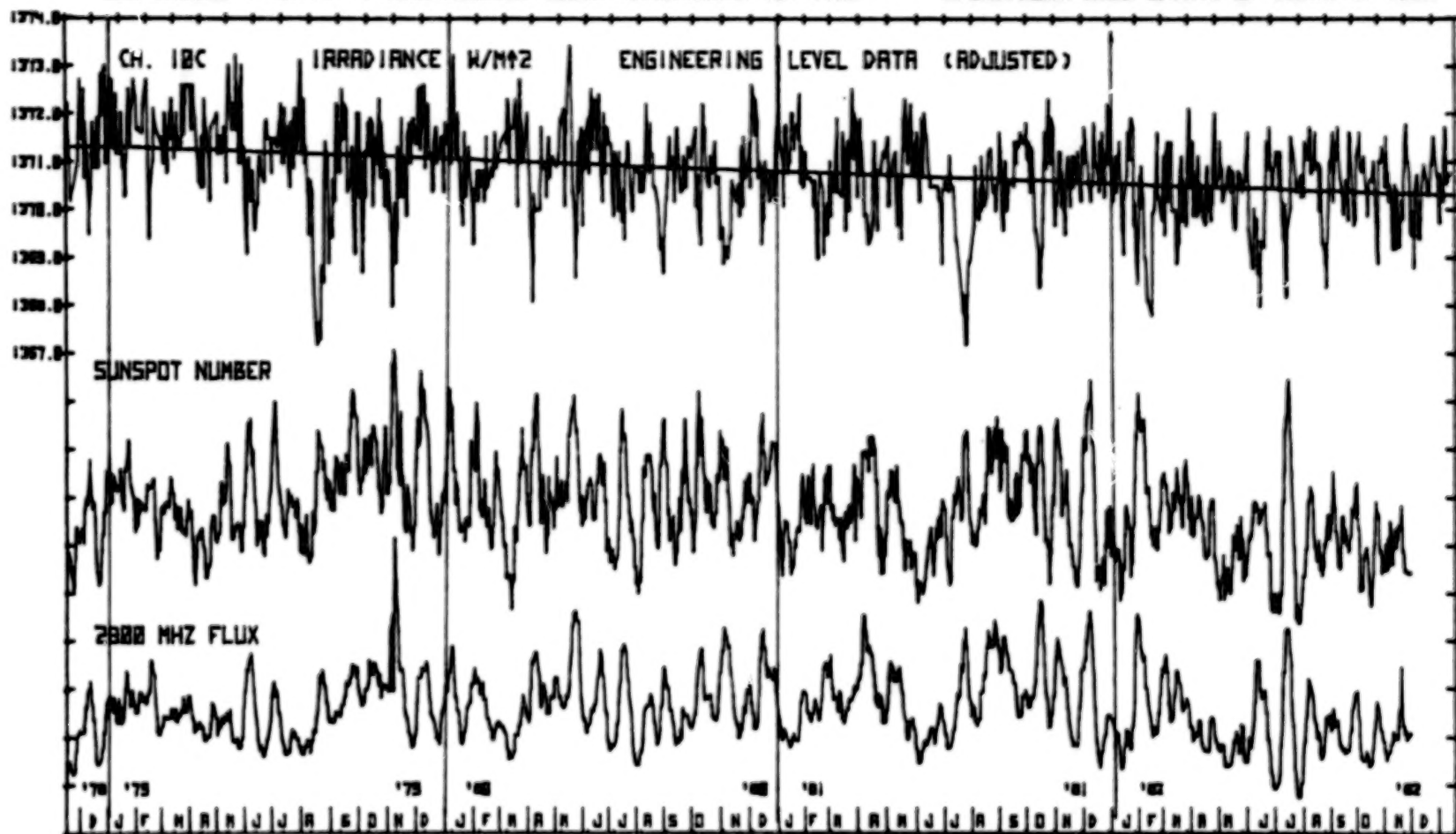


Figure 5

228

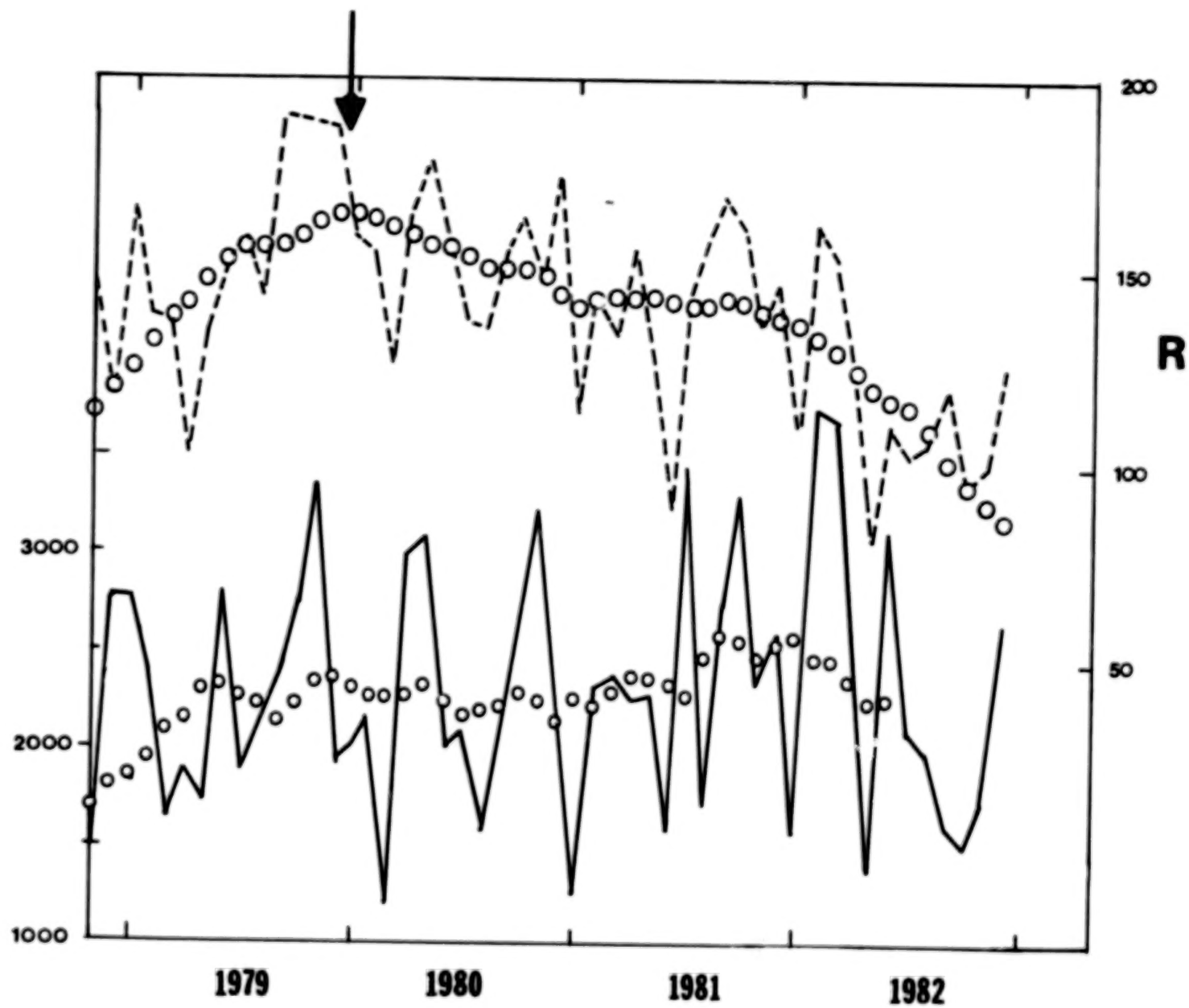


Figure 6

229

DISCUSSION OF EDDY PRESENTATION

SOFIA: ... integrated over the same size, when it's not something bigger?

EDDY: I hear your point, it says when the two are present you'd be very surprised because of the fact that they ought to be a great deal bigger than the spot areas. Is that true?

SOFIA: Even if it is equal and then lasts five times as long it's already much more than one time because they last the same amount of time. You have that curve going too high, and even when they're present at the same time it's arguable.

EDDY: It doesn't surprise me too much I guess, except maybe in the Greenwich measurements, which are certainly daily and continuous so you can't apply any factor to them about lifetimes; that's already present. In a sense that strengthens your argument. It's already there, it's averaged over every day of the year. Well, but I don't know, if one looks at photographs of the white light that doesn't surprise me.

LABONTE: Gary has a point to make on this particular subject.

CHAPMAN: Hot off the press! My graduate student was doing this yesterday, well it's just continuing on, hammering out more data, but for all the pitfalls of using monochromatic data, I still think to a good approximation that it should track the bolometric changes for things on the sun. And, this is a result of 41 data sets, different active regions. What we find is that the correlation of the limb photometer fluctuation, $\Delta B/B$, not corrected bolometrically, is highly correlated with the PSI index. The correlation coefficient is almost 0.9. This is the actual regression we got using this particular expression here, and it is what I recommend as the PFI index now. This number is almost exactly what you published, and so I suggest at most that it would need only a small correction. This is at $0.53 \mu m$. Now the thing that I really wanted to get across is the facular thing, the same kind of thing, a PFI which is being published in the proceedings that I gave to you yesterday. For the calibration of the calcium plage areas, the values I'm getting are 0.01 (note that this value is 0.009 in the published paper -editors) times the area of the plage from the Solar Geophysical Data. That's about one percent. There are no assumptions here. These are measurements, 41 data sets; if you take this functional form, which I think isn't bad, except at the extreme limb, and the area that's published in the Solar-Geophysical Data (by the government!) then the brightness in millionths is one percent of the plage area. So we're not going to have much more data than this by the way, so this cannot possibly change by very much.

SCHATTEN: Gary, what does this say in terms of energy balance?

CHAPMAN: Ah, let's see, well, that's an interesting question. I think, if you take 1 percent times the plage area, the plage area is typically at least 5 or 10 times the area the sunspots, the published values, of the calcium plage area and so it's not negligible.

HUDSON: If you did your integrals over those functions of μ , what are the ratios

of those functions? Maybe that's the other factor of ten.

CHAPMAN: Well, you have to know the life times.

SOFIA: No, the factor of 10 includes the life time.

CHAPMAN: No, not in this, right? You look at the average, well maybe, oh I see your saying that they live longer.

SOFIA: They live longer, a factor of 10 in life time.

CHAPMAN: I understand, you say just look at the published values, you see a mean area, a time-averaged area.

MOORE: Jack, if we take this possible [irradiance decline] bottoming out, [what does that] say about the lifetime of the storage?

EDDY: If you put in different storage life times, it doesn't affect the amplitude very much at all. You're never going to be able to say whether it's 10 years or 500,000 years; you'll have a hard time distinguishing between 5 and 10 [years]. You might be able to distinguish between a few months and a few years.

SCHATTEN: Of course we're finding out that the curve you drew looks nothing like the actual curve which is more [nearly] horizontal. It's quite possible the effects [you described] are going on. I agree with most of what you said, but this really doesn't allow us at present to distinguish between your model and ours; but these variables won't give a constant [solar output]; do you really think you can claim support for that shift? I think it's probably a secular trend of the type that Sabatino [Sofia] suggested, not the one that occurred for the facular shift, but one of the long term changes, in solar radius or something we don't know about.

EDDY: I'm sorry, in all those models there's the assumption that the only thing that drives the solar luminosity [fluctuations] is solar activity. I think we don't have that long term trend.

BLANK PAGE

TEMPORAL VARIATIONS OF SOLAR UV SPECTRAL IRRADIANCE
CAUSED BY SOLAR ROTATION AND ACTIVE REGION EVOLUTION

Richard F. Donnelly

Air Resources Laboratories, NOAA ERL, Boulder, Colorado 80303

Donald F. Heath

NASA Goddard Space Flight Center, Greenbelt, Maryland 20771

Judith L. Lean

CIRES, University of Colorado, Boulder, Colorado 80309

Gary J. Rottman

LASP, University of Colorado, Boulder, Colorado 80303

ABSTRACT

Variations in the solar 100 - 400 nm UV spectral irradiance caused by solar rotation and active region evolution, are discussed as a function of UV wavelength, CMD dependence, and in relation to the temporal variations in the total solar irradiance, 10.7 cm radio flux, sunspot number and Ca K plage data. Active region radiation at cm wavelengths includes a component proportional to the magnetic field. Active region evolution involves a more rapid growth, peak and decay of sunspots and their strong magnetic fields than the Ca K plages and their related UV enhancements. Major plages often last a rotation or more longer than the active region's sunspots. Large active regions, including those associated with major dips in the total solar irradiance, tend to produce the strongest peaks in 10.7 cm and sunspot numbers on their first rotation, while the Ca K plages and UV enhancements peak on the next rotation and decay more slowly on subsequent rotations. Differences in CMD dependencies cause temporal differences including the stronger presence of 13-day variations in the UV flux.

ATMOSPHERIC IMPORTANCE

Solar UV radiation is important because of its effects in the stratosphere, its influence on the terrestrial ozone layer and possible influence on climate through stratosphere-troposphere coupling. The O_3 layer is vital to life on Earth in its role of blocking solar UV radiation from the biosphere. The 220-285 nm band of solar UV radiation is primarily absorbed by ozone O_3 and is the major source of stratospheric heating and O_3 photodissociation. The 175-205 nm band is very important because it photodissociates O_2 . The resultant atomic oxygen leads to the production of O_3 and other odd-oxygen minor constituents that play an important role in the chemistry of the stratosphere.

The short-term UV variations caused by active region evolution and solar rotation are very important to stratospheric physics because the first accurate quantitative links between the measured solar UV variations and the observed stratospheric response are being made for these variations from

concurrent solar and stratospheric measurements from the NIMBUS-7 and SME satellites. Longer-term variations are of greater interest in the atmospheric sciences but currently the accuracy of measurements of long-term UV variations is insufficient. A combination of a long-term series of rocket and shuttle measurements is inadequate for determining the long-term variation unless we know the short-term variations at the time of each measurement in the series. In effect, the short-term variations act like noise in trying to measure the long-term variations. However, an accurate knowledge of the contribution of active region evolution and rotation effects on the full-disk UV flux is also important because it indicates the longer-term variations, like solar cycle variations, due to the physical process of the accumulation of more active regions on the solar disk at a given time. On the otherhand, we should not assume that all of the long-term variations are caused solely by what we now call active regions. Also, solar cycle variations in the characteristics of active regions, for example their latitude distribution and brightness, are important.

SOLAR UV OBSERVATIONS AND MODELS

Extensive measurements of the solar UV spectral irradiance have been made with the NIMBUS-7 satellite in the 160 - 400 nm wavelength range since November 7, 1978 (refs. 1, 2) and by the SME satellite in the 120 - 305 nm range starting on October 13, 1981 (ref. 3). Before these measurements were available, daily solar indices like the 10.7 cm solar radio flux (F10) measured near noon in Ottawa and the Zurich sunspot number (R) were used as indicators of UV flux variations (refs. 4,5). The UV flux observations sometimes vary quite differently than these general indices of activity. Two types of different temporal behavior are discussed below.

Several efforts are currently being made to model the solar UV temporal variations. The work of Cook et al. (ref. 4) has recently been extended by Lean et al. (refs. 6,7) using ground-based observations of Ca-K plages as input data to estimate the solar UV flux. Oster (ref. 8) based his modeling on the 10.7 cm solar radio flux data. The two types of differences presented below are also cases where the Lean model estimates the UV flux variations fairly well but no model based on simple linear regression analysis with either R or F10 could fit the UV observations well.

SIMILARITY OF UV VARIATIONS

Figure 1 shows four adjacent wavelength bands of solar UV flux with temporal variations caused by the combined effects of active region evolution (birth, growth, peak and decay, and sometimes rejuvenation) and solar rotation of active regions with an inhomogeneous distribution in longitude. These two types of effects cause fairly similar temporal variations as a function of wavelength for bandwidths of a few nanometers. In the figures of this paper, the flux in the 200-205 or 185-205 nm wavelength band is used as an example of the solar UV temporal variations. Compared to the differences between the temporal variations of the solar UV flux, total solar irradiance, sunspot number and 10.7 cm radio flux discussed below, the differences in relative temporal variations among the bands of UV flux in the 165-300 nm range are small from the viewpoint of their effects on the Earth's atmosphere and are

neglected here. Heath (ref. 9) discusses some of the differences in temporal variations at certain UV wavelengths that are important for long-term variations and understanding the physics of the solar variations.

MAJOR ACTIVE REGION EVOLUTION

During major dips in the total solar irradiance (S), the solar UV flux is enhanced. However, the concurrent UV enhancements are not major but are only average enhancements (ref. 9). The arrow in Figure 1 denotes the time of a major dip in S as observed by the NIMBUS-7 satellite (ref. 10). Note that the UV enhancement at the time of the arrow is only average. On the otherhand, the UV enhancement on the next solar rotation is about twice as large and is larger than average. Figure 2 shows that the relation between plage area and sunspot area is quite scattered. Plage brightening dominates the UV variations and sunspot darkening dominates the known variations in the total solar irradiance on active-region time scales. The temporal evolution of plages is longer term than that for the sunspots (ref. 11). In Figure 2, there is a tendency for this relation to evolve in a counter clockwise direction for individual active regions, with the peak sunspot area occurring earlier than the peak plage area. This trend is discussed below with further examples.

Figure 3 shows another example. Major new active regions emerged during the peak in June and continued to grow through the peak in mid July. Major dips in S occurred in both mid June and mid July (refs. 10, 14). However, both the observed and modeled UV flux grew a little more in the third peak in August while the decrease in S was small and the increases in both F10 and R had dropped to peak values more like those in June. Furthermore, the UV observations decreased only slightly below the August peak during the September peak and were still significantly higher than during the June peak. On the other hand, F10 during the fourth peak continued its decay and reached lower values than for all of the first three peaks.

Another example of this behavior occurred during the major dip in S of November 6 - 10, 1979 (ref. 10) and is illustrated in Figure 6 in ref. 13. The 10.7 cm radio flux was anomalously large during the major dip in S but smaller along with the sunspot number during the next rotation when the observed Lyman-alpha flux and the Ca-K modeled UV flux variation was much larger.

Note in Figure 3 that the model calculations were not available for September because the Ca-K plage data have not yet been published in Solar Geophysical Data (SGD). Because the model UV flux fits the UV observations so well, the Ca-K data should be continued to provide a backup in case the satellite UV measurements fail. The Ca-K observations are also important for comparisons with UV measurements in order to interpret the causes of the observed UV variations, to identify possible cases of drift of satellite instruments and to discover possible real solar UV variations that are not accounted for in the physical processes included in the Ca-K/UV model.

R peaks earlier and S dips and decays earlier than the UV flux peaks because the major active regions tend to peak in their sunspot activity earlier than in their plage activity where the latter dominates the UV enhancement. This is evident from comparing the sunspot count and areas given in the Solar

Geophysical Data Reports with the associated Ca-K plage area multiplied by its intensity. The reason why F10 also peaks earlier than the observed UV flux or the Ca-K modeled UV flux is not quite as obvious. Part of the slowly varying component of centimeter-wavelength solar radio emission is caused by gyroresonance emission that depends on the magnetic field strength in the low corona portion of the active region (ref. 15). These magnetic fields probably are proportional in strength to the sunspot magnetic fields and proportional in spatial extent to the area of the sunspots. Figure 4 shows a plot of the Ca-K plage area weighted by the intensity, which is used in the UV model, versus the sunspot area times its field strength for the largest active region involved in the activity in Figure 3 and for the rotations 1-3, which correspond to the peaks in June, July and August, respectively. Note that the August peak is largest in the plage data while the June and July peaks are large in the sunspot data, i.e. there is a clockwise trend in this figure. This suggests that the centimeter-wavelength gyroresonance emission peaked was larger for this active region during the June and July passages than during the August passage and may have caused the early peaks in F10 in Figure 3.

All of the major dips in S larger in magnitude than 0.2% in Hoyt and Eddy's model of the total solar irradiance (ref. 16) during the period 1969 - 1981 were examined. The UV flux modeled from Ca-K plage data was found to be larger on later rotations and both F10 and R peaked during the major dip in S. The size of the short-term enhancements in F10 to that in the Ca-K modeled UV flux was about twice that for the similar ratio for one rotation later. Typically, the major dip in S and the largest enhancements in F10 and R occurred for only one rotation and the peak in modeled UV flux or the Ca-K plage emission occurred on the next rotation of the regions, i.e. a two-peak growth sequence unlike the three peaks in Figure 3.

Note that the UV plage enhancements that accompany sunspot-blocking induced decreases in the total solar irradiance constitute a reduction in the radiation energy lost from sunspot blocking. For example, for a short-term decrease in S of about 0.1 %, the enhancement below 300 nm may correspond to about a 1% enhancement in the UV, which corresponds to about 0.01 % enhancement in S. Consequently, the UV flux enhancement corresponds to about 10 % of the magnitude of the concurrent decrease in S, which is not negligible. The slightly larger half-width with respect to the solar central meridian distance (CMD) for the UV data (7 - 8 days) relative to the S dips (6 days, ref. 9) also suggests a larger radiation pattern for the UV enhancement, thereby increasing the portion of energy that is blocked at visible and infrared wavelengths that emerges in the UV. The main point we want to make here is that the tendency for the UV and plage enhancements to peak on later rotations than the sunspot darkening or dip in S and to decay more slowly on subsequent rotations also tends to increase the portion of energy blocked by sunspots that is compensated by energy that emerges in the UV over several months. Presumably, this trend for a slower time dependence for major chromospheric plage activity means that the visible and near infrared emission from photospheric facula also occurs over a longer time than the sunspot darkening effects. The longer lifetime of facula would account for more of the radiant energy apparently blocked by sunspots. Summarizing, when considering the importance of facula-enhanced radiation relative to sunspot-blocked radiation, we should consider the following: (1) the relative areas of sunspots

and facula, (2) their contrasts, (3) that facula emit strongest at large CMD or radiate over a larger solid angle than the sunspot darkening (ref. 17), (4) the longer life of plagues and (5) the large percentage enhancements at UV wavelengths.

THIRTEEN-DAY SOLAR UV PERIODICITY

Figure 5 shows R, F10, and the modeled and observed solar UV flux in the 200 - 205 nm wavelength band. The observed UV flux in the bottom curve has been normalized to the initial value and has been detrended of a long-term decrease caused by degradation of a diffuser used in the NIMBUS-7 SBUV experiment for solar flux observations. Corrections for this long-term instrumental effect were not available for this study, but any remnant effects should not affect the characteristics of the short-term variations discussed here. These NIMBUS-7 observations are daily averages of typically three to four wavelength scans (160 - 400 nm) completed over several minutes. The two values connected with dashed lines were the only two cases where only one wavelength scan was taken and are therefore more susceptible to noise. The second curve from the bottom in Figure 5 is the modeled UV flux (ref. 6) based on the solar location, area and peak intensity of Ca-K plagues to estimate the UV plague emission. The F10 and R data are the final values published in SGD.

The important feature of Figure 5 is that the observed UV flux exhibits a main peak about every 13 days apart starting near the end of January. The modeled UV flux is very similar to the observed flux in that it too clearly shows the 13-day periodicity. The Ca K plague data used as input data to the model show that the 13-days between peaks is caused by the concentration of plagues at solar longitudes nearly 180° apart. Some differences between the modeled and observed flux do occur, partly because of missing Ca-K data caused by cloudiness and probably partly because the scaled plague data are a crude representation of the complex plague structures. These problems can be overcome through improved observing programs. The solar radio flux and sunspot number do not show a predominant 13-day periodic structure. Consequently, estimates of the solar UV flux based on linear relations with either of these indices likewise would not show clearly the 13-day structure that dominates these UV observations.

The peak near the end of March involves a shift in solar longitude of the active regions contributing one of the two peaks per solar rotation; therefore, Figure 5 includes two groups of 13-day periods, one ending about March 30th and the other beginning then. Cases of 13-day periods in solar UV data are fairly common but not frequent. Some additional cases are indicated in Table 1. Heath (ref. 18) reported the presence of 13-day peaks caused by two solar longitudes of concentrated plagues in solar UV observations from NIMBUS-4 in 1969 and 1970. The cases in Table 1 are based on the Ca-K plague model (ref. 6). In each of these cases, the 13-day periodicity is not a strong clear feature in the time dependencies of the 10.7 cm radio or sunspot data.

CMD DEPENDENCIES

The main reason why the 10.7 cm solar radio flux and sunspot number do not show the same 13-day temporal structure as the observed UV flux or the

model results based on Ca-K plage data is probably that the former have a much broader dependence on the solar central meridian distance (CMD) than do the latter. CMD is the solar longitude with respect to the central solar meridian viewed at Earth. Figure 6 shows our current knowledge of the CMD dependencies of the active region emissions of these data. If the active region stayed the same except it rotated around the sun so that our observing angle increased with respect to the solar radial through the active region, then on average the intensity would decrease with increasing CMD as shown.

The curve for 10 cm solar radio emission from active regions is based on an average of the observational results at 9.1 cm (ref. 19) and in the 8 - 10.7 cm range (ref. 20) and includes more than 100 active regions in order to average out the temporal variations of individual regions. The two UV curves are based on the Ca-K plage model (ref. 6) and include the effective area foreshortening for optically thick emission areas together with quiet-sun measurements of the center-to-limb variations in contrast (ref. 21). The UV curves are for the case of a solar latitude of 20° for the active region and 0° for the observed center of the solar disk. The sunspot curve drops below unity at large CMD because the sunspot number is usually dominated by small sunspots and because it is more difficult to see small sunspots at large CMD than near the center of the sun. (See ref. 23 for a derivation of the $R(\text{CMD})$ curve.) A synodic solar rotation rate of 27 days corresponds to 13.3° CMD per day, or a CMD variation half-width of about 7, 8, 10 and 12 days for 200 nm, 160 nm, sunspot numbers, and 10.7 cm flux, respectively. Note that in Figure 3, the major peaks of July and August, 1982, have half-widths of 8.1 and 7.7 days for the 185 - 205 nm observations, 8.2 and 6.6 days for the 200 - 205 nm model, 9.5 and 8.7 days for the sunspot numbers, and 11.0 and 11.6 days for F10, respectively.

According to Figure 6, F10 receives a fairly large contribution from both the group of active regions near the East solar limb and those near the West limb so their total effect is similar to that when either group of regions is near the center of the disk. Consequently, F10 does not have a strong minimum when the two groups of regions are near the limbs. Conversely, the UV plage emission does have a strong minimum at that time and a peak when one of the groups of active regions is near the center because the UV emission from regions near the limb is much weaker than from near the center. R is intermediate between these two cases. The UV half-width of about 7 to 8 days is narrow enough to permit deep enough valleys for two peaks per solar rotation to provide a strong 13-day periodicity.

CONCLUSIONS

1. Although the observed variations of the total solar irradiance are of the order of tenths of a percent, solar UV variations on active region time scales are of the order of one percent below 300 nm increasing to as large as eight percent at wavelengths below 205 nm or the Al I absorption edge (Figure 3).
2. Solar irradiance variations on active region time scales involve two processes, the temporal evolution of the regions (birth, growth, peak and decay) and the effects of solar rotation changing the direction from which the region is viewed at Earth. The delayed UV peak associated with major S dips primarily results from differences in temporal evolution of plagues and

sunspots while the 13-day UV periodicity is strongly linked to the UV solar-rotation dependence.

3. When large dips in the total solar irradiance occur due to the central meridian passage of strong young sunspots concentrated in a small range of solar longitude, the concurrent UV enhancements from the associated plages are not outstanding but are only average in intensity. On the next rotation, the UV enhancement is much larger while the total irradiance dip usually has diminished greatly. This behavior is a consequence of the plage evolution (growth, peak and decay) being slower than the sunspot evolution.

4. The 10.7 cm solar radio flux F10 and the sunspot number R also tend to have their strongest peak at the time of the major dip in the total solar irradiance and smaller enhancements on later rotations when the UV flux reaches its maximum. On subsequent rotations, the UV emission decays more slowly than F10 and R. This behavior is another consequence of the slower evolution of plages than sunspots where F10 is sensitive to the magnetic fields of active regions through the gyroresonance emission. Consequently, models of the UV temporal variations based on Ca-K plage data follow the observed UV variations on active region time scales more closely than estimates based on linear relations to either F10 or R.

5. The dependence of the UV emission on the solar central meridian distance (CMD) is narrower than that for R and F10 (Figure 6). Consequently, the temporal half-widths of peaks caused by the solar rotation of strong active regions concentrated in a small range in solar longitude tend to be shorter for UV radiations (120-300nm) than for R and F10 (Figure 3). When two concentrations of active regions occur nearly 180° apart in solar longitude, the UV irradiance can have a strong 13-day modulation while F10 and R do not have a dominant 13-day variation because the UV emission has a narrower CMD dependence (Figure 5).

REFERENCES

1. Heath, D. F., A. J. Krueger, H. A. Roeder and B. D. Henderson, The Solar Backscatter Ultraviolet and Total Ozone Mapping Spectrometer (SBUV/TOMS) for NIMBUS G, Optical Eng., 14, 323, 1975.
2. Heath, D. F., A Review of Observational Evidence for Short and Long Term Ultraviolet Flux Variability of the Sun, Sun and Climate, Centre National D'Etudes Spatiales, 18 Avenue Edouard - Belin, 31055 Toulouse Cedex, France, 447, 1980.
3. Rottman, G. J., C. A. Barth, R. J. Thomas, G. H. Mount, G. M. Lawrence, D. G. Rusch, R. W. Sanders, G. E. Thomas and J. London, Solar Spectral Irradiance, 120 - 190nm, October 13, 1981 - January 3, 1982, Geophys. Res. L., 9, 587, 1982.
4. Cook, J. W., G. E. Brueckner and M. E. VanHoosier, Variability of the Solar Flux in the Far Ultraviolet 1175-2100 A, J. Geophys. Res., 85, 2257, 1980.
5. Keating, G. M., The Response of Ozone to Solar Activity Variations: a Review, Solar Phys., 74, 321, 1981.
6. Lean, J. L., O. R. White, W. C. Livingston, D. F. Heath, R. F. Donnelly, and A. Skumanich, A Three-Component Model of the Variability of the Solar Ultraviolet Flux: 145-200 nm, J. Geophys. Res., 87, 10307, 1982.
7. Lean, J., Modeling Solar Spectral Irradiance Variations in UV Wavelengths, Workshop on Solar Irradiance Variations on Active Region Time Scales, NASA CP- , 19 . (Paper of this compilation.)
8. Oster, L., Solar Irradiance Variations, 1, Analysis of Modeling Techniques and Intercomparison of Ground-Based Data, J. Geophys. Res., 88, 1953, 1983.
9. Donnelly, R. F., D. F. Heath and J. L. Lean, Active-Region Evolution and Solar Rotation Variations in Solar UV Irradiance, Total Solar Irradiance, and Soft X Rays, J. Geophys. Res., 87, 10318, 1982.
10. Hickey, J., Status of Solar Measurements and Data Reduction for ERB - NIMBUS 7, Workshop on Solar Irradiance Variations on Active Region Time Scales, NASA CP- , 19 . (Paper of this compilation.)
11. Hudson, H., Observations of Solar Irradiance Variations on A. R. Timescales, Workshop on Solar Irradiance Variations on Active Region Time Scales, NASA CP- , 19 . (Paper of this compilation.)
12. Hinteregger, H., EUV Flux Variation During End of Solar Cycle 20 and Beginning of Solar Cycle 21, Observed from AE-C Satellite, Geophys. Res. Lett., 4, 231, 1977.
13. Lean, J. L., and A. Skumanich, Variability of the Lyman Alpha Flux with

Solar Activity, J. Geophys. Res., 88, 5751, 1983.

14. Willson, R., Status of the SMM - ACRIM Instrument and Data, Workshop on Solar Irradiance Variations on Active Region Time Scales, NASA CP- , 19 . (Paper , of this compilation.)
15. Marsh, K. A., and G. J. Hurford, High Spatial Resolution Solar Microwave Observations, Ann. Rev. Astron. Astrophys., 20, 497, 1982.
16. Hoyt, D. V., and J. A. Eddy, An Atlas of Variations in the Solar Constant Caused by Sunspot Blocking and Facular Emissions from 1874 to 1981, NCAR Technical Note No. NCAR/TN-194+STR, 1982.
17. Schatten, K. H., N. Miller, S. Sofia and L. Oster, Solar Irradiance Modulation by Active Regions from 1969 through 1980, Geophys. Res. L., 9, 49, 1982.
18. Heath, D. F., Space Observations of the Variability of Solar Irradiance in the Near and Far Ultraviolet, J. Geophys. Res., 78, 2779, 1973.
19. Riddle, A. C., The Quiet and Slowly Varying Components of 9.1 cm Radio Emission During the Solar Minimum, Sol. Phys., 7, 434, 1969.
20. Vauquois, B., Remarques sur le Rayonnement Radioelectrique Solaire sur 10 cm, Acad. Sci. Paris C. R., 240, 1862, 1955.
21. Samain, D., Solar Continuum Data on Absolute Intensities, Center to Limb Variations and Laplace Inversion Between 1400 and 2100A, Astron. Astrophys., 74, 225, 1979.
22. Foukal, P., and J. Vernazza, The Effect of Magnetic Fields on Solar Luminosity, Astrophys. J., 234, 707, 1979.
23. Puga, L. C., Studies of Ca-K plages and solar indices, Ch. 6 in NOAA-ERL-ARL Solar UV Radiation and Climate Research Project, NOAA Tech. Mem., ed. R. F. Donnelly et al., NOAA-ERL-ARL, Boulder, Colo., 1983.
24. Donnelly, R. F., D. F. Heath, J. L. Lean and G. J. Rottman, Differences in the temporal variations of solar UV flux, 10.7 cm solar radio flux, sunspot number and Ca-K plage data caused by solar rotation and active region evolution, accepted for publ. in J. Geophys. Res., 1983.

TABLE 1. Additional Examples of Thirteen-Day Periodicity in Solar UV Flux*

Dates		No. of Peaks	Average ^{**} Spacing	Comments
First Peak	Last Peak			
Feb. 25, 1970	June 13, 1970	9	13.5	Similar to Fig. 1.
Nov. 25, 1971	Jan. 29, 1972	6	13.0	Small Amplitude.
July 3, 1974	Sept. 6, 1974	6	13.0	
Sept. 7, 1978	Nov. 2, 1978	5	14.0	Longest Period
Mar. 4, 1980	May 23, 1980	7	13.3	

* Based on Ca-K plage data and the UV model of Lean et al. (ref. 6) for the years 1970 - 1981. The years 1975 - 1977 were too quiet in activity to obtain thirteen-day periods.

** Average spacing between peaks including the case in Figure 5 is 13.3 days.

FIGURE CAPTIONS

- Figure 1. Temporal variations of solar UV irradiance. The arrows denote the time of a major dip in the total solar irradiance.
- Figure 2. Ca-K plage area versus the associated sunspot area for individual active regions.
- Figure 3. Comparison of temporal variations of solar UV observations, UV model results based on Ca-K plage data, 10.7 cm solar radio flux and sunspot number during the growth, peak and early decay of major groups of active regions starting mid June, 1982 (ref. 24).
- Figure 4. Plage evolution versus sunspot evolution for an active region that is a major contributor to the temporal variations in Figure 3.
- Figure 5. Comparison of temporal variations of solar UV observations, UV model results based on Ca-K plage data, 10.7 cm solar radio flux and sunspot number during strong 13-day periodicity in the UV observations (ref. 24).
- Figure 6. Average dependence of the solar flux from active-regions as a function of the CMD location (ref. 24). The photospheric limb of the sun is on average at 90° . The UV emission for a region near the limb of the sun is very weak relative to when it is near the central meridian whereas the 10.7 cm sensitivity is quite high near the limb. The sunspot number is intermediate between the UV and 10.7 cm flux.

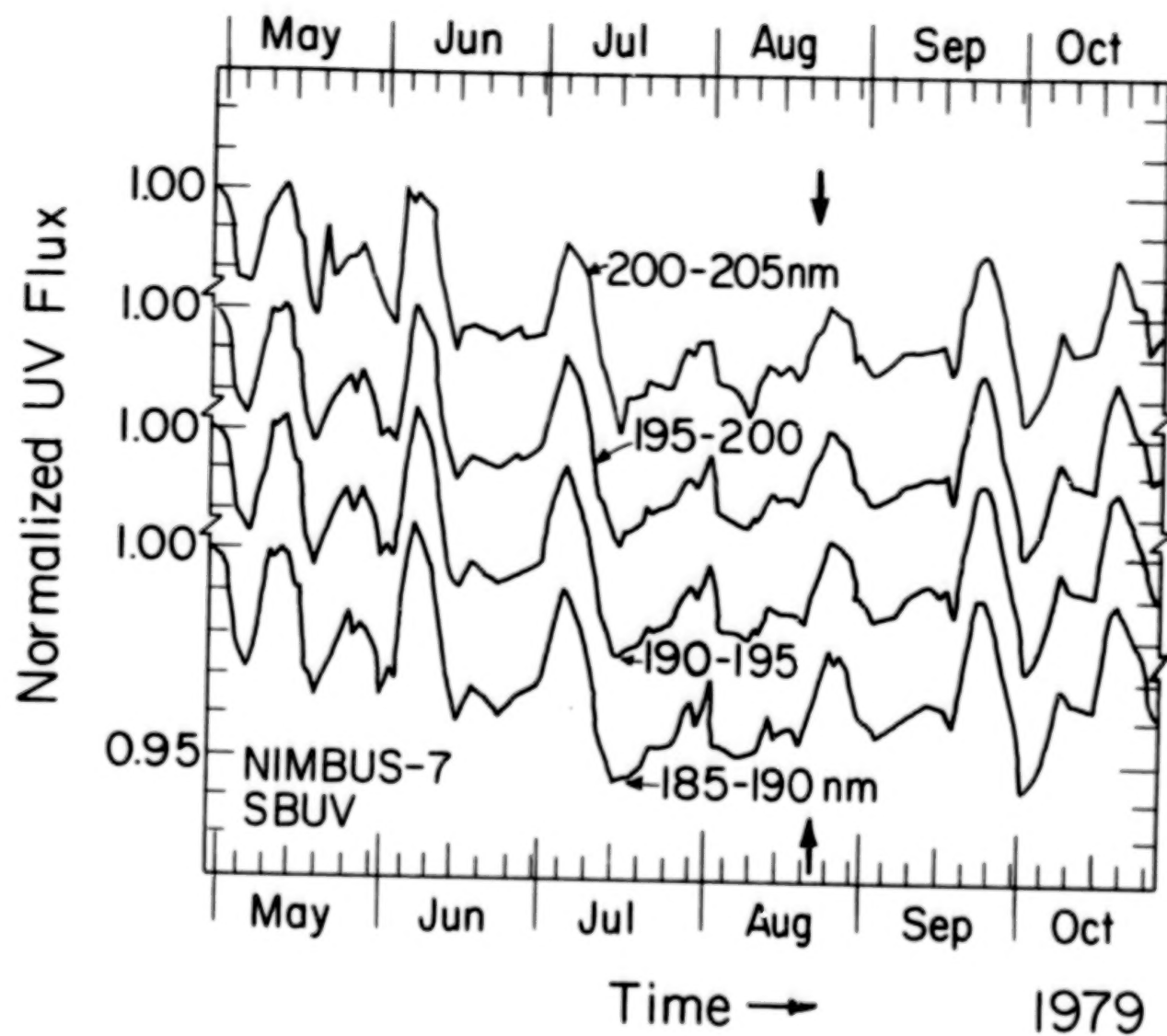


Figure 1

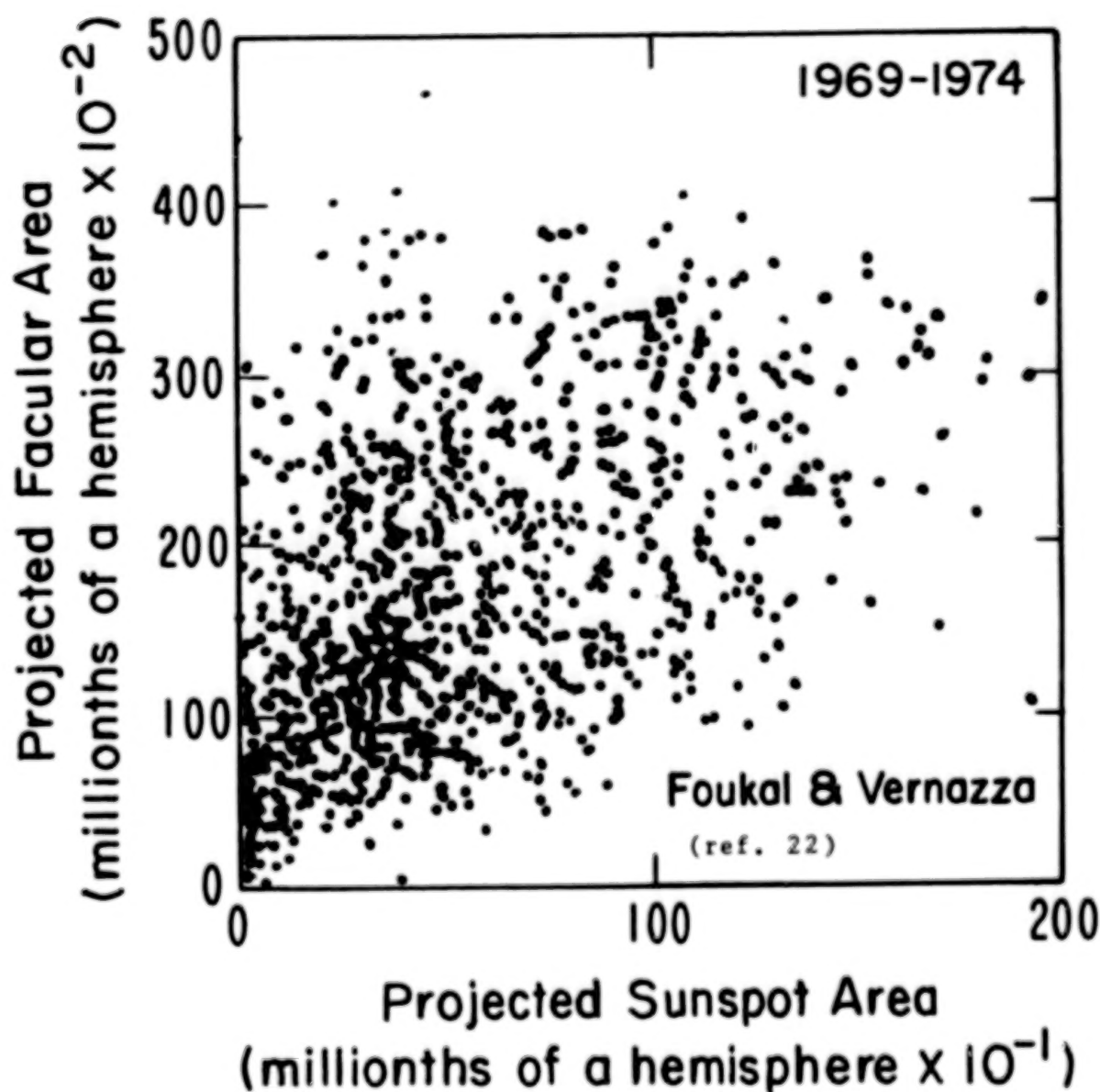


Figure 2

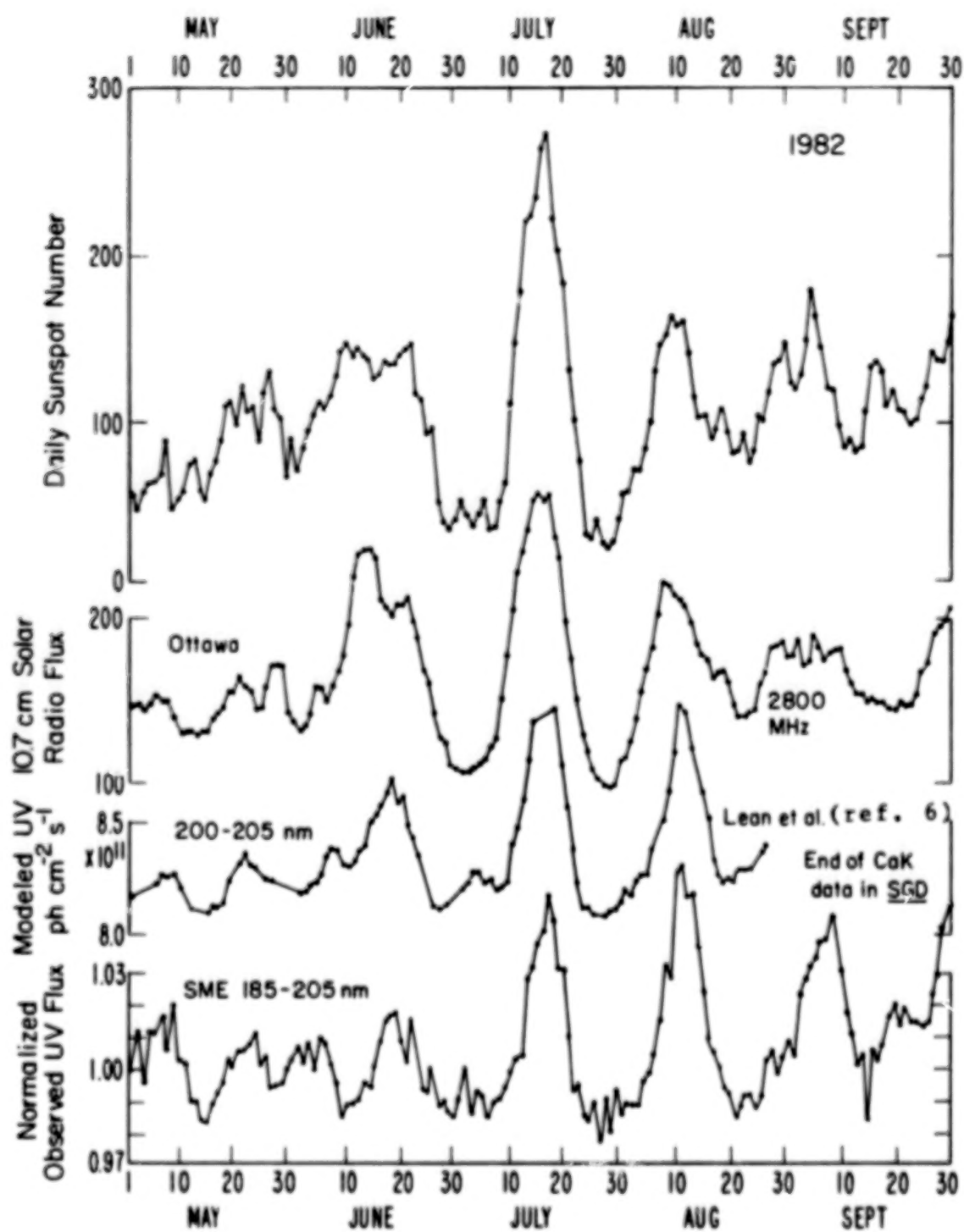


Figure 3

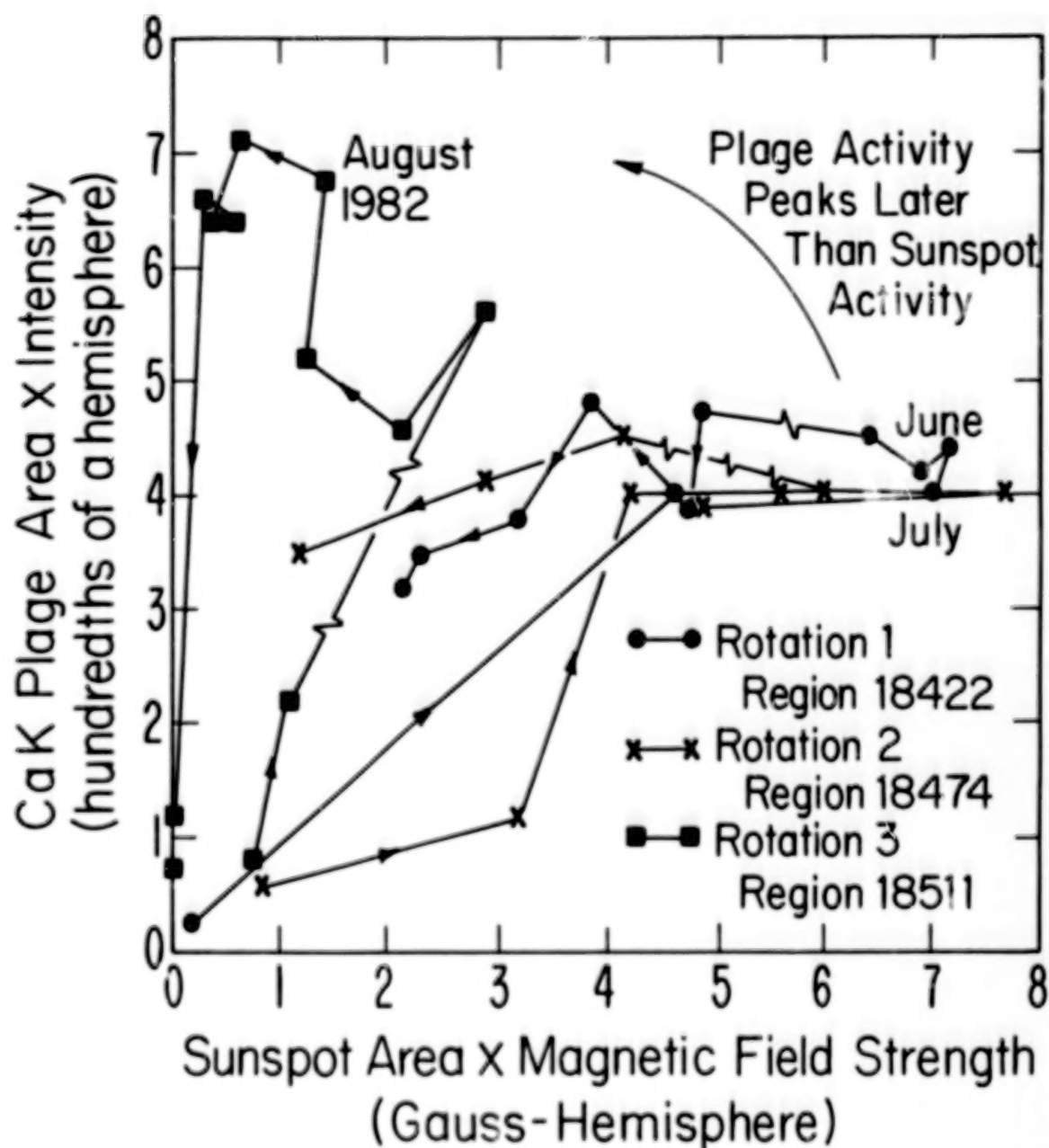


Figure 4

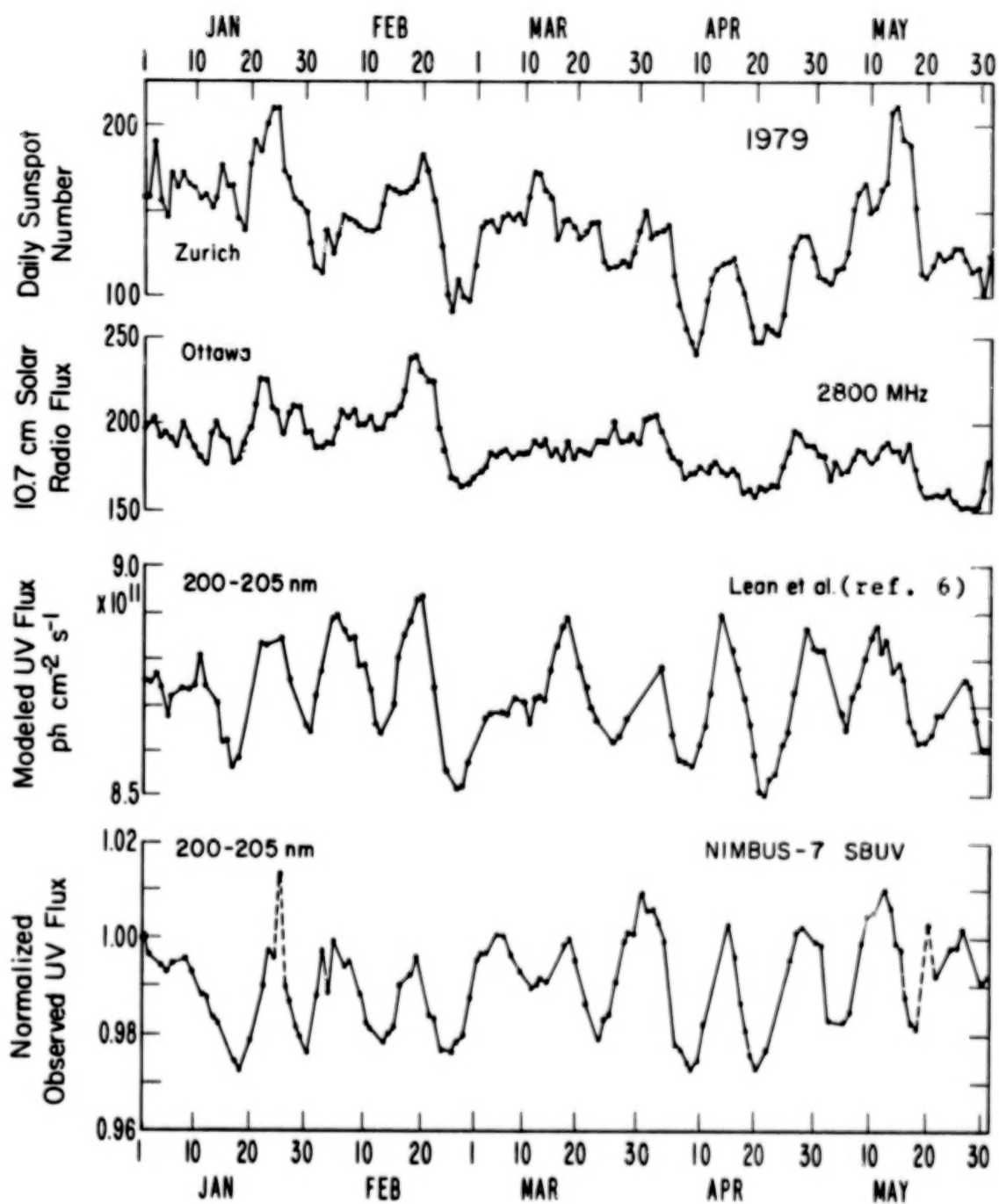


Figure 5

Average Normalized CMD Dependence for Solar Active Regions

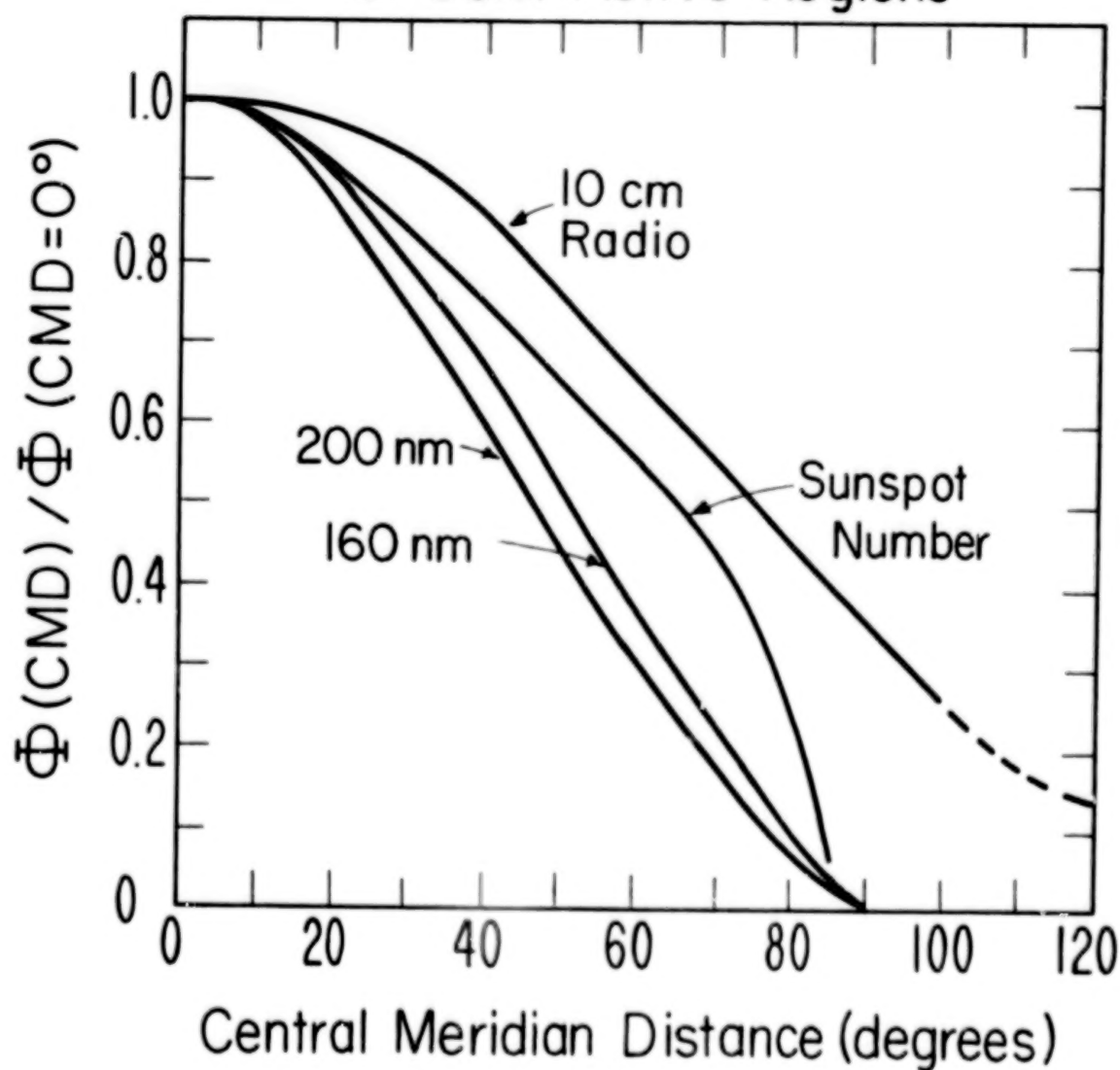


Figure 6

DISCUSSION OF DONNELLY PRESENTATION

FOUKAL: I wasn't sure what you're concluding from the comparison between the irradiance and the UV signal.

DONNELLY: Thank you for that question. Yesterday we were talking about faculae and how much do they contribute to the energy balance; you take a dip of the order of a tenth of a percent in the total solar irradiance in the total solar irradiance, look in the ultraviolet and you get enhancements of the order of 1% below 300 nm. The flux below 300 nm is of the order of 1% of the total solar irradiance. So that means the enhancement at the time of that dip in the total solar irradiance is of the order of .01% of the total solar irradiance. Now if you look at the amplifying effect because of [radiation pattern], the fact that in the UV you're radiating a little larger solid angle than you do in the dip [for] the sunspots you get a multiplying factor of about 3 which says that the UV enhancement going with that depletion in total solar irradiance [from] sunspots can be on the order of 0.03% compared to 0.1% in the total solar irradiance; that's about 30% of the dip that you're looking at in the missing energy and therefore in consideration of faculae, you cannot ignore the ultraviolet; it's an important portion of the energy [balance]. Now we can haggle about these numbers but you're not going to be able to make them negligible. There's a spectral dependence in the facular contribution [which] is important. Does that answer your question?

UNKNOWN: What was the question (laughter and Zirin guffaws)?

FOUKAL: Well, that's certainly an interesting rumination?. I was interested in a result that Hugh [Hudson] first brought out where they subtracted the calculated sunspot contribution in the ACRIM data and they found that the residuals correlated rather nicely with the 10.7 cm flux. That raised the question to us rather those residuals that Hugh was pointing out were due to excess UV emission; we know they correlate well with 10.7 cm, that looked pretty nice on our graph. In fact, I'm surprised that hasn't been followed up more. But our attempt to follow it up was along the line that we looked at the positions on the disk of the Ca K plages which are presumably responsible for the 10.7 cm emission [and was] found to correlate well with the flux; our idea was that if those plages were found to be concentrated near the center of the sun where we know that the faculae have very small contrast, then the contribution of the plages to the total irradiance could only come from their UV component. We know the UV contrast of plages is high near sun center. Whereas if we had found that it was strongly correlated with plages near the edge of the sun, it could have been caused either by the UV component of plage emission or by the fact they are limb brightened in the thermal [emission], namely in the continuum. so we hoped to find a clear distinction there but in fact it turned out to be inconclusive; that some of those residual humps were correlated well with Ca K plages near sun center, some of them were plages near the edges. It didn't look like there was a very clear distinction.

DONNELLY: I think to make the physics simpler, you should take the residuals and correlate them with Don Heath's UV measurements.

FOUKAL: We came to the same conclusion, and Don has sent us the measurements, so we're going to do that.

DONNELLY: The other point I want to make which is very important to this question whether the total solar irradiance measurements are really working well from here on out because the UV enhancement I'm talking about ..., which is why we're interested in whether the black paint on the instruments was working well at UV wavelengths, as we knew that most of what we were seeing was down here.

FOUKAL: I can shed some light on that because we had that concern too. We set up a measurement program at NBS as most of you know. We tested the specularity of the blacks that were used on Nimbus-7 at NBS. That result is published in Applied Optics. The specularity was excellent right down to 1800 Å which is as low as you can go.

DONNELLY: In answer to your earlier question with respect to the 10-cm flux fitting better with the residuals; because of the complexity in the physics of the 10 cm flux you're better off going directly to the UV.

MOORE: I didn't quite understand the point about 13 days [period]. What's going on in the sun?

DONNELLY: You're getting groups of active regions roughly 180° apart and they're just rotating, giving two peaks per rotation; it's important in the UV then that the CMP dependence from these regions be narrow enough that you get valleys when they're at the limb and peaks when they're near the center.

SOFIA: Do you mean facular area versus sunspot area?

DONNELLY: No, that's Ca K.

HUDSON: This is a workshop after all, so you won't mind if we sort of waffle a little bit. We took the integral of this, these two functions of μ and integrated those over μ to get the flux at the sun, the total flux per unit area. We seem to find that the integral of the top one [spots] is 2 and of the bottom one [faculae] is 1/2, very neat, isn't that right? (Yeah.) So, there's a factor of 4; put those together with the coefficients you get a factor of 10, and if you look at the correlation there, and sort of do your best fit about what the actual ratio is, it's on the order of 10 or 20, something like that. Anyway it comes out about right, so ...

UNKNOWN: What is right? 10 or 20 - what?

HUDSON: That, that (laughter). The time-integrated sunspot flux deficit is comparable to the time-integrated net facular re-emission!

DONNELLY: I'm not going to let you get away with not including the UV ...

HUDSON: One more statement! If there's overbalance, of course that explains the association of Maunder Minimum ...

EDDY: Of course ...?

MODELLING SOLAR SPECTRAL IRRADIANCE VARIATIONS
AT ULTRAVIOLET WAVELENGTHS

J. L. Lean

Cooperative Institute for Research in Environmental Sciences (CIRES)
University of Colorado/NOAA, Boulder, CO 80309

W. C. Livingston

Kitt Peak National Observatory, Tucson, AZ 85726

O. R. White

Lazy FW Ranch, Mancos, CO 81328

A. Skumanich

High Altitude Observatory, National Center for Atmospheric Research,
Boulder, CO 80307

ABSTRACT

We examine solar ultraviolet irradiance variations with solar activity by using a three component model of the CaII K chromospheric emission. This model, developed from ground based observations of the location, area and relative intensity of CaII K plage, in conjunction with measurements throughout solar cycle 21 of the full disc CaII K emission, includes the contributions to the ultraviolet flux from both plage and active network emission. Evolution and rotation of the plage regions on the solar disc (as recorded by the World Data Center of the National Oceanic and Atmospheric Administration) produce a 27-day modulation of the UV flux. Over longer time scales, such as the eleven year solar cycle, changes in the active network are an important source of UV flux variability, and are postulated to arise from the remnants of decayed magnetic features on the solar disc, and from the temporal behaviour of ephemeral regions. The model successfully replicates changes in the Lyman alpha flux related to the 27 day rotation of solar plage, outbreaks (or rounds) of activity over periods of a year or more, and the growth and accumulation of active regions over the eleven year solar activity cycle. At the longer ultraviolet wavelengths, from 200 to 300 nm, the rotation modulation of the UV flux, observed by the Solar Backscatter Ultraviolet experiment on the Nimbus 7 satellite, is well described by the model. Estimates of the magnitude of the solar cycle variability of the UV emission between 200 and 300 nm are presented but cannot currently be verified by available observations since the uncertainties pertaining to state-of-the-art UV flux measurements are larger than the calculated variability. If the cycle variability of the solar flux at wavelengths between 200 and 300 nm is indeed of the magnitude predicted by the model, then this emission must be considered as a source of long term variability in the total solar irradiance.

INTRODUCTION

This paper describes a three component (3C) model of solar UV irradiance variability, derived from ground based observations of solar active regions seen in Ca K emission at 393 nm. In the model, it is assumed that those areas on the solar disc enhanced in Ca K emission are also enhanced in UV emission. There exists an extensive data base characterizing the temporal variation of the Ca K solar emission. Observations of the Ca K emission from the full solar disc (sun as a star) have been made by O. R. White and W. C. Livingston at Kitt Peak (ref. 1), over both the short term (27 day) and longer (11 year) time scales of solar activity, during the current solar cycle. As well, spatially resolved observations of the location, area and relative brightness of the most intense, compact active areas enhanced in Ca K emission (called plage) have been recorded, almost daily, for the past few decades by the WDC/NOAA. It is possible to estimate the magnitude of the UV flux variability from this data base, providing the contrast for active region emission compared to that from the quiet sun, and the center-to-limb variation of the solar radiance at the UV wavelengths are known.

Figure 1 illustrates the similarities between the solar disc viewed at Lyman alpha, at 160 nm and at Ca K. The Lyman alpha and 160 nm photographs were taken by the Transition Region Camera (TRC) described by Bonnet et al. (ref. 2), and have a spatial resolution of about 1". It is evident that plage areas seen in Ca K are also seen as regions enhanced in emission at both Lyman alpha and at 160 nm. Figure 2 further illustrates the similarities between the Lyman alpha emission and the Ca K emission, and also some of the differences. Both photos in Figure 2 have a spatial resolution of about 2".5. The Lyman alpha photo is from Prinz (ref. 3) and the Ca K spectroheliogram is from Mt Wilson: they were taken on July 10, 1972, a period of moderate solar activity during the declining phase of the last solar cycle, #20. Again, those regions brightest in Ca K emission are also brightest in Lyman alpha emission. But note that regions near the limb are more easily observed in Lyman alpha than in Ca K. This is because the Lyman alpha radiance has essentially no center-to-limb dependence, while the Ca K emission at the limb is about half that from the disc center. As well, the contrast for plage emission compared to that from the quiet sun is about 6 for Lyman alpha whereas it is about 2.5 for Ca K. The Ca K plage map in Figure 2 shows the plage regions recorded by the WDC/NOAA for the same day. Only the brightest, most compact, active areas were identified as plage. It is quite evident that a significant fraction of the solar disc was covered by areas of enhanced UV emission that were not recorded by the WDC/NOAA; this is particularly obvious in the Lyman-alpha photograph, and is demonstrated quantitatively in the intensity histogram in Figure 3. By subtracting the quiet sun component (fitted by a Gaussian distribution) from the full distribution, it was estimated that about 25% of the disc, on July 10, 1972, was covered with active network.

It is generally well recognized that the WDC records do not account for all of the active area on the disc. This follows from the work of Sheeley (ref. 4), and Harvey and Martin (ref. 5), who made detailed studies of both Ca K spectroheliograms and magnetograms. To model properly the temporal behaviour of the UV flux it is necessary to know the true fraction of the

solar disc covered by active area at different times throughout the solar cycle. We can obtain a quantitative estimate of this active area fraction by using the WDC/NOAA records in conjunction with the measurements of the Ca K flux from the full solar disc. If we calculate the Ca K flux from the quiet sun plus the WDC plage areas and subtract this from the measured full disc flux, the difference can be attributed to the Ca K emission from active areas other than those recorded by the WDC, a component which we call "active-network" (see Figure 3).

VARIABILITY OF THE CaII K EMISSION WITH SOLAR ACTIVITY

Figure 4 shows the behaviour of the Ca K1.0 Å index from both the center of the solar disc and from the full solar disc, throughout the current solar cycle, as measured at Kitt Peak by White and Livingston (ref. 1). At the center of the disc, in selected quiet regions, the Ca K emission remains constant throughout the cycle, implying the constancy of the quiet sun emission (ref. 6). In contrast, the Ca K emission from the full solar disc increases from solar minimum (1976) to solar maximum (1979). At least part of the Ca K flux variability (on both short and long times scales) evident in this figure can be attributed to the evolution and rotation of the plage areas. Figure 5 illustrates how solar rotation generates changes in the projected plage area, when viewed from earth, for a few active rotations near the maximum of the current solar cycle. We can thus expect the Ca K (and also the UV) flux from the full solar disc to be modulated by solar rotation. Such rotational modulation has indeed been observed in full disc solar observations, and is illustrated in Figure 6, for both the Ca K and the Lyman alpha flux. The Ca K data were taken by W. C. Livingston at Tucson, and the Lyman alpha data by G. J. Rottman on the LASP/SME satellite (ref. 7). Using the plage area data from the WDC/NOAA, we can calculate the expected magnitude of the solar flux modulation due to solar rotation, for both the Ca K and Lyman alpha emission, if we know the quiet sun emission from the center of the disc and from the full solar disc, the center-to-limb variation, and the contrast for plage emission relative to that from the quiet sun (ref. 6).

For the Ca K line, the center-to-limb variation has been measured by White and Suemoto (ref. 8). Data for the Ca K plage contrasts are shown in Figure 7, as a function of the observed relative brightness listed in the WDC records. The contrast for "observer intensity" $I^{obs} = 3$ is from the measurements of Lemaire et al. (ref. 9), and the relative variation of plage contrast with observer intensity was provided by R. Hedeman.* Calculated plage related variations are compared with full disc Ca K observations in Figure 8. It is evident that the relative changes with solar rotation are well reproduced but the absolute magnitude of the calculated plage emission is significantly less than that measured from the full solar disc. Of course, by increasing the plage contrast and/or the area by a factor of about 2 (see ref. 6), it is possible to increase the calculated plage flux, but then the observed rotation modulation would be overestimated. So the good fit of the rotation modulation suggests that the plage contribution to the full disc Ca K emission can be successfully reproduced using the WDC plage area together

* Private communication, 1982.

with independently measured plage contrasts. If the Ca K emission from the quiet sun (undisturbed chromosphere) remains constant throughout the solar cycle, as evidenced by the center disc observations of White and Livingston (ref. 1 and Figure 4a), then it is necessary to postulate a source of enhanced Ca K emission, additional to plage, in order to explain the full disc Ca K flux variability measured over the solar cycle (Figure 4b).

The work of Harvey and Martin (ref. 5) suggests that ephemeral regions (ER), which are small bi-polar regions not large enough to be identified as plage, may be an important source of enhanced Ca K flux. We can estimate their contribution to the full disc Ca K emission as follows. Figure 9 (from ref. 5) shows the growth of a typical ER, observed with about 2".5 resolution. The top graph shows the total magnetic flux from the ER and the bottom graph shows the area, typically equal to about $3 \times 10^8 \text{ km}^2$, or 0.01% of the solar hemisphere. If we divide the total flux by the area, at various times during the lifetime of the ER, we can estimate the magnetic field to be around 55G. The Ca K emission from an active region increases linearly with magnetic field. According to Skumanich, Smythe and Frazier (ref. 10), the magnetic field in the Ca K network, which has a contrast of about 1.27, is 26G, and a magnetic field of 55G corresponds to a contrast of 1.42. Note that this value is much less than the plage contrast of 2.3 (see Figure 9). We can also estimate, from the results of Harvey et al. (ref. 11) the fraction of the solar disc covered by ERs at different times throughout the solar cycle. In 1970 there were, on average, 373 ERs present on the disc, decreasing to 179 in 1973 and to 88 in 1975. With a typical area of 0.01% of the solar hemisphere, about 3.7% of the hemisphere was covered with ERs in 1970, decreasing to 1.8% in 1973 and to 0.9% in 1975. Thus the average number of ERs appears to vary in phase with the solar cycle, allowing us to parameterize the ER fractional hemispheric area in terms of the total plage area on the disc, smoothed over three rotations, and calibrated by the 1970, 1973 and 1975 ER counts. This is consistent with the identification of the ERs as simply the small scale end of a broad spectrum of active regions. Using this parameterization, and a contrast of 1.42, we can estimate the ER contribution to the full disc Ca K flux at different times throughout the current solar cycle.

In Figure 10, the calculated Ca K emission from both plage and ERs is shown. The combined flux from both plage and ER still underestimates the observed full disc flux near solar maximum; for this reason we have assumed additional enhanced Ca K emission from the Ca K network (with contrast 1.27) which is formed, for the most part, around the borders of the supergranule cells. On the same figure, the combined emission from both plage, ER and network is compared with the full disc measurements made at Kitt Peak. This figure demonstrates that, having obtained reasonably good estimates of the plage emission (as verified by the agreement between the calculated and observed magnitude of the rotational modulation, see Figure 7), it is not possible to reproduce the solar cycle variability of the full disc Ca K flux measured at Kitt Peak without postulating the existence of additional sources of enhanced Ca K emission. In summary, by using the full disc Ca K flux data measured at both Tucson and Kitt Peak, it has been possible to first calibrate the WDC plage areas and then to estimate how the fractional area of this additional source, which we have called active network (ER plus additional

network area), varies throughout the solar cycle.

Our estimate of the magnitude of the fractional active network area present on the solar disc at different times throughout the solar cycle is very sensitive to our calculation of the Ca K rotation modulation. Figure 8 demonstrates that we have reproduced the daily rotational modulation observed during 1982 by W. C. Livingston at Tucson. However, it is evident in Figure 10 that the full disc Ca K observations made by White and Livingston (ref. 1) at Kitt Peak are not fit particularly well by the calculated rotation modulation. Differences between the Tucson daily Ca K data (Figure 8) and the Kitt Peak solar cycle measurements (Figure 10) are being investigated. Meanwhile, it is important to recognize that increasing the calculated rotation modulation, to better fit the Kitt Peak data in Figure 10, would lead to a decrease in our estimate of the active network fractional area, which we use in the following sections to examine solar variability at other wavelengths.

LYMAN ALPHA FLUX VARIABILITY

Assuming that active areas (both plage and active network) enhanced in Ca K emission are also enhanced in emission at other UV wavelengths, we can now investigate the solar flux variability at other UV wavelengths, for example at Lyman alpha (ref. 12). We can estimate the plage and network contrast at Lyman alpha from Prinz's (ref. 3) intensity distribution of Lyman alpha radiances (Figure 3); there the plage-quiet sun contrast is about 6 and the network-quiet sun contrast is about 2 (see ref. 12 for a more detailed discussion). Figure 11 compares the calculated Lyman alpha flux variation throughout 1979 with data from Hinteregger's AE-E satellite experiment (ref. 13), which measured the Lyman alpha flux from the full solar disc. The rotation modulation is well reproduced, in both magnitude and period, and the 3C model estimates the rotation modulation better than other models based on either the 10.7cm flux or the sunspot number. This is discussed in more detail by Donnelly et al. in another paper in this volume (ref. 14). Figure 12 illustrates that over the longer time scale of the solar cycle, when the active network emission becomes as important as the plage emission, the model also reproduces the observed changes in the Lyman alpha emission, both from the AE-E satellite, and the LASP rocket measurements. This is discussed further by Lean and Skumanich (ref. 12). We note that Vidal-Madjar's (ref. 15) Lyman alpha model, derived from the OSO-5 Lyman alpha observations, is also a three component model: Vidal-Madjar found that the observed Lyman alpha flux variation was better correlated with a three component approach, than with a two component model based only on daily solar activity indices. The models of Cook et al. (ref. 16) and Bossy and Nicolet (ref. 17) are both two component models. The comparisons, in Figures 11 and 12, of the calculated Lyman alpha flux variability with the available full disc Lyman alpha observations illustrate that the 3C model developed from the Ca K observations can be extended to model the variability of other UV emissions from the sun.

ESTIMATING SOLAR FLUX VARIATIONS: 200 - 300 NM

Of special importance for interpreting the observed changes in the spectrally integrated (total) solar irradiance is the variability in UV wave-

lengths longer than 200 nm. The solar flux between 200 and 300 nm represents about 1% of the total solar irradiance; solar flux variability at these wavelengths is generally assumed to be negligible in terms of its contribution to changes in the total solar irradiance. Recent observations by the Solar Backscatter Ultraviolet (SBUV) experiment on the Nimbus 7 satellite (ref. 18) provide evidence that the solar flux at wavelengths at least as long as 260 nm exhibit a variation associated with solar rotation (ref. 19); we can expect an even larger variation over the 11 year solar cycle. The magnitude of the solar cycle variability at these wavelengths is not well known, because measurements of the absolute solar UV irradiances are difficult and have large uncertainties, typically greater than 15% - 25%; however, we can use the three component model to estimate the probable magnitude of this variability (ref. 20).

An example of the rotation modulation of the solar flux at 205 nm, detected by SBUV during 1979, is shown in Figure 13. The projected plage area is also shown and demonstrates the high degree of correlation between the two. The data presented sample a period near solar maximum: the rotation modulation is smaller at times near solar minimum since there are fewer plages on the disc. The rotation modulation also decreases with wavelength: the bottom graph in Figure 13 shows the ratio of the maximum to minimum flux for three distinct solar rotations labelled A, B and C in the graph above. At 200 nm there is about a 3% modulation which drops sharply to 1% at wavelengths longer than 207.5 nm, the aluminium I ionization edge. A plateau of constant modulation extends up to about 251 nm, the onset of Mg I ionization, with the variability decreasing at longer wavelengths. The Mg II lines, which are of chromospheric origin, can be seen to be more variable than the surrounding continuum emissions, which originate in the photosphere. Assuming that the rotation variability at these longer UV wavelengths is, like that at the shorter wavelengths, associated with changes in the plage area on the solar disc, we can use the short term SBUV observations to obtain estimates of the plage contrast (i.e. that factor by which the plage emission must be enhanced above the quiet sun emission in order to explain the observed rotation modulation). The plage contrasts calculated in this way are shown in Figure 14. At the shorter wavelengths, less than 210 nm, there is good agreement with the measurements reported by Cook et al. (ref. 16). At wavelengths longer than the Al I edge, Cook et al. set the plage contrast to unity. However, if the plage emission at these wavelengths was not enhanced above that from the surrounding quiet sun, rotation modulation would not be detected, contrary to the SBUV observations.

In addition to plage contrasts, we also need to estimate the network contrasts. Figure 15 shows the calculations by Herse (ref. 21) of the contrast of bright structures on the disc, at wavelengths from 200 nm to 100 μ m. This empirical facular model was derived by Herse from a statistical study of facular grains, observed at wavelengths 200 nm, 210 nm, 310 nm and 460 nm with high spatial resolution (0".5) in regions of the solar disc covered by predominantly non-plage features. Herse's observations indicated that the excess emission from network features was about half that from the brighter plage areas. In Figure 15 the mean contrasts (averaged over position on the solar disc) for the mean facular grains, degraded to a resolution of 2".5 (by dividing by a factor of 4, as recommended by Herse) can be seen to be in good

agreement with the network excess emission (contrast -1) determined as half that from plages, where the plage contrasts are those in Figure 14 (i.e. deduced from the SBUV short term observations). Other estimates of facular contrast, averaged over all wavelengths, reported by Foukal (ref. 22) and Hoyt and Eddy (ref. 23), are provided in Figure 15 for comparison.

Having estimated the active region contrasts (both plage and network) at these longer UV wavelengths, we can estimate the flux variability over the solar cycle associated with the increase in the active area fraction, as determined from the analysis of the Ca K data. These estimates are shown in Figure 16. The minimum expected variability (dotted line) is that due to the increase in plage regions alone (from 0 to 5% of the disc, as documented by the WDC/NOAA). The cycle variability due to twice the plage area is also shown (dash-dot line). The solid line is the variability expected from an increase of 0 to 5% of the disc fraction covered by plage plus an increase of 0 to 40% of the hemispheric fraction covered by active network. The calculated variability is 25% at 200 nm, dropping to 10% at wavelengths from 210 to 250 nm and to only a few percent at 300 nm. The radiation at 300 nm originates in approximately the same region of the solar atmosphere as does the visible continuum radiation at 500 nm (ref 24). Ground based observations indicate that the variability at 500 nm is no more than a few percent (ref. 16) which is quite consistent with these calculations. In Figure 17 the calculated variation in the solar flux from 200 to 205 nm, for the period around the maximum of the current solar cycle, is compared with available observations. The rocket data are from LASP (refs. 25,26) and Mentall et al. (ref. 27). H refers to the SBUV measurement at the time of launch (ref. 19). The error bars indicate limits of $\pm 10\%$ which is an optimistic estimate of the accuracy of these experiments. This figure demonstrates that the measurement uncertainties are greater than the calculated variability and therefore the available observations can neither confirm nor refute the model calculations.

TOTAL SOLAR IRRADIANCE VARIABILITY

The change, from solar minimum to solar maximum, in the total energy radiated from the sun at wavelengths between 200 and 300 nm is calculated by the 3C model to be of the order of 0.5 to 0.7 Watt/m² (14.7 Watt/m² in 1976; 15.4 Watt/m² during December 1979). This represents about 1/20th percent of the total solar irradiance. To put this in the perspective of the total solar irradiance (S) variations, Figure 18 compares the calculated variability over the wavelength interval 200 - 300 nm with the variability due to sunspot blocking, as calculated by Hoyt and Eddy (ref. 23). The important point is that, while the UV variability may not contribute significantly to the short term changes in the total solar irradiance, the active network term means that, over longer time scales, in order to properly interpret changes in S it may be necessary to understand the UV variations. Note that the cavity radiometers used to measure the changes in S (refs. 28, 29) are sensitive to radiation at wavelengths longer than about 180 nm, so they are capable of detecting any changes in the UV emission at wavelengths from 200 to 300 nm. Even if the magnitude of the UV variability is half that suggested by these calculations, it still must be considered as a source of variability in S. It is not yet known how the total solar irradiance varies over the solar cycle -

whether it is out of phase with the sunspot number, as suggested by Hoyt and Eddy's (ref. 23) calculations, whether it is in phase, as suggested by Reid and Gage's (ref. 30) analysis of the variations in the height of the tropical tropopause, or whether there is no average change; this is a very fundamental gap in our understanding of the causes of the total solar irradiance behaviour. Figure 19 illustrates this current confusion. The model of Hoyt and Eddy (ref. 23) considers primarily the effects of sunspot blocking on the total solar irradiance whereas Schatten et al. (ref. 31) include a greater contribution from the faculae (average effect at all wavelengths). They determined the magnitude of the faculae contribution by fitting a model to the daily ACRIM data (ref. 29) and then extrapolating the fitted parameters to longer time scales (ie the solar cycle). This is, in effect, a two component approach to faculae emission. Recall, however, that, at least at the UV wavelengths, because of the three components, the daily variations due to plage regions underestimate the variations over the solar cycle.

A potential problem with extrapolating total solar irradiance models derived from daily observations over time scale of many solar cycles, is that the sunspot areas and the facular areas may not necessarily vary proportionately. Figure 20 shows, from the work of Brown and Evans (ref. 32), that the 11 year cycles in the sunspot areas are modulated somewhat differently than the 11 year cycles in the facular areas. Assuming that the changes in the UV are better represented by the faculae areas than by sunspot areas, we see that the relative effects of the UV flux variability and of sunspot blocking may well be different during different solar cycles. Although Figure 21 (ref. 20) is quite speculative, it provides an attempt to predict quantitative changes in the total solar irradiance due to both enhanced UV emission from active regions and sunspot blocking; these calculations are compared with a model based on simple sunspot blocking and minor facular emission (ref. 23).

CONCLUSIONS AND FUTURE WORK

The 3C model calculations described above represent an attempt to understand solar variability at different ultraviolet wavelengths. As emphasized by Foukal (ref. 22), to properly understand the causes of total solar irradiance variability requires an understanding of spectral irradiance variability. Our present knowledge of solar ultraviolet irradiance variability over the solar cycle, especially at wavelengths between 200 and 300 nm, is inadequate for understanding variations in the total solar irradiance. The 3C model calculations suggest that active area emission other than that from plage areas is an important source of UV flux variability and that this variability may need to be incorporated in models of S if the total solar irradiance variability is to be properly interpreted.

Uncertainties in the Ca K plage contrasts and areas generate uncertainties in our calculation of the rotation modulation of the Ca K flux, and hence in the deduced fractional active network area. Our estimates of the UV flux variability which use Ca K active network fractional area data as input reflect these uncertainties. Little is known about the average (in a statistical sense) contrasts for plage and network emission at either Ca K or the UV wavelengths. Intensity distributions of the entire solar disc at Ca K

and at different UV wavelengths are needed to provide these data. Quantitative information about the spatial correlation between the Ca K and UV active areas is essential for improving the 3C model.

The lack of statistically averaged data characterizing surface inhomogeneities on the solar disc when observed at Ca K is an unnecessary source of uncertainty in our model calculations. Although Ca K spectroheliograms are made routinely, little effort has been directed towards defining the intensity distribution function for the whole solar disc (in the same way that Prinz, ref. 3, characterized the Lyman alpha emission). Analyses of Ca K spectroheliograms, similar to that shown in Figure 3 for Lyman alpha, would yield valuable information about the average Ca K plage contrasts and areas, as well as estimates of the fractional network area and contrast, at different times throughout the solar cycle. Such data would provide an important check on the active area parameters used in the model calculations of both the Ca K and the UV flux variability.

Continued observation and interpretation of the Ca K emission from the full solar disc, during the descending phase of the current solar cycle, is essential for improving our understanding of the evolution, with solar activity, of magnetically active features on the solar disc. Although during the rising phase of the solar cycle, the Ca K flux was well correlated with the plage index (a measure of projected plage area weighted by a relative brightness estimate), Keil and Worden (ref. 33) have recently reported that during 1980 and 1981 the Ca K emission did not decline as rapidly as the plage index. They offer the explanation that, although the amount of plage is decreasing, the field associated with the plage is not dissipated; rather it is rearranged into the network where it can still contribute to an enhanced calcium emission but not show up as plage. Alternately, the plage may simply become too diffuse to be included in the somewhat subjective plage index. Both of these scenarios are consistent with our findings that, in order to explain the observed full disc Ca K flux variations, it is necessary to invoke a source of Ca K emission additional to the measured plage areas. However, while our parameterization of this third component (the active network term in our model) as a linear function of the total plage area on the solar disc, smoothed over seven rotations (see ref. 6 for a more complete discussion), appears quite satisfactory for the ascending phase of the solar cycle, a more detailed quantitative prescription of magnetic flux breakup and loss by reconnection and submergence is probably required to better model the Ca K flux variations during the descending phase of the solar cycle.

In order to utilize the Greenwich faculae record, which extends back to 1905, the correspondence between total plage area on the disc, and the white light faculae seen on the limb must be quantitatively established. This will allow a more reliable calculation of the UV fluxes during past times.

During the next few years data from the Nimbus 7, SMM, and SNE satellites should provide more simultaneous, continuous and reliable data for both the total solar irradiance and the spectral irradiance variability than have yet been available. Such data will enable improvements to be made in models such as the three-component model described in this paper, and allow solar variability models to better reconstruct the past history of the solar irradiance.

REFERENCES

1. White, O. R. and W. C. Livingston, Solar luminosity variations III, Calcium K variation from solar minimum to maximum in cycle 21, *Astrophys. J.*, 249, 798, 1981.
2. Bonnet, R. M., M. Bruner, L. W. Acton, W. A. Brown, M. Decaudin and B. Foing, Rocket photographs of fine structure and wave patterns in the solar temperature minimum, *Astron. Astrophys.*, 111, 125, 1982.
3. Prinz, D. K., The spatial distribution of Lyman alpha on the sun, *Astrophys. J.*, 187, 369, 1974.
4. Sheeley, N. R., The average profile of the solar K line during the sunspot cycle, *Astrophys. J.*, 147, 1106, 1967.
5. Harvey, K. L. and Sara, F. Martin, Ephemeral active regions, *Solar Physics*, 32, 389, 1973.
6. Skumanich, A., Lean, J. L., O. R. White and W. C. Livingston, The sun as a star: Three component analysis of chromospheric variability in the Calcium K line, Submitted to *Astrophys. J.*, 1983.
7. Rottman, G. J., O. R. White and W. C. Livingston, Correlation of solar ultraviolet irradiance with the Kitt Peak CaII K index, *EOS*, 64, 280, 1983.
8. White, O. R. and Z. Suemoto, A measurement of the solar H and K profiles, *Solar Phys.*, 3, 523, 1967.
9. Lemaire, P., P. Gouttebroze, J. C. Vial and G. E. Artzner, Physical properties of the solar chromosphere deduced from optically thick lines: I. Observations, data reduction and modelling of an average plage, *Astron. Astrophys.* 103, 160, 1979.
10. Skumanich, A., C. Smythe and E. N. Frazier, On the statistical description of inhomogeneities in the quiet solar atmosphere I. Linear regression analysis and absolute calibration of multichannel observations of the Ca^+ emission network, *Astrophys. J.*, 200, 747, 1975.
11. Harvey, K. L., J. W. Harvey and S. F. Martin, Ephemeral active regions in 1970 and 1973, *Solar Physics*, 40, 87, 1975.
12. Lean, J. L. and A. Skumanich, Variability of the Lyman alpha flux with solar activity, *J. Geophys. Res.*, 88, 5751, 1983.
13. Hinteregger, H. E., K. Fukui and B. R. Gilson, Observational, reference and model data on solar EUV, from measurements on AE-E, *Geophys. Res. Lett.*, 8, 1147, 1981.

14. Donnelly, Richard F., Donald F. Heath, Judith L. Lean and Gary J. Rottman, Temporal variations of solar UV spectral irradiance caused by solar rotation and active region evolution, Workshop on Solar Irradiance Variations on Active Region Time Scales, NASA CP- , 1983. (Paper of this compilation.)
15. Vidal-Madjar, A., the solar spectrum of Lyman alpha 1216 A, in The Solar Output and its Variation, O. R. White (ed.), Colorado Associated University Press, Boulder, CO, p 213, 1977.
16. Cook, J. W., G. E. Brueckner and M. E. Van Hoosier, Variability of the solar flux in the far ultraviolet 1175 - 2100 A, J. Geophys. Res., 85, 2257, 1980.
17. Bossy, L. and M. Nicolet, On the variability of Lyman alpha with solar activity, Planet. Space Sci., 27, 907, 1981.
18. Heath, D. F., R. F. Donnelly, S. D. Bouwer and G. Merrill, Nimbus 7 SBUV observations of solar UV spectral irradiance variations caused by solar rotation and active region evolution, NOAA Technical Memorandum, ERL/ARL, 1983.
19. Heath, D. F., A review of observational evidence for short and long term ultraviolet flux variability of the sun, Sun and Climate, International Conference, Toulouse, France, 30 Sept - 3 Oct, 1980.
20. Lean, J. L., Estimating the variability of the solar flux between 200 and 300 nm, J. Geophys. Res., in press, 1983.
21. Herse, M., High resolution photographs of the sun near 200 nm, Solar Phys., 63, 35, 1979.
22. Foukal, P., Sunspots and changes in the global output of the sun, Workshop on sunspots, Sacramento Peak Observatory, July 14-17, 1981.
23. Hoyt, D.V. and J. A. Eddy, An Atlas of variations in the solar constant caused by sunspot blocking and facular emissions from 1874 to 1981, NCAR Technical Note 194+STR, HAO, NCAR, Boulder, CO, May, 1982.
24. Vernazza, J. E., E. H. Avrett and R. Loeser, Structure of the solar chromosphere. III. The underlying photosphere and temperature minimum region, Astrophys. J. Suppl. Series, 30, 1, 1976.
25. Mount, G. H. and G. J. Rottman, The solar spectral irradiance 1200 - 3184 A near solar maximum: July 15, 1980, J. Geophys. Res., 86, 9193, 1981.
26. Mount, G. H. and G. J. Rottman, The solar absolute spectral irradiance 1150 - 3173 A: 17th May, 1982, J. Geophys. Res., 88, 5403, 1983.
27. Mentall, J. E., J. E. Frederick and J. R. Herman, The solar irradiance from 200 to 300 nm, J. Geophys. Res., 86, 9881, 1981.

28. Willson, R. C., S. Gulkis, M. Janssen, H. S. Hudson and G. Chapman, Observations of solar irradiance variability, *Science*, 211, 700, 1981.
29. Hickey, J. R., L. L. Stowe, H. Jacobowitz, P. Pellegrino, R. H. Maschhoff, F. House and T. H. Vonder Haar, Initial solar irradiance determinations from Nimbus 7 cavity radiometer measurements, *Science*, 208, 281, 1980.
30. Reid, G. C. and K. S. Gage, On the annual variation in height of the tropical tropopause, *J. Atmospheric Sciences*, 38, 9, 1981.
31. Schatten, K. H., N. Miller, S. Sofia and L. Oster, Solar irradiance modulation by active regions from 1969 through 1980, *Geophys. Res. Lett.*, 9, 49, 1982.
32. Brown, G. M. and D. R. Evans, The use of solar faculae in studies of the sunspot cycle, *Solar Phys.*, 66, 233, 1980.
33. Keil, Steven L. and Simon P. Worden, Variations in the solar Calcium K-line 1976 - 1982, Submitted to *Astrophys. J.*, 1983.

LIST OF FIGURES

1. Photographs of the sun on 23 September 1980 at a) Lyman alpha (ref. 2), b) CaII K and c) 160 nm in the UV continuum (ref. 2). The Lyman alpha and 160 nm data have a spatial resolution of about 1" while that of the Ca K data is 2".5.
2. Photographs of the sun on 10 July 1972 at a) Lyman alpha, 121.57 nm (ref. 3) and b) CaII K, 393.3 nm (R. Howard, private communication). The CaII plage areas recorded by the WDC/NOAA are identified in c). The spatial resolution of both photographs is about 2".5 X 2".5.
3. Intensity distribution for the Lyman alpha emission from the quiet sun, active network and plage regions on 10 July, 1972, from the Lyman alpha spectroheliogram in Figure 2a (ref. 2).
4. Observation of the K1.0 index a) at the center of the disc in 1' x 3' quiet regions and b) for the entire disc (flux) for solar cycle 21 (ref. 1). The horizontal line in (a) indicates the mean and in (b) the calculated quiet sun flux value (see ref. 6)
5. Variation in the projected plage area with solar rotation near the peak of solar cycle 21, observed in CaII K emission.
6. Comparison of rotational modulation of the full disc Lyman alpha flux measured by the SME satellite, with the CaII K1.0 index measured at Tucson, for the period 13 October 1981 to 16 September 1982 (ref. 7).
7. The relation between plage contrast (compared to quiet sun) and the WDC/NOAA observer brightness. The contrast at observer brightness 3 (open circle) was measured by Lemaire et al. (ref. 9) and the relative variation (solid line) is from R. Hedeman (private communication, 1982).
8. Comparison of the full disc K1.0 rotational modulation measured at Tucson (heavy line) and at Kitt Peak (dots) with the calculated plage emission (fine line) for the period 17th September, 1981 to 11th August, 1982.
9. Growth of a typical ephemeral region (at 2".5) showing a) total magnetic flux and b) area (open circles) and major axis (crosses) from Harvey and Martin (ref. 5). An area of $3 \times 10^8 \text{ km}^2$ (0.01% of the solar hemisphere) and magnetic field of 55 Gauss were assumed as average values.
10. Model calculations of the quiet sun, plage and ephemeral region emission compared to the full disc observations (filled circles) of the K1.0 index made at Kitt Peak (ref. 1). Note that the data and the calculations refer to, on the whole, monthly sample points.

11. The rotation modulation (27 day variability) of solar Lyman alpha flux during 1979. The AE-E data (ref. 13) are compared with calculations from a) this model, b) Cook et al.(ref. 16), c) Bossey and Nicolet (ref. 17) and d) Vidal-Madjar (ref. 15).

12. Solar Lyman alpha irradiance variability for the ascending phase of solar cycle 21 as a) Observed by AE-E (adjusted, following ref. 12) and calculated by b) this model, c) Cook et al.(ref. 16), d) Bossey and Nicolet (ref. 17), and e) Vidal-Madjar (ref. 15). The dashed lines are the average, calculated irradiances for 1976 and 1979 (see ref. 12).

13. Comparison of the temporal variability of a) the solar flux at 205 nm, during 1979, observed by the SBUV experiment on the Nimbus 7 satellite by Heath et al.(ref. 18) and b) the projected CaII K plage area for the same time. In c) is shown the magnitude of the rotation modulation of the solar flux observed by SBUV at wavelengths between 180 and 300 nm, for the three strong rotations labelled A,B and C in b).

14. Plage contrast from 180 to 300 nm, derived from the SBUV observations and the CaII K plage data shown in Figure 13 b) and c), and explained more fully in ref 20. The contrast data of Cook et al. (ref. 16) are included for comparison at wavelengths shorter than 210 nm.

15. Data for the excess emission from the network at wavelengths from 200 nm to 100 μ m. The calculations by Herse (ref. 21) at disc center with 0".5 resolution (dashed line), and averaged over the disc with 2".5 resolution (dotted line) are compared with values deduced from Figure 14 (solid line, see text). The measurement by Skumanich et al. (ref. 10) at disc center with 2".5 resolution is indicated by the cross, and the shaded values are the faculae contrasts averaged over all wavelengths adopted by Foukal (ref. 22) and Hoyt and Eddy (ref. 23).

16. The cycle variability of the solar ultraviolet flux from 180 to 300 nm, calculated by the three-component model. Estimates of the variability corresponding to the plage areas alone, and to twice the plage areas, are included for comparison.

17. Comparison of the modelled flux averaged over the wavelength interval 200-205 nm (solid line) with the SBUV observations (dots) and available rocket measurements (letters) from July 1978 to June 1982. The letters H, L and M refer to, respectively, Heath (ref. 19), Mount and Rottman (ref. 26) and Mentall et al. (ref. 27). The error bars represent $\pm 10\%$.

18. a) Contribution of the calculated solar flux variability at wavelengths between 200 and 300 nm to changes in the total solar irradiance, compared with the sunspot blocking calculated by Hoyt and Eddy (ref. 23) from 1979 to 1981.

b) Total solar irradiance variability during 1979 - 1981 calculated as the sum of the enhanced UV emission and the sunspot related deficit, shown in (a). Note the long term downward trend apparent in the calculated total irradiance throughout 1979 to 1981.

19. Comparison of the total solar irradiance near solar minimum, and near solar maximum, calculated by the models of a) Hoyt and Eddy (ref. 23) and b) Schatten et al. (ref. 31).

20. a) Model calculations by Hoyt and Eddy (ref. 23) of the total solar irradiance variations due primarily to sunspot blocking for the period 1870 to 1980, compared with

b) the temporal variations in the sunspot area and faculae area reported by Brown and Evans (ref. 32), for the same period.

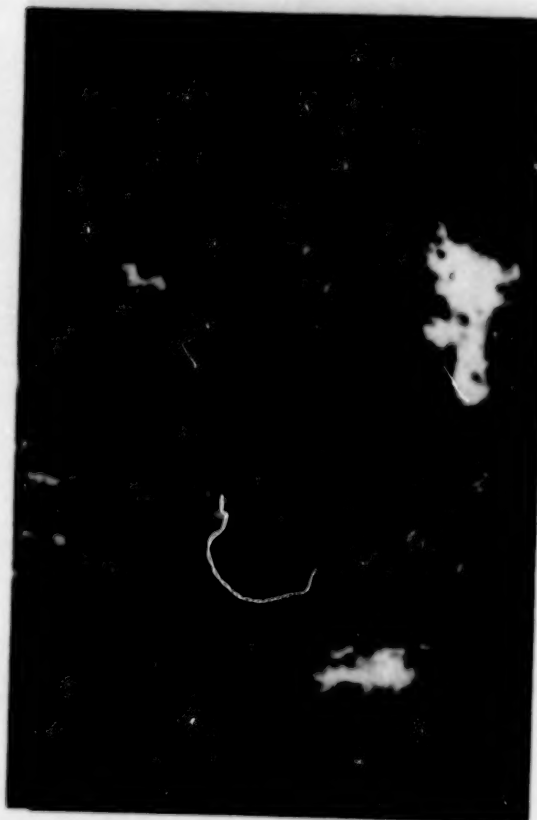
21. Calculated relative changes from 1905 to 1975 in a) the UV (200 to 300 nm) and sunspot blocking, together with b) the resulting prediction for the total irradiance variations, compared with the (predominantly sunspot blocking) model of Hoyt and Eddy (ref. 23).

Solar Disc: 23 Sept 80

a) Lyman Alpha



b) Calcium K
(SPO)



c) 160 nm

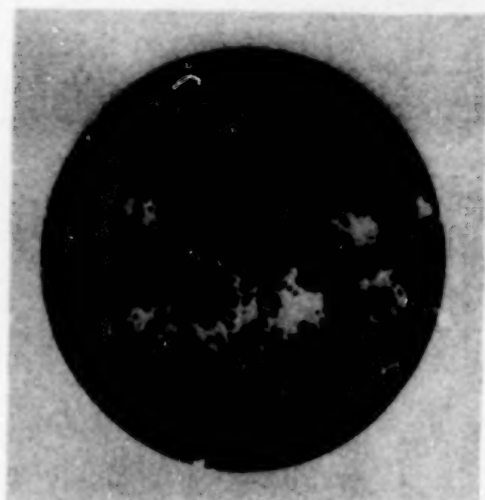


268

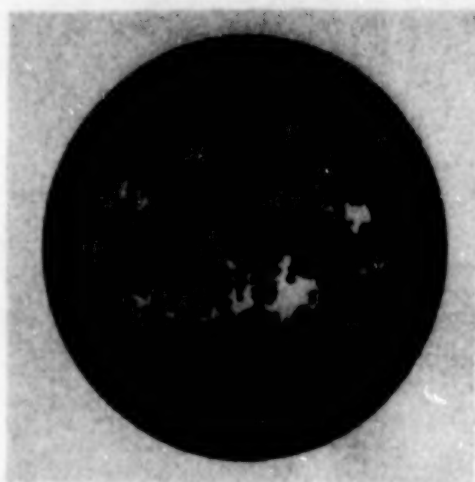
Figure 1

268

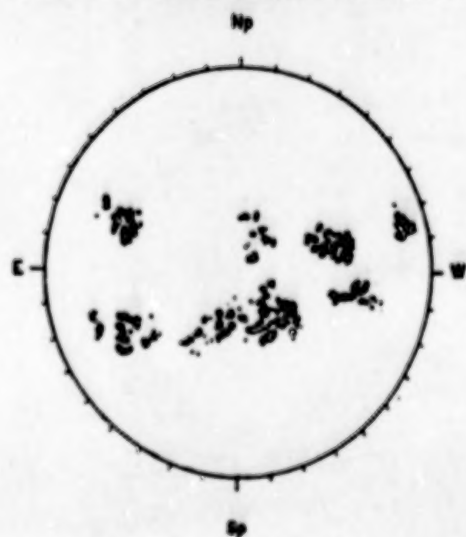
SOLAR DISC: 10 JULY 1972



a) Lyman α



b) Ca II K



c) Ca II K Plage Map

Figure 2

269

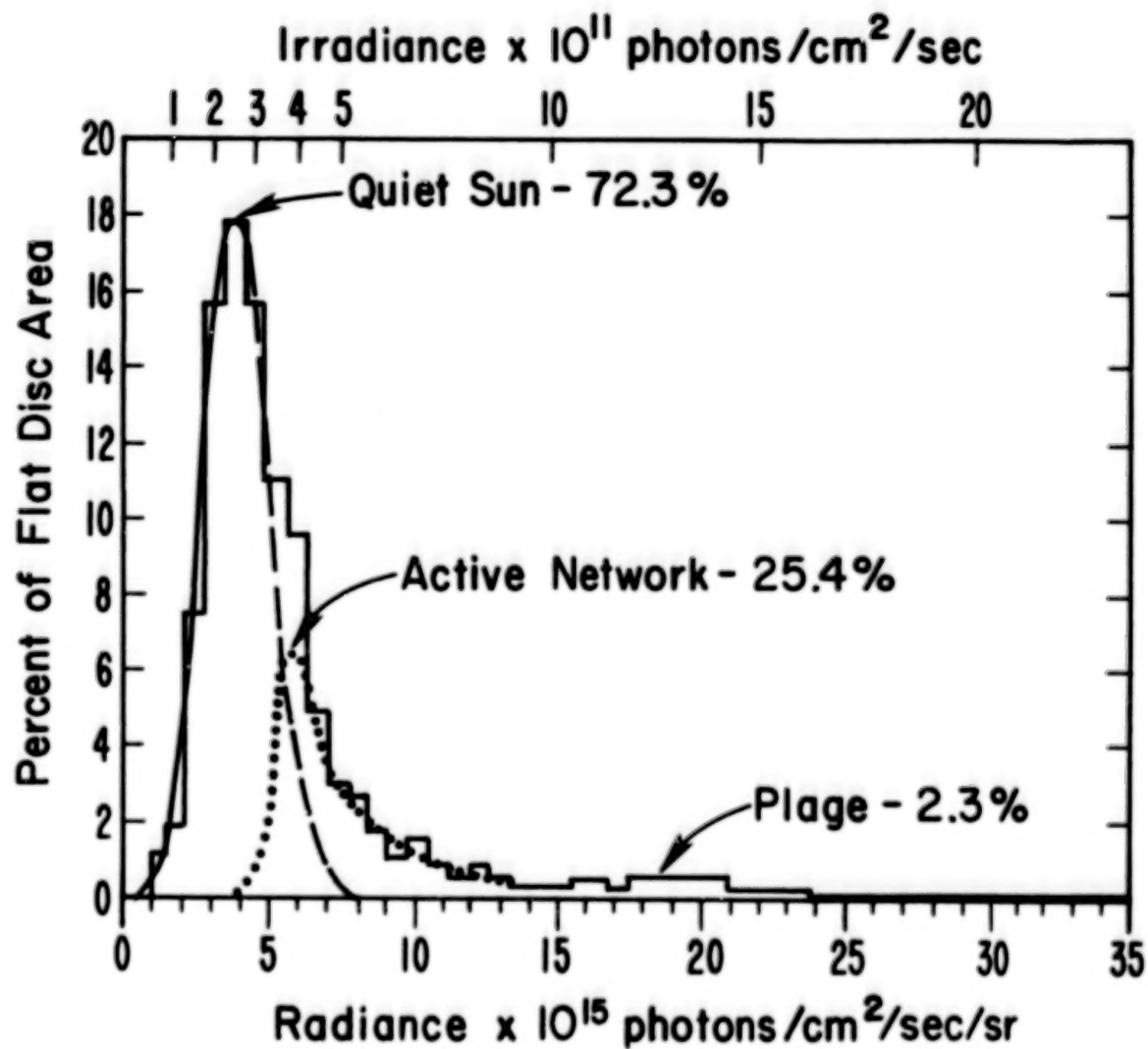


Figure 3

270

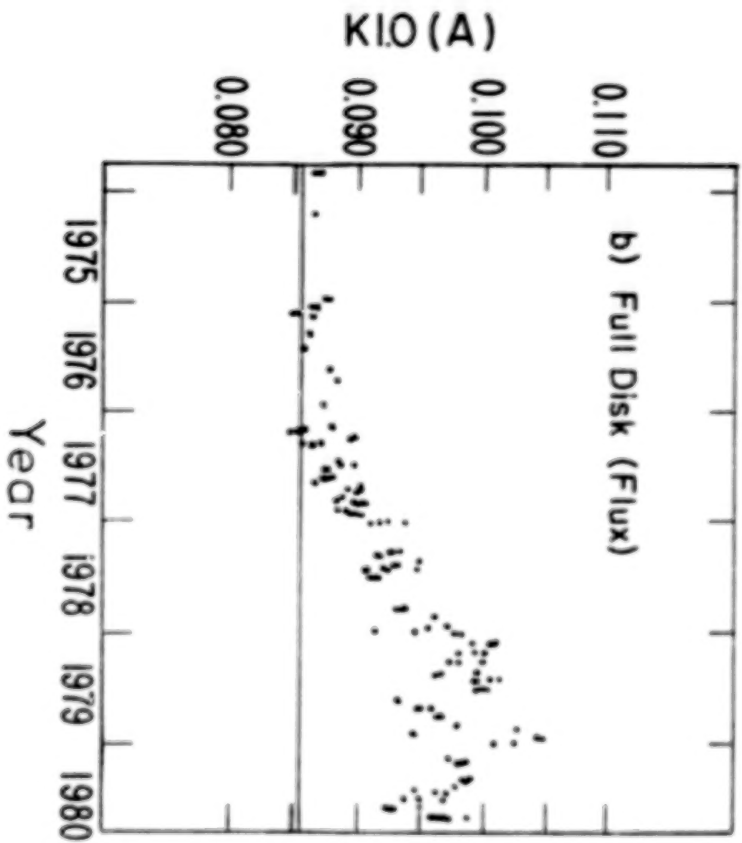
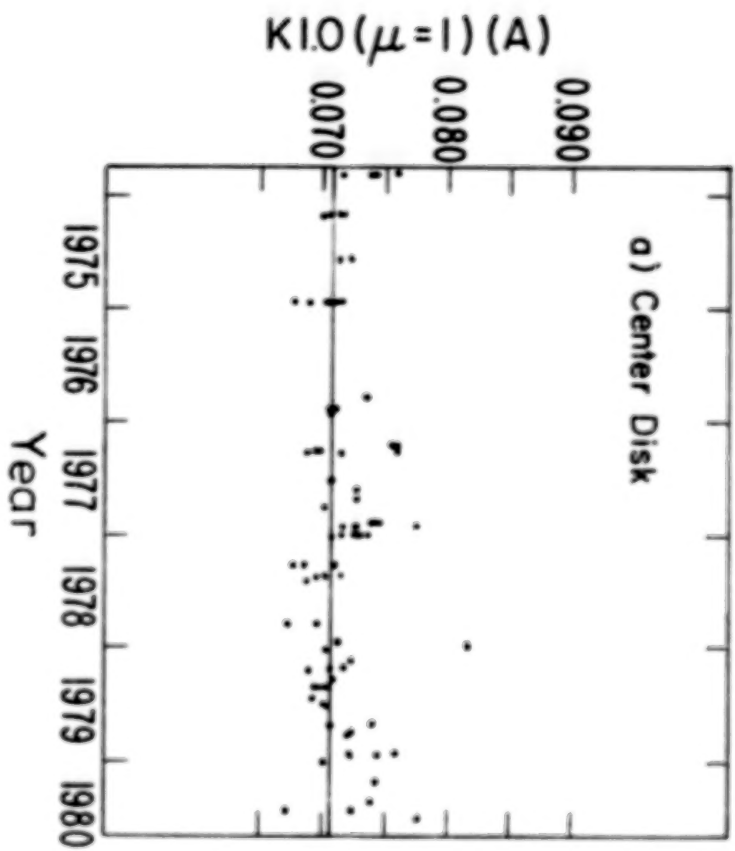


Figure 4

271

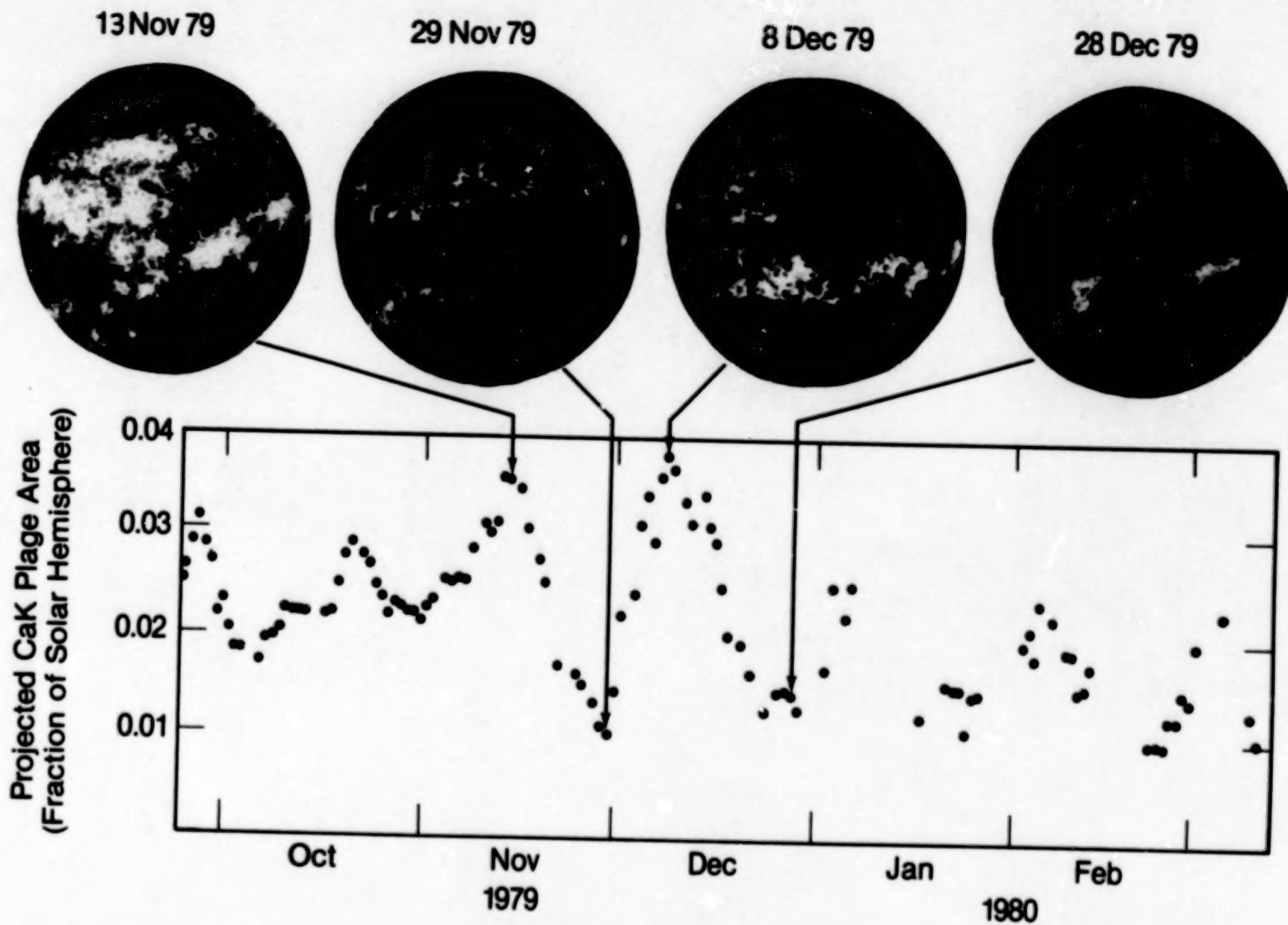


Figure 5

272

• Ca II KI.0 - Tucson
— Lyman alpha - SME

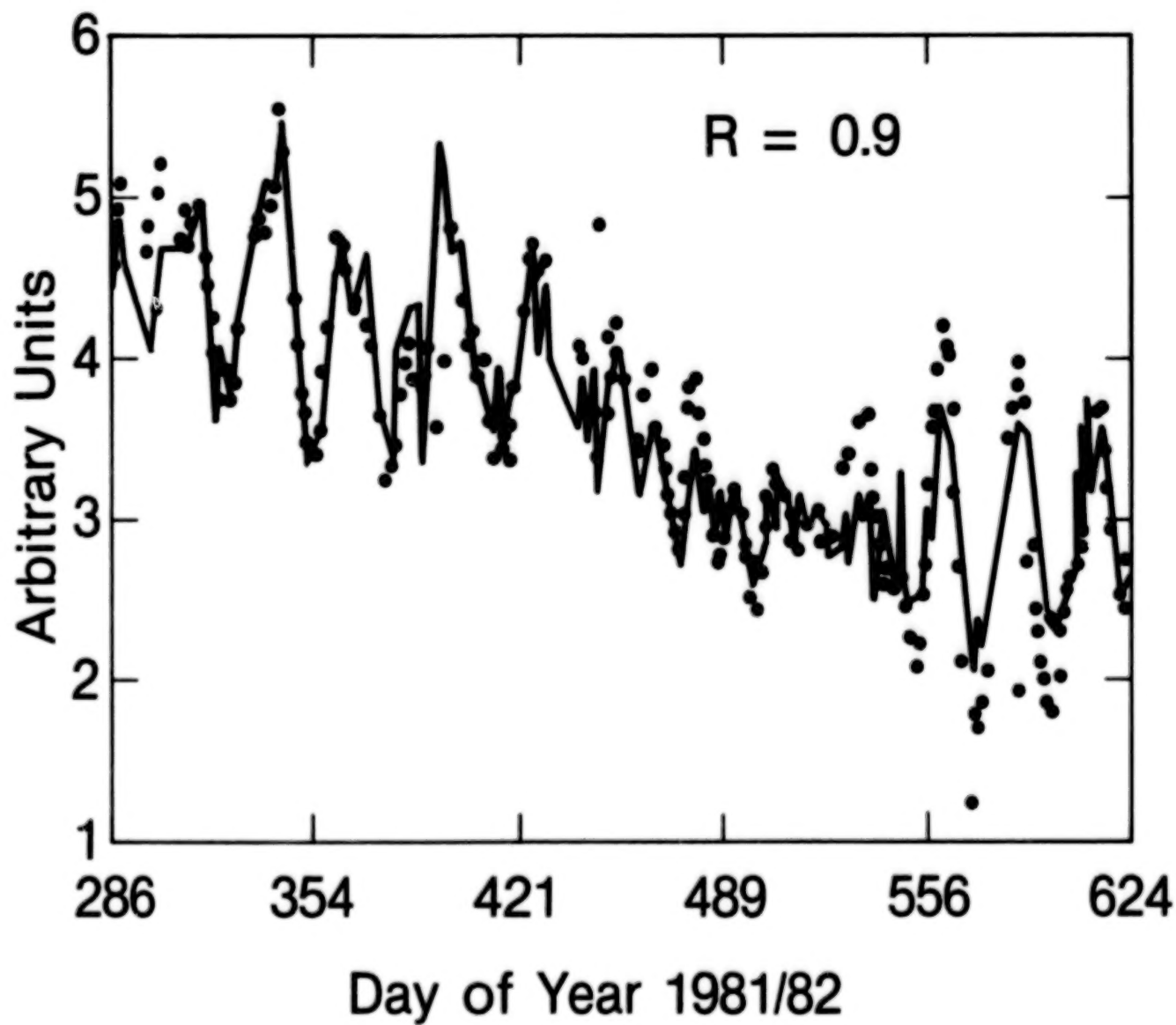


Figure 6

273

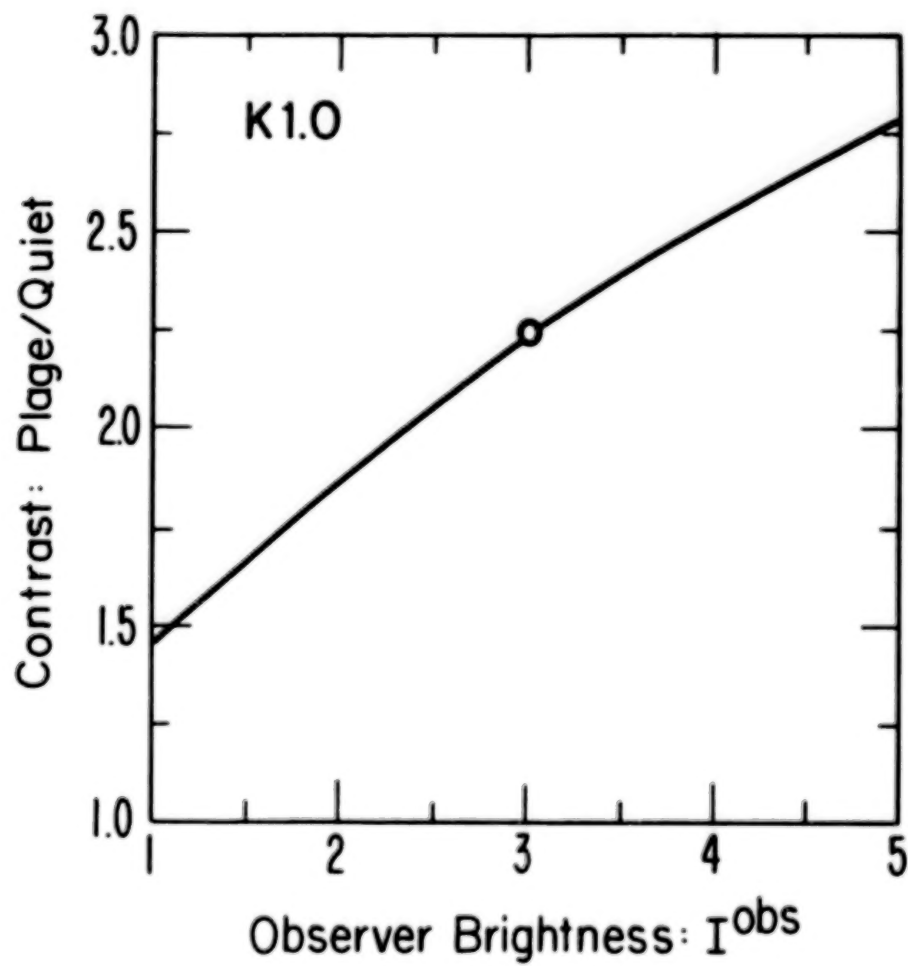


Figure 7

274

- Full Disc, Measured at Kitt Peak
- Full Disc, Measured at Tucson
- Plage, Calculated from WDC/NOAA data

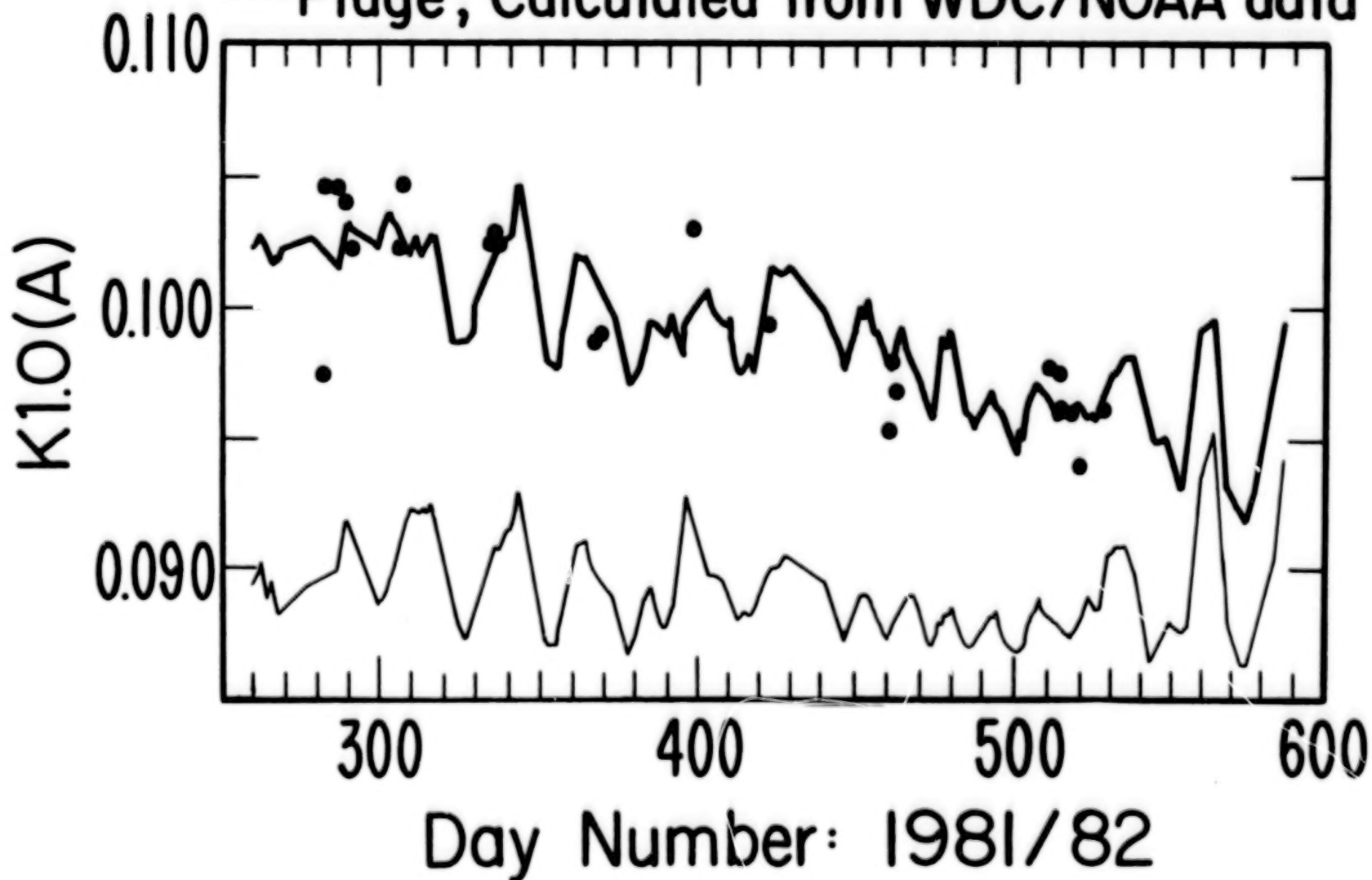


Figure 8

275

Typical Ephemeral Region Growth (2".5)

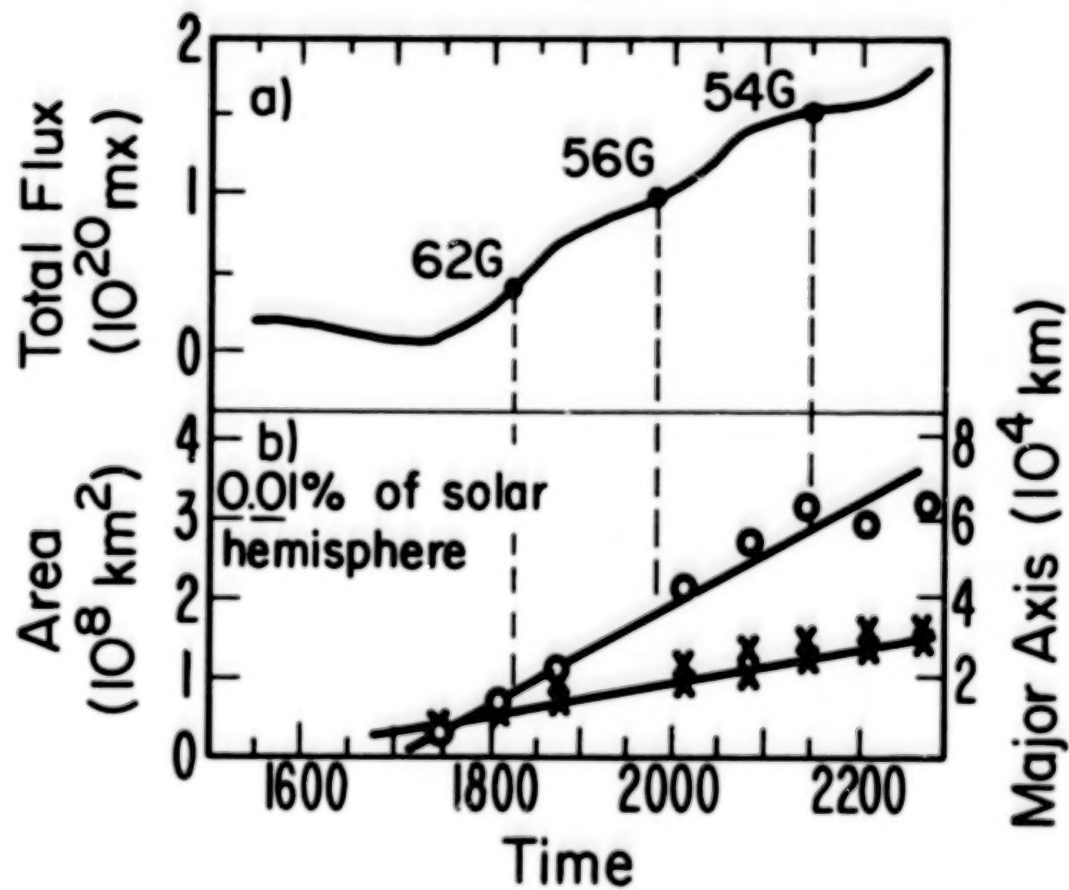


Figure 9

276

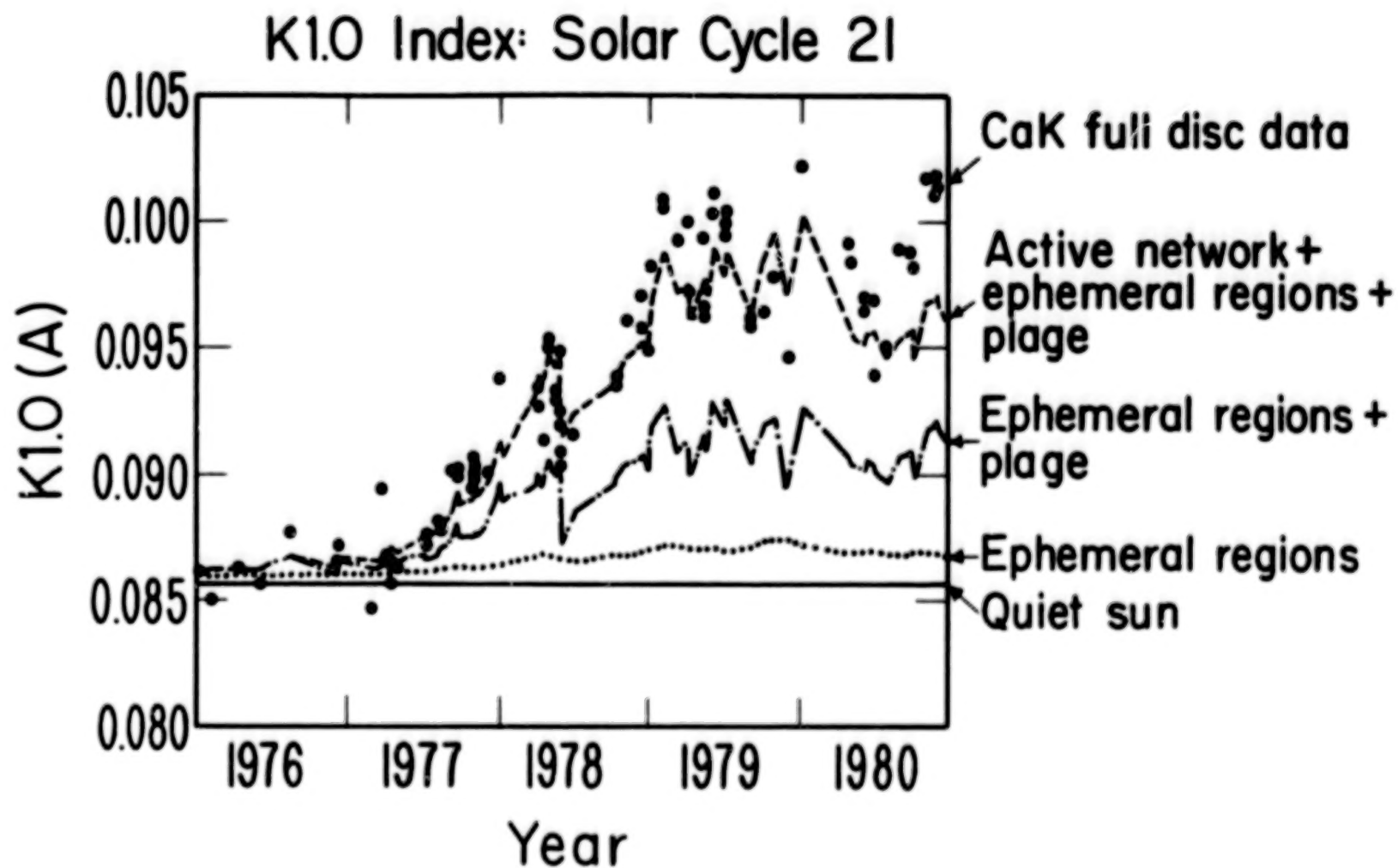
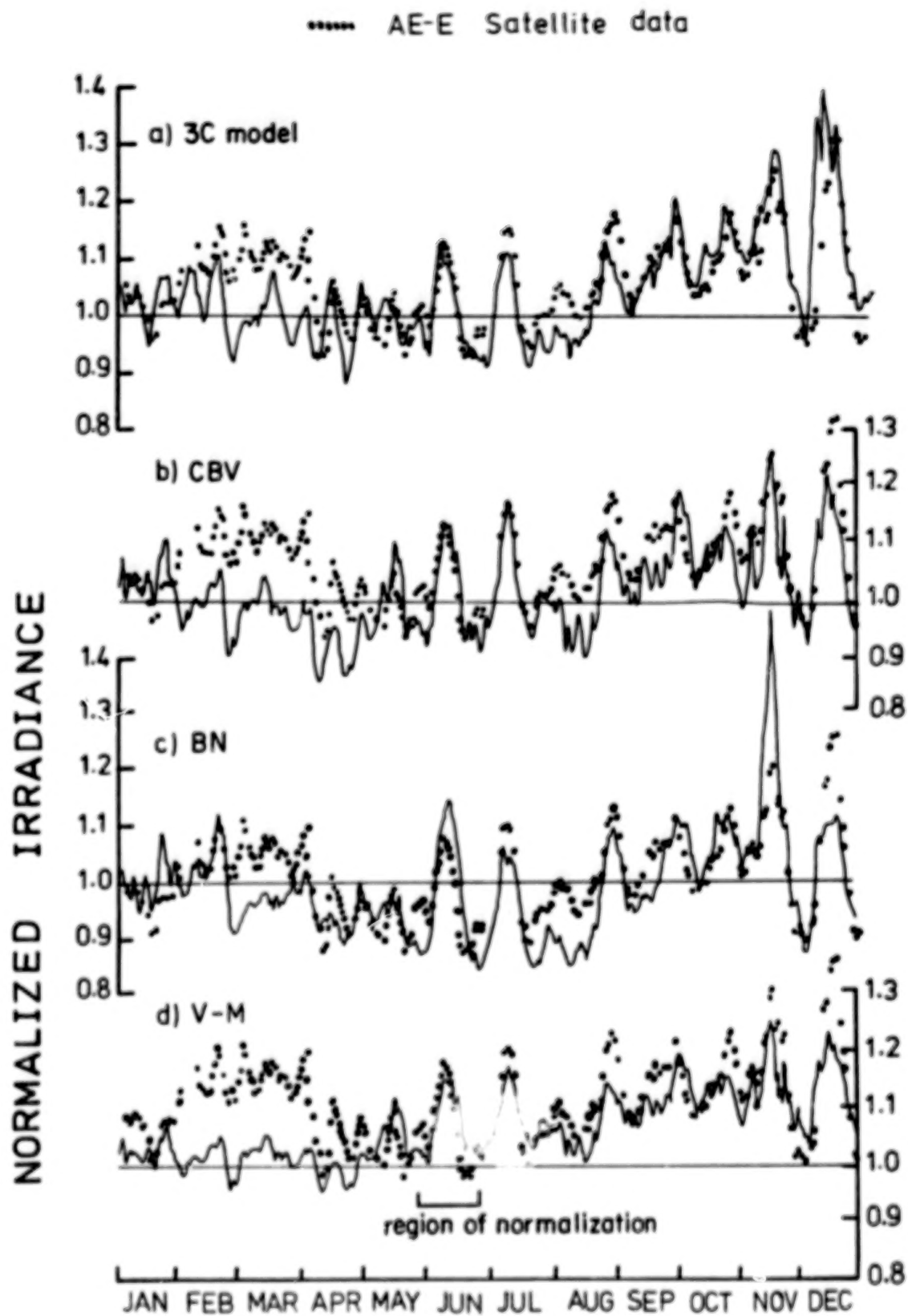


Figure 10

277



1979

Figure 11

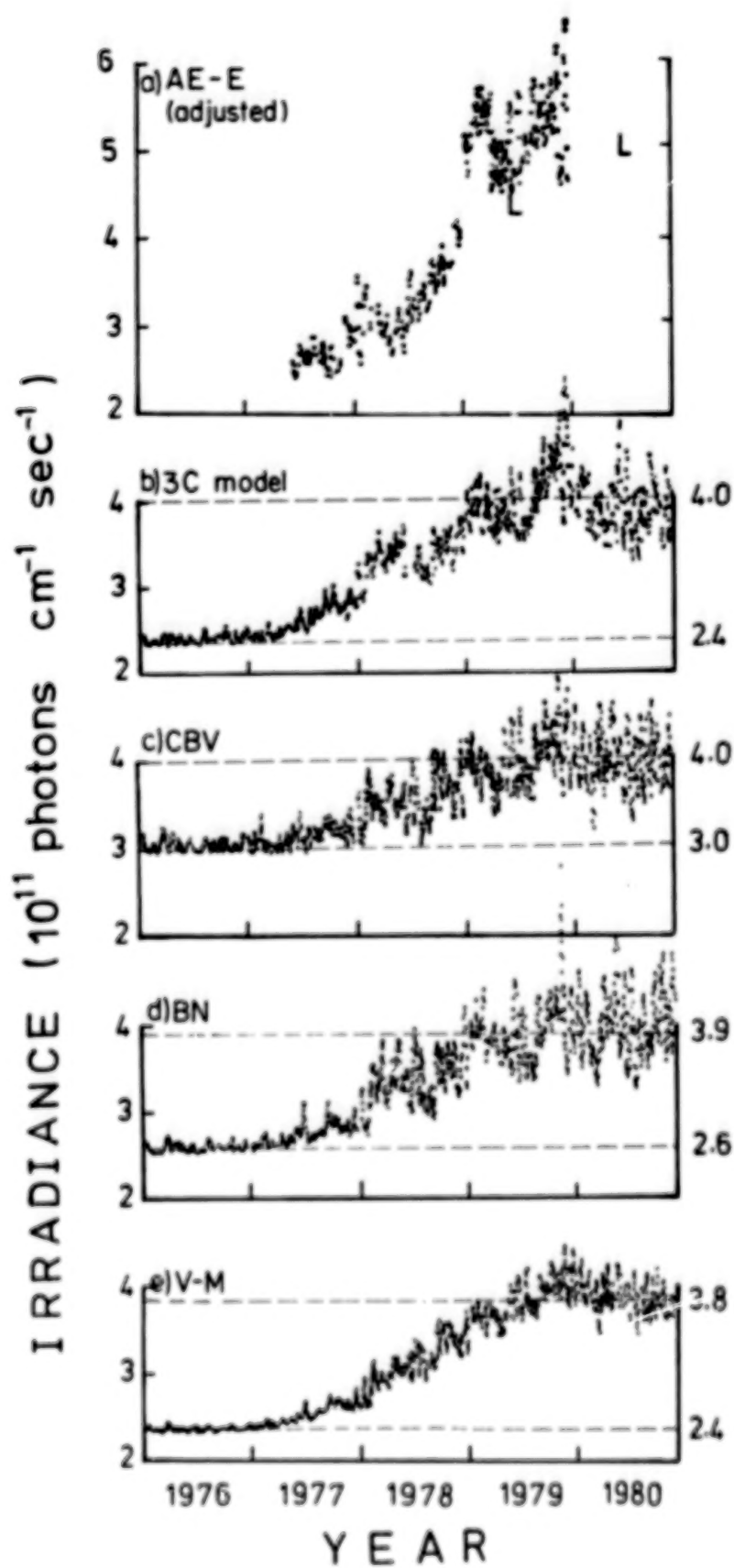


Figure 12

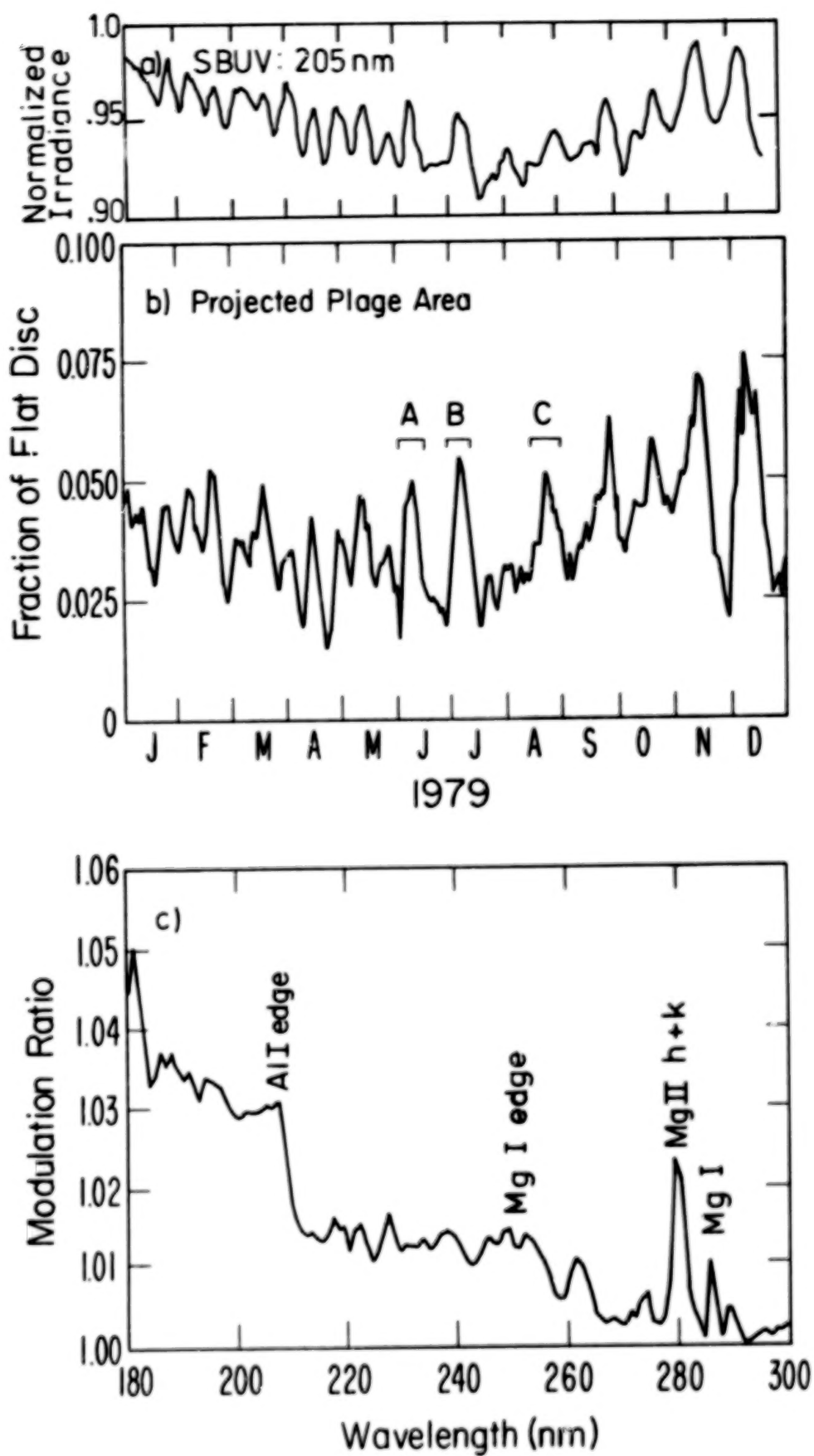


Figure 13

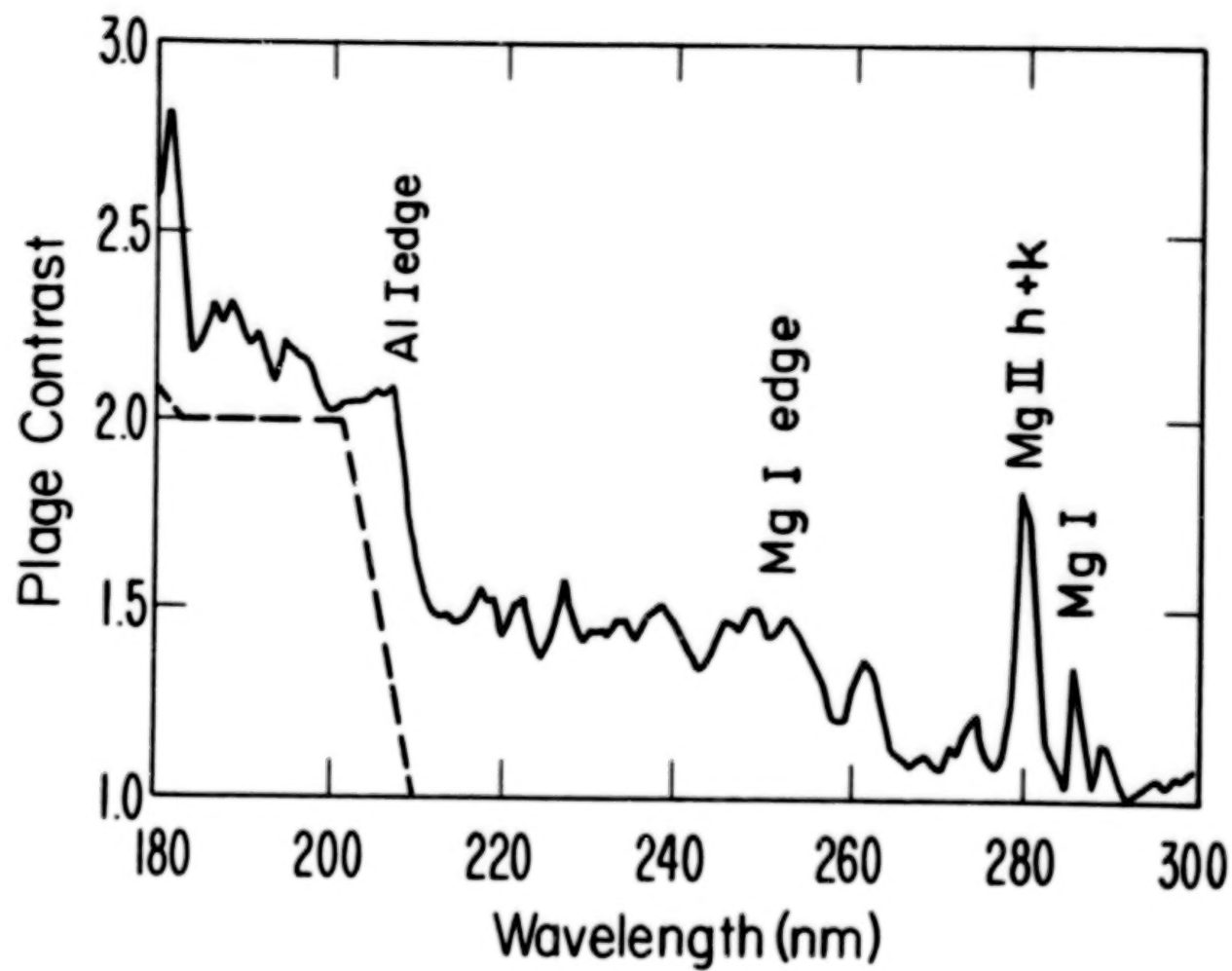


Figure 14

281

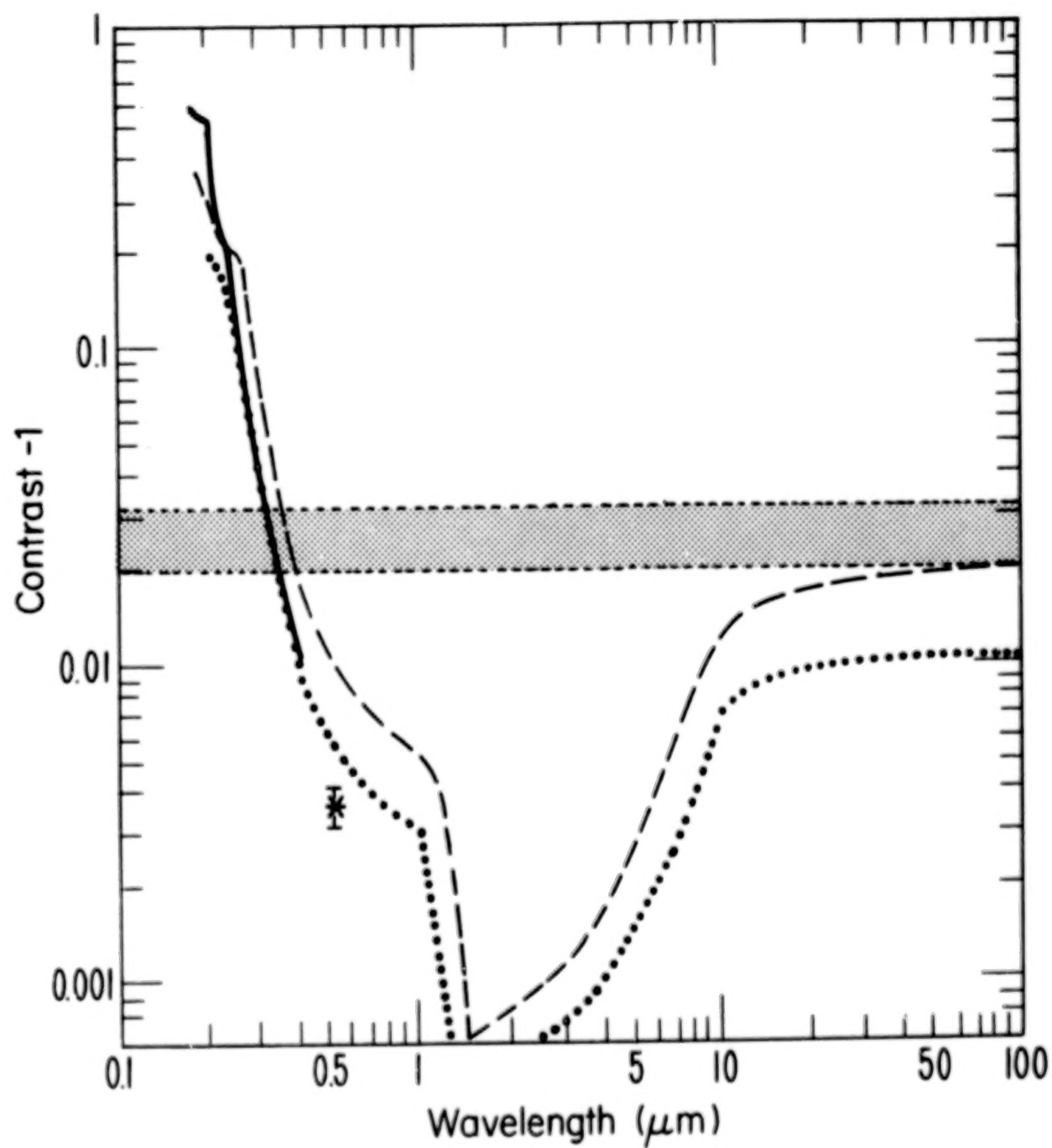


Figure 15

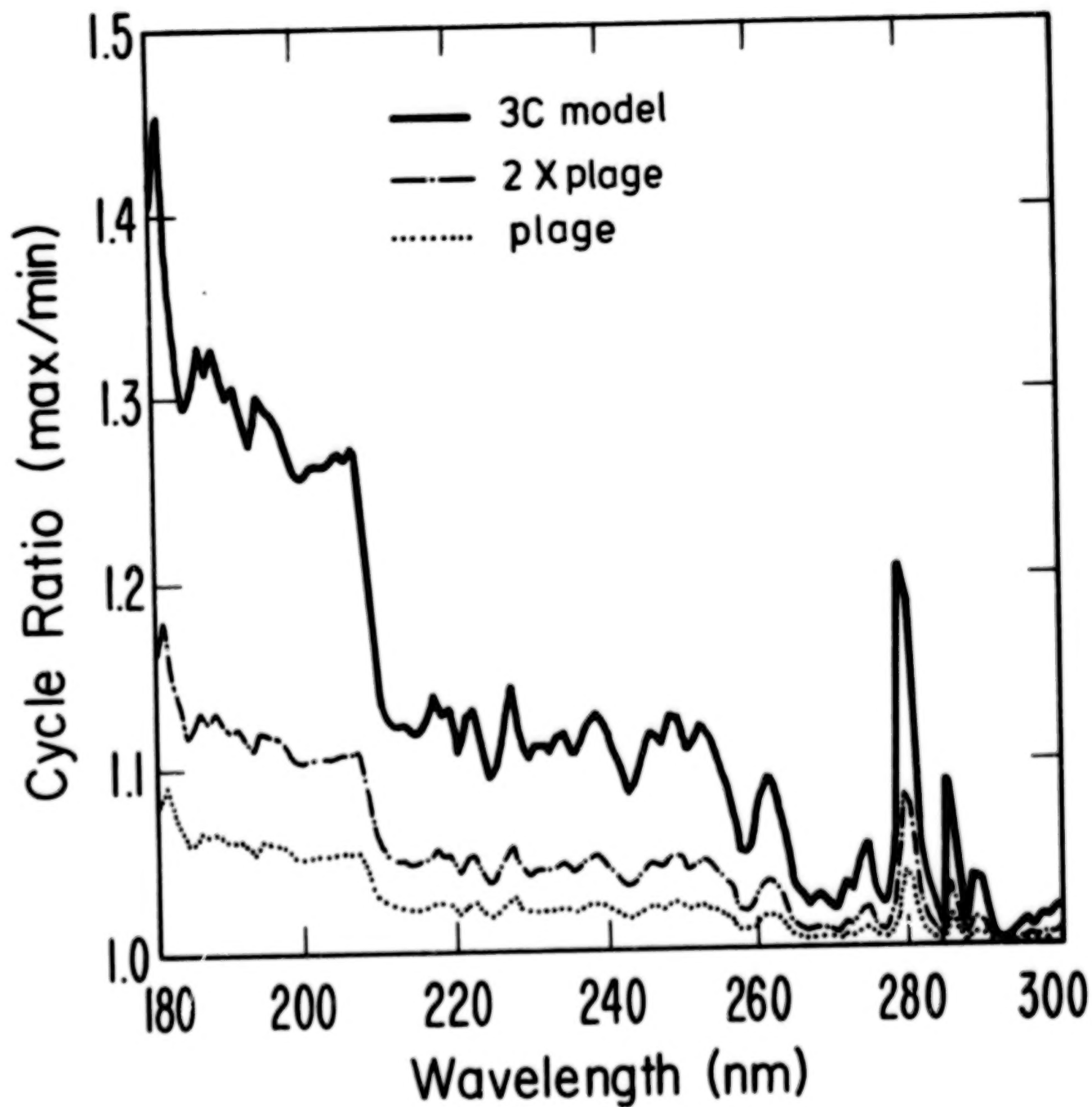


Figure 16

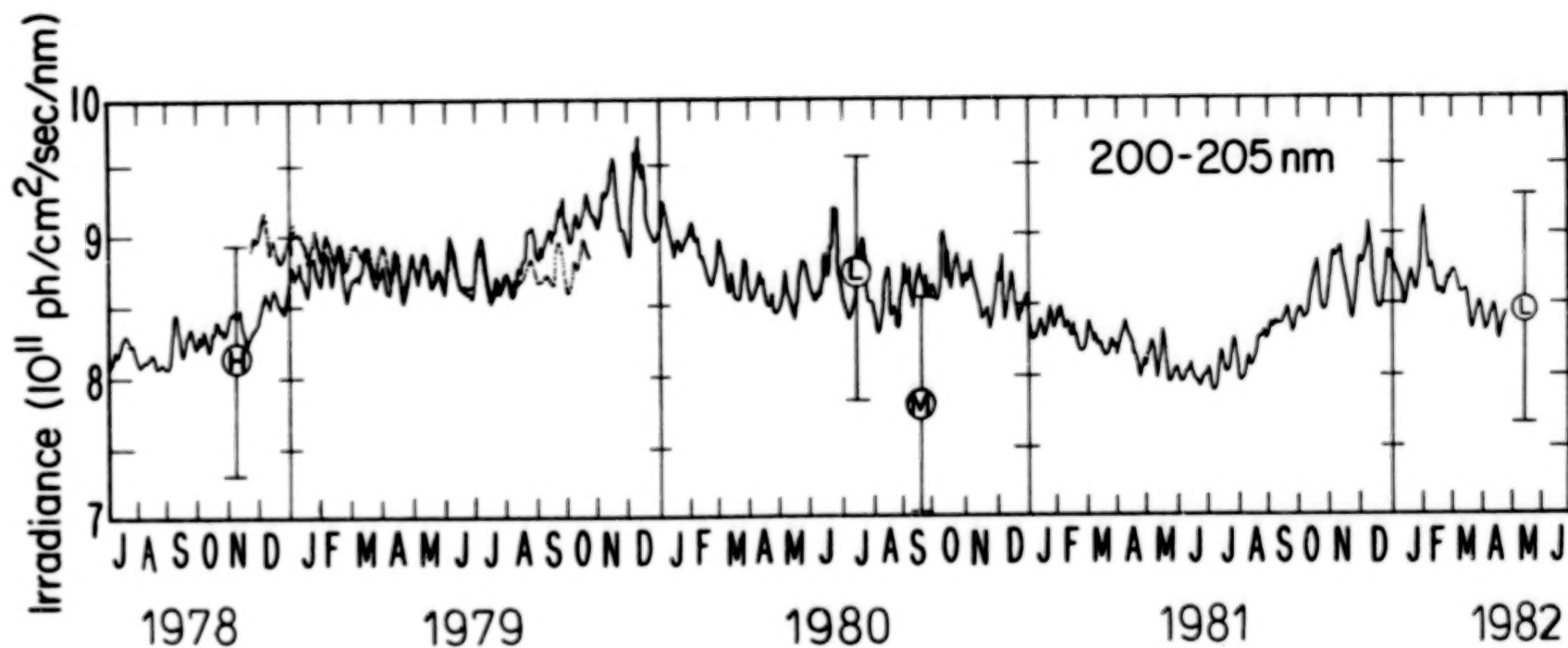


Figure 17

284

PERCENT CHANGE: TOTAL SOLAR IRRADIANCE

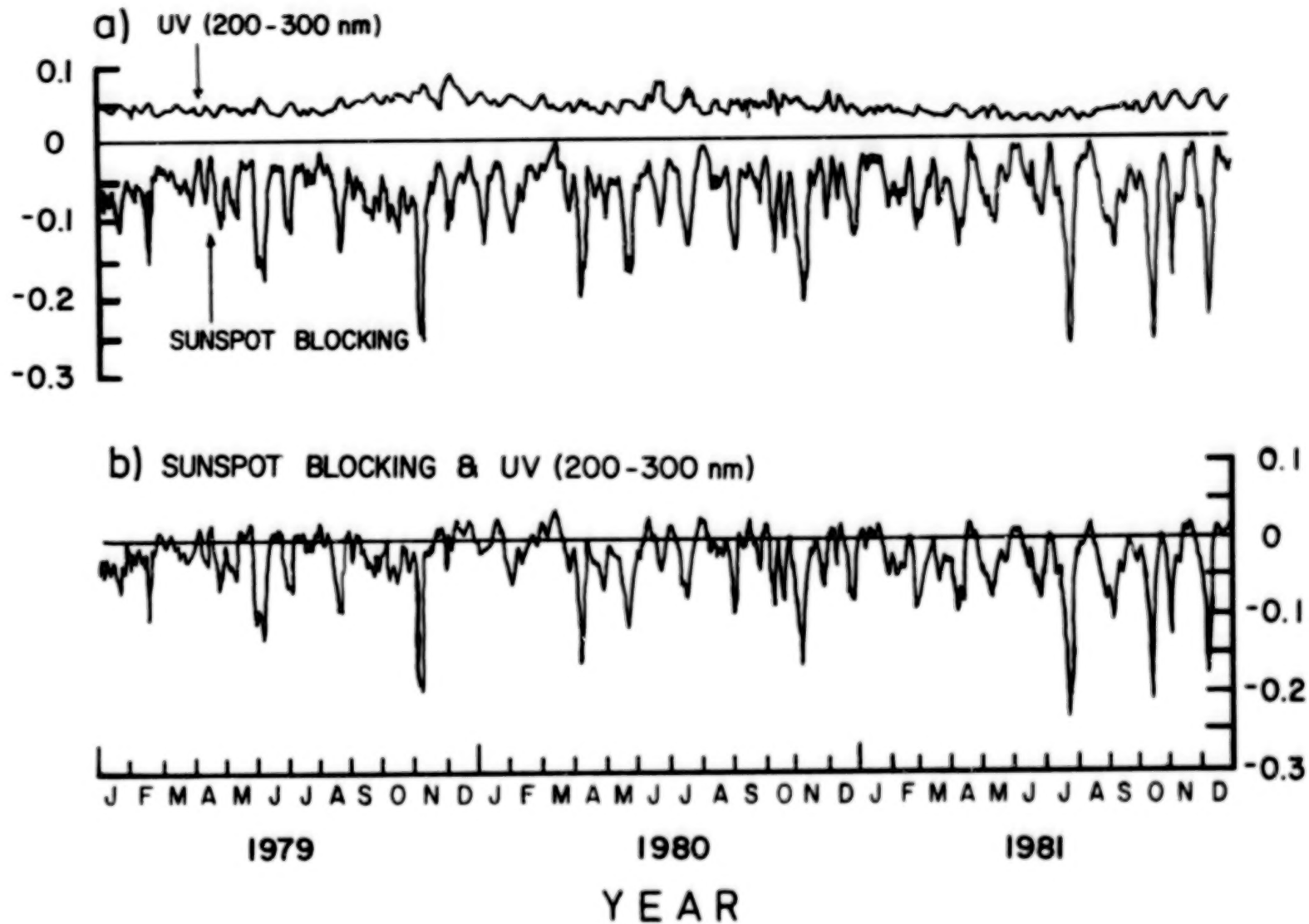


Figure 18

285

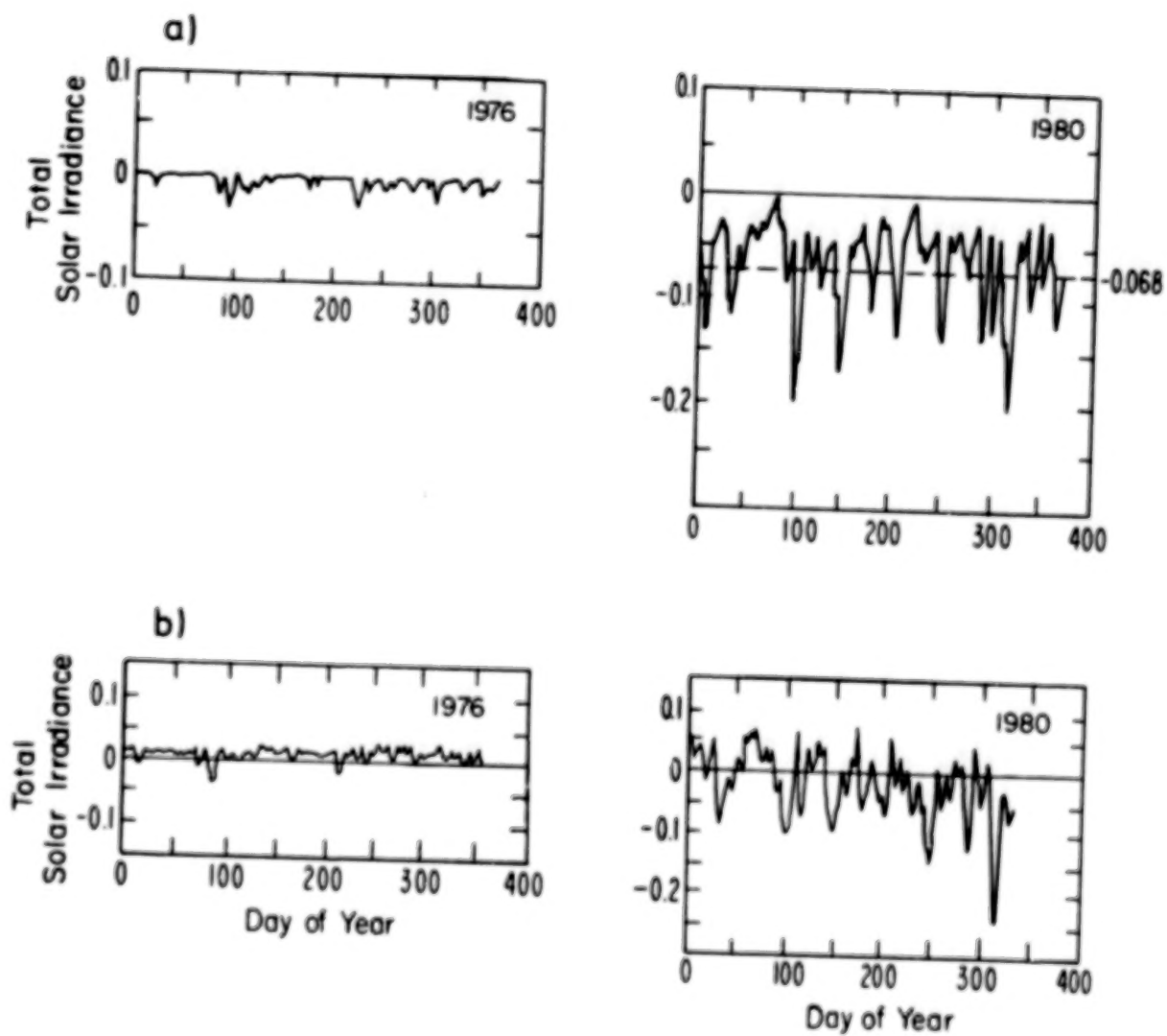


Figure 19

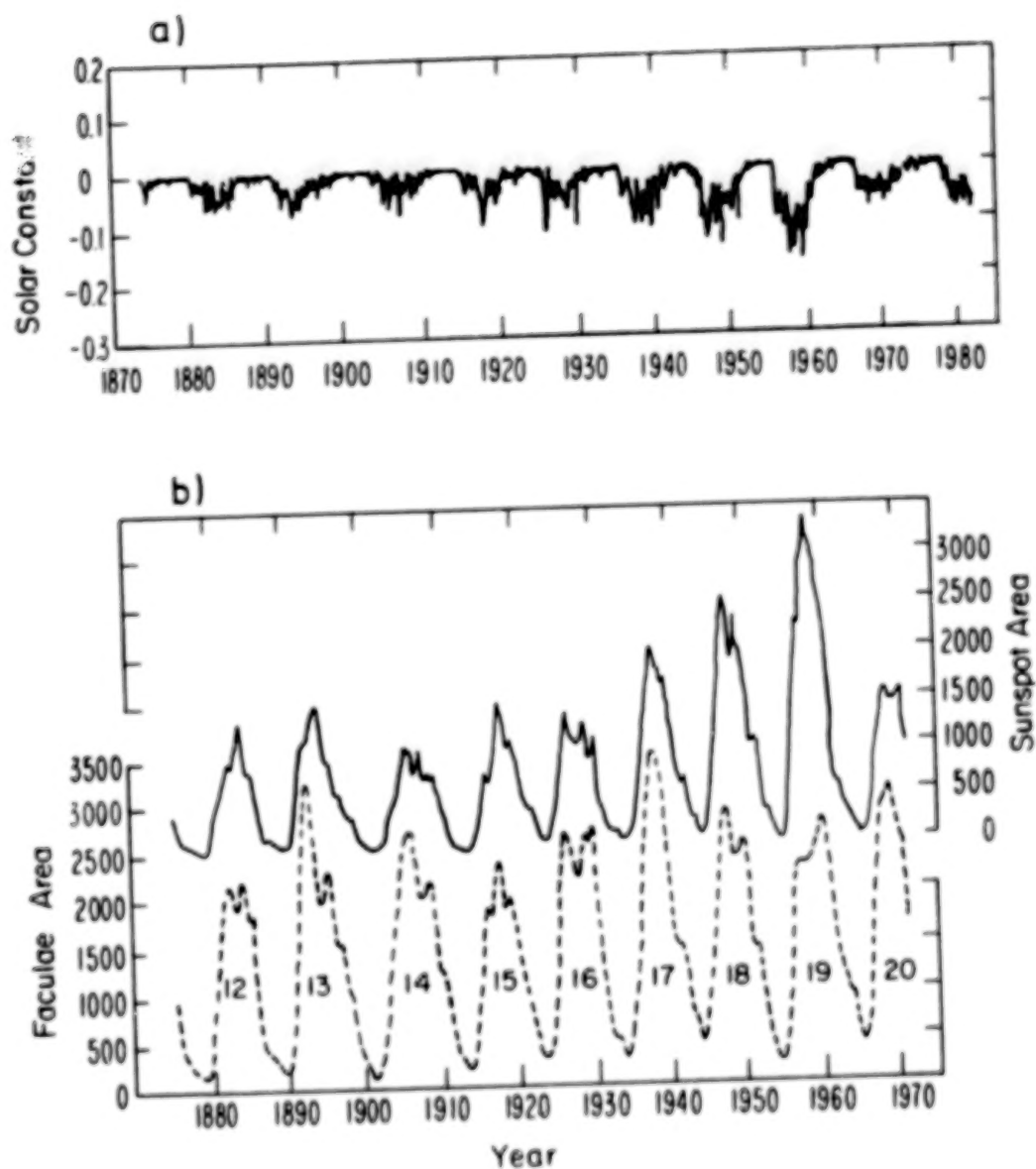


Figure 20

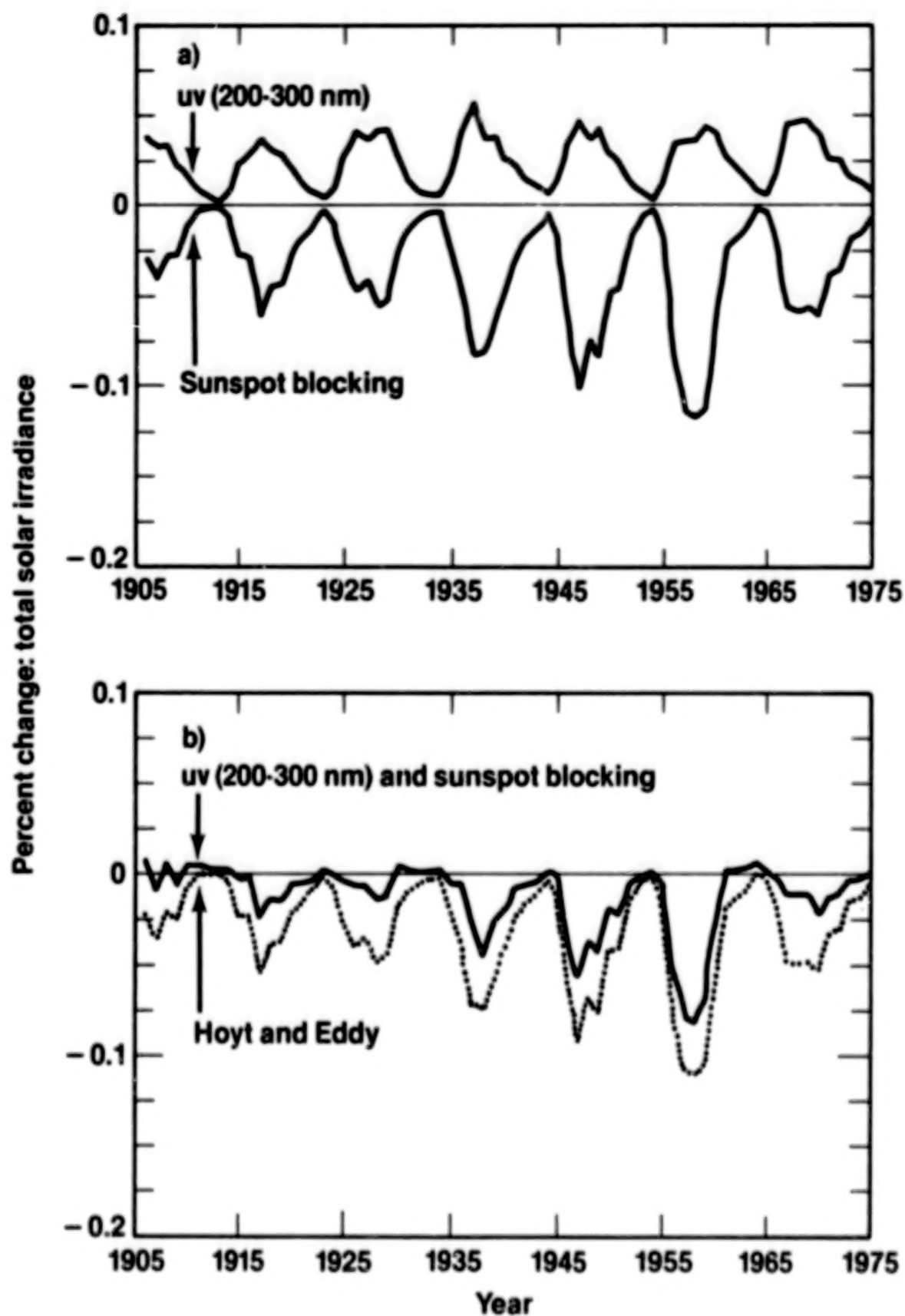


Figure 21

DISCUSSION OF LEAN PRESENTATION

ZIRIN: Why not just measure the UV pictures to find the feature contrasts?

DONNELLY: No one ever bothered to, they never saw it was important.

SCHATTEN: The UV contribution is in the model since the model is fit to the ACRIM data.

LEAN: If you only fit to the daily variations, that leaves out the slowly varying components.

Editor's note: No paper was received for Don Heath's presentation, so the following transcription of some of the interesting points has been put together.

DISCUSSION OF HEATH PRESENTATION

HEATH: Our results are from an instrument which really was not designed to do solar physics. The primary objectives of these measurements are to detect changes in the ultraviolet albedo of the Earth in the ozone absorption region, to detect long-term changes in the stratospheric ozone, and to identify the physical mechanisms which are responsible for these long-term changes. Nevertheless, the instrumentation has several advantages. We had to have scattered-light rejection by six orders of magnitude over about 200 angstroms. We had to have extremely high radiometric stability since we were trying to measure albedo changes of half a percent. We had to have extremely high wavelength precision, stability as well as linearity.

There are two parts to the solar problem. One is to determine whether or not there is any evidence of changes taking place, and the other is to interpret the physical processes responsible for the changes. For our purposes the biggest problem is in what the Sun is doing in the ultraviolet; the ozone exists solely because of ultraviolet radiation coming from the Sun.

Here you see the solar spectral irradiance data with good evidence for 27-day variability. I will concentrate on the modulation during one solar rotation period, the ratio of maximum to minimum. Our data begin one year prior to solar maximum and continue three years after. I am going to describe briefly the work that we're doing in trying to check long-term changes in the solar spectral irradiance, as well as a series of studies of the aluminum ionization edge where you have the least change in the emitting region in the solar atmosphere. We take the ratio of magnesium II to magnesium I as a temperature indicator by comparing it with a blackbody spectrum.

There are a number of interesting features which I will show you; one has to do with the ratio of the enhancement of that region to that of Mg I and the other one has to do with the appearance and disappearance of the Fe I emission lines and the behavior of the aluminum ionization continuum and [some] emission lines.

The instrument that we use to make these measurements has a 10 angstrom spectral bandpass. It's fortunate that the dynamic range required to make solar measurements in the region from 1600 to 4000 angstrom is exactly the same as what we need to measure the atmospheric albedo, so it makes an ideal instrument. Just to give you an idea of the quality of the daily measurements, we make a measurement approximately once per day at the northern hemisphere and this is the solar flux at 205 nm, 2050 angstrom, which is the short wavelength [band]... [of] observation [averaged] over a year, this is the 27-day peak and these are the 13 1/2 day peaks that correspond to active regions about 180° apart in solar longitude and, as Jack Harvey mentioned earlier, [...these go from modes in which you] have a typical 13 1/2 day forcing of having two active longitudes, and then it will suddenly make a transition over to only one active longitude; but this gives you some idea of the stability of the data and don't attach any significance to the long term changes for that is on instrumental [effect]. Now if we look at the Mg II h and k lines, that is ... at 2800 angstrom, here again we see these series of 13 1/2 day strong signals [with] a 27-day modulation. This has an instrumental dip connected into it, but you can sort of think of it as

though [you've] subtracted out part of this.

I want to concentrate more on the modulation with time, and one of the things that comes in, which should be rather obvious, is that over this 4-year period, that there are periods when the amplitude of the modulation of the Mg II, singly ionized is the same all the way up to 1982. In terms of the rotational modulation, there has been this very high level of solar activity until the day when Jack showed this curve; this curve is the 205 nm long-term changes. But this is different than the Mg II h and k. We've taken out, to the best of our ability, the instrumental changes in the instrument's sensitivity [and you can think of it in terms of a series of residuals that are] departures from a slowly-varying...drift..., but the surprising thing is, apart from the repeating of the series of peaks of very strong 27-day variation, the maximum in UV radiation occurs in late 1981, [whereas] sunspot maximum was in 1979. An this feature becomes stronger and stronger as you approach the region of the temperature minimum. At first, as I said, I didn't believe this; I thought it was just some artifact; now I'm beginning to believe that there may be some substance to this delayed UV radiation. This is very important as far as understanding what's producing the long term behavior in ozone. People over a number of years have made studies of the relationship between ozone and sunspot number, and for the most part the effect has more or less fallen by the wayside because you observe that the maximum effect in the long term changes in the ozone occurred one to two years after sunspot maximum and for this reason it was thrown out. But now, based on what we're seeing, and what Jack was showing in the He I line, perhaps [one] should reconsider this question.

EDITOR'S NOTE: Dick Willson made a second presentation, for which the text and figures are incorporated into his paper published in these proceedings. The discussion for this presentation follows here.

DISCUSSION OF WILLSON PRESENTATION

HUDSON: Will the calibration of the ACRIM spin-stabilized data get better - do you plan to re-analyze the calibration?

WILLSON: Yes, but I am pleased with the calibration I am using now.

POUKAL: In the spin-stabilized data you don't use the reference provided by the back of the shutter. Also, what about the time constants involved in the measurement?

WILLSON: We do not use data that do not give a minimum duration of solar viewing. It's reasonable to say that our criterion is not definitive; the analysis will be sharp enough to ... As a matter of fact, in the spin mode, the instrument looks into cold space once for each solar sample, which is a far better calibration.

POUKAL: And that correction is well enough known that it's small compared to the error bar that you have there?

WILLSON: Oh, that correction is about 0.06%.

POUKAL: Then the error bar on that correction makes a negligible contribution.

DONNELLY: Now that you leave your shutter open all the time, do you see any evidence of rapid degradation relative to the reference?

WILLSON: No, we don't.

SOFIA: I would like the other modelers to produce a residual graph the way we have done, to see if there is any sustained discontinuity roughly at 0.2% decrease after the new mode of operation that might indicate something instrumental as opposed to something that's changing on the sun.

WILLSON: I've noticed from your results yesterday, where you said you did see what could be interpreted as a level shift, however, your level shift occurred some time in February, about 6 months too late.

SOFIA: Yes, on the other hand the residuals are pretty large. But it did seem to be a few months later.

ZIRIN: I guess the long-term data will really settle this question of sunspots versus plages. Either it will relax to the average between them, or it will relax to a quiet sun value....

SCHATTEN: If Hickey's data had a general trend...

WILLSON: That brings me to my next point.

MOORE: What if you just fit '81 to '82 and forget about 1980 and 1981; what kind of slope do you have?

WILLSON: I haven't done that; it would be interesting to do.

DONNELLY: What if you just do the fit for the days that you both have data and not fill in any data which makes a controlled bias, do you still get as good an agreement?

WILLSON: That's something worth doing; I haven't done it.

HUDSON: We could take your data and just throw out the days...

CHIPMAN: That's not the same thing, because one of the reasons for this later result is that Hickey's data underweights the latest part of the last year...

WILLSON: You're right Eric, it wouldn't give an accurate representation of the real slope, but Dick's right too in that it would give an estimation of whether or not throwing those out, we both get the same result, albeit not a very interesting one.

SOFIA: Another way of looking, though, is if you divide [it] right there in February - the ACRIM data before and after - there seems to be a shift in level.

WILLSON: Where is this famous shift in levels? I'm not seeing something! (some laughter).

SOFIA: Here it is! The level up here is there! And afterwards it's there! You don't look at the trend, you fit to the first half from there to there, and there it is, and then you look at this one and there it is; it's a bit lower whereas here there is no obvious shift or trend.

CHIPMAN: That's not very fair.

HUDSON: That's not a meaningful statement because of course if there's a trend the means will be different. Is the data powerful enough to support a higher-order fit than a linear trend? With all the noise that's there it is hardly very satisfactory even to do a linear fit.

CHAPMAN: What is the linear trend with time just for the spin-stabilized part of the data?

WILLSON: I haven't separated it out. Just for 1980, it was 0.04% for 300 days, which is 0.05% per year.

CHAPMAN: So it wasn't constant; what was the uncertainty in that? Was that a two- or three-sigma result?

WILLSON: Yeah, at least.

CHAPMAN: So there was already a downward trend, it's dangerous when you're fitting two different slopes that are very small when the signal is that noisy. I just don't think it's valid to try to, with your eye, to fit two things together like that [discussion continues briefly].

SCHATTEN: Perhaps what you could do is a separate analysis up until the time you redid your method of analysis, and then another one afterwards and presumably those two curves would look somewhat similar to what you have ... and that would enable you to see [any change in slope] and would also perhaps give you a feeling for the uncertainty, which you say is only about 0.02% or of that order.

WILLSON: OK, we'll do that.

FINAL DISCUSSION OF GROUND-BASED OBSERVING PROGRAMS

The editors felt that improved ground-based observations could go a long way towards improving the understanding of the variations of solar irradiance on active-region time scales. The improvements probably should include strengthening of the traditional synoptic observing programs, the introduction of new technology in old or new measurements, and a renewed focus on interpretation and theory. The participants in this workshop were therefore urged to contribute brief comments on directions that they felt would be useful. We summarize our own ideas on p. 313 in "A Global Irradiance Program."

BLANK PAGE

Drift-scan Photometry and Astrometry

Hugh S. Hudson

I would like very briefly to mention an idea proposed by Gordon Hurford, who unfortunately isn't here. He suggests that drift scans of a one-dimensional diode array would be a good way to get high-quality photometry and astrometry of spots - he was interested particularly in the astrometry, because of the problem of image registration. He envisions multiple scans going on all day long, with a simple alt-azimuth mount that would just step to the next position and then freeze there to await the arrival of the Sun. The diodes would be aligned north-south so that each would scan out a strip. For calibration, a 90° rotation would enable them all to scan the same strip in sequence. Isn't that a nice idea?

DISCUSSION

EDDY: Is this something that's really going to happen?

HUDSON: No, the point is that Gordon is too busy to do it. I thought that the ideas might fit into somebody else's observations. For example, Tim Brown's diameter instrument might be adaptable.

EDDY: The idea is to make one observation a day?

HUDSON: No, as often as you want to, just by stepping the telescope and then locking it down.

HARVEY: Watch out for seeing! Tom Duvall and I have measured the solar radius that way, a lot, and it isn't as easy as it might seem.

ZIRIN: It's easy to do, but just you wait and see!

BLANK PAGE

Facular Data Base for SMM-ACRIM Comparison

David L. Glackin and Richard C. Willson, JPL

Solar irradiance variations as observed with the SMM-ACRIM instrument should be compared with observed data on solar faculae during data analysis and interpretation. Unfortunately, no data now exist which contain accurate measures of facular area and intensity. We propose the creation of such a data base at JPL, because the facilities exist here for high-volume, computation-intensive image analysis.

We would like to discuss a joint program with a ground-based observatory having a set of analog or digital full disc images of the sun which can be calibrated and which cover the time span of past ACRIM observations. They might be taken at, e.g., $\lambda 3840$. We envision first a proof-of-concept study in which once- or twice-daily images are used. Image digitization (if necessary), calibration, contrast enhancement, perspective projection (if necessary), scene segmentation into faculae, spots, and quiet photosphere and measurement of the statistical properties of the faculae would be carried out in the Image Processing Laboratory (IPL). Digitization of analog images would be done on a PDS microdensitometer. Scene segmentation would be done with a supervised classification algorithm first developed for earth resources studies. Comparison with ACRIM data would then be made at JPL.

Such a program would provide information and experience regarding the types of data that should be collected during the next phase of SMM. We envision a more detailed study with higher time resolution full disc data, and perhaps better calibration.

This data base should allow a more accurate assessment of the effects of solar faculae on the solar variability than has been possible to date. It might also provide a strong argument for inclusion of a full-disc imaging instrument on the proposed JPL SDO (Solar Dynamics Observatory) spacecraft.

DISCUSSION OF GLACKIN PRESENTATION

EDDY: Can you use these methods to find bright and dark features?

GLACKIN: You can use them for any kind of feature.

COFFEY: Can you digitize the MacMath films?

GLACKIN: Are they calibrated?

DONNELLY: Yes.

unknown: All it takes is money.

NEWKIRK: Why do you want to use an ultraviolet band?

unknown: We want to see faculae all over the disk

NEWKIRK: Then you won't match the ACRIM, because the contrast will be different from the bolometric.

FOUKAL: The ultraviolet contrast is not small.

NEWKIRK: Then you ought to use various passbands.

FOUKAL: Spectra can be taken down to 3200 \AA , so we can measure the contrast of faculae as a proxy for the UV.

New Techniques for Global Activity Monitoring

Harold Zirin

Big Bear Solar Observatory

Since September 1981, Big Bear has taken responsibility for observation and measurement of calcium plage regions, the continuation of the long string of observations from the former McMath-Hulbert Observatory. In the summer of 1982, we began making digital measurements, digitizing calcium images from a Vidicon camera by passing them through a Quantex image processor. Software has been written for computer measurement of both area and total brightness of each plage. The photometry of the present system is probably better than the visual estimates used for the McMath numbers. Care has been taken to normalize the system by choosing plage brightness levels that give results to match to old system. The total apparent disk K-line brightness can also be measured. This work was interrupted by the ending of NOAA funding in 1982, but funding for an additional year was obtained, so that all data through October 1, 1983 will be reduced. We do not know whether there will be future funding for this program.

I should note that this work is significantly aided by the use of the full disk magnetograms provided by the Kitt Peak National Observatory (courtesy of J. Harvey), which are used as a backup and for help in region identification.

The availability of digital image processing systems makes it relatively easy to produce digital data on the calcium brightness as well as white light images and the like. We are planning to regularly record white light and H-alpha images in addition to the K-line images presently being recorded. New image processing equipment that the observatory is obtaining should make the reduction of this data relatively simple. In view of the importance of and interest in the global solar activity conditions, we expect in the future to build a separate building for such monitoring, as well as the measurement of global pulsation. It is unfortunate that just as such measurements have become easy it has become extremely difficult to fund them. Regardless of funding we will continue to record the digital images, saving them for reduction when funding becomes available.

DISCUSSION OF ZIRIN PRESENTATION

DONNELLY: Why do the spots show up so well on your K line pictures?

ZIRIN: The filter has a 0.4 \AA bandpass.

SOLAR & TERRESTRIAL ATMOSPHERES SPECTROMETER - STAS*

Peter L. Smith^(a), W.H. Parkinson^(a), and W.K. Fowler^(b)

(a) Harvard-Smithsonian Center for Astrophysics

(b) Ball Aerospace Systems Division

MOTIVATION AND OBJECTIVE:

Solar radiation between 120 and 360 nm dominates the photochemistry of the mesosphere and stratosphere¹. Many atmospheric molecules, both major and minor, show very complex and fundamentally narrow structure in their photodestruction cross sections at these wavelengths. Understanding of the photochemical processes in the terrestrial atmosphere requires knowledge of both the cross sections and of the ultraviolet solar spectral irradiance with the highest possible resolution and radiometric accuracy.

At present, there is considerable uncertainty not only in the absolute value of the ultraviolet solar spectral irradiance but also in its variability, especially at high spectral resolution². The Solar & Terrestrial Atmospheres Spectrometer (STAS), which has been selected by NASA for Definition Phase study, is planned for ultraviolet irradiance measurements with the highest possible resolution and radiometric accuracy. STAS will have a spectral resolving power more than 50 times greater than any other instrument planned for such measurements³.

THE STAS INSTRUMENT:

The spectral resolution goal of STAS, $\Delta\lambda \leq 0.0015$ nm (15 mÅ), was the principal influence on the design. We have selected a 3-m focal length, diffraction limited, f/15, modified Czerny-Turner spectrometer with off-axis paraboloids in an orientation first proposed by Hill⁴. STAS will not have a telescope; the optics will be filled by the diffraction pattern of the slit. Ray-tracing analysis showed that the spectrometer design was superior to more familiar instruments for our purposes. With a 3600 l mm^{-1} , holographically-ruled grating and 7 μm slits, the spectral resolution requirement will be achieved within any 4 nm band. The bands will be selected by grating rotation and studied by focal plane scanning. The ray trace analysis showed that an infinitely narrow line would have a width of ≤ 0.0008 nm (8 mÅ) when scanned. Preliminary consideration of the sensitivity of the performance to optical imperfections and misalignments as well as to thermal effects showed that the design goal of $\Delta\lambda \leq 0.0015$ nm can be reached with presently-available technology.

Two photomultipliers with different photocathodes and a number of cut-off and band-pass filters will be used to remove out-of-band scattered light. Provision for the use of a predisperser will also be made. Deuterium and tungsten filament irradiance sources will be included for in-flight calibration of the instrument detection efficiency.

*Supported by NASA Contract NAS-5-26557 to Harvard College.

1. Simon, P.C., Planet. Space Sci. 26, 355 (1978).
2. Simon, P.C., Sol. Phys. 74, 273 (1981).
3. Brueckner, G.E., Advances in Space Research 2, No. 4, 177 (1982).
4. Hill, R.A., Applied Optics 8, No. 3, 575 (1969).

DISCUSSION OF SMITH PRESENTATION

EDDY: What is the field of view of the instruments?

SMITH: The whole Sun.

STATUS REPORT- ARIZONA SOLAR VARIABILITY PROGRAM

James M. Palmer, Optical Sciences Center, Univ. of Arizona, Tucson, AZ 85721.

This brief report outlines the current status of the long-term solar variability study under way since October 1980. The program is under the direction of principal investigators B. M. Herman and W. L. Wolfe. The program goals are (1) to determine the intrinsic variability of the spectral output of the sun, (2) to determine the specific optical modification of the radiation due to the earth's atmosphere, and (3) to relate these variations to climate changes. The approach is to deploy ground-based observatories to measure the direct component of the solar spectral irradiance in the wavelength range 300-1800nm with accuracies approaching 0.1% for a 22 year period. In addition, supplemental measurements of atmospheric variables will be made to further characterize the atmosphere.

REQUIREMENTS ANALYSIS AND ATMOSPHERIC CORRECTIONS- Based on the Langley method employed, the instrument bandwidth varies from 2nm at the shorter wavelengths to 10nm at the longest wavelengths. The field of view is 40 arc-min to minimize effects of multiple scattering while allowing some tracking inaccuracies. The motion of the sun requires that the maximum integration (dwell) time be 1 sec at high (~5) air mass. Higher air masses are excluded. Separate studies are under way to determine the effects of vertical and horizontal inhomogeneities and to perfect appropriate statistical analysis procedures.

SITE SELECTION- Desirable site characteristics include high (>2.5km) elevation, within $\pm 35^\circ$ of the equator, with accessibility, power, good "seeing", clear weather and political stability. After looking at some 300 existing sites, our tentative selections are Mt. Lemmon, AZ (2.75km, 32°N) and Mauna Loa, HI (4km, 19°N) for the first two sites. A potential third site is sought in the Chilean Andes.

INSTRUMENTATION- All of the instrumentation has been designed and approved at the conceptual level and the detailed design is progressing nicely. The spectroradiometer features an adjustable siderostat for precise tracking, an integrating sphere for depolarization, two double monochromators, each with its own optimized detector and appropriate electronics. The entire system is automated with distributed computing facilities. The auxiliary instrumentation includes separate radiometers for ozone, water vapor and atmospheric aerosol characterization, precise measurement of the solar zenith angle, total radiation using active-cavity radiometers and pertinent meteorological factors.

CALIBRATION- The calibration of the instrument will be accomplished using the self-calibration technique developed by NBS. We have achieved errors <0.1% from 400-900nm and are attempting to extend this range to 300-1800nm. Other calibrations include instrumental slit function, wavelength (verified with Fraunhofer lines) and periodic scale verifications using portable absolute filter radiometers.

Funding is provided by NOAA under grant NA80RAD00065.

BLANK PAGE

Comments on the Need for Ground-Based Observations
for Research on Solar Variations on Active Region Time Scales

by

Richard F. Donnelly

July 21, 1983

1. In support of total solar irradiance research, daily sunspot and facula measurements should be made with a more quantitative scaling of areas and intensities than in current sunspot sketches. Active observers should be consulted for their advice. For example, their sketches probably involve some time integration that smooth out some of the short-term effects of seeing; so I don't think high speed photos should be used. Some sort of video scan system that makes use of time diversity to decrease seeing effects should probably be used. I think that more than two areas (umbra and penumbra) should be scaled for sunspots, for example some preselected intensity relative to the quiet photosphere at similar solar central angles. A letter survey of those who observe sunspots and facula and those who model S should be made to get their combined opinions. Geoffrey Brown of England should be consulted about facula measurements.

2. Facula contrasts as a function of CMD in the 300 - 500 nm band with 1 nm resolution and wavelength steps should be made daily for a year before sunspot minimum arrives. Data for about a hundred regions should be analyzed to determine the average and standard deviations of their contrasts as a function of CMD, wavelength and peak brightness. If the results are too varied, monitoring measurements should be made after the one year. Occasionally, when major active regions are developing rapidly, measurements should be made about every ten minutes for a couple of days.

3. In support of research of solar UV variability, its stratospheric effects and possible effects on climate, daily Ca-K measurements should be made. Full disk measurements over the central 1A band core with high absolute accuracy relative to the adjacent photospheric continuum, like those of W. C. Livingston and O. R. White at Kitt Peak, should be continued. Although their monthly measurements at the McMath tower have high accuracy, the daily measurements made in Tucson need to be demonstrated to have sufficient accuracy. In the meantime, Jack Harvey's 10830A He-line measurements should be continued daily. Eventually, we probably don't need both Ca-K & He, but Harvey and Livingston should best be able to describe their pro's and con's. Ca-K spatial data with about 10 arc seconds spatial resolution should be raster scanned daily. On a few rare occasions of rapid active region growth, measurements every 10 seconds should be made. I think Zirin's current Ca-K effective bandwidth may be a little too wide. I think a central bandwidth of 1 A is appropriate but the bandpass should be attenuated very rapidly outside this range. Scattered light problems need to be carefully solved. Intensity scalings should aim at more than a one intensity contour for active regions, more like every 5% in intensity from 0.8 to 1.5 X's the intensity of the "quiet sun" at comparable solar central angles for central angles in the range 0 - 70° with different criteria for larger CMD. These raster scan scalings should permit UV modeling to take into account large filaments and plagues as well as the major plagues.

BLANK PAGE

D. H. Bruning

A perplexing problem in the study of the solar irradiance is the cause of the residuals obtained by subtracting the computed photometric sunspot index (PSI) from the ACRIM irradiance measurements. While some of the irradiance residual was thought to be due to the neglect of variations of individual sunspot contrast in the PSI model, recent observations by Chapman (Bull. Am. Astr. Soc. 15, 719, 1983) have shown that accurate sunspots areas coupled with PSI can completely account for the observed sunspot irradiance deficit. It is possible that these data are not representative of all sunspots and further observations are needed to show whether this is the case. The facular contrast, especially near the limb, is not well determined, but the contribution of faculae to the day-to-day irradiance variation still appears to be smaller than that required to explain the irradiance residuals. Other possible causes that need to be investigated observationally are the variations in the limb darkening or photospheric temperature gradient, and the presence of active network in the irradiance deficit and excess signals.

Another point of disagreement between authors is the placement of the zero point or quiet sun level for the irradiance. Since this quiet sun level affects the measurement of variations over the solar cycle length periods, it is important that some agreement is reached upon what the quiet sun level is defined to be.

While measurements of the facular contrast are perhaps best left to space-borne instruments such as SOT, many important irradiance observations such as measurements of the limb darkening, sunspot area and sunspot contrast can still be made using ground-based instruments. It is not necessary to obtain high spectral resolution or to cover very many spectral regions since we are interested primarily in the temporal variations of the irradiance. Observations should be obtained daily and might be best obtained with a dedicated instrument, since daily observations are not feasible at many observatories. A dedicated instrument also could be designed to minimize sources of instrumental error such as scattered light.

BLANK PAGE

A GLOBAL IRRADIANCE PROGRAM

H. S. Hudson
Center for Astrophysics and Space Sciences, UCSD

G. A. Chapman
California State University, Northridge

B. J. LaBonte
University of Hawaii

This workshop has provided abundant evidence that the quality of present ground-based observations seriously limits our ability to study the physical mechanisms responsible for the observed variations of total and spectral irradiance. The areas of sunspots and faculae have been thus far the basic tools for intercomparison with the solar flux variations. As a substitute for faculae, which are generally not observed by synoptic programs at present, proxy data such as Ca plage have widely been used. The shrinkage of synoptic observing programs has eliminated even this, however, from the standard Solar-Geophysical Data compilations. In any case the tools used for compiling the synoptic data are archaic and perhaps should be allowed to expire if they can be replaced by superior techniques. There has been almost no application of modern detector and data-processing technology to the synoptic measurements, and it is clear that the order-of-magnitude improvement that these approaches make possible will put the synoptic data back at the forefront of research.

We assume that the importance of the solar physics and the terrestrial impact of the processes governing active-region time scales will cause a continuing program of spacecraft bolometric and spectral irradiance measurements. We address here the ways in which ground-based observations can most effectively help to resolve the important issues, and to complement the space program successfully.

Direct observations of solar brightness are now possible, with the aid of new technology, and solar brightness measurements should become an important item in a new program of precise solar global measurements. Photometric observations at Kitt Peak, San Fernando Observatory, and elsewhere have produced residual noise levels well below one percent precision. Systematic, routine observations with this precision would directly clarify the present controversy over the energetics of spots and faculae. If such observations could be carried out with sufficiently high resolution, spot areas could be determined photoelectrically, and this would be another useful input for modeling.

In addition to white-light observations, systematic and quantitative measurements of a chromospheric line are essential. The calcium K line or the helium 10830 line (see the paper by Harvey in these proceedings) would be suitable in principle. The K line is more traditional, but the 10830 line has the added advantage that it shows the presence of coronal holes quite clearly.

The usefulness of modern, professional global measurements extends beyond

the immediate needs of the irradiance modeling that we have emphasized. Indeed, the traditional synoptic data gathering doubtless began before solar constant was known to 10%. Other objectives for comprehensive data would include the presence of large-scale systematic patterns in the solar atmosphere, of which coronal holes would be a good example; monitoring for white-light flares, which has never been done photoelectrically; and possibly solar seismology. The inclusion of observations in spectral lines is aimed at these additional objectives, rather than for the purpose of providing a substitute for direct white-light photometry.

The continuity and uniformity of data represents a very important aspect of any routine observation devoted to solar global properties. It is not possible at present to predict the nature of longer-term variations in the observables, yet these would be the most important for studies of the nature of the solar cycle and of the solar structure deeper in the interior. Long-term observing programs of the greatest utility for these purposes need stable, secure support. The Greenwich solar measurements or the Harvard astronomical plate collection are two good examples that continue to produce exciting research results long after the observations were discontinued. For example, the latter are applicable to γ -ray astronomy although γ -rays were not known even in laboratories when the programs began! In this sense we can distinguish the routine global measurements from individual research programs, which can aim to achieve better observations for specific goals. The support needed for the two kinds of programs is not comparable and should not be competitive.

To conclude this discussion, we present in Table 1 a set of parameters describing the desired new departure in synoptic observations. The entries in the table represent our own opinions and are probably far from definitive. It is abundantly clear from the papers in these proceedings, and from the detailed comments of the workshop participants, that new programs of a type that we might describe as a "global irradiance program" would be able to make very powerful contributions to our knowledge of the fundamental causes of solar activity and the structure of the solar interior.

Table 1

Target Specifications of a Global Irradiance Program

Quantity	Angular Resolution	Photometric Precision	Frequency of Observation
White light	Few arc sec	$\sigma = 0.2\%$	Hourly
Calcium K	" "	$\sigma = 1\%$	Daily
He 10830	" "	" "	" "
Magnetic Field	" "	$\Delta B = 10$ gauss	Hourly

Notes: The "few arc sec" resolution intends to match the level of seeing at the sites of observation. The hourly frequency of observation appears to be necessary to resolve the most rapid time variations observed in the total irradiance by the Solar Maximum Mission. Completeness of time coverage is very important and suggests multiple observing sites, or eventually observations from a dedicated monitoring satellite.

LIST OF PARTICIPANTS

B. Alton	The Eppley Laboratory 12 Sheffield Ave. Newport, RI 02840
David H. Bruning	Mt. Wilsona and Las Campanas Observatories 813 Santa Barbara Street Pasadena, CA 91107
Gary A. Chapman	Department of Physics and Astronomy California State University 18111 Nordhoff Street Northridge, CA 91330
Eric Chipman	NASA Headquarters SC-7 Solar and Heliospheric Physics Office Washington, DC 20546
Helen E. Coffey	World Data Center A for Solar Terrestrial Physics National Oceanic and Atmospheric Administration D631 Boulder, CO 80303
John W. Cook	Naval Research Laboratory, code 4163 Washington, DC 20375
Richard P. Donnelly	Space Environmental Laboratory NOAA Environmental Research Laboratory Boulder, CO 80303
James P. Dowdy	ES-52, Space Science Laboratory NASA-Marshall Space Flight Center Huntsville, AL 35812
Dainis Dravins	Lund Observatory Box 1107 S-22104 Lund SWEDEN
Lawrence Dunkelmann	Laboratory for Optical Astronomy NASA-Goddard Space Flight Center Greenbelt, MD 20771
John A. Eddy	High Altitude Observatory Box 3000 Boulder, CO 80307

Peter V. Foukal	Atmospheric and Environmental Research, Inc. 840 Memorial Drive Cambridge, MA 02139
Tomas E. Gergely	Astronomy Program University of Maryland College Park, MD 20742
Mark S. Giampapa	Center for Astrophysics 60 Garden Street Cambridge, MA 02138
David L. Glackin	168-427 Jet Propulsion Laboratory 4800 Oak Grove Drive Pasadena, CA 91103
John W. Harvey	Kitt Peak National Observatory 950 N. Cherry Avenue Tucson, AZ 85726
Karen L. Harvey	Solar Physics Research Corporation 4720 Calle Desecada Tucson, AZ 85726
Donald F. Heath	Bennett's Point, Box 153 Queenstown, MD 21658
J. Hickey	The Eppley Laboratory 12 Sheffield Avenue Newport, RI 02840
Robert Howard	Mt. Wilson Observatory 813 Santa Barbara Street Pasadena, CA 91107
Hugh S. Hudson	CASS C-011 University of California, San Diego La Jolla, CA 92093
Gordon Hurford	Solar Astronomy 296-33 Caltech Pasadena, CA 91125
Harrison P. Jones	Laboratory for Astronomy and Solar Physics NASA S.W. Solar Station P.O. Box 26732 Tucson, AZ 85726
Barry LaBonte	Institute for Astronomy University of Hawaii 2680 Woodlawn Drive Honolulu, HI 96822

L. Larmore	Office of Naval Research Green Street Pasadena, CA 91105
John K. Lawrence	Department of Physics and Astronomy California State University Northridge, CA 91130
J. Lean	Space Environment Research Laboratory NOAA Environmental Research Laboratory Boulder, CO 80303
K. Libbrecht	c/o Harold Zirin Caltech 354-33 Pasadena, CA 91125
Ronald Moore	Space Science Laboratory NASA-Marshall Space Flight Center ES52 Huntsville, AL 35812
Gordon A. Newkirk	National Center for Atmospheric Research High Altitude Observatory P.O. Box 3000 Boulder, CO 80307
A. Nordlund	National Center for Atmospheric Research High Altitude Observatory P.O. Box 3000 Boulder, CO 80307
J. Palmer	University of Arizona Optical Sciences Center Tucson, AZ 85721
Alan P. Patterson	Big Bear Solar Observatory Caltech 40386 N. Shore Drive Big Bear City, CA 92314
D. Rabin	Space Science Laboratory ES52 NASA Marshall Space Flight Center Huntsville, AL 35812
C. Rapley	Department of Physics and Astronomy Mullard Space Science Center, University of London Holmbury St. Mary Dorking, Surrey ENGLAND RH5 6NT

Kenneth H. Schatten	Laboratory for Planetary Atmospheres NASA Goddard Space Flight Center Greenbelt, MD 20771
Andrew Skumanich	High Altitude Observatory National Center for Atmospheric Research P.O. Box 3000 Boulder, CO 80303
Peter Smith	Harvard College Observatory 60 Garden Street Cambridge, MA 02138
Sabatino Sofia	7204 Panorama Drive Derwood, MD 20855
Steven T. Suess	Space Environmental Laboratory NOAA/ERL Boulder, CO 80303
S. Tomczyk	Department of Astronomy SCI-B3 University of Southern California Los Angeles, CA 90007
Richard Willson	Jet Propulsion Laboratory 171-400 4800 Oak Grove Drive Pasadena, CA 91103
Harold Zirin	Caltech 354-33 Pasadena, CA 91125

1. Report No. NASA CP-2310		2. Government Accession No.		3. Recipient's Catalog No.	
4. Title and Subtitle Solar Irradiance Variations on Active Region Time Scales				5. Report Date May 1984	
				6. Performing Organization Code EZ	
7. Author(s) B. J. LaBonte, G. A. Chapman, H. S. Hudson, and R. C. Willson, Editors				8. Performing Organization Report No.	
9. Performing Organization Name and Address Astrophysics Division NASA Office of Space Science and Applications Washington, DC 20546				10. Work Unit No.	
				11. Contract or Grant No.	
12. Sponsoring Agency Name and Address National Aeronautics and Space Administration Washington, DC 20546				13. Type of Report and Period Covered Conference Publication	
				14. Sponsoring Agency Code	
15. Supplementary Notes B. J. LaBonte: University of Hawaii at Manoa, Honolulu, Hawaii. G. A. Chapman: California State University at Northridge, Northridge, California. H. S. Hudson: University of California at San Diego, La Jolla, California. R. C. Willson: Jet Propulsion Laboratory, California Institute of Technology, Pasadena, California.					
16. Abstract Variations of the total solar irradiance have become an important new tool for studying the sun since the deployment of a new generation of precise solar flight instrumentation, such as the ACRIM I experiment on the Solar Maximum Mission in 1980. The study of variations of the spectral irradiance observed in the EUV has also developed rapidly. The largest variations of the total irradiance occur on time scales of a days to weeks and are caused by solar active regions. Efforts to model the radiative effects of active regions are proceeding apace and the first round of results from these has appeared in the literature. Disagreements have quickly surfaced in this new field and a topical workshop was convened at The California Institute of Technology in June 1983, to provide both formal and informal opportunities for dialog between those actively working in this area. The papers resulting from this workshop are collected here, along with a transcription of the discussions.					
17. Key Words (Suggested by Author(s)) Solar Variability/Solar Constant			18. Distribution Statement Unclassified - unlimited Subject Category 92		
19. Security Classif. (of this report) Unclassified	20. Security Classif. (of this page) Unclassified	21. No. of Pages 310	22. Price A14		



END

9-14-84